# ACOUSTIC INDOOR LOCALIZATION EMPLOYING CODE DIVISION MULTIPLE ACCESS

**A Thesis Submitted to**
**the Graduate School of Engineering and Sciences of**
**İzmir Institute of Technology**
**in Partial Fulfillment of the Requirements for the Degree of**

**MASTER OF SCIENCE**

**in Electrical and Electronics Engineering**

**by**
**Cem SERTATIL**

**February 2010**
**İZMİR**

We approve the thesis of **Cem SERTATIL**

**Assist. Prof. Dr. Mustafa A. ALTINKAYA**
Supervisor

**Assist. Prof. Dr. Barış BOZKURT**
Committee Member

**Assist. Prof. Dr. M. İ. Can DEDE**
Committee Member

**15 February 2010**

**Prof. Dr. F. Acar SAVACI**
Head of the Department of
Electrical and Electronics Engineering

**Assoc. Prof. Dr. Talat YALÇIN**
Dean of the Graduate School of
Engineering and Sciences

# ACKNOWLEDGEMENTS

I would like to express my sincere gratitude to my supervisor Assist. Prof. Dr. Mustafa Aziz Altınkaya not only for his valuable support and guidance but also for his gentle behavior throughout my research. I am very proud that I had the chance to work with him.

I would like to express my sincere gratitude to Assoc. Prof. Kosai Raoof who provides me a new vision for his support and guidance during my research in France.

I would like to express my sincere gratitude to Assist. Prof. Dr. Barış Bozkurt for allocating his office for this research, sharing his equipment and involving to my thesis committee.

I would like to express my sincere gratitude to Assist. Prof. Dr. Mehmet İsmet Can Dede for involving to my thesis committee.

I would like to express my sincere gratitude to Heads of the Department of Electrical and Electronics Engineering Prof. Dr. Ferit Acar Savacı and former Heads of the Department of Electrical and Electronics Engineering Assoc. Prof. Mehmet Salih Dinleyici for their supports.

I would like to thank international relations office of İYTE for their help of carrying through my research in France.

I would like to thank all my friends for their help, support and friendship. Especially, I would like to thank Can Sümer and Alper Bayrak for sharing their house with me and helping with my thesis. I would also like to thank İlhan Baştürk, Refik Fatih Üstok, Mehmet Emre Çek and Mert Aydın for their moral motivation.

Finally, I owe gratefulness to my family for their support and endless love through my life.

# ABSTRACT


## ACOUSTIC INDOOR LOCALIZATION EMPLOYING CODE DIVISION MULTIPLE ACCESS

Indoor localization becomes a demand that comes into prominence day by day. Although extensively used outdoor location systems have been proposed, they can not operate in indoor applications. Hence new investigations have been carried on for accurate indoor localization in the last decade.

In this thesis, a new indoor location system, that aims to locate an entity within an accuracy of about 2 cm using ordinary and inexpensive off-the-shelf devices, has been proposed and an implementation has been applied to evaluate the system performance. Therefore, time of arrival measurements of acoustic signals, which are binary phase shift keying modulated Gold code sequences using direct sequence spread spectrum technique, are done. Direct sequence-code division multiple access is applied to perform simultaneous accurate distance measurements and provides immunity to noise and interference.

Two methods have been proposed for the location estimation. The first method takes the average of four location estimates obtained by trilateration technique. In the second method, only a single robust position estimate is obtained using three distances while the least reliable fourth distance measurement is not taken into account.

The system performance is evaluated at positions from two height levels using two sets of variables determined by experimental results. The precision distributions in the work area and the precision versus accuracy plots depict the system performance for different sets of variables. The proposed system provides location estimates of better than 2 cm accuracy within 99% precision. Eventually, created graphical user interface provides a user friendly environment to adjust the parameters.

# ÖZET

## KOD BÖLÜŞÜMLÜ ÇOKLU ERİŞİM KULLANIMIYLA AKUSTİK BİNA İÇİ KONUMLAMA

Bina içi konumlama günden güne önem kazanan bir ihtiyaç haline gelmektedir. Yaygın olarak kullanılan açık hava yer bulma sistemleri önerilmiş olmasına rağmen bu sistemler bina içi uygulamalarda çalışamamaktadır. Bundan dolayı özellikle son on yılda yüksek doğruluklu bina içi konumlama için yeni araştırmalar sürdürülmüştür.

Bu tezde, sıradan ve uygun fiyatlı hazır aygıtlar kullanılarak bir nesneyi yaklaşık 2 santimetre bir hatayla konumlamayı amaçlayan yeni bir bina içi yer bulma sistemi önerilmiş ve sistemin performansını görmek amacıyla sistem uygulaması yapılmıştır. Bu yüzden doğrudan dizi yayılı izge tekniği kullanılarak ikili evre kaydırmalı anahtarlama ile modüle edilmiş Gold kod dizilerinden oluşan akustik sinyallerin uçuş zamanı ölçülmektedir. Eş zamanlı yüksek doğruluklu mesafe ölçümleri için doğrudan dizi-kod bölüşümlü çoklu erişim uygulanmakta ve gürültü ile girişime bağışıklık sağlanmaktadır.

Konum belirleme için iki yöntem önerilmiştir. İlk yöntem, trilaterasyon tekniği ile elde edilen dört farklı konum kestiriminin ortalamasını almaktır. İkinci yöntemde ise gürbüz bir konum kestirimi üç ayrı mesafe kullanılarak yapılmakta, dördüncü en güvenilmez ölçümle bulunan mesafe hesaba katılmamaktadır.

Sistemin performansı yerden iki farklı yükseklikteki konumlarda deneysel sonuçlarla belirlenen iki farklı değişken kümesi kullanılarak değerlendirilmektedir. Çalışma alanındaki kesinlik dağılım grafikleri ve kesinlik-doğruluk grafikleri farklı değişken kümeleri için sistemin performansını ortaya koymaktadır. Önerilen sistem %99 kesinlikle 2 santimetreden daha iyi doğrulukla konum kestirimleri sağlamaktadır. Son olarak oluşturulmuş grafik arayüzü sistemin parametrelerini ayarlamak üzere kullanımı kolay bir ortam sağlamaktadır.

# TABLE OF CONTENTS

# LIST OF FIGURES

# LIST OF TABLES

# LIST OF ABBREVIATIONS

| | |
|---|---|
| 2D | Two Dimensional |
| 3D | Three Dimensional |
| ABL | Anchor-Based Localization |
| AFL | Anchor-Free Localization |
| AHL | Ad-Hoc Localization |
| AHLoS | Ad-Hoc Localization System |
| AoA | Angle of Arrival |
| BPSK | Binary Phase Shift Keying |
| CDMA | Code Division Multiple Access |
| DAT | Data Acquisition Toolbox |
| DGPS | Differential GPS |
| DS-CDMA | Direct Sequence CDMA |
| DSSS | Direct Sequence Spread Spectrum |
| FDMA | Frequency Division Multiple Access |
| FFH | Fast Frequency Hoping |
| FH-CDMA | Frequency Hoping CDMA |
| FHSS | Frequency Hoping Spread Spectrum |
| FSK | Frequency Shift Keying |
| GPS | Global Positioning System |
| GUI | Graphical User Interface |
| ID | Identification |
| IR | Infrared |
| LAL | Local Area Localization |
| LAN | Local Area Network |
| LLT | Location Lookup Table |
| LoS | Line of Sight |
| LPF | Low-Pass Filter |
| LPS | Local Positioning System |
| MAI | Multiple Access Interference |
| MDS | Multidimensional Scaling |
| NIC | Network Interface Card |

| | |
|---|---|
| PC | Personal Computer |
| PN | Pseudo Noise |
| PSD | Power Spectral Density |
| PSK | Phase-Shift-Keying |
| RADAR | Radio Detecting and Ranging |
| RF | Radio Frequency |
| RFID | Radio Frequency Identification |
| RSSI | Received Signal Strength Indication |
| RToF | Return Time of Flight |
| SFH | Slow Frequency Hoping |
| SONAR | Sound Navigation and Ranging |
| SS | Signal Strength |
| SSMA | Spread Spectrum Multiple Access |
| TDMA | Time Division Multiple Access |
| TDoA | Time Difference of Arrival |
| TDoF | Time Difference of Flight |
| TH | Time Hopping |
| TH-CDMA | Time Hoping CDMA |
| ToA | Time of Arrival |
| ToF | Time of Flight |
| US | Ultrasound |
| WAL | Wide Area Localization |
| WLAN | Wireless Local Area Network |
| WSN | Wireless Sensor Network |

# CHAPTER 1

# INTRODUCTION

Localization is a newly emerged technology that simplifies everyday life. Until today, numerous investigations have been carried out about localization. Although accurate outdoor location systems have been proposed, they can not operate properly in indoor applications. Among these, Global Positioning System (GPS) (Daly 1993) is an outstanding and effective outdoor location system that has world wide coverage. Nevertheless, GPS can not perform indoor localization. Therefore, specific location systems are needed for indoor localization applications. Especially in the last decade, the investigation about indoor localization has gained momentum, and the significance of indoor localization has been well established. There are many useful localization applications improving everyday life. Just a few examples can be given as follows. Enterprises use indoor localization in order to localize their employees and their properties. In hospitals, doctors can be localized by an indoor location system, so they can reach their patients on time. In museums, visitors can be provided with information regarding their current location or the system can show advertisements or location information to the user.

The aim of this thesis is to reach approximately 2 cm accuracy within sufficient precision using ordinary inexpensive devices. Thereby an indoor location system that uses acoustic signals has been proposed and an implementation has been applied in order to see the overall performance of the system. First of all, the related research activities about indoor localization will be revisited to have an idea about what have been proposed until today.

## 1.1. Indoor Localization Research

In this section, a representative set of outstanding indoor location systems will be given. This would be helpful to the reader to see the progress of indoor localization and enable his/her compare the proposed system with the other indoor location systems.

An early localization effort is Active Badge system (Want, et al. 1992) that is based on infrared (IR) signals and is used to localize people in an office environment. A badge worn by a person emits a unique code that is perceived from receptors at the fixed points. The master station processes data and displays it in a visual form. The system provides room-granularity accuracy. The drawbacks of the system are influence of the direct sunlight and dead spots.

In 1997, another system called BAT system (Harter, et al. 2002) that uses ultrasound (US) signals instead of IR signals has been proposed. A small US transmitter, Bat, that is attached to the people emits a short unencoded pulse when base station transmits a radio message containing its identifier. The receivers placed at known position record the Time of Arrival (ToA) of any signal from the Bat. Consequently, the location of Bat is estimated by a central unit within 9 cm tolerance of its true position for 95 percent of the measurements using multilateration technique.

Around the beginning of the new millennium, Radio Frequency (RF) signals have begun to be used for indoor applications. RADAR system (Bahl and Padmanabhan 2000; Bahl, et al. 2000) based on RF signal measures the Signal Strength (SS) and signal to noise ratio of the signals emitted from several known points with several known directions using three base stations and constructs models for signal propagation during off-line phase. In real-time phase, the user coordinates are estimated in two dimensions by matching the result obtained during the real-time phase with the data obtained during off-line phase. The system estimates the user's location within 3 m accuracy and 50% precision.

Another system which is also proposed in 2000 is Cricket system (Priyantha, et al. 2000; Priyantha 2005). That system uses RF and US signals concurrently to measure distance by calculating Time Difference of Arrival (TDoA) of these signals. In Cricket System, beacons emit unmodulated US signals constructed by long enough radio messages. The location of a beacon is estimated by applying trilateration technique. It has room-granularity within an accuracy of a few inches. The difference of this system compared to its rivals is the firstly used decentralized and privacy-oriented structure.

The Cricket Compass system (Priyantha, et al. 2001) was improved from the Cricket system and it provides information about the orientation of the receiver. It uses V-shaped five US transducers to measure the phase differences in the received US signals.

In 2002, Dolphin system (Hazas and Ward 2003; Hazas and Hopper 2006) that uses Direct Sequence-Code Division Multiple Access (DS-CDMA) method for simultaneous distance measurements as in GPS has been proposed. US ranging signal is modulated by 511 bits long Gold code using Binary Phase Shift Keying (BPSK). Two types of location systems have been proposed: polled and centralized location system and privacy oriented location system. In polled and centralized system, the receivers are fixed to the ceiling and the location of emitter is estimated by applying multilateration technique using direct ToF measurement. It has approximately 2 cm accuracy. In privacy-oriented location system, the emitters are fixed to the ceiling while the receivers are roaming. This type of system can be synchronous or asynchronous. In the synchronous case, location of the receiver is estimated by conventional multilateration. On the other hand, in asynchronous case location of the receiver is estimated by using direct sequence pseudorange measurements. The system has 4.9 cm accuracy within 67% returned readings for synchronous case and 26.6 cm accuracy within 48% returned readings for asynchronous case.

SmartLOCUS system (Cyril, et al. 2003) that is a self-assembling system consisting of ad-hoc networking nodes has been proposed one year later. It provides ease in adding new nodes. It uses RF and US signals concurrently to measure distances between nodes as Cricket system does. Additionally, RF signals are used to share the location data among nodes. The system has a distance accuracy of about 20 cm and the measurements are performed multiple times to get accuracy about 1 cm.

In the following year, Radio Frequency Identification (RFID) technology has been used in indoor location systems. LANDMARC (Location Identification based on Dynamic Active RFID Calibration) system (Ni, et al. 2004) uses a number of RFID readers and tags. The RFID readers have eight different power levels. Based on the received SS, the RFID reader determines which level the received power corresponds to. The process is implemented for each power level of each tag. Location of an object is estimated only with a low accuracy using the SS data.

Another system (Piontek, et al. 2007) was improved from the Cricket system in 2007. In that system, the US pulses are encoded by thirteen chips long Barker code and modulated with BPSK to achieve greater accuracy in distance measurements. Besides that the update rate is improved by synchronizing the active beacons. The overall accuracy of the system is within 10 cm.

Eventually, acoustic signals were firstly used in 3D-LOCUS Local Positioning System (LPS) (Prieto, et al. 2007) that is based on acoustic transducers and can determine the mobile target position with sub-centimeter accuracy. In 3D-LOCUS LPS, acoustic sound signals are modulated by 32 chips long Golay code using BPSK. The system can perform in three different configurations: centralized, privacy oriented and bidirectional. The results are obtained for the four different test conditions: Time Division Multiple Access (TDMA), Code Division Multiple Access (CDMA), TDMA with airflows and CDMA with airflows.

Some specifications of these indoor location systems were illustrated in Table 1.1. These specifications are emitted signal, measurement technique, location estimation technique, structure, spread spectrum technique and performance of the system.

Table 1.1. Specifications of Indoor Location Systems

| | Emitted Signal | Measurement Technique | Location Estimation Technique | Structure | Spread Spectrum Technique | Accuracy and Precision |
|---|---|---|---|---|---|---|
| Active Badge (1992) | IR | Connectivity | Proximity | Centralized | - | Coarse-grained Room-granularity |
| BAT (1997) | US | ToA | Multilateration | Centralized | - | Fine-grained 9 cm (95%) |
| RADAR (2000) | RF | RSSI | Fingerprinting or Triangulation | Centralized | - | 3 m (50%) Room-granularity |
| Cricket (2000) | RF and US | TDoA or Connectivity | Trilateration or Proximity | Decentralized Privacy-oriented | - | a few inches Room-granularity |
| Cricket Compass (2001) | RF and US | Phase Difference | - | Decentralized Privacy-oriented | - | 3˚ ± 30˚ 5˚ ± 40˚ |
| Dolphin (2002) | US | ToA | Multilateration | Polled and centralized | DS-CDMA 511 Gold Code BPSK | 2.1 cm accuracy with 95% confidence (75% readings returned) |
| | | | | Privacy-oriented | | Synchronous 4.9 cm accuracy with 95% confidence (67% readings returned) |
| | | | | | | Asynchronous 26.6 cm accuracy with 95% confidence (48% readings returned) |
| SmartLOCUS (2003) | RF and US | TDoA | - | Decentralized Self-assembling | - | 20 cm distance accuracy |
| LANDMARC (2004) | RF (RFID) | RSSI | Proximity or Fingerprinting | Decentralized | - | Coarse-grained |
| (Piontek, et al. 2007) | RF and US | TDoA | Multilateration | Decentralized Privacy-oriented | DS-CDMA 13 Barker Code BPSK | 10 cm |
| 3D-LOCUS (2007) | Acoustic | ToA | Trilateration | Centralized | DS-CDMA 32 Golay Code BPSK | 12.6 mm accuracy with 95% confidence (96.2% valid readings) |
| | | | | Privacy-oriented | | 13.5 mm accuracy with 95% confidence (94.7% valid readings) |
| Proposed System (2010) | Acoustic | ToA | Trilateration | Centralized | DS-CDMA 511 Gold Code BPSK | 2 cm accuracy with 99% precision |

## 1.2. Thesis Outline

In this chapter, the history of indoor localization and the motivation of this thesis work are considered. The remaining chapters are organized as follows.

In Chapter 2, the background of localization subject is given. Some definitions are clarified and comprehensive classification is done.

In Chapter 3, spread spectrum concept, CDMA and spreading codes are handled respectively in consecutive sections.

In Chapter 4, the proposed location system and its implementation are introduced. Devices used in the setup and their technical details, the preparation of work area, procedure of localization and Graphical User Interface (GUI) are mentioned.

In Chapter 5, the simulation results are presented. The transfer function gain of the system, the effect of selection of the variables to the performance, the precision distribution through the work area and the precision versus accuracy relations are analyzed, respectively.

Finally, in Chapter 6, conclusion and contribution of the work presented in this thesis are given and some possible future works are suggested to extend this research.

# CHAPTER 2

# BASICS OF LOCALIZATION

This chapter gives background on localization subject, which is very important to comprehend what is done in this thesis. The chapter is divided into three sections. In the first section, an introduction to localization is done. Then some concepts related to localization are revealed in section 2.2, followed by a classification in localization in section 2.3.

## 2.1. Introduction to Localization

From the beginning of history, localization has been a fundamental necessity for human beings. Localizing prey or food source for feeding and localizing predatory or danger source in order to survive are the primary vital necessity since the first men. Sensing abilities (like seeing, hearing abilities etc.) of human have provided the ways to meet this essential need.

Today, diverse methods and devices are used to get accurate localization in order to fulfill the modern world's needs. From simple daily tasks to military applications, localization takes place in many aspects of modern life. Therefore investigations about localization get important increasingly day by day. These investigations lights the way of developing innovative technologies about localization.

If localization is handled entirely as a topic, the investigation becomes very hard to deal with. That is because localization topic covers an excessive field. Indoor (in-building) localization, outdoor localization, underwater localization and localization in robotics are some prominent subtopics of the localization. A considerably accurate indoor localization method was accomplished in this thesis. Therefore, first some general concepts related to localization were clarified. Then indoor localization topic was handled by classifying them in order to give some knowledge and new vision to the reader.

## 2.2. Some Concepts Related to Localization

The concepts that are handled in this section are common to all location systems. Knowing these concepts provides reader an easy reading of papers related with this thesis. Firstly, definition of accuracy, precision, granularity, range and scale must be elucidated.

Accuracy or grain size of a location system is the closeness measurement of distance to the actual position of the target. On the other hand, precision of a location system is the percentage of relevant occurrences. For instance, GPS has 1 to 3 meter accuracy with 99 percent precision. There is a trade-off between accuracy and precision. They are inversely correlated, since the precision of a system can be increased by just decreasing the accuracy of that system. For more information, refer to (Hightower and Borriello 2001).

Granularity in a location system refers to the smallest scale that the target can be localized in that system. For instance, Active Badge system has a room-granularity. So system can not localize the target in portion smaller than a room size.

Range of a location system refers the size of entire influence area of that location system from smallest distance to the largest distance. For instance, LANDMARC that uses RFID tags has a 150 feet range.

Scale of a location system refers to the coverage area and the number of objects located in that area per unit infrastructure per each time interval. For instance, GPS reach to unlimited number of users in worldwide with its 24 satellites.

### 2.2.1. Physical vs. Symbolic Localization

Physical localization requires the exact physical location of an entity or node in a defined coordinate system. The words “entity” and “node” will be used interchangeably throughout this thesis. GPS is an example to physical location systems. GPS provides spatial location information of the receiver as latitude, longitude and altitude. Thus, it determines exact physical location of the GPS receiver. Additionally, the system that has been proposed in this thesis can be given as an example to physical location systems. As it will be mentioned extensively in the sequel, the coordinates of the receiver node, consisting of a microphone, are found in three-dimensional space. On

the other hand, symbolic localization never requires an exact physical location as in physical localization. It states location of an entity (node) by referring to predefined entities. Bar code scanner system is a good example for symbolic location system. Symbolic localization can only provide substantially coarse grained physical location.

### 2.2.2. Relative vs. Absolute Localization

In relative localization, nodes are localized in reference to a coordinate system that is independent of external references. On the other hand, in absolute localization, external references are used to define a coordinate system in which nodes are located. Relative localization is generally used for ad-hoc systems. The nodes in ad-hoc system can be localized relatively using Multidimensional Scaling (MDS) method. A relative coordinate system can be transformed into an absolute coordinate system using known references. The proposed system performs absolute localization.

### 2.2.3. Centralized vs. Distributed Localization

Centralized localization can be explained as nodes are localized by performing the whole computation in a central unit. The unit can be a central node inside system or can be an outside unit like a PC or can be a combination of both. In the proposed system, a PC was used to perform the whole computation as a central unit. The usage of centralized system necessitates simpler devices in indoor localization. However, the deployment of a centralized localization is not convenient for outdoor localization and Ad-Hoc Localization (AHL). In such a case, distributed localization may be more useful. In distributed localization, each node performs its computation separately. As an indoor location system, Cricket System is an example of distributed locations system due to its decentralized structure. In fact, privacy concern is an important issue for centralized localization. In centralized localization, all node locations are known by central unit, so central unit can track all nodes. In some cases, this violates some privacy concerns. For instance, employees in a company may feel uncomfortable due to the tracking of their employer. In these cases, distributed localization must be preferred. Distributed location systems use methods requiring less computation because of cost, size and energy consumption concerns. This in turn might reduce system accuracy.

### 2.2.4. Anchor-Based vs. Anchor-Free Localization

In Anchor-Based Localization (ABL), special nodes called ‘anchor nodes’ which assign their coordinates by manual configuration or using a location system like GPS are used. Thus, other nodes can determine their absolute locations by using the knowledge of anchor nodes’ coordinates. Contrary to ABL, in Anchor-Free Localization (AFL), there is no special node like ‘anchor nodes’. Instead, local measurements are done in order to determine nodes positions in a relative coordinate system. Pre-configured coordinates are not used. The proposed system in this thesis uses four fixed emitter nodes with assigned coordinates as in ABL. Thereby the location of the receiver node can be found in absolute coordinate system.

### 2.2.5. Incremental vs. Concurrent Localization

Incremental localization and concurrent localization are appropriate for wireless ad-hoc location system. Incremental localization algorithm starts with a set of nodes with assigned coordinates like anchor nodes. Then other nodes are added to this set respectively by calculating their coordinates using the knowledge of the nodes whose coordinates are already computed previously. In concurrent localization, all nodes calculate and refine their coordinates concurrently. The procedures of incremental localization and concurrent localization are shown respectively in Figure 2.1 and Figure 2.2.

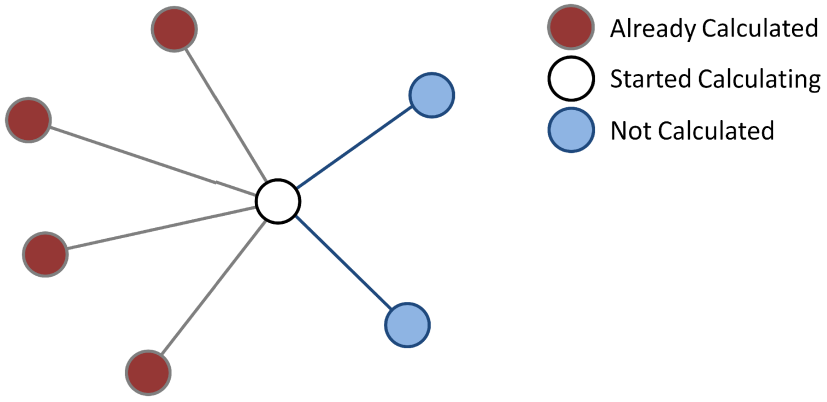


Figure 2.1. Incremental localization procedure

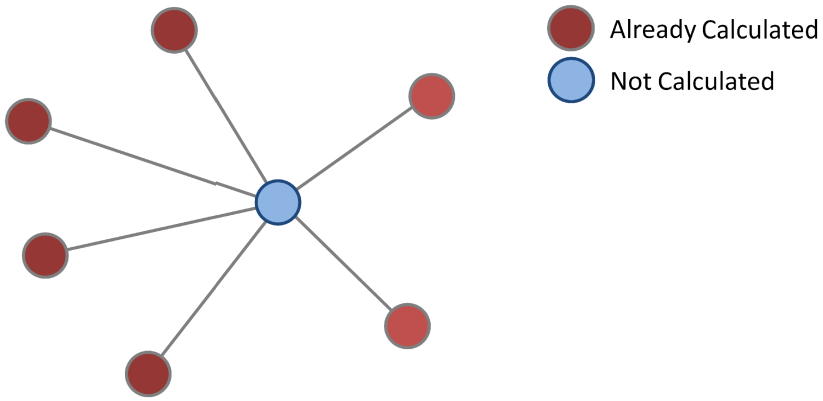


Figure 2.2. Concurrent localization procedure

### 2.2.6. Fine-Grained vs. Coarse-Grained Localization

Fine-grained localization, or range-based localization, involves determining location of an entity by measuring distances or angles between the entity and specific nodes. Measuring the Received Signal Strength Indication (RSSI) or Time of Flight (ToF) are the most often used methods to measure the distance. Angle of Arrival (AoA) is another method for fine-grained localization that estimates the angles. All GPS, RADAR and Cricket system are examples for fine-grained location system. Furthermore, the system that has been proposed in this thesis is also an example for fine-grained localization. In this system, distance measurements are made with an accuracy of millimeters by using the method of ToF. On the other hand, coarse-grained localization, or range-free localization, does not require any distance or angle measurements. Connectivity is a coarse-grained method. Cricket system can also be given as an example for coarse-grained location system, because it can be adjusted for both type of localization. The main advantage of coarse-grained localization is the requirement of less infrastructure and computation. Thereby the cost is less. However, accuracy of coarse-grained localization is relatively low, which is the main disadvantage. Both of two localizations have their own area of use. If an accurate localization is needed, then fine-grained localization has to be chosen, on the other hand, if not, there is no need for fine-grained localization. Choosing the coarse-grained localization would be more sensible.

### 2.2.7. Active, Cooperative, Passive and Blind Localization

In active localization, location system emits and receives back signals to localize a target. Sound Navigation and Ranging (SONAR) system localizes target by processing the returned sound signal from the target. That's why SONAR system is an active location system. In cooperative localization, target cooperates with location system in order to find its position. Target emits specific signal and cooperative location system assigns the location of the target using the emitted signal from the target. BAT system is a prominent example for cooperative location system. A base station periodically sends a radio signal in order to trigger targets called Bats to send ultrasonic signal. As a result of that, the base station calculates distances and assigns the location of the target. In passive localization, location system detects the location of the target from observations that it does. Habitat monitoring systems can be an example of passive location systems. A bird in a nature can be monitored using its characteristic voice. In blind localization, location system detects location of target without any priori knowledge about its characteristic. This type of localization needs more computation and may not be noise immune. Beamforming method, that uses arrays of receivers or transmitters to obtain directionality or sensitivity of signal, can be used for blind localization.

### 2.2.8. Wireless vs. Wired Communication System

Wireless communication systems transfer communication data over a distance without using any wires. Today wireless location systems are preferred due to their ease of deployment and large coverage area. Wireless location systems can be used for both indoor and outdoor localization conveniently. Wired communication systems transfer communication data through a wired network. Wired location systems can be used for indoor localization. Most of the indoor location systems use wired communication, because it requires less complex devices. Proposed system also uses wired communication. All of the transducers are connected to the central unit through wires. But it is possible to make it wireless using wireless equipment like RF communication devices. As a consequence, the process of changing a wired system to a wireless system might bring an additional cost.

### 2.2.9. Context-Aware, Location-Aware and Tracking-Aware Systems

Context-aware systems sense the environmental changes using their sensors and adopt their behavior to this changing environment. These systems need to know not only the location of the user but also location of devices that is related to the users such as printers in an office. BAT system is a good example for context aware systems. Location-aware systems determine the location of an entity but do not track that entity. Cricket system can be given as an example for location-aware systems. Tracking-aware systems track and store the location information of entities. The knowledge of change in location provides time and location information to the user. In habitat monitoring, this information is very essential. For instance, ZebraNet (Juang, et al. 2002) is a wild life tracking system in which sensors are attached to the zebras to get information about their movements, migration pattern, and such that. A motion-aware system is generally used for virtual reality and motion capture in computer animation industry. The system must determine the person's position and orientation with a high degree of precision. Hence, this kind of a system is quite expensive. MotionStar DC magnetic tracker uses magnetic field pulses to assign the position and orientation.

### 2.2.10. Static, Adaptive and Predictive Localization

Localization must be repeated periodically to ensure that the error in the location estimates are at an acceptable level or to track changes in the location of the target. This is called dynamic localization. There are three types of dynamic localization which are static, adaptive and predictive localization, respectively. In static localization, the localization period is constant and does not change with any action of the user. The system localizes the target every $t$ seconds. This type of localization is simple but exposed to errors. Since the performance varies with the mobility. Although it can give less erroneous results while the target moves slowly, in the case of fast movement, it might give much erroneous results. In addition to that, the power consumption is not good, because it consumes power even in a case that the target does not move. In adaptive localization, the localization period is not constant and changes with the mobility. The system adapts its localization period corresponding to velocity of the target. If the velocity of the target is high, then localization period will be short,

similarly, if the velocity of the target is low, then localization period will be long. The change in localization period saves computation and power, but it may also cause some error if sudden velocity changes occur. In predictive localization, dead reckoning method is used to choose the localization period of the system. Dead reckoning is a method that estimates location of an entity using previously detected location or using the known velocity of that entity. Thereby the path can be predicted by using dead reckoning method and if the prediction is accurate, the location estimate is updated without performing actual localization. This means an increment in localization period which provides less power consumption. For more information refer to (Tilak, et al. 2005).

## 2.3. Classification of Localization

In this subsection localization is classified according to scale, emitted signal, measurement technique, location estimation technique, structure and usage. Figure 2.3 illustrates the classification of localization. For more information refer to (Pandey and Agrawal 2006)

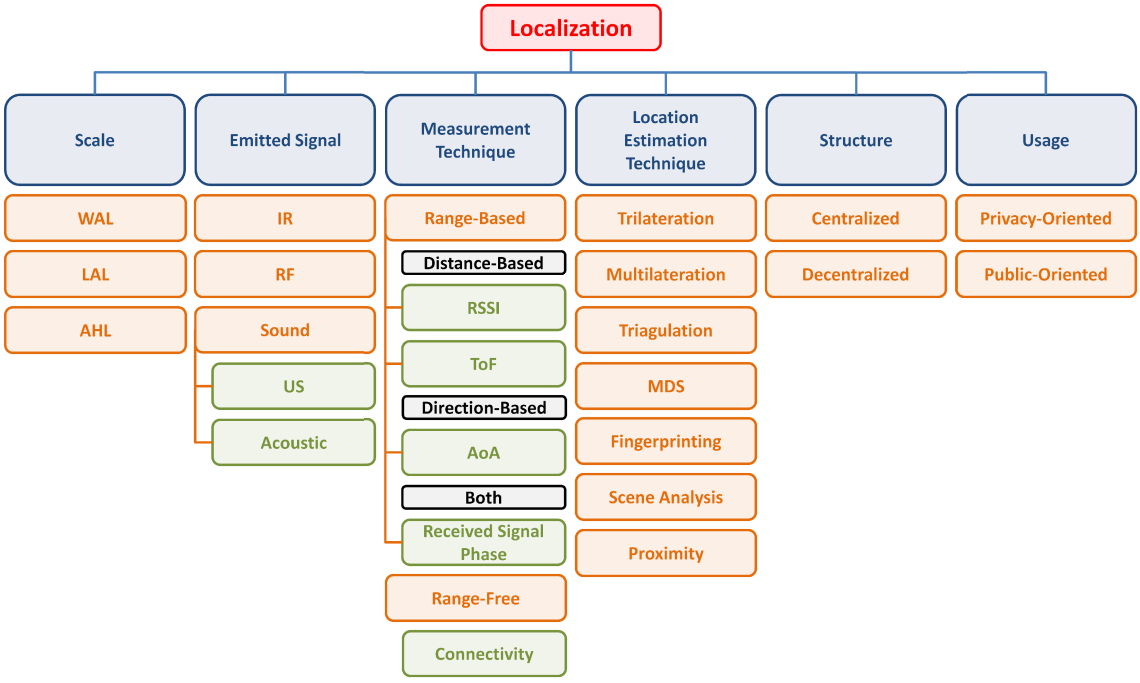


Figure 2.3. Classification of localization

### 2.3.1. Scale

Location systems differ by their coverage area, the number of users connected to them and their network topology. Thus localization may be classified into Wide Area Localization (WAL), Local Area Localization (LAL) and Ad-Hoc Localization (AHL) according to its scale.

#### 2.3.1.1. Wide Area Localization (WAL)

Wide Area Localization (WAL) provides a wide area deployment and coverage of a huge number of users. It is commonly used for wireless outdoor applications. The broadcasting devices may be costly and require no power constraint, since they broadcast through wide area. GPS and E911 application for cellular phone perform WAL to locate their users. GPS provides service with its 27 satellites (3 satellites are for back-up) to the entire surface of the earth. The difficulty of WAL is to achieve a good accuracy throughout the entire deployment area.

#### 2.3.1.2. Local Area Localization (LAL)

Local Area Localization (LAL) provides a narrower area deployment compared to WAL and does not require such costly devices as in WAL. It is commonly implemented for indoor applications. It is convenient for enterprise and commercial establishment. Active Badge, BAT, RADAR, Cricket, Dolphin and 3D-LOCUS systems are all LAL applications. Among these Active Badge system is tested in an enterprise, while RADAR system is tested on the second floor of a three storey building.

#### 2.3.1.3. Ad-Hoc Localization (AHL)

Ad-Hoc Localization (AHL) requires low power consumption, computation and communication cost. Integrating a new node to the system does not require any exterior intervention in Ad-Hoc Localization System (AHLoS). Wireless Sensor Network (WSN) performs AHL using anchor nodes. SmartLOCUS is a prominent example for AHLoS, since it is self-assembling and has an autonomous management.

### 2.3.2. Emitted Signal

Infrared (IR), Radio Frequency (RF), sound and combinations of them are used in location systems. Each of them has a unique characteristic that provides advantage for different purposes when compared to the others. These are very effective on the performance of the location system. One important issue is that they may use the same frequency spectrum but they show different specifications on that spectrum. Hence the performance of location system varies. Using a combination of them may increase the performance of the system as in Cricket system. In Cricket system, RF and US signals are emitted concurrently from the object. Taking the advantage of the difference in velocities between RF and US, the distances are measured.

#### 2.3.2.1. Infrared (IR)

Infrared (IR) is generally used for coarse-grained localization. The precision of the system is related to the line-of-sight (LOS) between the emitter and receiver. The drawbacks of IR are limited transmission with LOS, low transmission range of IR transducers, low accuracy of location system and influence of sunlight. Despite all, IR can be a good choice for localization requiring room-granularity. Active Badge system uses IR to localize working people in an office environment. A kind of tag attached to people, emits a unique coded IR signal every 15 seconds. IR sensors are placed inside every room in that office. All sensors are connected to each other and constitute a sensor network which is controlled by a master station. The master station processes the data sent from the sensors and puts it into a visual form. Small and low cost IR transducers of Active Badge provide an advantage.

### 2.3.2.2. Radio Frequency (RF)

Radio Frequency (RF) is commonly used for communication. Mobile phones, Wireless Local Area Network (WLAN) and such use RF spectrum to communicate. GPS, RADAR and SpotON (Hightower, et al. 2000) location systems also use RF for distance measurements. The advantages of RF are inexpensive and off-the-shelf RF products, easy deployment, and accurate time measurements with clocks that have enough time resolution. For instance, each base station and mobile host is equipped with an ordinary Network Interface Card (NIC), based on Lucent's WaveLAN™ RF LAN technology in RADAR system. This NIC can be found in every laptop and can be bought from every technology market. This widespread usage of RF product makes it preferable for location systems. The drawback of RF location system is the need of expensive and very precise clocks in order to measure the distance accurately. For instance, GPS uses very precise atomic clocks. The other drawbacks of RF are multipath, shadowing and attenuation of signal.

### 2.3.2.3. Sound

Additional to IR and RF, sound is also used for localization. The slower velocity of sound compared to RF velocity, make it possible to obtain very accurate distance measurements with inexpensive clocks. Today, location systems using sound have reached subcentimeter accuracy with inexpensive infrastructure. For instance, 3D-LOCUS LPS achieves that accuracy by using acoustic transducers that can be bought from every technology market. Sound signals are considered in three groups according to their frequency spectrum as infrasound, acoustic and ultrasound (US). Figure 2.3 illustrates the frequency spectrum of them. Although acoustic sound and US are used for indoor localization, there is no deployed infrasound location system to our best knowledge.


Figure 2.4. Frequency spectrum of sound

#### 2.3.2.3.1. Ultrasound (US)

Ultrasound (US) is used in location systems such as BAT, Cricket, SmartLOCUS, and Dolphin System. These systems can localize objects with centimeter accuracy using US transducers. Although several US transducers are available in the market, finding broadband and omnidirectional transducers is a bit problematic. In fact, as a result of this challenge, US transducer called 'Dolphin unit' was manufactured by hand in Dolphin system. These manufactured transducers have broader frequency spectrum compared to ordinary ones. Thanks to this broader frequency spectrum Dolphin Systems implements Direct Sequence Spread Spectrum (DSSS) technique as in GPS. For this, 511 bits Gold code is modulated with a 50 kHz carrier signal using BPSK. The Dolphin system has accuracy about 4.9 cm with %95 confidence.

#### 2.3.2.3.2. Acoustic

Recently, acoustic transducers also come into use for localization, because of their broadband and omnidirectional characteristic. Acoustic transducers are firstly used in 3D-LOCUS LPS that also implemented DSSS technique. Contrary to Dolphin System, in 3D-LOCUS LPS 32 chips long Golay code is used instead of 511 bits long Gold code. The 3D-LOCUS LPS has subcentimeter accuracy. The proposed system also uses basic low-cost acoustic transducers. The proposed system is handled comprehensively in the following chapter.

### 2.3.3. Measurement Technique

Range-based and range-free measurement techniques are used to measure distances in location systems. Range-based measurement techniques are preferred for the location system requiring high accuracy, while range-free measurement techniques are preferred for the location system requiring less accuracy. The challenge in implementing range-based measurements is the requirement of more expensive devices when compared to range-free measurement. By the help of the range-based measurement techniques, today location systems can achieve subcentimeter accuracy.

### 2.3.3.1. Range-Based Measurement Techniques

Received Signal Strength Indication (RSSI), Time of Flight (ToF), Received Signal Phase and Angle of Arrival (AoA) measurement techniques are range-based measurement techniques. Range-based measurement techniques can also be classified as distance-based, direction-based or both. While RSSI and ToF are distance-based, AoA is direction-based and Received Signal Phase is both.

#### 2.3.3.1.1. Received Signal Strength Indication (RSSI)

Received Signal Strength Indication (RSSI) depends on power measurement of received signal whose transmission power is known already. This measurement technique is low cost and simple, and moreover it can be implemented with ordinary RF communication devices. Signal strength denoted by *SS* varies inversely with distance *d*,

$$SS = \frac{1}{d^n} \tag{2.1}$$

where *n* is the path loss exponent. In free space, SS diminished proportionally with square of distance ($d^2$). The attenuation of SS causes some difficulties for WAL and AHL in outdoor applications. Multipath, reflection, shadowing, fading and mobility effect the SS measurement, therefore the accuracy of location system is reduced. RSSI provides less accuracy compared to other techniques. For instance, RADAR system that performs RSSI has an accuracy of 3 meters.

#### 2.3.3.1.2. Time of Flight (ToF)

Time of Flight (ToF) leans on measurement of flight time ($t_{\mathrm{ToF}}$) of a signal that propagates with a constant velocity *v*. The distance *d* can be found as

$$d = t_{\mathrm{ToF}} \times v \tag{2.2}$$

Measuring ToF of a high frequency signal like RF signal which has a velocity that approaches to the speed of light, $3x10^8$ meter per second, can provide high accuracy. However, in order to reach that high accuracy, very expensive and high resolution (by six orders of magnitude) clocks must be used. In addition, order of nanoseconds time resolution brings out a synchronization problem. Hence transmitters and receiver must be synchronized very precisely. For instance, GPS operates with RF signal and measures ToF by using very precise atomic clocks in their transmitter. Instead of that, measuring ToF of sound signal provides high accuracy with inexpensive clocks. Since the propagating velocity of sound (approximately 343 meters per second at 20˚C and absolute pressure 1 bar) is much slower than the propagating velocity of RF.

ToF can be measured in different ways; Time of Arrival (ToA), Return Time of Flight (RToF) and Time Difference of Arrival (TDoA).

In Time of Arrival (ToA), the elapsed time is measured from the beginning of transmission to the perception at the receiver. The product of ToA with the propagating velocity gives the distance from the emitter to the receiver. GPS measures ToA of RF signal in order to measure elapsed time between satellites and receiver. At least four elapsed times are measured in order to localize the receiver. Although satellites are synchronized among them, there is no synchronization among the satellites and the receivers. Hence satellites broadcast their actual location and exact transmission time so that GPS devices can calculate their positions from time differences without any synchronization.

In Return Time of Flight (RToF), there is no need of time synchronization as in ToA. Since the received signal is retransmitted with a latency. Hence RToF ($t_{\mathrm{RToF}}$) is

$$t_{\mathrm{RToF}} = 2t_{\mathrm{ToF}} + t_{\mathrm{latency}} \tag{2.3}$$

where $t_{\mathrm{latency}}$ denotes latency. If the occurred latency is known, then ToA and distance can be calculated. RToF does not require knowledge of transmission time and synchronization among emitters and receivers. Therefore, RToF is convenient for active location systems.

Time Difference of Arrival (TDoA) or Time Difference of Flight (TDoF) can be measured in three cases. In the first case, more than one signal with different propagation velocities are used concurrently to measure TDoA between the signals. For instance, Cricket system measures TDoA of RF and US signals and estimates the distance from relative delay of them. The RF signal propagate at a velocity of $3x10^8$ meter per second, while US signals propagates at a velocity of 343 meters per second at 20˚C and absolute pressure 1 bar. The temperature of the medium must be clarified since the propagation velocity of sound differs with change in temperature. This difference in velocities between signals causes a time difference as shown in Figure 2.5.

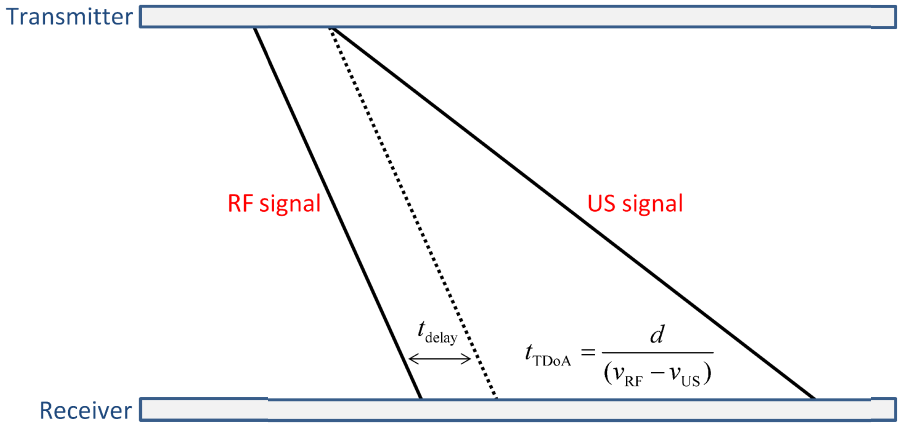


Figure 2.5. Time Difference of Arrival (TDoA)

TDoA without any time delay can be calculated as

$$t_{TDoA} = \frac{d}{(v_{RF} - v_{US})} \tag{2.4}$$

where $d$ denotes the distance, $v_{RF}$ denotes the velocity of RF and $v_{US}$ denotes the velocity of US. In the second case, the differences in time of arrivals measured between different emitters and a receiver can be taken as TDoA. In the third case, the time differences between the arrivals of a signal at different receivers are also defined as TDoA.

#### 2.3.3.1.3. Angle of Arrival (AoA)

Angle of Arrival (AoA) is a direction-based measurement technique. It assigns the direction of arrival signal by analyzing the phase or time difference between the signal's arrival at different receivers or antennas. In order to analyze the phase or time difference for radio signal and sound signal, directional antennas or antenna arrays and microphone arrays are used, respectively. The accuracy of the direction measurement is given as an angle. The drawback of this technique is the sensitivity to multipath. This is why it is not convenient for indoor applications.

#### 2.3.3.1.4. Received Signal Phase

Received Signal Phase measurement technique can be used for two purposes; the first one is to improve the accuracy of distance measurements and the second one is to assign the direction of the object. For an indoor location system, it is possible to use the received signal phase measurement technique together with ToF and SS measurement techniques to fine-tune location estimation. For example, the accuracy of Differential GPS (DGPS) which is about 20 m can be improved to sub-meter scale by measuring the carrier phase. On the other hand, Cricket Compass system can assign its orientation by using 'V' shaped passive ultrasonic transducers array that provides phase difference measurements.

### 2.3.3.2. Range-Free Measurement Techniques

Range-Free measurement techniques do not measure distance or direction. Instead, they provide hearing and connectivity information. Their accuracies are very low compared to range-based measurement techniques. This kind of a technique is commonly used for ad-hoc location systems that do not require very accurate localization and have power limitation.

Connectivity is a range-free measurement technique. It indicates that the receiver is within the transmission range or not. Thus it provides relative distance information. The region where the receiver is located can be determined by using the connectivity information of more than one transmitter. Assume that there are three

transmitters and the transmitters have three levels of power as in Figure 2.6. The receiver can get the connectivity information of transmitter A, transmitter B and transmitter C. For instance, receiver is in the second level power transmission region of transmitter A, the third level power transmission region of transmitter B and the third power level transmission region of transmitter C. In order to estimate the location of the receiver, a predefined Location Lookup Table (LLT) can be used.

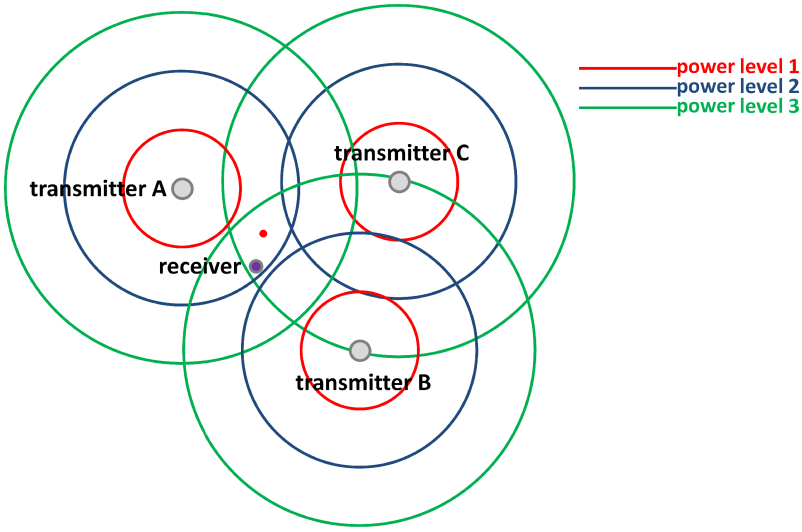


Figure 2.6. Connectivity

Connectivity commonly uses RSSI of RF signals and its accuracy is very low compared to other techniques. In addition to that LLT must be constructed again, if a change is occurred in the environment. LANDMARC system uses connectivity information in order to localize. Its RFID readers have eight different levels. Based on the received SS by the RFID reader, the reader determines if a power level can be assigned to the transmitter or not. The process is implemented for each power level of each transmitter. Eventually, the connectivity information is formed.

### 2.3.4. Location Estimation Technique

Location estimation techniques assign the location of an object using distance, direction or closeness information that is gained from measurement techniques. While some location estimation techniques provide very accurate localization as trilateration, some location estimation techniques as Min-Max provide less accuracy. In this subsection, location estimation techniques are handled in the order of trilateration,

multilateration, triangulation, multidimensional scaling, fingerprinting, scene analysis and proximity. For more information refer to (Bucur 2006).

### 2.3.4.1. Trilateration

Trilateration computes the location of a node in $n$ dimensional space by measuring distance to $n$+1 reference nodes. In order to measure the distance, range-based ToF or RSSI measurement techniques must be used. Trilateration provides an accurate localization.

In order to compute two dimensional (2D) position of an object, three non-collinear references are needed. The coordinates of the references and the distances of these references to the object must be known.

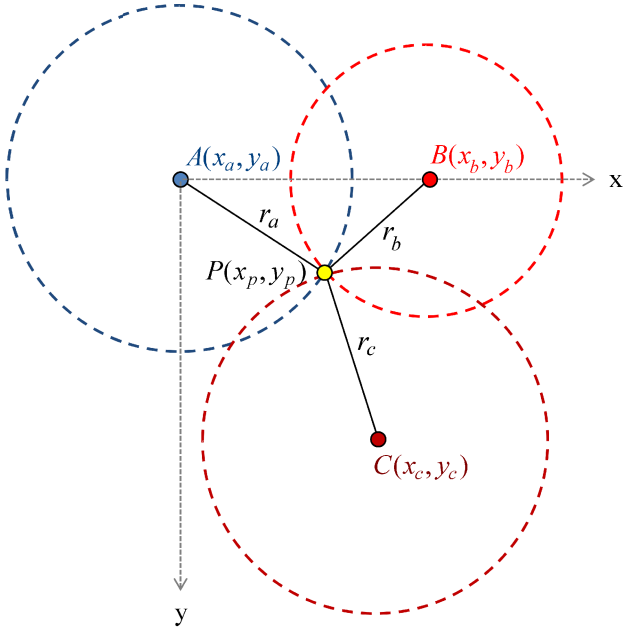


Figure 2.7. 2D trilateration with three non-collinear references

As it is seen in Figure 2.7, the coordinates of the nodes $A$, $B$ and $C$ and the distances from these nodes to the node, $P$, are known.

Using this knowledge, the equations below can be written

$$\begin{aligned}(x_p - x_a)^2 + (y_p - y_a)^2 &= r_a^2,\\ (x_p - x_b)^2 + (y_p - y_b)^2 &= r_b^2,\\ (x_p - x_c)^2 + (y_p - y_c)^2 &= r_c^2,\end{aligned} \tag{2.5}$$

where $r_a$, $r_b$ and $r_c$ are the distances from the nodes $A$, $B$ and $C$ to the node $P$, respectively.

In order to make the computation easily, it can be assumed that $(x_a,y_a)=(0,0)$ and $(x_b,y_b)=(x_b,0)$. Therefore the equations reduce to

$$\begin{aligned}x_p{}^2 + y_p{}^2 &= r_a^2\\ (x_p - x_b)^2 + y_p{}^2 &= r_b^2\\ (x_p - x_c)^2 + (y_p - y_c)^2 &= r_c^2.\end{aligned} \tag{2.6}$$

The coordinates $x_p$ and $y_p$ are found as in the equations (2.7) and (2.8), respectively:

$$x_p = \frac{x_b^2 + r_a^2 - r_b^2}{2x_b}, \tag{2.7}$$

$$y_p = \frac{x_c^2 + y_c^2 + r_a^2 - r_c^2 - 2x_p x_c}{2y_c}. \tag{2.8}$$

After calculating $x$ and $y$, the coordinate system can be transformed into previous case where no assumption is done.

It is also possible to implement the 2D trilateration with two references, if one of the solutions can be eliminated. As it is seen in the Figure 2.8, there are two solutions, because of the intersection of two circles. But one solution may be eliminated in a case that the solution is out of the solution region. Hence, one solution that is desired remains. The coordinates $x_p$ and $y_p$ can be found by solving of the intersection of two circles.

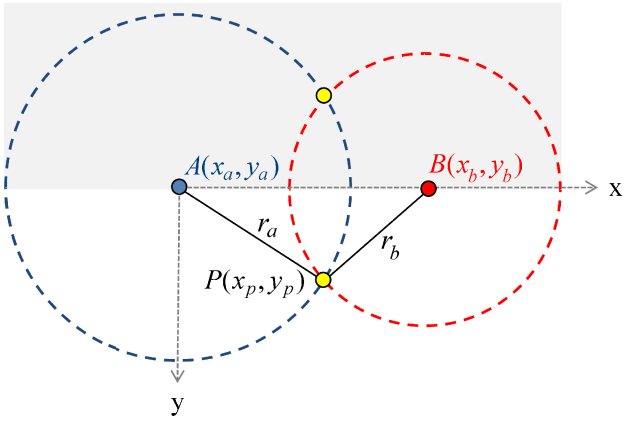


Figure 2.8. 2D trilateration with two references

Although four references are needed in order to compute three dimensional (3D) position of an object using trilateration, three references can also be sufficient in the case of one that the solutions is out of the solution region.

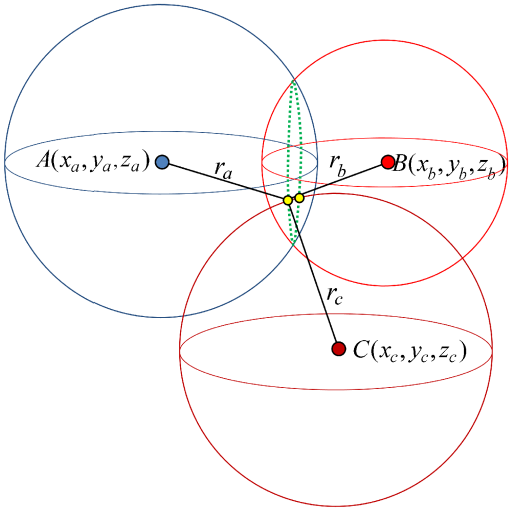


Figure 2.9. 3D trilateration

The intersection of two spheres composes a circle and the intersection of that circle with another sphere brings out two points as solution. In short, intersection of three spheres brings out two points as solution, as it is seen in Figure 2.9. Assuming the coordinates as $A$=(0,0,0), $B$=($x_b$,0,0) and $C$=($x_c$,$y_c$,0) simplifies the computation. This simplified planar representation is shown in Figure 2.10.

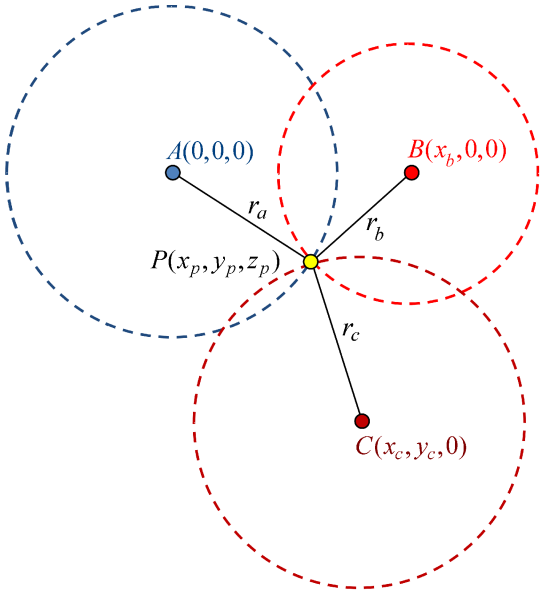


Figure 2.10. 3D trilateration with three references

The equation of the three spheres with the centers $A$, $B$ and $C$ can be written as

$$\begin{aligned} x_p^{\,2} + y_p^{\,2} + z_p^{\,2} &= r_a^2 \\ (x_p - x_b)^2 + y_p^{\,2} + z_p^{\,2} &= r_b^2 \\ (x_p - x_c)^2 + (y_p - y_c)^2 + z_p^{\,2} &= r_c^2 \end{aligned} \tag{2.9}$$

where $r_a$, $r_b$ and $r_c$ denote the respective radii. The coordinates $x_p$ and $y_p$ are found as in the equation (2.10) and equation (2.11) respectively;

$$x_p = \frac{x_b^2 + r_a^2 - r_b^2}{2x_b}, \tag{2.10}$$

$$y_p = \frac{x_c^2 + y_c^2 + r_a^2 - r_c^2 - 2x_p x_c}{2y_c}. \tag{2.11}$$

Note that, these two equations have exactly the same form as their 2D trilateration counterparts, namely the equations (2.6) and (2.7) respectively, due to the chosen zero $z$-coordinate of the center points $A$ and $B$. Then, the $z$-coordinate of the node, $P$, is found as

$$z_p = \mp\sqrt{r_a^2 - x_p^{\,2} - y_p^{\,2}}. \tag{2.12}$$

As it is seen from the Equation (2.12), the computation gives two solutions in $z$ coordinate. One of them is positive and the other one is negative. Choosing the right solution, the coordinates of the object can be found. Additionally, it is also possible to make a coordinate system transformation. Hence, first the three points are transformed into $A$=(0,0,0), $B$=($x_b$,0,0) and $C$($x_c$,$y_c$,0), after computation the results can be transformed to the real coordinate system.

In the proposed system, trilateration is performed by taking four ToA distance measurements to localize the microphones. The procedure is handled comprehensively in Chapter 4.

### 2.3.4.2. Multilateration

Multilateration computes the location of a node in $n$-dimensional space by measuring relative distances from $n$ references to a $(n+1)^{th}$ points to that node. TDoA measurements are applied in order to calculate the relative distances. Shortly, a receiver can be located by measuring the TDoA of signals transmitted from three or more synchronized transmitters. Multilateration differs from trilateration, since multilateration uses relative distances, while trilateration uses absolute measurements of distance. At least four references are needed to perform multilateration, since relative distances are measured with respect to one of the references. Hence, three equations can be obtained when there are four reference points.

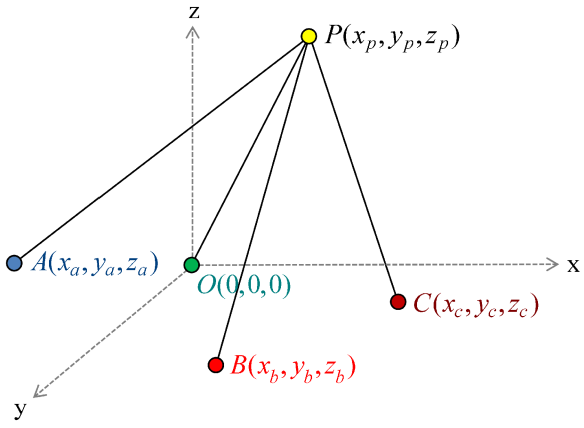


Figure 2.11. 3D multilateration with four references

In Figure 2.11, four reference nodes, $A(x_a,y_a,z_a)$, $B(x_b,y_b,z_b)$, $C(x_c,y_c,z_c)$ and $O(0,0,0)$ which is located in the origin of the coordinate system and unknown node $P=(x_p,y_p,z_p)$ are shown.

The time of flights from reference nodes $A$, $B$, $C$ and $O$ are given as

$$\begin{aligned} t_A &= \frac{1}{v}\sqrt{(x_p-x_a)^2+(y_p-y_a)^2+(z_p-z_a)^2}, \\ t_B &= \frac{1}{v}\sqrt{(x_p-x_b)^2+(y_p-y_b)^2+(z_p-z_b)^2}, \\ t_C &= \frac{1}{v}\sqrt{(x_p-x_c)^2+(y_p-y_c)^2+(z_p-z_c)^2}, \\ t_O &= \frac{1}{v}\sqrt{x_p{}^2+y_p{}^2+z_p{}^2} \end{aligned} \tag{2.13}$$

respectively, where $v$ denotes the velocity. The differences of time of flight give TDoA which are given in the form:

$$\begin{aligned} \tau_A &= t_A - t_O = \frac{1}{v}\left(\sqrt{(x_p-x_a)^2+(y_p-y_a)^2+(z_p-z_a)^2}-\sqrt{x_p{}^2+y_p{}^2+z_p{}^2}\right), \\ \tau_B &= t_B - t_O = \frac{1}{v}\left(\sqrt{(x_p-x_b)^2+(y_p-y_b)^2+(z_p-z_b)^2}-\sqrt{x_p{}^2+y_p{}^2+z_p{}^2}\right), \\ \tau_C &= t_C - t_O = \frac{1}{v}\left(\sqrt{(x_p-x_c)^2+(y_p-y_c)^2+(z_p-z_c)^2}-\sqrt{x_p{}^2+y_p{}^2+z_p{}^2}\right). \end{aligned} \tag{2.14}$$

The Equations (2.14) are hyperboloid equations, and the solution of these three equations gives $x$, $y$ and $z$ coordinates of the unknown object.

Multilateration can be applied when there is no synchronization between transmitters and receiver. Therefore, it is preferred by many location systems. But it must be kept in mind that the transmitters must be synchronized among each other in order to find the time differences.

### 2.3.4.3. Triangulation

Triangulation computes the location of a node in *n*-dimensional space by measuring one distance and *n* angles. While the distance can be measured by using either ToF or RSSI measurements, the angles are measured by using AoA measurements. Phased antenna arrays and multiple antennas with known separation that measure time difference are used to measure the angle. 2D triangulation requires one length measurement and two angle measurements. On the other hand, 3D triangulation requires one length measurement, one azimuth measurement and two angle measurements in order to localize an object.

### 2.3.4.4. Multidimensional Scaling (MDS)

Multidimensional Scaling (MDS) is a set of data analysis techniques. It determines relative locations of the object in *n*-dimensional space from the data that approximate the distances between pairs of the objects. This technique is commonly used for ad-hoc location system of sensor networks. Distances needed for MDS can be calculated using one of these measurement techniques; ToF, RSSI or connectivity information. There are many types of MDS techniques. The usually applied ones are classical MDS, metric MDS, non-metric MDS, weighted MDS and generalized MDS.

### 2.3.4.5. Fingerprinting

SS measurement does not always give expected results as in the theoretical strength-distance relation since it suffers form the effects multipath, reflection, shadowing, fading and mobility in environment. In order to handle this challenge, fingerprint technique is implemented. Fingerprint technique consists of two separate phases. During the first phase, called offline (training) phase, SS of radio signals that are emitted from different transmitters are measured at various predefined locations throughout the deployment area. The SS values are recorded into LLT and a radio map of deployment area is created. During the next phase, called online (real-time) phase, currently measured SS values at an unknown location are compared with the SS values in the LLT. Thereby the unknown location can be estimated by matching measured SS

values with the most suitable SS values in the LLT. For instance, RADAR implements fingerprint technique and it constructs an LLT.

Fingerprint technique can increase the accuracy of a location system, however the time consuming and tedious process for constructing an LLT and the need of reconstruction of LLT due to the environmental changes are significant drawbacks of the technique.

### 2.3.4.6. Scene Analysis

Scene Analysis location estimation technique depends on scene observation from a particular point and draws conclusions about the location of the observer or relative location of the object in that scene. There are two types of scene analysis; static and differential. In static scene analysis, observed features are looked up in a predefined LLT that maps observed features to a location. This analysis requires a previous scene analysis in order to construct an LLT. On the other hand, differential scene analysis estimates the location from the movement detection between consecutive frames. While the difference between scenes in consecutive frames gives information about location of the observer, the difference in objects in consecutive frames gives information about objects locations. Scene analysis location estimation technique does not require any measurements of angle or distance and provides passive localization. The drawbacks are requirement of expensive computation devices and expensive vision devices like camera, computational difficulty and changing LLT with respect to changing environment.

### 2.3.4.7. Proximity

Proximity is based on closeness information of an object to a certain object with known location. Connectivity information is needed to derive the location of that object. Using proximity, just coarse-grained localization can be achieved. There are three general approaches to sensing the proximity: detecting physical contact, monitoring roaming and observing automatic Identification (ID) systems (Hightower and Borriello 2001).

Detecting physical contact is the most basic method of sensing proximity. Pressure sensors, touch sensors and capacitive field detectors are used for detecting physical contact.

Monitoring roaming is based on sensing if an object is in the range of one or more transducers or not. For example, Active Badge location system uses active badges that emit IR signals in order to sense in which room they are. As another example, LANDMARC system uses connectivity information that is gathered from different transmitters and localizes the receiver.

Observing automatic ID systems also provides location information. Credit card point-of-sale terminals, electronic card lock logs and identification tags are worked with observing automatic ID principle. If the locations of these systems are known, then the location of the object can be determined.

### 2.3.5. Structure

Localization diverges as centralized or decentralized localization according to its structure.

#### 2.3.5.1. Centralized Localization

In centralized localization, a central unit controls the other components that constitute the location system. The entire computation take place in that central unit. The location information can either be monitored in that unit or sent to subscribers if there is a demand. Centralized localization provides ease in computation, but it can be faced with deployment problem. Active Badge, BAT, RADAR, Dolphin, 3D-LOCUS systems and in addition to them the proposed system are centralized location systems.

### 2.3.5.2. Decentralized Localization

In decentralized localization, there is no central unit as in centralized localization. The computations are performed separately. The decentralized structure provides ease of deployment but requires more infrastructures to perform computation separately. Especially, decentralized localization is preferred for outdoor applications and AHL. Crickets, SpotON, SmartLOCUS system are examples of indoor decentralized localization.

## 2.3.6. Usage

Location systems are divided as privacy-oriented or public-oriented location systems according to their usage.

### 2.3.6.1. Privacy-Oriented Localization

Privacy concern is an important issue for localization that has to be missed out by producers of location systems. For some reasons, users do not want others to know their location. For instance, in an enterprise employees do not want their employer knows their location every time. This occasion may put pressure on employees and they may feel uncomfortable. This issue is handled in Active Badge (Want, et al. 1992) and Cricket (Priyantha, et al. 2000) systems. The privacy-oriented localization requires decentralized and self computing system structure. Since there is always a probability that someone gets the location information of the user in centralized location system. Regardless, the user can broadcast its location information if he or she wants to. Cricket system and GPS are examples for privacy-oriented system.

### 2.3.6.2. Public-Oriented Localization

Public-oriented localization is discussed when there is no privacy concern. The location information can be known by center or shared with the users who want to know that information. Most of the location systems are public-oriented.

# CHAPTER 3

# SPREAD SPECTRUM

This chapter gives information about spread spectrum concept, code division multiple access and spreading codes, respectively.

## 3.1. Introduction

Spread spectrum is a technique which is firstly used in military communications starting from 1970's. Nowadays, spread spectrum is used in public domain. The most remarkable spread spectrum applications are in digital communication. The third generation mobile telephone system, shortly 3G, is based on spread spectrum communication. Although it is not known by majority, spread spectrum is used to obtain accurate time measurements and velocity measurements for a long time other than digital communication. GPS uses Direct Sequence Spread Spectrum (DSSS) technique in order to get precise ToF measurement. In addition to GPS, Dolphin, 3D-LOCUS and the proposed location system also use this technique. Therefore, spread spectrum concept and techniques, Code Division Multiple Access (CDMA) and spreading code will be explained in this section.

## 3.2. Spread Spectrum Concept

Narrowband systems work with the idea of transmitting as much as possible data in a narrow frequency band. In contrast, spread spectrum systems utilize a much wider frequency band with respect to narrowband systems. A spread spectrum system expands the bandwidth of the signal, $W$ in Hz, while its data rate $R$ in bits/s, remains constant. This process spreads the energy of the signal over a wide bandwidth and reduces the Power Spectral Density (PSD) of that signal possibly below the noise level. At the aimed receiver, the narrowband signal is reproduced by despreading the spread signal power where the uncorrelated noise and other interference are not affected. Figure 3.1 shows how spreading bandwidth overcomes the narrowband interference.

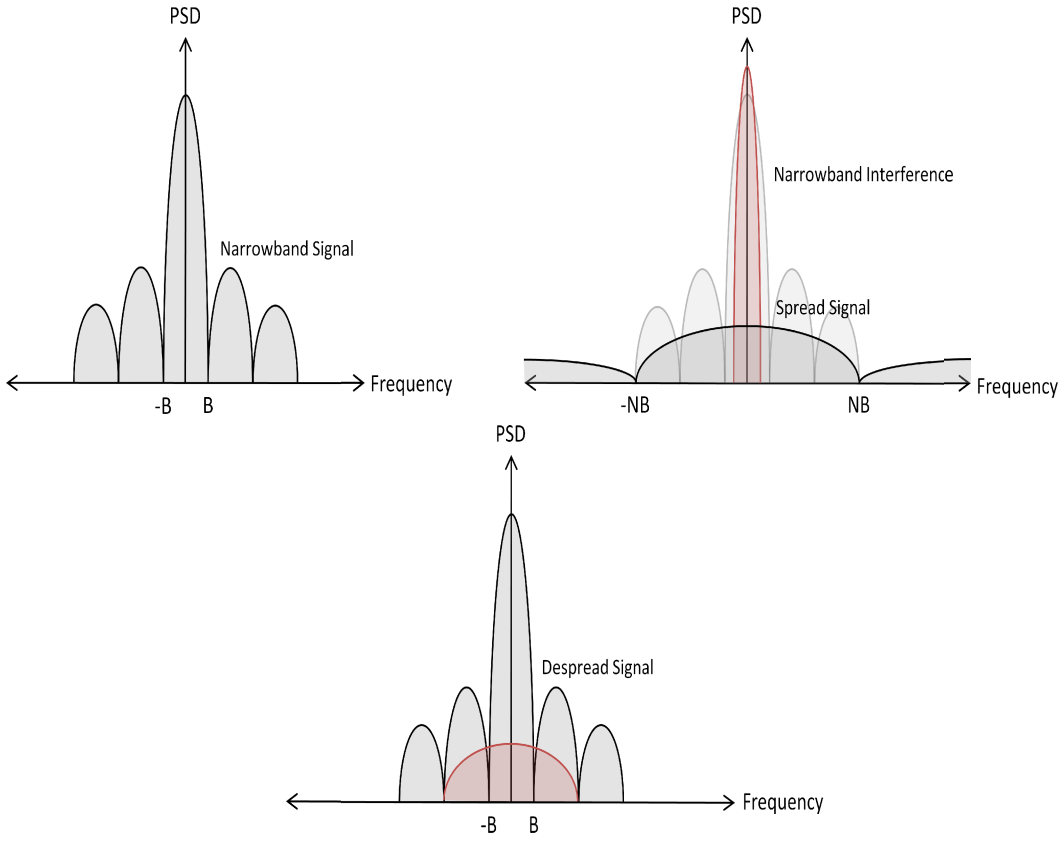


Figure 3.1. Spread and despread bandwidth of narrowband signal

$N$ denotes the bandwidth expansion factor and can be found from

$$B_e = N = \frac{W}{R}. \tag{3.1}$$

This spreading process is realized by applying spread spectrum techniques that are used for

- Combating with intentional interference due to jamming,
- Suppressing the effect of interference arising from other users,
- Suppressing the effect of self-interference caused from multipath propagation,
- Coding the signal in order to ensure its privacy,
- Making the signal undetectable to unintended listeners by transmitting it at low power.

The best way of expanding a signal bandwidth is coding. Coding extends the number of bits in a data sequence. In order to maintain the input data rate, the transmitted data rate has to be increased. Consequently, increase in the transmitted data rate requires an expansion in bandwidth. In spread spectrum, a special code called pseudo-random or pseudo-noise (PN) code (sequence) is used for that purpose. PN code is a binary sequence that has

- Nearly equal number of zero and ones,
- Low correlation between shifted versions of itself,
- Low cross-correlation with the other sequences,
- High auto-correlation in synchronization.

The spread spectrum system can be generally modeled as in Figure 3.2. Firstly, binary input data sequence is encoded. After encoding process, the encoded data sequence is modulated with Phase Shift Keying (PSK) or Frequency Shift Keying (FSK) using the PN code generated in the PN code generator. Then the modulated signal passes through the channel and it is demodulated with the same PN code generated in PN code generator of the receiver. Finally, demodulated signal is decoded and binary output data is attained. The important issue that should not be missed out is the requirement of synchronization between generated PN codes. If synchronization can not be provided, the demodulation does not occur.

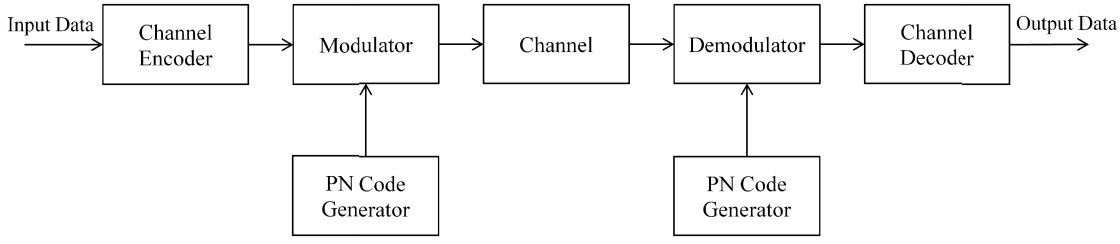


Figure 3.2. Spread spectrum system model

There are three distinct spread spectrum techniques: Direct Sequence Spread Spectrum (DSSS), Frequency Hopping Spread Spectrum (FHSS) and Time Hopping (TH). These spread spectrum techniques are treated in the following subsections.

### 3.2.1. Direct Sequence Spread Spectrum (DSSS)

Direct Sequence Spread Spectrum (DSSS) technique is commonly used in commercial applications. Especially in digital communication, DSSS technique provides various advantages to the user. Binary Phase Shift Keying (BPSK) and *M*-ary Phase Shift Keying modulations are applied to shift the phase of the carrier pseudorandomly by using PN codes in DSSS technique. In BPSK modulated DSSS, binary data sequence is enhanced by multiplying each bit with predetermined PN code that has a higher chip rate $R_c$ bits/s than binary data sequence has. This procedure can be modeled in Figure 3.3 and Figure 3.5.

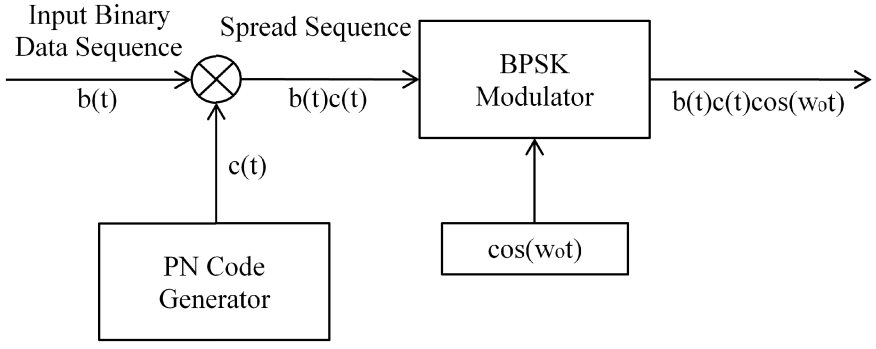


Figure 3.3. Block diagram of BPSK modulated DSSS transmitter

At transmitter, bits in data sequence and chips in PN sequence generated by PN code generator are converted into bipolar form before multiplication. This means that bits and chips consisting of {1,0} are mapped to {1,−1} respectively. Alternatively, summation in modulo 2 can be implemented without converting the data to bipolar form. The multiplication of these two bipolar sequences constitutes a new sequence called Spread Sequence that has the same chip rate as the PN sequence. Eventually, the spread sequence is modulated with BPSK modulation.

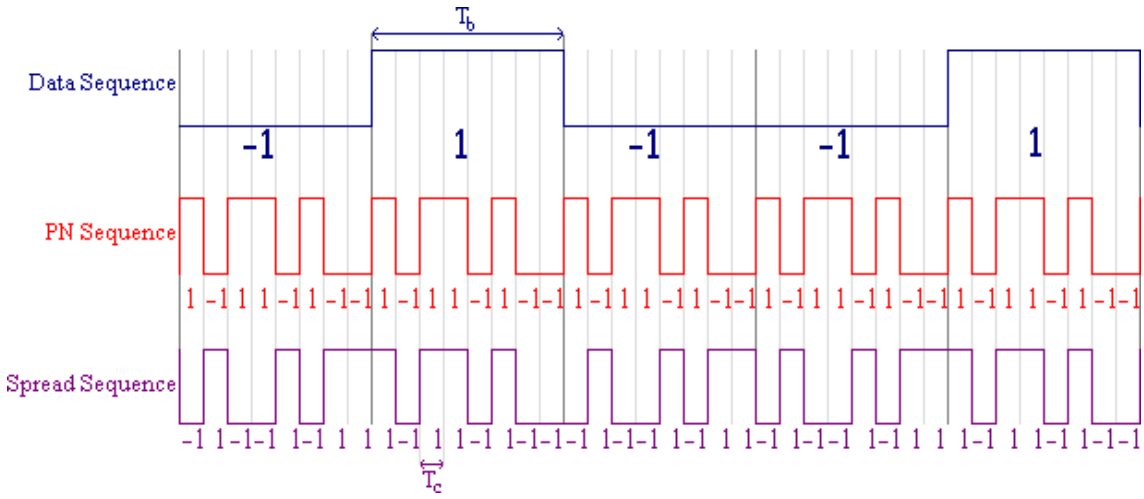


Figure 3.4. Data Sequence, PN Sequence and Spread Sequence in baseband

The process of obtaining the spread sequence is illustrated in Figure 3.4. The duration for transmitting each bit in data sequence is denoted as $T_b$ and the duration for transmitting each chip in PN sequence, called chip interval, is denoted as $T_c$, as they are shown in the figure. It is possible to find the bandwidth expansion factor, or spreading factor, by using Equation (3.2)

$$B_e = \frac{T_b}{T_c} \tag{3.2}$$

where $B_e$ must be an integer.

At the receiver, the received signal is multiplied with the same PN sequence again for despreading. After BPSK demodulation the binary data sequence is reconstructed. Figure 3.5 illustrates the block diagram of the receiver.

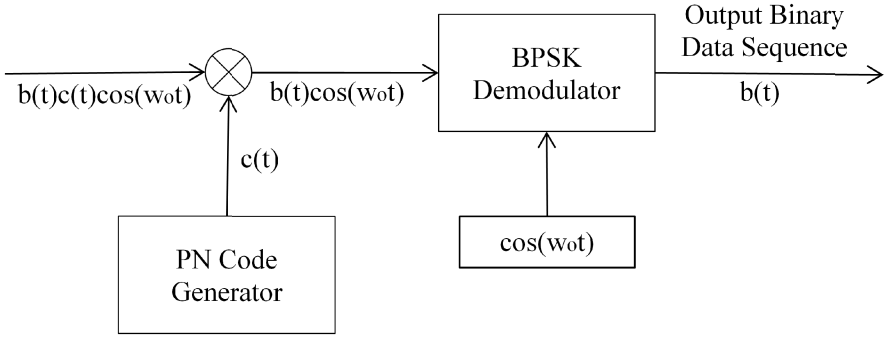


Figure 3.5. Block diagram of BPSK modulated DSSS receiver

Some DSSS systems use a short code, whereas the others use a long code. Short code systems use a PN sequence for each data bit, while long code systems use a PN sequence for more than one data bits.

### 3.2.2. Frequency Hoping Spread Spectrum (FHSS)

Frequency Hoping Spread Spectrum (FHSS) technique is especially used for military applications, since frequency hoping assures signal privacy from unintended listeners and provides freedom in communication to the user. As a distinction from DSSS technique, FHSS technique divides the available channel bandwidth into *N* subchannels (frequency slots) and hops between these subchannels according to a PN sequence while transmitting data. FHSS technique uses FSK modulation to shift the carrier of data signal pseudorandomly. The modulation frequency is determined with respect to PN sequence and data signal is modulated with that frequency in each time interval. Figure 3.6 illustrates an example of data transmission in FHSS.

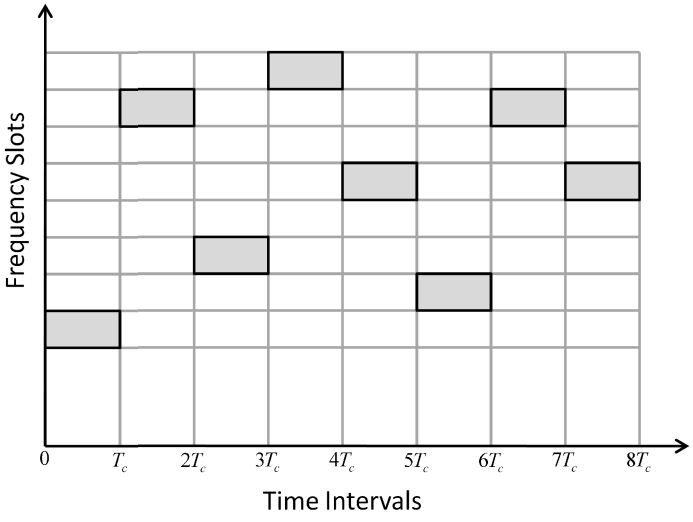


Figure 3.6. FHSS with one symbol in each interval

The occupied channel bandwidth for transmission is related to the number and the bandwidth of the subchannels. But it should not be missed out that it has to be equal or less than the available bandwidth.

FHSS signal is a narrowband signal and does not occupy the whole bandwidth as the DSSS signal does. It occupies only a subchannel in a time, but it spreads to the whole bandwidth by frequency hopping.

Figure 3.7 and 3.8 illustrate block diagrams of FHSS transmitter and FHSS receiver, respectively.

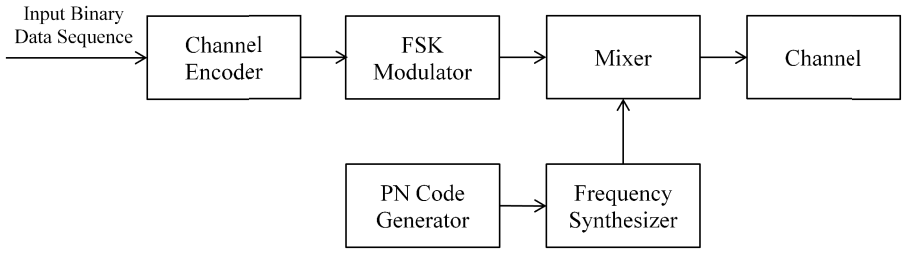


Figure 3.7. Block diagram of FHSS transmitter

At the transmitter, PN code generator generates a PN sequence that determines the output of the frequency synthesizer. FSK modulated data signal is combined with the output of the frequency synthesizer at the mixer and then the combined data signal is transmitted through channel.

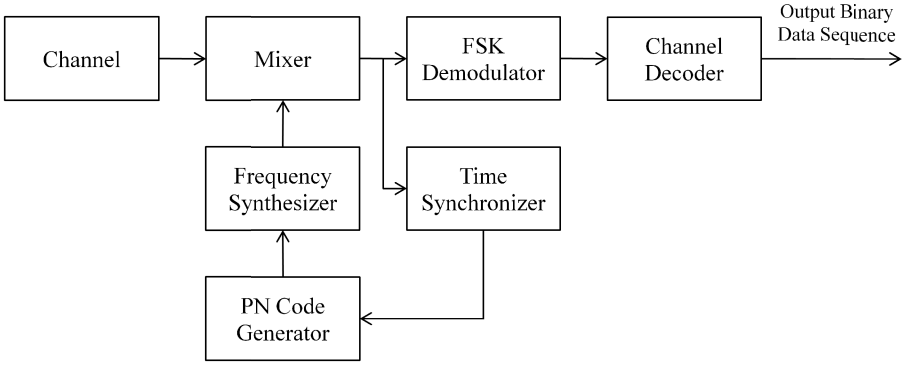


Figure 3.8. Block diagram of FHSS receiver

At the receiver, a PN code generator is used to control the frequency synthesizer which is synchronized with received signal. The received signal is combined with the output of the synthesizer again and eventually the output is demodulated by means of FSK modulator.

FHSS techniques can be divided into two according to their hopping rate. If the hopping rate is higher than the symbol rate, one speaks of Fast Frequency Hopping (FFH) and contrarily if the hopping rate is equal to or lower than the symbol rate, one speaks of Slow Frequency Hopping (SFH).

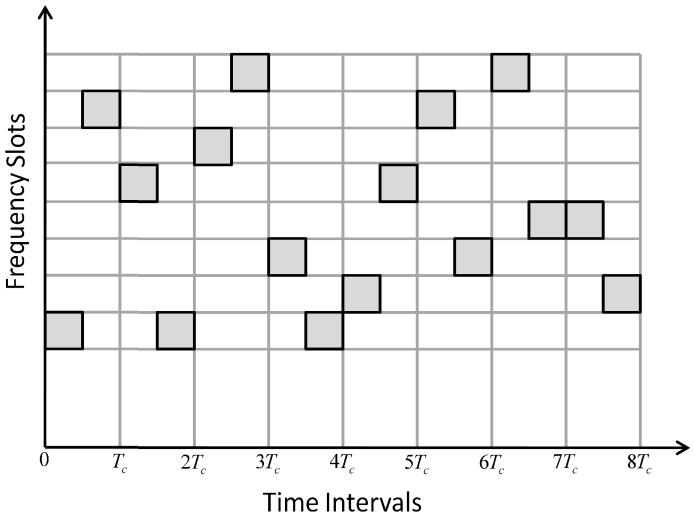


Figure 3.9. Fast Frequency Hopping (FFH)

In FFH, carrier frequency changes during the transmission of a symbol so that there are multiple hops per symbol, as shown in Figure 3.9.

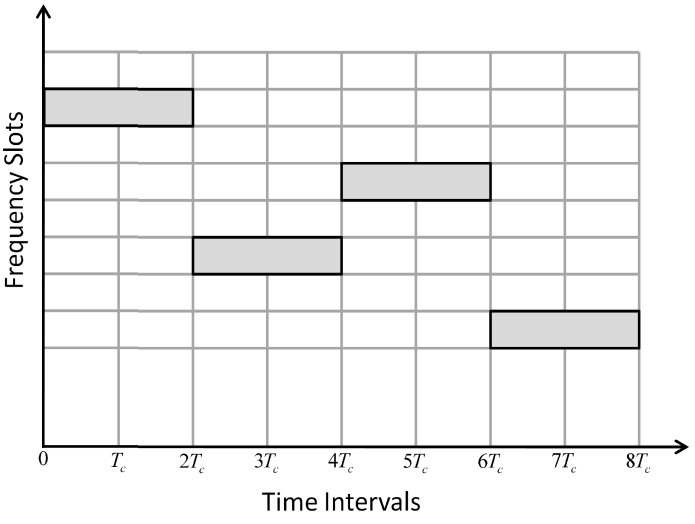


Figure 3.10. Slow Frequency Hopping (SFH)

On the other hand, one or more symbols are transmitted in a hop interval in SFH, as shown in Figure 3.10.

### 3.2.3. Time Hoping (TH)

In Time Hoping (TH) technique data signal is transmitted in bursts at pseudorandomly assigned time intervals. Time is divided into frames, which is selected to be larger than the reciprocal of the data rate and each frame is divided into *M* time slots. During each frame data signal is transmitted from one of the *M* time slots that is assigned by using the PN sequence. Shortly, TH uses whole frequency bandwidth but just a time slot, while data signal is transmitted. Figure 3.11 illustrates data signal transmission of TH with respect to frequency and time.

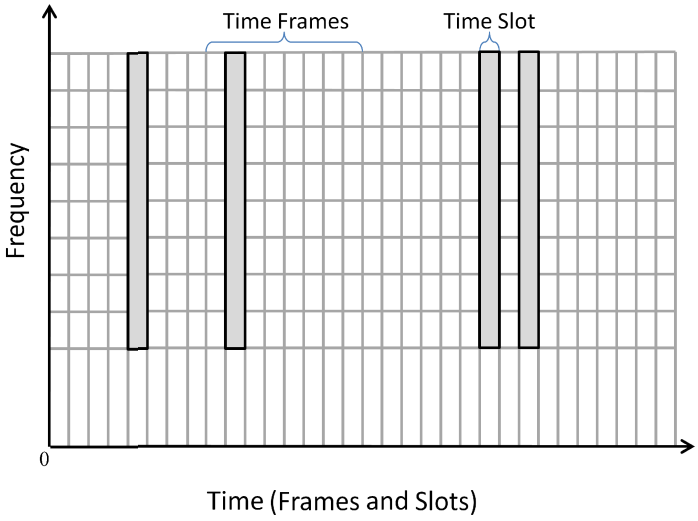


Figure 3.11. Time Hoping (TH)

In addition to all these spread spectrum techniques, combinations of these techniques can also be implemented. By the way, the specific advantages of each technique can be combined in one.

## 3.3. Code Division Multiple Access (CDMA)

Multiple access is used to share a common channel with a number of users. There are several different methods for multiple access. One simple method is to divide time into frames and subdivide the frames into time slots in which only particular user can transmit data. This multiple access method is called Time Division Multiple Access (TDMA). Another method is to subdivide the available channel bandwidth into

subchannels where only particular user occupies that frequency band. This multiple access method is called Frequency Division Multiple Access (FDMA). These two methods may be inefficient in cases where the frequency slots or time slots are assigned to users which do not send or receive data. The third multiple access method overcomes this challenge. Code Division Multiple Access (CDMA) or Spread Spectrum Multiple Access (SSMA) is a multiple access method where different users share the same frequency band at the same time. In this method, each user has a unique code that allows the user to spread the data signal.

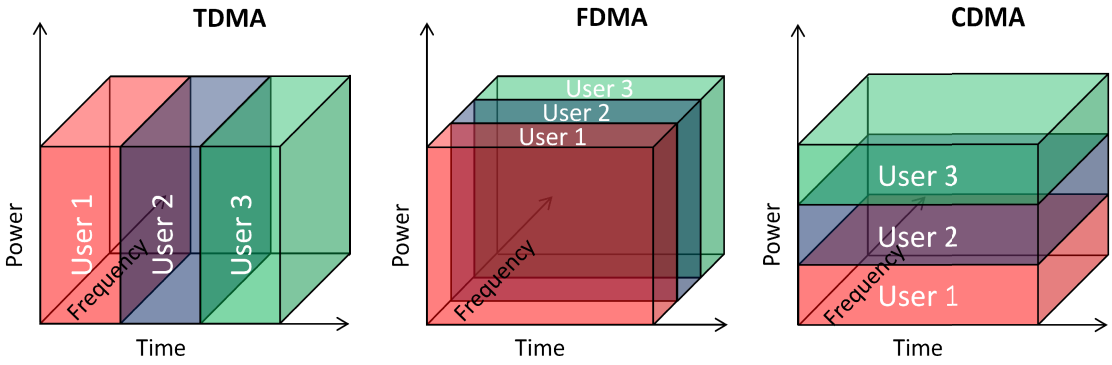


Figure 3.12. TDMA, FDMA and CDMA

CDMA uses spread spectrum techniques for data transmission. There are several types of CDMA which differ in the spreading technique utilized such as Direct Sequence CDMA (DS-CDMA), Frequency Hopping CDMA (FH-CDMA) and Time Hoping CDMA (TH-CDMA).

Figure 3.13 illustrates how data transmission is realized in DS-CDMA. Assume that there are two users sharing the same medium, i.e., the same frequency band at the same time. Data signals for both users are spread to the frequency band by using unique codes and they are transmitted through the channel. Finally each data signal is reconstructed separately by despreading the desired data signal using its unique code at the receiver.

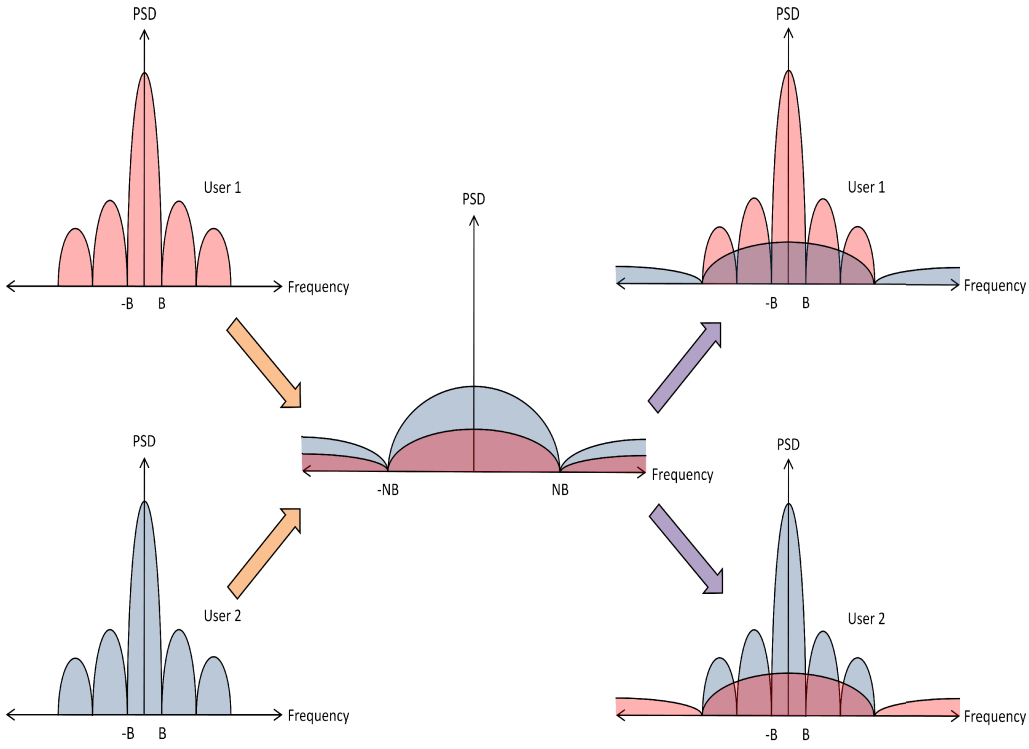


Figure 3.13. DS-CDMA

CDMA can be realized in two ways, synchronously or asynchronously. In synchronous CDMA, data signals of different users are transmitted simultaneously, so that there is no time shift between users in received data at the receiver. Thus orthogonal codes are used for synchronous CDMA, since they have zero cross-correlation while there is no offset between them. An example of synchronous DS-CDMA in baseband is illustrated in Figure 3.14.

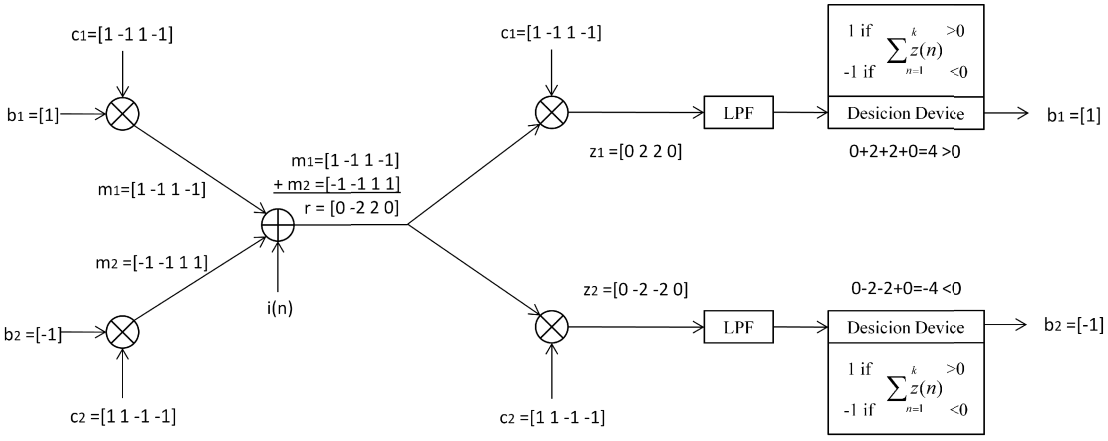


Figure 3.14. An example of synchronous DS-CDMA in baseband

In this example, the channel effects are neglected. $b(n)$ denotes a bipolar data sequence, while $c(n)$ denotes a bipolar code taken from an orthogonal code set. After multiplication of bipolar data sequence and bipolar orthogonal code of both users, the generated data signals are transmitted over the same channel. At the receiver, the incoming signal is multiplied with each user's orthogonal code. Later the outcome passes through a Low Pass Filter (LPF). Finally the output of the LPF is imported into a decision device where the sequence is summed and decides if it is 1 or −1. So, the bipolar output is determined.

In asynchronous CDMA, the data signals of different users are transmitted at arbitrary starting times, thus there is no synchronization between codes. In this case PN codes (sequences) are used since they have very low correlation between any two shifted versions of the same sequence and low cross-correlation between any two sequences. The spreading will be explained in detail in the following subsection.

CDMA encounters some challenges that affect its performance. Multiple Access Interference (MAI) is one them which denotes the interference from the other users sharing the same channel. To overcome MAI, the number of users must be kept below a level or longer codes must be used.

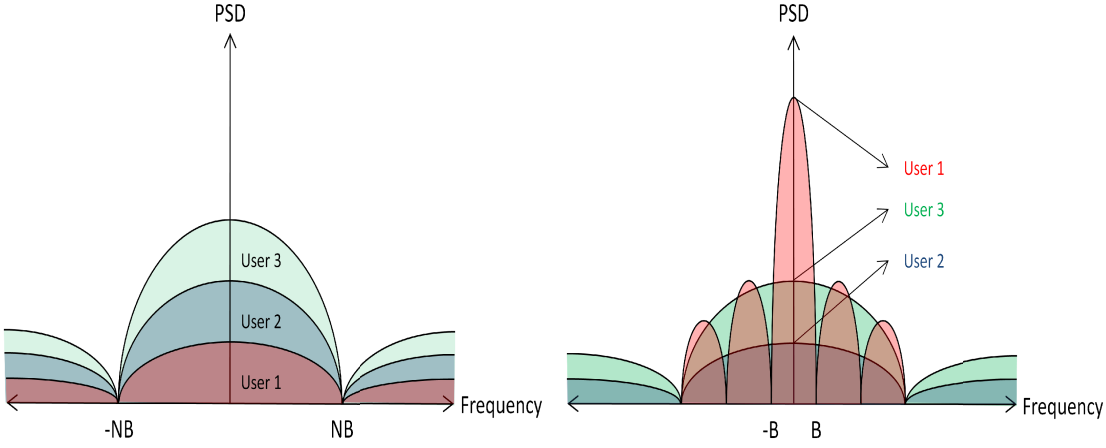


Figure 3.15. MAI

Another difficulty related to CDMA is near-far effect. The data signals transmitted from different transmitters reach to the receiver with different powers. A data signal transmitted from a close transmitter has much more power than a data signal transmitted from a far transmitter. As a result, the data signal with more power may

mask the data signal with low power. This is called near-far effect. Power control is implemented to overcome this challenge. Figure 3.16 illustrates near-far effect and power of received signals with or without power control.

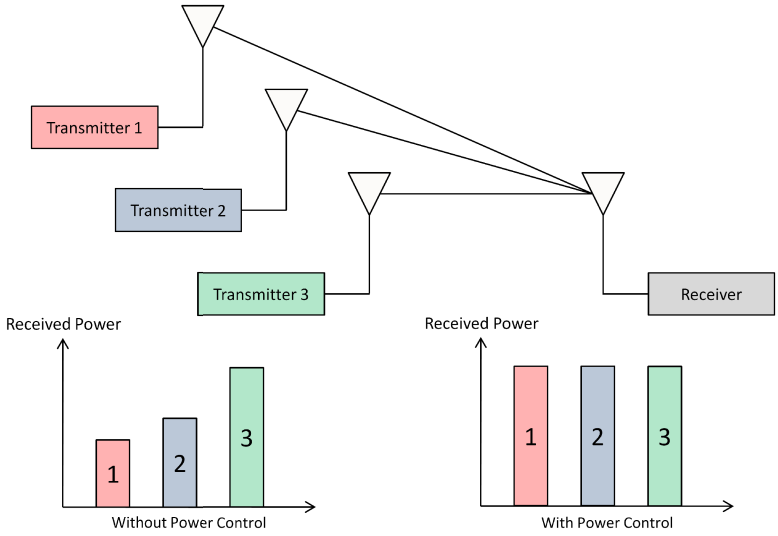


Figure 3.16. Near-far effect

The third challenge is multipath propagation. In multipath propagation, the transmitted signal arrives to the receiver through more than one path. This causes time shifts and different levels of attenuation because of the difference in propagation distances. Thus, several replicas of the transmitted signal are received each with a different time shift and power. In order to overcome this challenge shifted correlators' outputs are combined in the receiver. This type of a receiver is called a rake receiver.

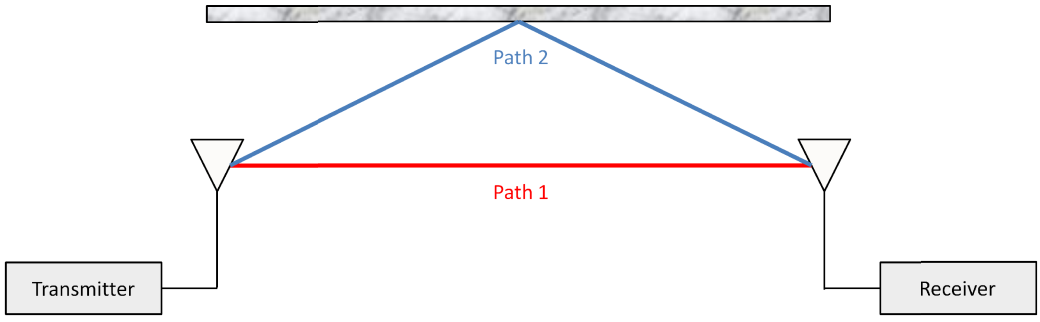


Figure 3.17. Multipath propagation

Attenuation (fading), that can be referred as diminishing of SS with respect to distance, and shadowing, which can be referred as diminishing of SS caused by obstacles, also pose problems in CDMA.

## 3.4. Spreading Codes

Spreading codes or spreading sequences are very crucial in spread spectrum. As mentioned before they are used for spreading process in spread spectrum techniques. The spreading sequences can be classified as orthogonal sequences and pseudo-random or pseudo-noise (PN) sequences according to their auto-correlation and cross-correlation properties.

Auto-correlation function can be defined as the scalar product of a code with its shifted copy. It can be expressed as below

$$R_{xx}(k) = \sum_{n=1}^{N} x_n x_{n+k} \tag{3.2}$$

and can be normalized as

$$R_{xx}(k) = \frac{1}{N} \sum_{n=1}^{N} x_n x_{n+k} \tag{3.3}$$

where $x_n$, $k$ and $N$ denote the $n^{th}$ code-bit, the amount of shift and the length of the code, respectively. It is desired that, the auto-correlation function is zero or at least approximately zero in the case of non-synchronization. Auto-correlation property is especially required in location systems for an exact determination of propagation time. Besides that, it is also very useful in communication for separating the multipath in order to avoid interference.

Cross-correlation function can be defined as the scalar product of a code with a shifted version of another code. It can be expressed as below

$$R_{xy}(k) = \sum_{n=1}^{N} x_n y_{n+k} \tag{3.4}$$

and can be normalized as

$$R_{xy}(k) = \frac{1}{N} \sum_{n=1}^{N} x_n y_{n+k} \tag{3.5}$$

where $x_n$, $y_{n+k,}$ and $N$ denote the $n^{th}$ code-bit of $x$, the $(n+k)^{th}$ code-bit of $y$, the amount of shift and the length of the code, respectively. For a good cross-correlation, the cross-correlation function should be also zero or approximately to zero. Cross-correlation is important in order to separate the signal of the desired user in communication.

Spreading codes are treated in two categories as in the figure below.

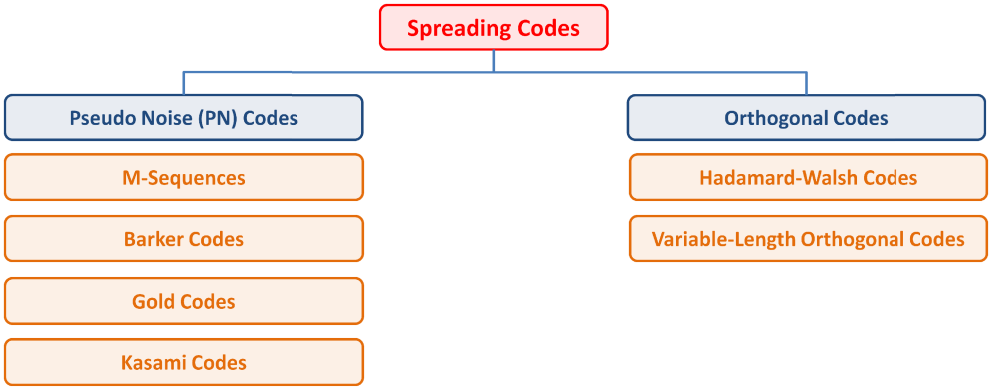


Figure 3.18. Classification of spreading codes

Orthogonal sequences are used for synchronous CDMA, since their cross-correlation is zero in synchronization, so that MAI does not affect the user. On the other hand, PN sequences are used for asynchronous CDMA since they have low cross-correlation even in case of non-synchronization.

### 3.4.1. Pseudo Noise (PN) Codes

Pseudo-Random sequence or PN sequence is a periodic binary sequence whose each period consists of a set of code that has low autocorrelation with its shifted copies (shows auto-correlation property similar to white noise) and has low cross-correlation with sets of codes at other periods. PN sequences are not random, they are deterministic, and however they look as if they are random. The selection of the code is effective on system capability, since the performance varies with the type and length of the code. PN codes with a longer period results in a higher spreading factor which in turn give much better results.

### 3.4.1.1. M-Sequences

Maximum-Length sequence or shortly *m*-sequence is generated by an *m*-stage shift register with linear feedback. The sequence has a length of $N=2^m-1$ and consists of $2^{m-1}$ ones and $2^{m-1}-1$ zeros. It is periodic with *N*.

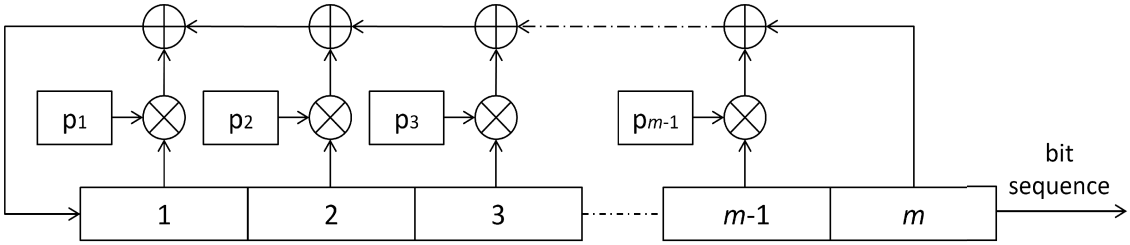


Figure 3.19. *m*-sequence generator

An *m*-sequence generator can be modeled as in Figure 3.19. The $p_i$ where $i=\{1,2,3,\ldots,m-1\}$ are assigned 1 or 0 according to the feedback polynomial,

$$P(x) = 1 + p_1 x + p_2 x^2 + ..... + p_{m-1} x^{m-1} + x^m \tag{3.6}$$

There is a short notation for polynomials. For instance, the feedback polynomial, $P(x)=1+x+x^3+x^5$ can be described with as [5,3,1] and can be modeled as below.

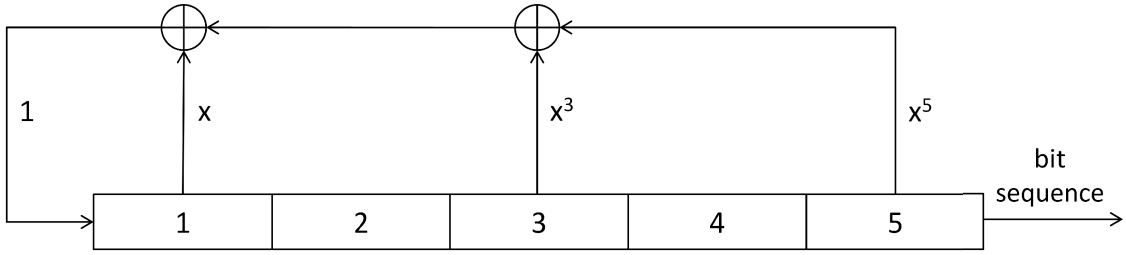


Figure 3.20. *m*-sequence generator model for $P(x)=1+x+x^3+x^5$

The generated *m*-sequence is determined by mainly three factors that are the length, *m*, and the initial state of the shift register and the feedback polynomial. The zero state is not allowed, and the length of the sequence or in other words the period, *N*, can not exceed $2^m-1$.

The periodic auto-correlation of an *m*-sequence is

$$R_{xx}(k) = \begin{Bmatrix} N & (k=0) \\ -1 & (1 \le k \le n\text{-}1) \end{Bmatrix} \tag{3.7}$$

and it is normalized as

$$R_{xx}(k) = \begin{Bmatrix} 1 & (k=0) \\ -1/N & (1 \le k \le n\text{-}1) \end{Bmatrix} \tag{3.8}$$

where

$$R_{xx}(k+rN) = R_{xx}(k) \tag{3.9}$$

and $r$ is an integer. Also, cross-correlation is not as well-behaved as autocorrelation. It varies with each *m*-sequence; however peak cross-correlation values can be determined.

Table 3.1. *m*-sequence

| *m* | *N* | Number of *m*-sequences | Peak cross correlation | Normalized peak cross correlation | Feedback polynomials |
|---|---|---|---|---|---|
| 3 | 7 | 2 | 5 | 0.71 | [3,1] |
| 4 | 15 | 2 | 9 | 0.60 | [4,1] |
| 5 | 31 | 6 | 11 | 0.35 | [5,3] [5,4,3,2] [5,4,2,1] |
| 6 | 63 | 6 | 23 | 0.36 | [6,1] [6,5,2,1] [6,5,3,2] |
| 7 | 127 | 18 | 41 | 0.32 | [7,1] [7,3] [7,3,2,1] [7,4,3,2] [7,6,4,2] [7,6,3,1] [7,6,5,2] [7,6,5,4,2,1] |
| 8 | 255 | 16 | 95 | 0.37 | [8,4,3,2] [8,6,5,3] [8,6,5,2] [8,5,3,1] [8,7,6,1] [8,7,6,5,2,1] [8,6,4,3,2,1] |
| 9 | 511 | 48 | 113 | 0.22 | [9,4] [9,6,4,3] [9,8,5,4] [9,8,4,1] [9,5,3,2] [9,8,6,5] [9,8,7,2] [9,6,5,4,2,1] [9,7,6,4,3,1] [9,8,7,6,5,3] |
| 10 | 1023 | 60 | 383 | 0.37 | [10,3] [10,8,3,2] [10,4,3,1] [10,8,5,1] [10,8,5,4] [10,9,4,1] [10,8,4,3] [10,5,3,2] [10,5,2,1] [10,9,4,2] [10,9,7,6,4,1] [10,7,6,4,2,1] [10,9,8,7,6,5,4,3] [10,8,7,6,5,4,3,1] |
| 11 | 2047 | 176 | 287 | 0.14 | [11,2] [11,8,5,2] [11,7,3,2] [11,5,3,2] [11,10,3,2] [11,6,5,1] [11,5,3,1] [11,9,4,1] [11,8,6,2] [11,9,8,3] [11,10,9,8,3,1] |

### 3.4.1.2. Barker Codes

Barker codes are finite length ($N=2^m-1$) sequences. They have maximum auto-correlation of 1 when they are not aligned. Table 3.2 illustrates Barker codes.

Table 3.2. Barker codes

| Length of code | Barker codes | |
|---|---|---|
| 2 | 1 −1 | 1 1 |
| 3 | 1 1 −1 | |
| 4 | 1 1 −1 1 | 1 1 1 −1 |
| 5 | 1 1 1 −1 1 | |
| 7 | 1 1 1 −1 −1 1 −1 | |
| 11 | 1 1 1 −1 −1 −1 1 −1 −1 1 −1 | |
| 13 | 1 1 1 1 1 −1 −1 1 1 −1 1 −1 1 | |

### 3.4.1.3. Gold Codes

Gold codes are generated by the combination of two *m*-stage shift registers with linear feedback. Therefore, two *m*-sequences with length $N=2^m-1$ are generated. Summation in modulo-2 of first *m*-sequence and the cyclically shifted versions of the second *m*-sequence constitute $2^m-1$ new sequences. The new sequences and two *m*-sequences constitute $2^m+1$ Gold codes with length $N=2^m-1$. Figure 3.21 illustrates the Gold code generator.

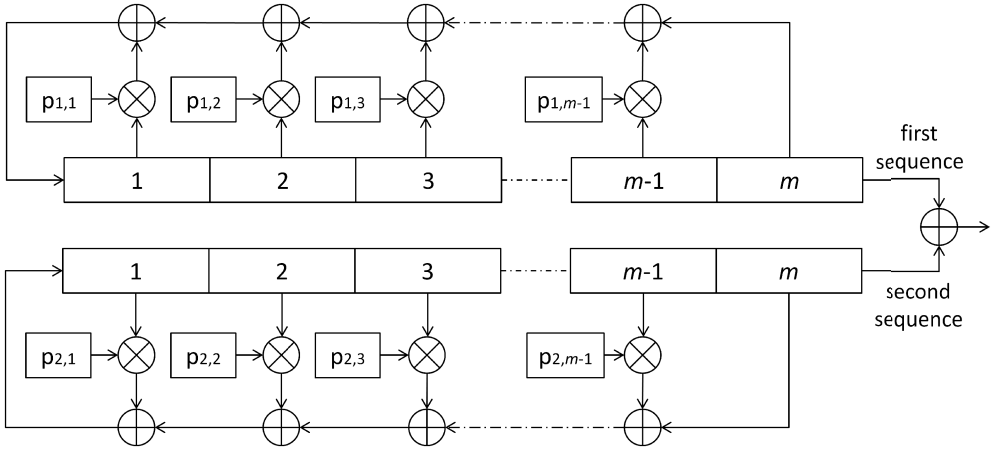


Figure 3.21. Gold code generator

The auto-correlation function of a Gold code is not two-valued as in the case of *m*-sequences. The cross-correlation functions and the off-peak autocorrelation function are three-valued $\{-1, -t(m), t(m)-2\}$, where

$$t(m) = \begin{Bmatrix} 2^{(m+1)/2}+1 & \text{when } m \text{ is odd} \\ 2^{(m+2)/2}+1 & \text{when } m \text{ is even} \end{Bmatrix}. \tag{3.10}$$

Preferred pairs of *m*-sequences are used in order to get three-valued cross-correlation and off-peak auto-correlation function. Table 3.3 illustrates these pairs.

Table 3.3. Gold codes

| *m* | *N* | Number of Gold codes | 3 values of correlation | | | Normalized peak correlation | Preferred pairs of *m*-sequences |
|---|---|---|---|---|---|---|---|
| 5 | 31 | 33 | 7 | −1 | −9 | 0.29 | [5,3] [5,4,3,2] |
| 6 | 63 | 65 | 15 | −1 | −17 | 0.27 | [6,1] [6,5,2,1] |
| 7 | 127 | 129 | 15 | −1 | −17 | 0.13 | [7,3] [7,3,2,1] |
| | | | | | | | [7,3,2,1] [7,5,4,3,2,1] |
| 8 | 255 | 257 | 31 | −1 | −33 | 0.13 | [8,7,6,5,2,1] [8,7,6,1] |
| 9 | 511 | 513 | 31 | −1 | −33 | 0.06 | [9,4] [9,6,4,3] |
| | | | | | | | [9,6,4,3] [9,8,4,1] |
| 10 | 1023 | 1025 | 63 | −1 | −65 | 0.06 | [10,9,8,7,6,5,4,3] [10,9,7,6,4,1] |
| | | | | | | | [10,8,7,6,5,4,3,1] [10,9,7,6,4,1] |
| | | | | | | | [10,8,5,1] [10,7,6,4,2,1] |
| 11 | 2047 | 2049 | 63 | −1 | −65 | 0.03 | [11,2] [11,8,5,2] |
| | | | | | | | [11,8,5,2] [11,10,3,2] |

Gold codes are useful since a large number of codes can be generated with good auto-correlation and cross-correlation properties. But their auto-correlation function is worse compared to *m*-sequences. For more information about Gold code refer to (Proakis 2001)

### 3.4.1.4. Kasami Codes

There are two kinds of Kasami codes: small set and large set of Kasami codes. The large set of Kasami codes contains both the Gold codes and small set of Kasami codes as subsets.

Generation of small set of Kasami codes is similar to the generation of Gold codes. First, an *m*-sequence with length $N=2^m-1$ called the long sequence is generated by an *m*-stage shift register with linear feedback. Then another *m*-sequence with length $2^{m/2}-1$ called the short sequence is formed by taking every $(2^{m/2}+1)^{th}$ bit of the long sequence. The short sequence is enlarged to a length of $N=2^m-1$ by adding $2^{m/2}+1$ repetitions end to end. The summation in modulo-2 of long *m*-sequence and all $2^{m/2}-2$ cyclically shifted copies of enlarged short *m*-sequence constitute $2^{m/2}-1$ new sequences. The new sequences and the long *m*-sequence constitute $2^{m/2}$ Kasami codes with length $N=2^m-1$.

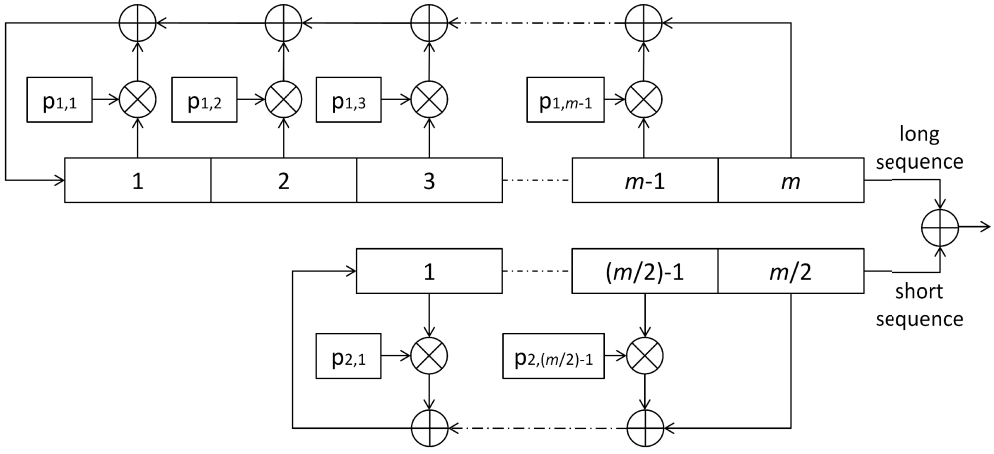


Figure 3.22. Kasami code generator

The cross-correlation and off-peak auto-correlation function in small set of Kasami codes are also three valued $\{-1, -s(m), s(m)-2\}$ where

$$s(m) = 2^{m/2} + 1 \tag{3.11}$$

The $s(m)$ is nearly half of the $t(m)$, so Kasami codes offer better cross-correlation and off-peak auto-correlation with respect to Gold codes. The drawback of small set of Kasami codes are that;

- Codes with length $N=2^m-1$where $m$ is odd can not be generated,
- Number of small set of Kasami codes generated with $m$ is approximately half of Gold codes generated with $m$.

The normalized peak correlation values of small set of Kasami codes can be observed from Table 3.4.

Table 3.4. Small set of Kasami codes

| $m$ | $N$ | Number of Kasami codes | 3 values of Correlation | | | Normalized peak correlation |
|---|---|---|---|---|---|---|
| 4 | 15 | 4 | 3 | −1 | −5 | 0.333 |
| 6 | 63 | 8 | 7 | −1 | −9 | 0.143 |
| 8 | 255 | 16 | 15 | −1 | −17 | 0.067 |
| 10 | 1023 | 32 | 31 | −1 | −33 | 0.032 |
| 12 | 4095 | 64 | 63 | −1 | −65 | 0.016 |

## 3.4.2. Orthogonal Codes

Hadamard-Walsh codes and Variable-Length Orthogonal codes are kinds of orthogonal codes.

### 3.4.2.1. Hadamard-Walsh Codes

The Hadamard-Walsh codes are generated from Hadamard matrix that is a symmetric square matrix whose elements are 1 or −1 and its rows and columns are mutually orthogonal to each other. The Hadamard matrix can be represent as below.

$$H_N = \begin{bmatrix} H_{\frac{N}{2}} & H_{\frac{N}{2}} \\ H_{\frac{N}{2}} & -H_{\frac{N}{2}} \end{bmatrix} \tag{3.12}$$

where $H_1=[1]$, $N=2^n$ and $n=(1,2,\ldots,k)$. The rows and columns of the matrix $H_N$ are the Hadamard-Walsh codes. The Hadamard matrix for $n=(1,2,3)$ are as below.

$$H_2 = \begin{bmatrix} 1 & 1 \\ 1 & -1 \end{bmatrix}, H_4 = \begin{bmatrix} 1 & 1 & 1 & 1 \\ 1 & -1 & 1 & -1 \\ 1 & 1 & -1 & -1 \\ 1 & -1 & -1 & 1 \end{bmatrix}, H_8 = \begin{bmatrix} 1 & 1 & 1 & 1 & 1 & 1 & 1 & 1 \\ 1 & -1 & 1 & -1 & 1 & -1 & 1 & -1 \\ 1 & 1 & -1 & -1 & 1 & 1 & -1 & -1 \\ 1 & -1 & -1 & 1 & 1 & -1 & -1 & 1 \\ 1 & 1 & 1 & 1 & -1 & -1 & -1 & -1 \\ 1 & -1 & 1 & -1 & -1 & 1 & -1 & 1 \\ 1 & 1 & -1 & -1 & -1 & -1 & 1 & 1 \\ 1 & -1 & -1 & 1 & -1 & 1 & 1 & -1 \end{bmatrix}. \quad (3.13)$$

$H_N$ matrix is an $N \times N$ square matrix that generates $N$ orthogonal codes with $N$ bits. Except the code whose bits are all 1, the other $N-1$ codes have equal number of 1, and $-1$, as it seen in the above examples.

Hadamard-Walsh codes are orthogonal that means their cross-correlations are zero only when they are synchronized otherwise their cross-correlation values are not small. Therefore, they can be only used with synchronous CDMA.

### 3.4.2.2. Variable-Length Orthogonal Codes

The Variable-Length Orthogonal codes are similar to Hadamard-Walsh codes. Dissimilarly, they are arranged and numbered according to tree structure.

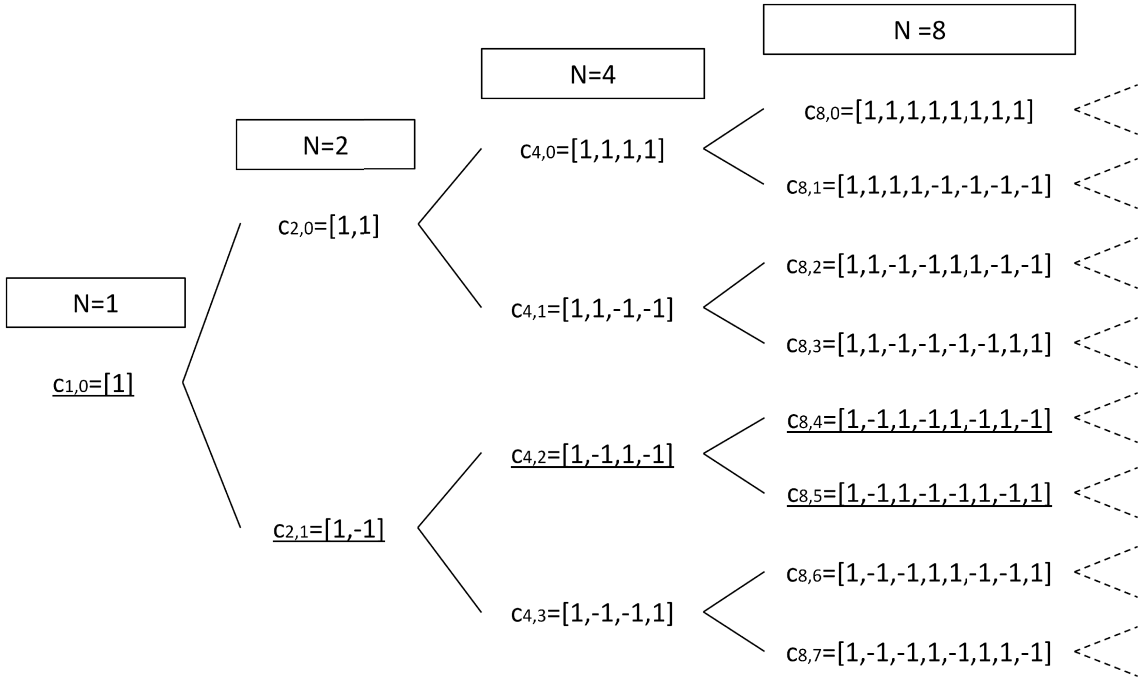


Figure 3.23. Tree Structure for Variable-Length Orthogonal codes

The tree structure for Variable-Length Orthogonal codes is illustrated in Figure 3.23 and can be formulated as below (Schulze and Lüders 2005).

$$\begin{aligned} c_{2N,2m} &= [c_{N,m}, c_{N,m}], \quad m = 0,1,....., N-1 \\ c_{2N,2m+1} &= [c_{N,m}, -c_{N,m}], \quad m = 0,1,....., N-1 \end{aligned} \tag{3.14}$$

where $N$ is spreading factor that is a power of 2.

The codes with the same length of code $N$ are orthogonal to each other as illustrated in Figure 3.23. For instance, $c_{4,0}$, $c_{4,1}$, $c_{4,2}$ and $c_{4,3}$ are orthogonal to each other. It should not be missed out that if a code is used in a connection, neither that code nor a code that is a descendant or ancestor of that code can not be used, since these codes are not orthogonal to each other. Assume that $c_{4,2}$ is used in a connection, then $c_{1,0}$, $c_{2,1}$, $c_{4,2}$, $c_{8,4}$, $c_{8,5}$ and so on are not allowed to be used in other connections.

As Hadamard-Walsh code, Variable-Length Orthogonal codes can just be used with synchronous CDMA not with asynchronous CDMA because of the same reason mentioned before.

# CHAPTER 4

# LOCATION SYSTEM SETUP

A new indoor location system that is based on acoustic transducers has been proposed in this thesis. It uses acoustic signals to locate several microphones physically in 3D coordinate system. A centralized unit, PC, performs the computations and controls the system. The location system can locate the microphones attached to the entities simultaneously using DS-CDMA signals with accuracy order of centimeters. The CDMA signals emitted from the speakers are BPSK modulated Gold code sequences. Good auto-correlation properties of these codes are used in obtaining accurate time measurements whereas their good cross-correlation property provides high processing gains and in turn simultaneous measurement possibility of all the required distances without making a significant disturbance to each other. The distances are estimated by using ToA measurement technique and the locations are estimated by using trilateration technique.

Acoustic signals were preferred due to their low velocity. As it was mentioned before, the low velocity makes an accurate localization possible with available inexpensive devices. A centralized unit was used for ease of computation. The centralized location system can work with basic devices since the nodes do not need to make any computations. DS-CDMA was used in the location system that provides: simultaneous signal emission from speakers and robustness of the signal to noise and interference. Gold code sequence was preferred since a large number of codes can be generated with good auto-correlation and cross correlation properties. Orthogonal codes are not proper candidates for this system since times of arrivals of the signal to the microphone are different. Hence orthogonal codes can not be separated from each other. Small set of Kasami codes comprise only the codes generated from even number of shift registers, so they are not suitable, either. On the other hand, *m*-sequences and Barker code sequence do not have many codes. Trilateration technique was preferred rather than multilateration for ease in computation. Trilateration requires synchronization between transmitters and receivers, while multilateration requires only synchronization between receivers to measure the pseudoranges. Although speakers and

the receivers are synchronized in the proposed system, some delays occurred in transmission. Hence another microphone was used in order to find the delays. Trilateration technique provides more accurate results compared to multilateration technique, since the multilateration technique requires more distance measurements and harder computations.

This chapter introduces implementation of the proposed location system in which ordinary and inexpensive off-the-shelf devices are used. The rest of the chapter considers devices used in the setup and their technical details, the preparation of work area, procedure of localization and Graphical User Interface (GUI).

## 4.1. Devices and Technical Details

Cost is one of most important issues for suppliers and customer. Inexpensive products with the same capability are preferred to expensive ones. Therefore ordinary and inexpensive devices are used in this location system implementation. Most of them are off-the-shelf devices that can be found easily in the market. Some devices are made by hand in order to reduce the cost, but they can be also bought with a small cost. The devices are listed as;

- Personal Computer (PC)

An ordinary PC is sufficient for this implementation; however the system operates more efficiently with a more powerful PC. The important issue is that PC must be capable to run MATLAB program that is a high level language and provides an interactive environment. In addition to that, it is suggested to choose a PC that has RS232 and FireWire (IEEE-1394) ports for this implementation. If there is no RS232 connection in PC, the RS232 to USB converters can also be used.

- Sound Card

A sound card that has at least four uniform outputs and two uniform inputs is required for data transmission. PreSonus Firebox 6x10 FireWire Recording Interface is used in this implementation. It has four uniform output and two uniform input which is in accordance with the requirement. It can sample analog data up to 96 kHz. The technical details are also illustrated in Table 4.1 below.

Table 4.1. Technical details of PreSonus Firebox 6x10 FireWire Recording Interface

| | |
|---|---|
| Preamp Bandwidth | 10 kHz to 50 kHz |
| Preamp Input Impedance | 1.3 kΩ |
| Instrument Input Impedance | 1 MΩ |
| Preamp THD | <0.005% |
| Preamp EIN | −125 dB |
| Preamp Gain | 45 dB |
| Line Input Impedance | 10 kΩ |
| TRS Output Impedance | 51 Ω |
| TRS Main Output Impedance | 51 Ω |
| Headphone Output | 150 mW/CH 20 Hz to20 kHz |
| Phantom Power | 48 V ± 2 V |
| Power Supply | Ext. Line Transformer, Internal Switching |
| Bus Power | Six-pin FireWire Port |
| Analog to Digital Converters | 24 bits/ up to 96 kHz |
| ADC Dynamic Range | 107 dB |
| Digital to Analog Converters | 24 bits/ up to 96 kHz |
| DAC Dynamic Range | 107 dB |
| IEEE 1394 | 400 mbps |

- Amplifier

Alpin USA-204 150x4 Amplifier that is an inexpensive four channel car amplifier is used for amplifying data signal before data signal is emitted from speakers. The amplifier has four distinct channels and they can operate simultaneously. The technical details are given in Table 4.2.

.

Table 4.2. Technical details of Alpin USA-204 150x4 Amplifier

| | |
|---|---|
| Frequency Response | 20 kHz – 50 kHz |
| Power per Channel | 150 W |
| Signal to Noise Ratio | 85 dB |
| Speaker Impedance | 4 Ω - 16 Ω |
| Input Sensitivity | 0.2 V – 0.4 V |

- Speakers

Jameson Js 21 Tweeters are chosen due to their low cost and easiness of availability. Four Jameson Js 21 Tweeters are used for emitting amplified data signals.

- Microphones

Microphones are made by hand in order to reduce the cost, but they also can be bought. At least two microphones are needed for this implementation. The schematic of the microphones is illustrated in Figure 4.1.

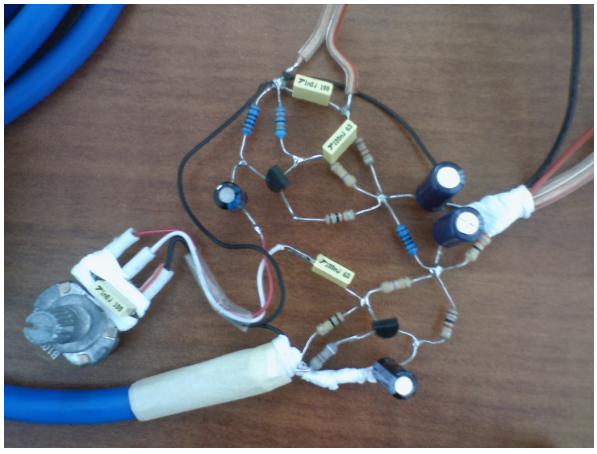

Figure 4.1. The photo of microphone

- Digital Thermometer

A digital thermometer is also required in order to measure environment temperature. This is essential to calculate the sound velocity. Digital thermometer is also made by hand. Figure 4.2 illustrates the photo of the digital thermometer.

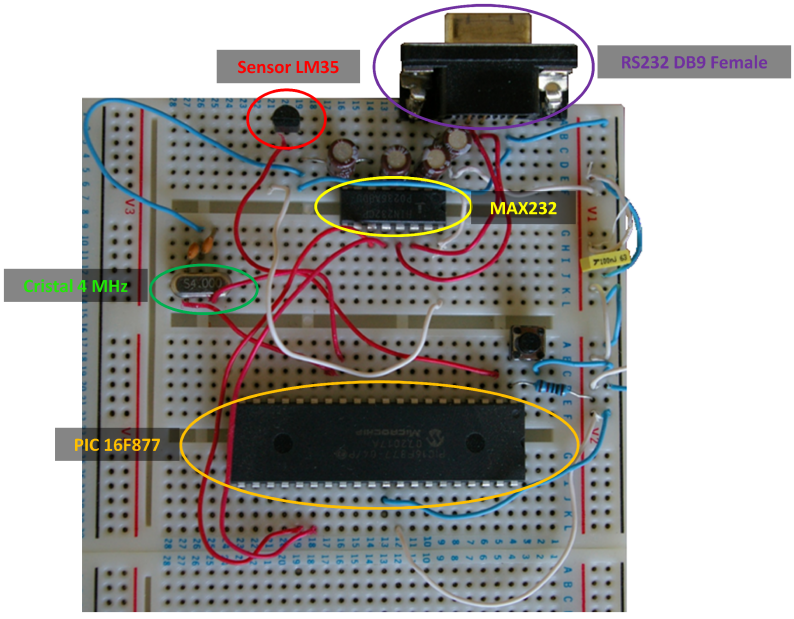


Figure 4.2. Digital thermometer

All these devices mentioned above constitute the hardware of the system and it can be modeled as in the Figure 4.3.

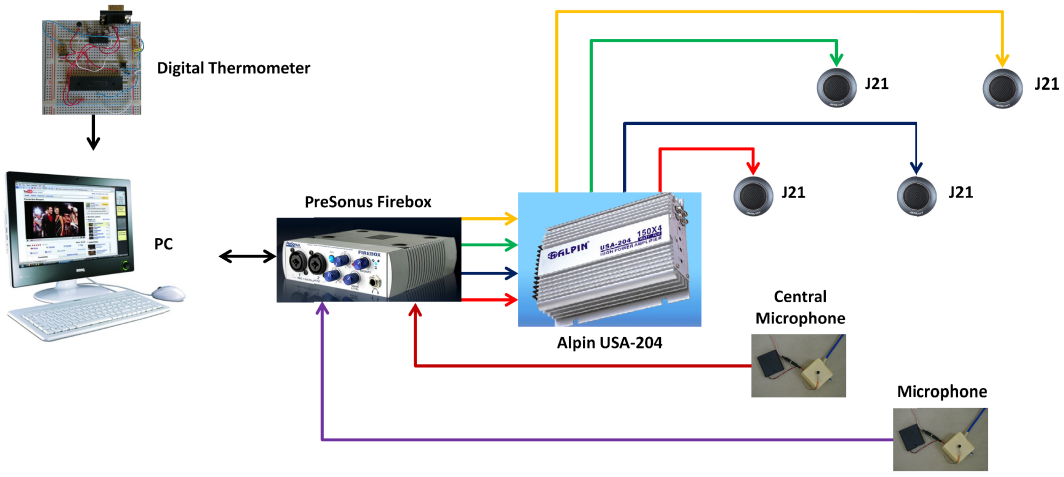


Figure 4.3. Connection diagram of location system

On the other hand, MATLAB, a forth generation programming language and computation environment, is used as software. All codes are written and GUI is designed in MATLAB. Data Acquisition Toolbox (DAT) of MATLAB provides data transmission between PC and sound card. For information about DAT, refer to Data Acquisition Toolbox™ 2 User's Guide.

## 4.2. Preparation of Work Area

After the devices were provided, an office in the Department of Electrical & Electronics Engineering at İzmir Institute of Technology was allocated. In order to attain a uniform work area, some modifications are made in that office as listed below.

- First of all, technical equipments were gathered. An oscilloscope, a signal generator, a voltage source, a soldering iron and a multimeter were used for this implementation.

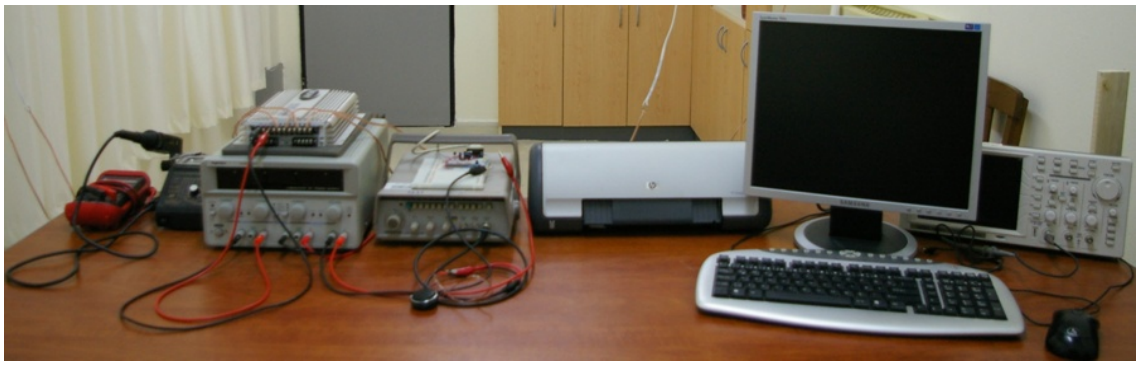

Figure 4.4. The equipment used for implementation

- Ceiling was covered to reduce the reflections.

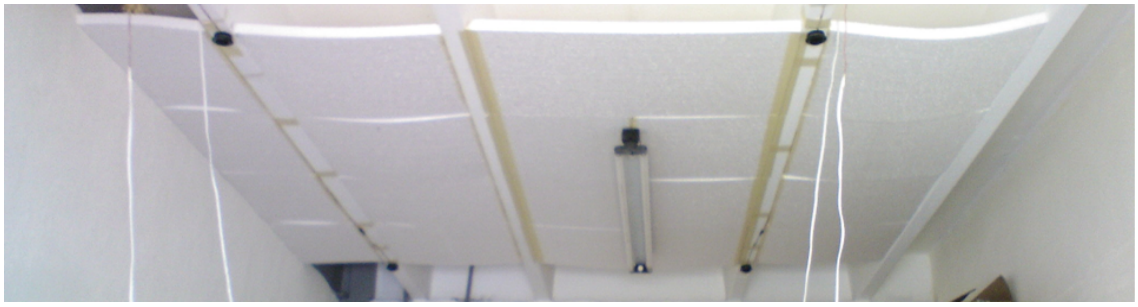

Figure 4.5. Ceiling

- Floor was covered with carpet.

Figure 4.6. Floor

- The area was encircled with curtain.

Figure 4.7. Curtain encircles the area

These arrangements were done in order to reduce the effects of exterior influences and multipath disturbances due to the reflections. So, a uniform work area is constituted.

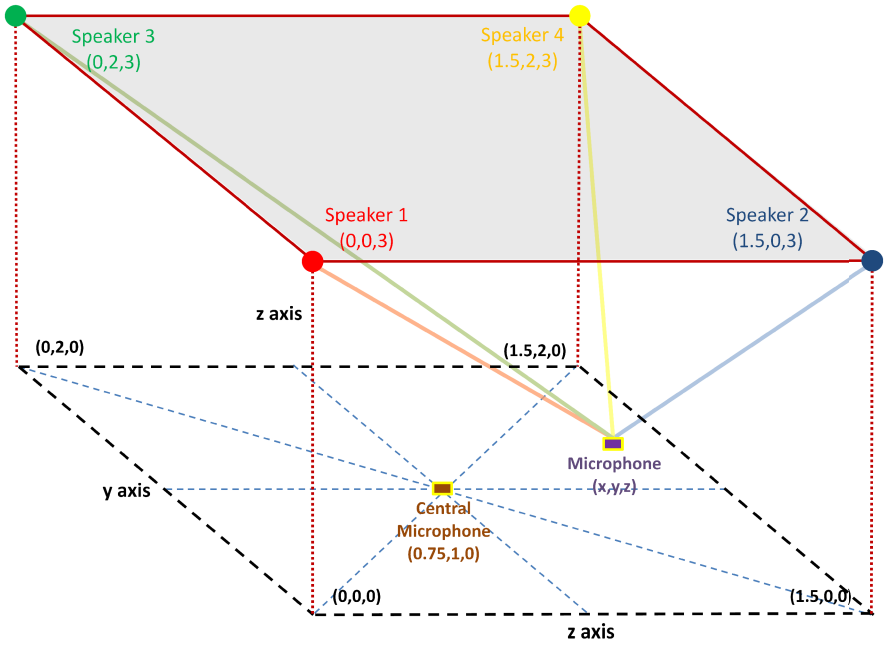


Figure 4.8. The setup at the office

The experimental setup was built as in Figure 4.8. The dimensions of the area are 1.5 m in width, 2 m in length and 3 m in height. The speakers were placed to the corner of the ceiling as it seen in the figure. Central microphone was placed to a fixed point that is the centre of the floor because of equal closeness to the speakers. If required the fixed point can be moved. The other microphone was used for obtaining its location. The system can also locate more than one microphone simultaneously, if the microphones are connected to the system. But in this implementation only one microphone is used for locating its position.

## 4.3. Procedure of Localization

The procedure of localization in the proposed location system is as below:

1. Determining variables,
2. Measuring temperature of environment,
3. Calculating velocity of sound,
4. Creating Gold code matrix,
5. Selecting randomly four distinct Gold codes,
6. Creating sampled data signal,
7. Transmitting data signals,
8. Receiving aggregated data signal,
9. Finding delays,
10. Finding distances,
11. Estimating location by applying trilateration.

### 4.3.1. Determining Variables

There are three kinds of variables. Some variables have to be redefined each time before the process starts due to the requirements. Some variable are calculated during the process and some variables are fixed for the setup. Still they can be changed, if a change is occurred in the setup.

Variables that have to be redefined before the process are:

- sampling frequency of sound card,
- chip frequency of data signal,
- carrier frequency of data signal,
- number of shift registers of Gold code generator,
- amplitudes of each signal data,
- number of phase shifts in data signal,
- method of trilateration.

Variables that are calculated or measured during process are:

- ratio of carrier frequency to chip frequency,
- length of the bit sequence of Gold code,
- temperature of environment,
- Gold code matrix.

Variables that are fixed for the setup are:

- microphone record time,
- coordinates of four speakers,
- coordinates of the central (fixed) microphone.

### 4.3.2. Measuring Temperature of Environment

The temperature of the environment has to be obtained, since the calculation of sound velocity requires precise temperature information. There are two ways of obtaining the temperature; one way is measuring the temperature by using thermometer and second way is to estimate the temperature from calculations. Measuring the temperature with a digital thermometer was preferred in the proposed system due to its smaller computational requirement. The hand made digital thermometer was connected to PC from serial port (RS232). The measured voltage data was imported to the PC and the temperature was calculated from that imported data.

### 4.3.3. Calculating Velocity of Sound

After obtaining the temperature of the environment, velocity of sound that is needed to calculate distances was calculated. Actually, temperature is not the only criterion for obtaining velocity of sound; humidity and wind are also effective on velocity of sound. However, influence of humidity can be neglected since it is less effective compared to the influence of temperature. The wind may also be very effective But it was also neglected, since the implementation took place indoor. The velocity of sound as a function of the temperature can be found as;

$$v_{\text{Sound}} = 331.3\sqrt{1+\frac{T}{273.15}} \tag{4.1}$$

where $T$ is the temperature in ˚C. For more information about the influence of wind, refer to (Martin, et al. 2002).

### 4.3.4. Creating Gold Code Matrix

The number of shift registers $m$ that can be chosen from 5 to 11 had been defined previously as a variable. By using $m$, the length of the bit sequence of Gold code, $n$, was calculated as;

$$n = 2^m - 1 \tag{4.2}$$

where $n$ can get a value between 31 bits to 2047 bits. Eventually, a matrix was generated with dimensions $n \times n+2$ as in Figure 4.9.

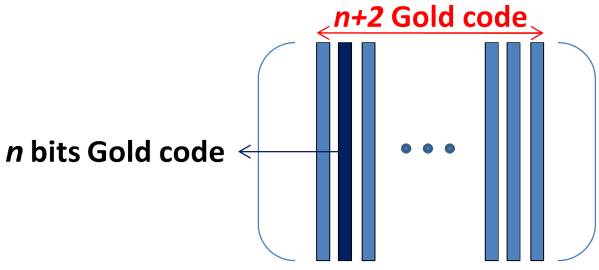


Figure 4.9. Gold code matrix

The code matrix consists of $n$+2 Gold codes, each $n$ bit long. This matrix is regenerated each time in this implementation. This causes redundant computation, which reduces the update rate. As a remedy, Gold code matrix can be stored in a table and the Gold codes can be extracted from that table when they are needed. Therefore the Gold codes can be reached from that table without any computation.

### 4.3.5. Selecting Randomly Four Distinct Gold Codes

After generating the Gold code matrix corresponding to a predefined $m$, four distinct Gold codes were selected from $n$+2 Gold codes, randomly. The codes must be distinct since each code is assigned to a speaker. The four codes that have good auto-correlation and cross-correlation properties can be selected, but in this implementation it is preferred to select the codes randomly in order to see general attitude of the system.

### 4.3.6. Creating Sampled Data Signals

The selected Gold codes were modulated with BPSK. The process can be revealed with an example. Assume that a data signal was created from a bit sequence [−1,1,1,−1−1] in a case that sampling frequency is 96000 Hz, chip frequency is 5000 Hz, carrier frequency is 10000 Hz, signal amplitude is 1 and the number of phase shifts is 3.

Firstly a square wave of half the chip frequency was generated. It was sampled with a frequency that is a multiple of sampling frequency and number of phase shifts that is 288 kHz for this example. Then the square wave was converted into bipolar code with chip frequency. At last, the bipolar code was modulated with BPSK signal at the carrier frequency. The steps of obtaining the BPSK-modulated CDMA code are shown in Figure 4.10.

(a)

(b)

(c)

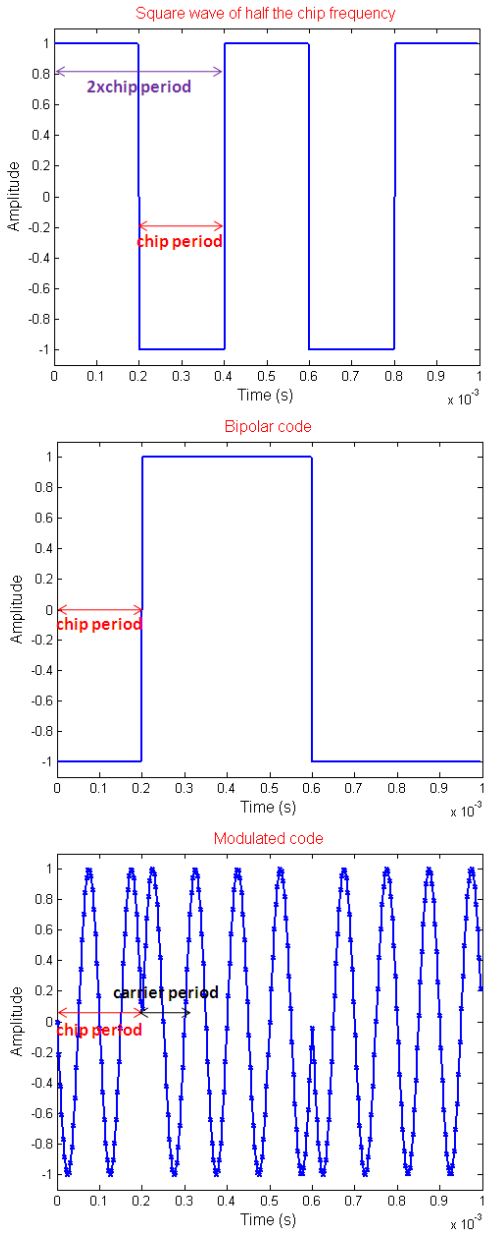


Figure 4.10. (a) Square wave of half the chip frequency (b) Bipolar code [−1,1,1,−1,−1] (c) Modulated code

Eventually, three vectors of modulated data were stored, the original sampled and modulated code vector and its one sample and two sample shifted versions. These stored data vectors which are BPSK-modulated CDMA codes sampled at 96 kHz are shown in Figure 3.11.

(a)

(b)

(c)

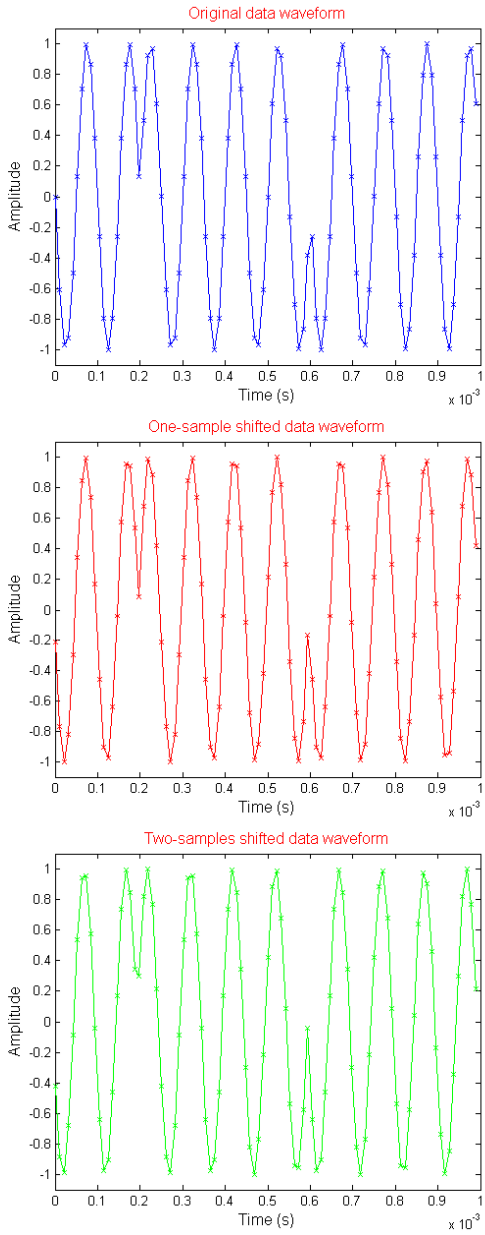


Figure 4.11. (a) Original data waveform (b) One-sample shifted data waveform (c) Two-samples shifted data waveform

The phase can be calculated as difference corresponding to a time shift;

$$\varphi = \frac{2\pi f_{\text{chip}}}{k.f_{\text{sampling}}} \tag{4.3}$$

where $k$ denoted the shift in number of samples, $f_{\text{chip}}$ is the chip frequency and $f_{\text{sampling}}$ is the sampling frequency. These shifted versions of data signals were used for correlation, so they were not transmitted by the speakers.

This process was performed for each data channel which is assigned a distinct speaker; where each speaker has its own Gold code. In order to gain time and reduce computation, the generated data signals for each speaker can be saved and used every time. Therefore the processes of creating Gold code matrix, selecting four distinct Gold codes and creating sampled data signals can be skipped. However in this implementation every process was done every time.

### 4.3.7. Transmitting Data Signals

The four distinct original (not shifted) data signals were transmitted simultaneously from speakers. Each speaker transmitted the data signal that belongs to it. The sound card was configured for four channels by constituting two stereo channels objects in MATLAB. During data transmission process some delays may occur.

### 4.3.8. Receiving Aggregated Data Signal

Two microphones were used in this implementation. One microphone was located to a fixed location, centre of the floor, and determined the delay of each speaker. The microphones received the aggregated data signal. A stereo channel object was generated for that process in MATLAB.

### 4.3.9. Finding Delays

In order to obtain the delay for a speaker, the difference between the computed time and the measured time must be found. First, the distance between a speaker and the central microphone was calculated by using basic geometry. Then the number of sampling periods, $L$, that is needed for a signal to travel from the speaker to the central microphone was computed as

$$L = \frac{d_{\text{cal}} \cdot f_{\text{sampling}}}{v_{\text{sound}}} \tag{4.4}$$

where $d_{\text{cal}}$ is the calculated distance.

After computing $L$, aggregated data signal that is received by the central microphone was correlated with the original data signal and the shifted versions. The peak correlation values for each correlation were found and the maximum one was selected. Then the instance of the maximum peak correlation in terms of sampling period, $l_{pp1}$, was found.

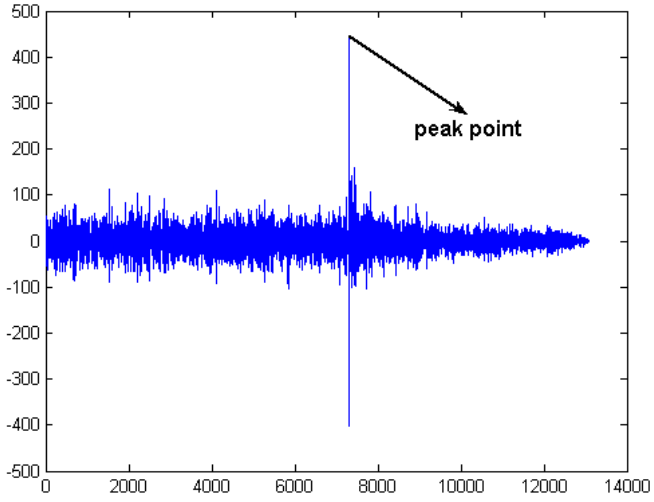


Figure 4.12. Peak point in correlation

Eventually, substituting $L$ from $l_{pp1}$ gave the delay, $l_d$, for that speaker. This process was repeated for the other speakers in order to find the delays for each speaker.

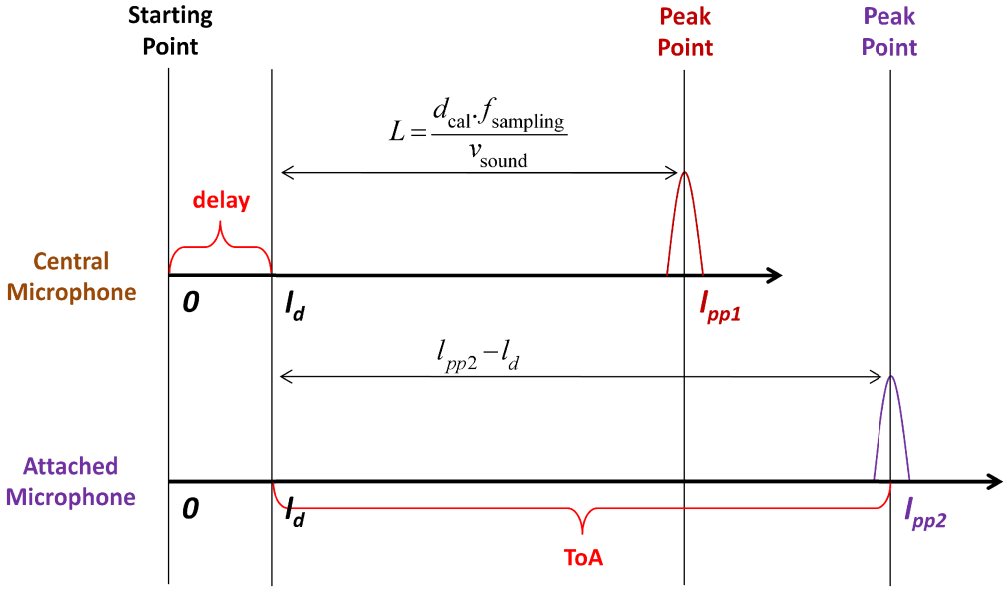


Figure 4.13. Finding delay and distance process

### 4.3.10. Finding Distances

Time of Arrival (ToA) measurement technique was used for finding the distances. The process for finding distances is similar to the process for finding delays. The acquired signal from the other microphone was correlated with the original data signal and shifted versions by using convolution. The correlations gave a high peak because of Gold code correlation properties. The peak correlation values for each correlation were found and the maximum one was selected. The time of the new peak point, $l_{pp2}$, was found as in previous process. The measured distance $d_m$ was found as

$$d_m = \frac{(l_{pp2} - l_d).v_{\text{sound}}}{f_{\text{sampling}}}. \tag{4.5}$$

This process was repeated for each speaker to find the four distinct distances.

### 4.3.11. Estimating Location by Applying Trilateration

Trilateration technique was applied to localize the microphone. The four distances were computed in the previous process. Indeed, three distances are sufficient to locate an object by using trilateration technique. Therefore three distances out of four can be chosen in four ways, so four different points for the microphone can be computed.

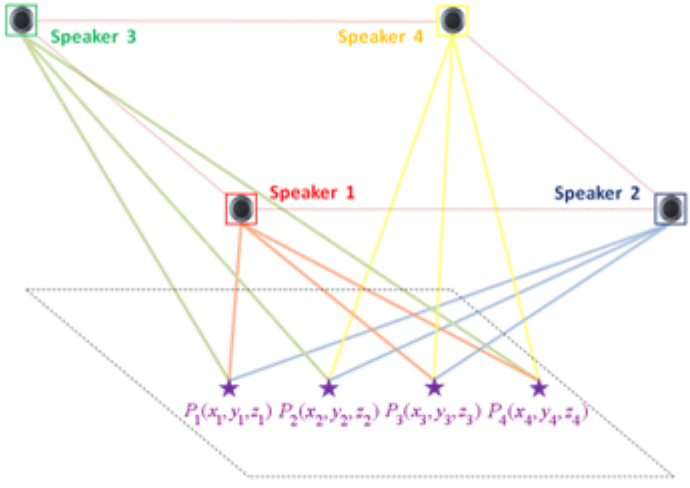


Figure 4.14. Four different coordinate respect to four distances

As a result of that, two methods were proposed;

Method 1 uses all four distances and computes the coordinates of four different points as in Figure 4.15. Then it takes the average of them, in order to find $x_p$, $y_p$ and $z_p$.

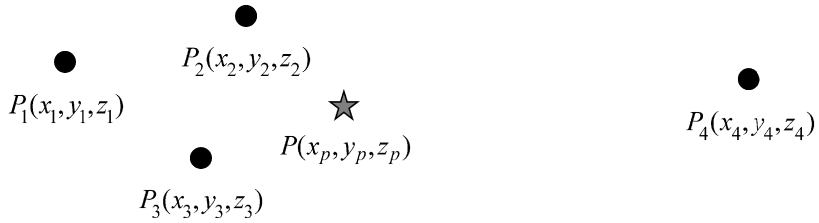


Figure 4.15. The average $x_p$, $y_p$ and $z_p$

$$\begin{aligned} x_p &= (x_1 + x_2 + x_3 + x_4)/4 \\ y_p &= (y_1 + y_2 + y_3 + y_4)/4 \\ z_p &= (z_1 + z_2 + z_3 + z_4)/4 \end{aligned} \tag{4.6}$$

Method 2 uses only three distances. In order to select three distances out of four, one distance has to be eliminated. First of all, peak correlation values obtained from each speaker's data are checked and the minimum is selected. Then the distance computed from the speaker data with minimum peak correlation value is eliminated. Finally $x_p$, $y_p$ and $z_p$ are calculated by applying trilateration technique.

It can be said that Method I considers all of the four distance measurements evenly reliable and gives them equal weight in obtaining the location estimate. On the contrary, Method II eliminates the most suspectable distance measurement corresponding to the smallest correlation peak. So, one might suggest that Method II will give a more robust localization estimate.

## 4.4. Graphical User Interface (GUI)

A GUI was created for convenience of the utilization. It consists of fourteen different partitions as seen in Figure 4.16. Orange labeled partitions are allocated for plots and illustrate the plots. Yellow labeled partitions are buttons. Red labeled partitions set variables that are fixed for the setup. Brown labeled partitions set variables that have to be redefined before each simulation run and blue labeled partitions represent the results.

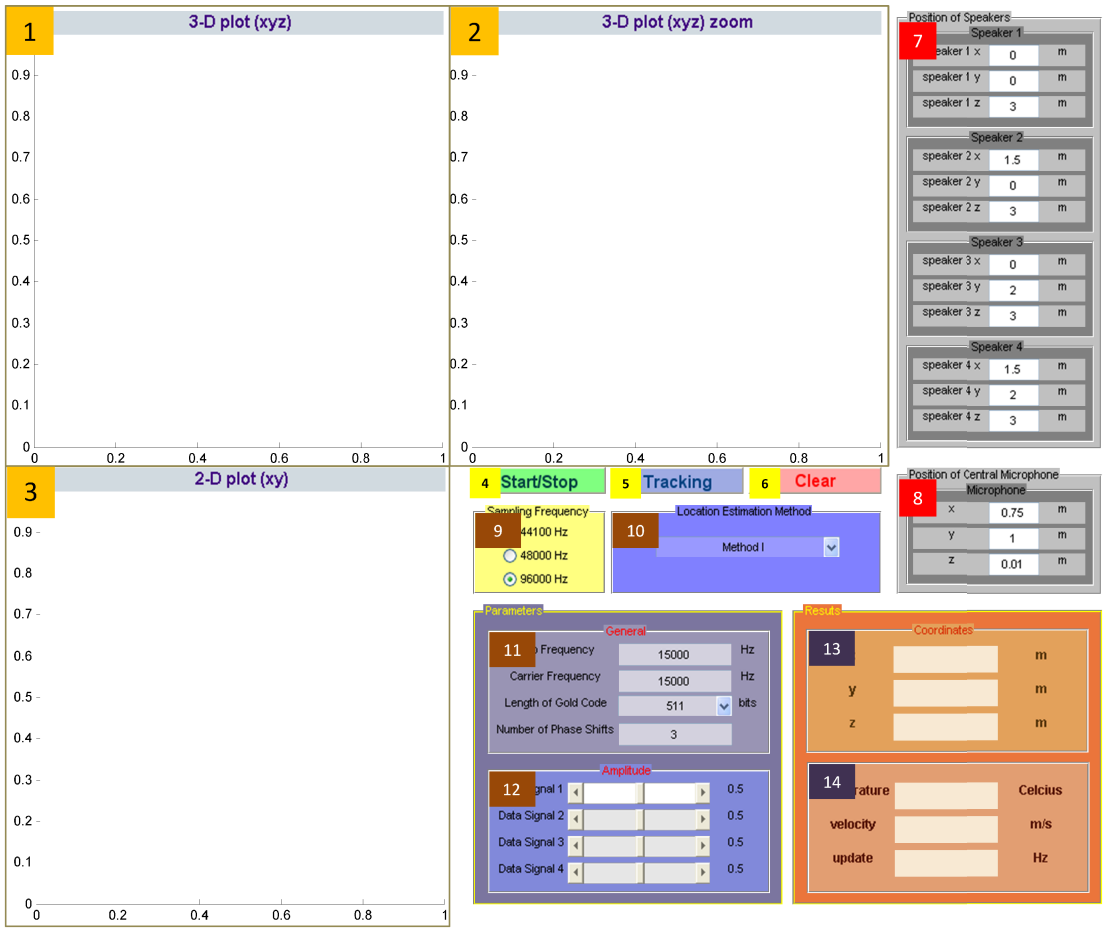


Figure 4.16. Graphical User Interface

The partitions can be listed as:

1. 3D plot (xyz)

   Three-dimensional plot illustrates the location estimate.

2. 3D plot (xyz) zoom

   Location estimate is illustrated more obviously by zooming in three-dimension.

3. 2D plot (xy)

   Location estimate is illustrated in two-dimensions.

4. Start/Stop button

   The start/stop button is used to start or stop the process. Once this button is pressed, it stays pressed and the process starts and when it is pressed again, it restores to its initial aspect and the process stops.

5. Tracking button

   When tracking button is selected, the localization process is repeated until it is deselected. So it enables seeing several location estimations in the same plot.

6. Clear button

   Clear button clears all plots and results when it is pressed.

7. Position of Speakers

   Position of each speaker is set to predefined $x$, $y$ and $z$ values of the setup. It can be set again, when a change is occurred in the setup. A warning appears if any characters except numbers are entered.

8. Position of Central Microphone

   Position of central microphone is set to predefined $x$, $y$ and $z$ value of the setup. It can be set again, when a change is occurred in the setup. A warning appears if any characters except numbers are entered.

9. Sampling Frequency

   Sampling frequency can be selected among 44100 Hz, 48000 Hz and 96000 Hz.

10. Location Estimation Method

    Method I or Method II can be chosen as location estimation method.

11. General Parameter

    Chip frequency, carrier frequency, length of Gold code and number of phase shift can be set in general parameter. Chip frequency and carrier frequency can take a value between 5000 and 20000. They are set to 15000 Hz as initial settings. A warning appears if any characters except numbers or any numbers out of range are entered. Length of the Gold code can be chosen among 31, 63, 127, 255, 511, 1023 and 2047. Number of phase shifts must be an integer.

12. Amplitude of Data Signal

    Amplitudes of data signals can be controlled by sliding the slider. The current value is illustrated beside the slider. The amplitude can take values between 0 and 1. It must be stated that; data signals 1, 2, 3 and 4 refer to the signals emitted from speakers 1, 2, 3 and 4, respectively.

13. Estimated Coordinates

    Estimated results of $x_p$, $y_p$ and $z_p$ are represented.

14. Other Results

    Temperature, velocity of the sound and update rate are represented.

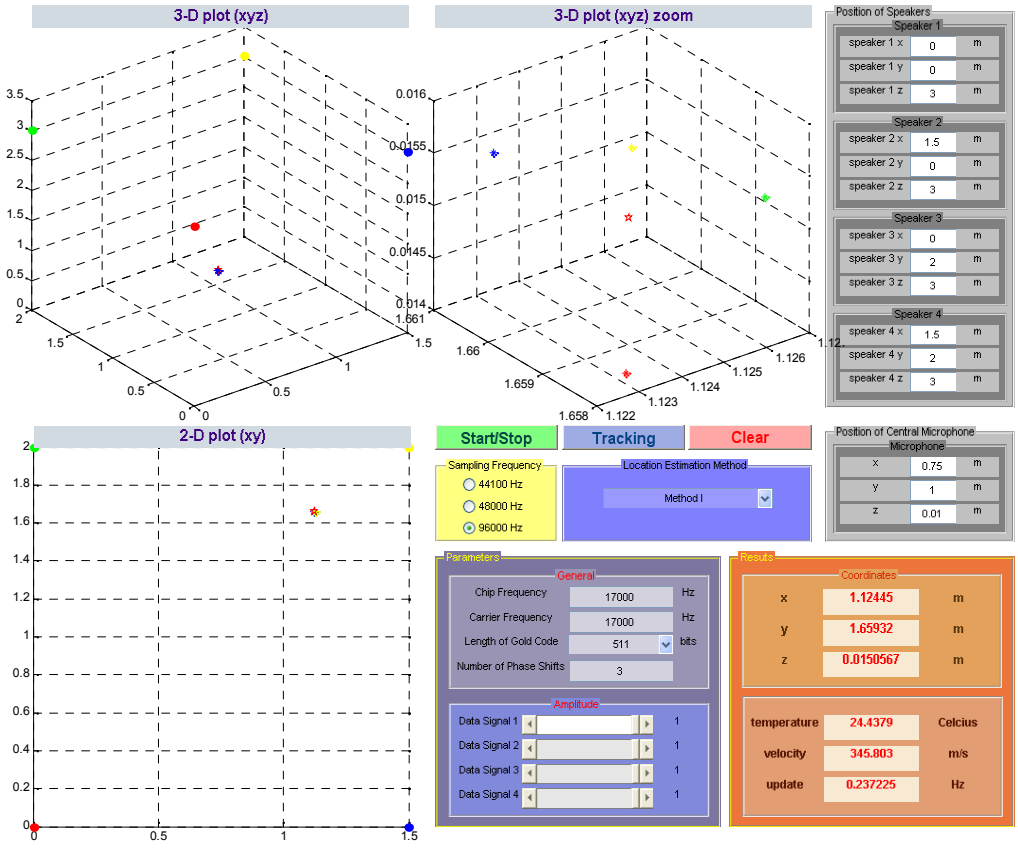


Figure 4.17. GUI in progress that uses Method I

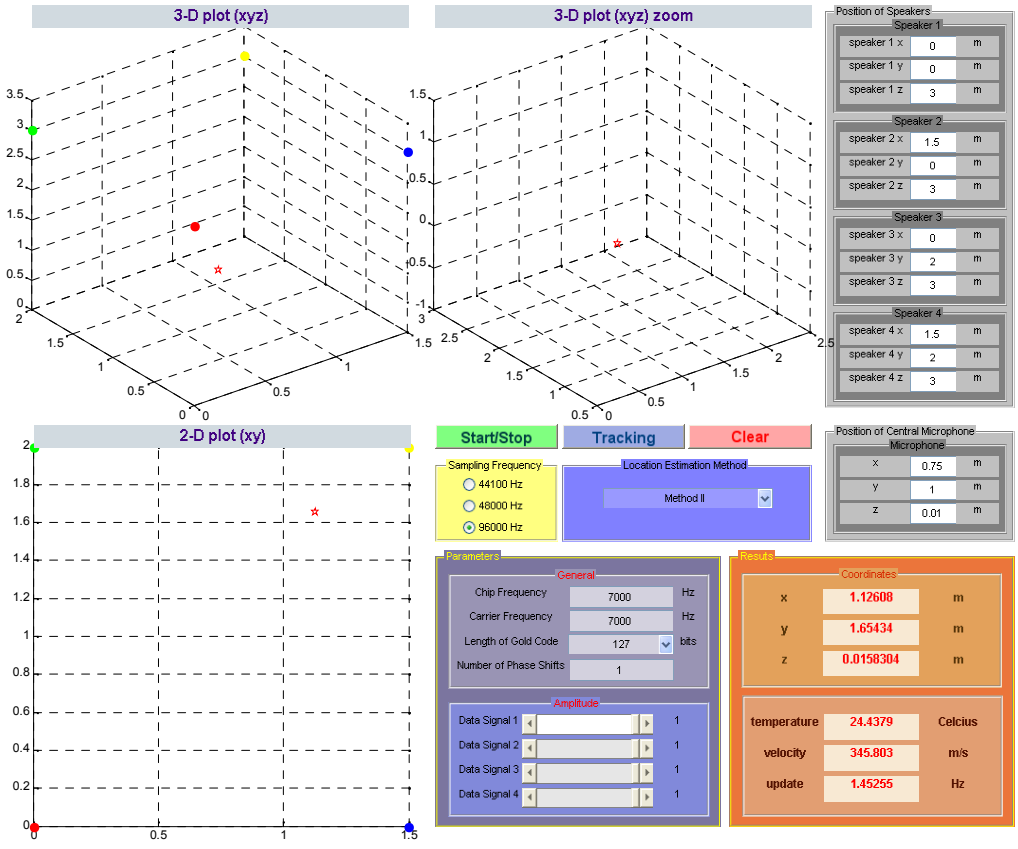


Figure 4.18. GUI in progress that uses Method II

Figure 4.17 and 4.18 illustrate sample simulations where Method I and Method II are applied, respectively. As it is seen, there are four colored circles in 3D and 2D plots: red circle, blue circle, green circle and yellow circle indicates the position of the speaker 1, speaker 2, speaker 3 and speaker 4, respectively. In Figure 4.17, it can be also seen that four location estimates and the average of them is indicated. The red point indicates the location estimate that is obtained by trilateration using distances between microphone and speaker 1, speaker 2, speaker 3. The blue point indicates the location estimate that is obtained by trilateration using distances between microphone and speaker 1, speaker 2, speaker 4. The green point indicates the location estimate that is obtained by trilateration using distances between microphone and speaker 1, speaker 3, speaker 4. The yellow point indicates the location estimate that is obtained by trilateration using distances between microphone and speaker 2, speaker 3, speaker 4. The star indicates the average of these four location estimates. The average results are represented in results partition. Opposite to the previous case, there is only one location estimate that is indicated with a red star in Figure 4.18.

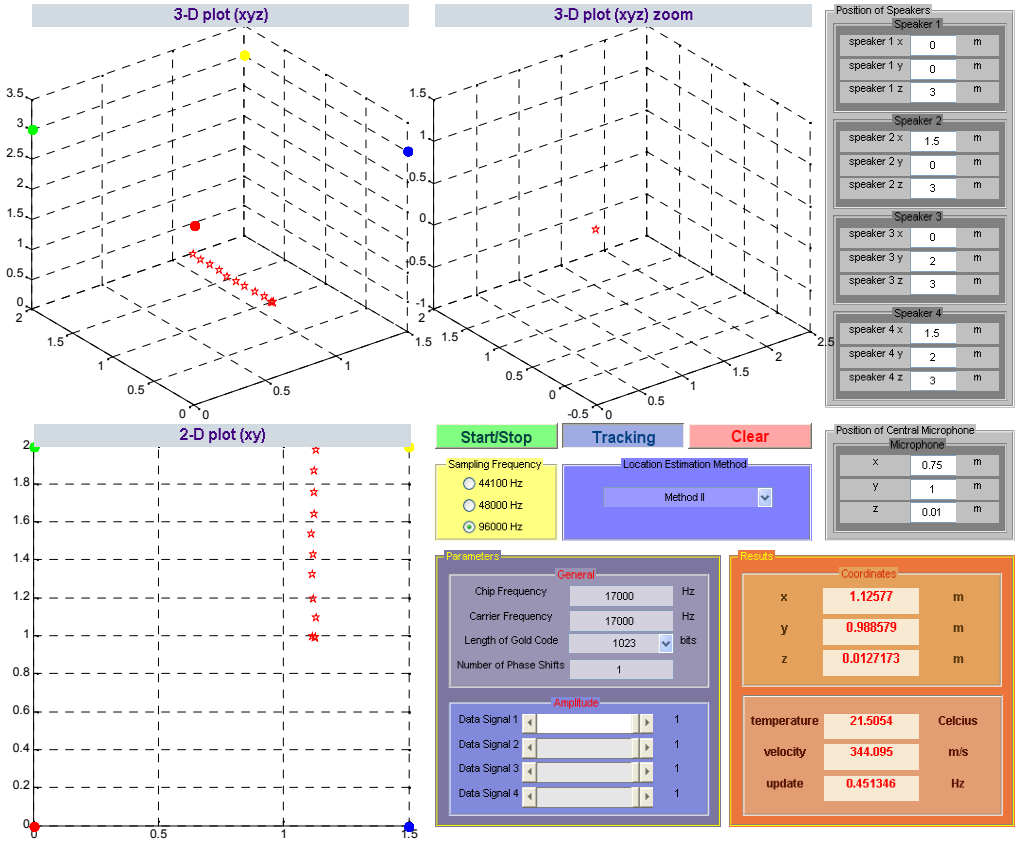


Figure 4.19. GUI in tracking mode

A sample in tracking mode is illustrated in Figure 4.19, where the path can be easily seen. This tracking mode provides tracking-aware property to the system and shows that it is also suitable for application, where the movement of the entity is considered.

# CHAPTER 5

# EXPERIMENTAL STUDY

This chapter considers implementation results of location system that we have proposed. Firstly, transfer function gain of the system was handled. Then optimum variables were selected. The performance of the proposed location system was investigated at predefined points in work area. Eventually, the precision distribution of the area and precision versus accuracy graphs were illustrated.

First of all, transfer function gains of system with respect to each speaker were obtained. A chirp signal from 0 Hz to 25 kHz was emitted from speaker 1 and acquired by a microphone that was three meter below the speaker as in Figure 5.1.

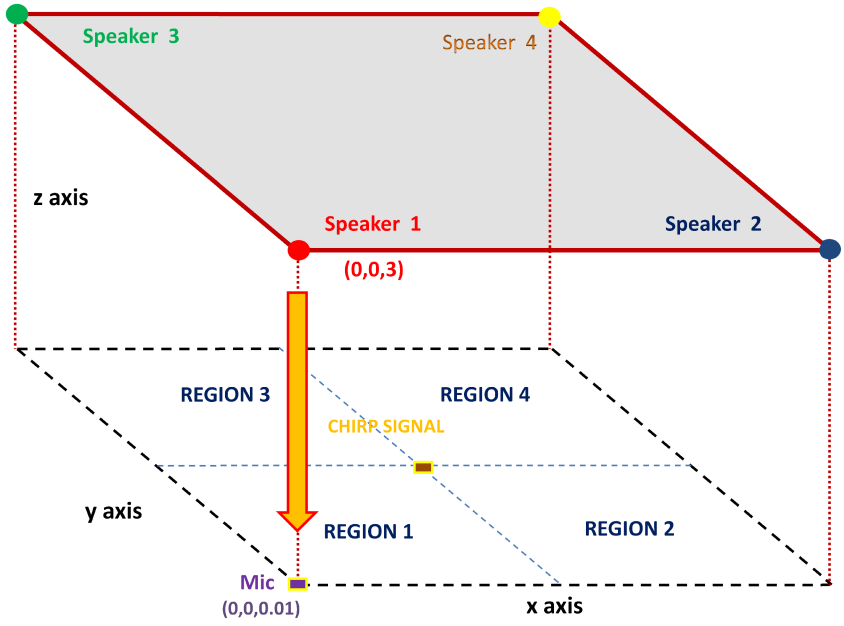


Figure 5.1. Speaker and microphone positions during the process

Initially, the speaker and microphone were looking face to face in order to obtain transfer function gain at 0 degrees incline. Then the microphone was rotated 20, 40 and 60 degrees in its axis respectively and the transfer function gains were obtained for each case. The process was repeated for the other speakers as well and the consecutive figures were attained.

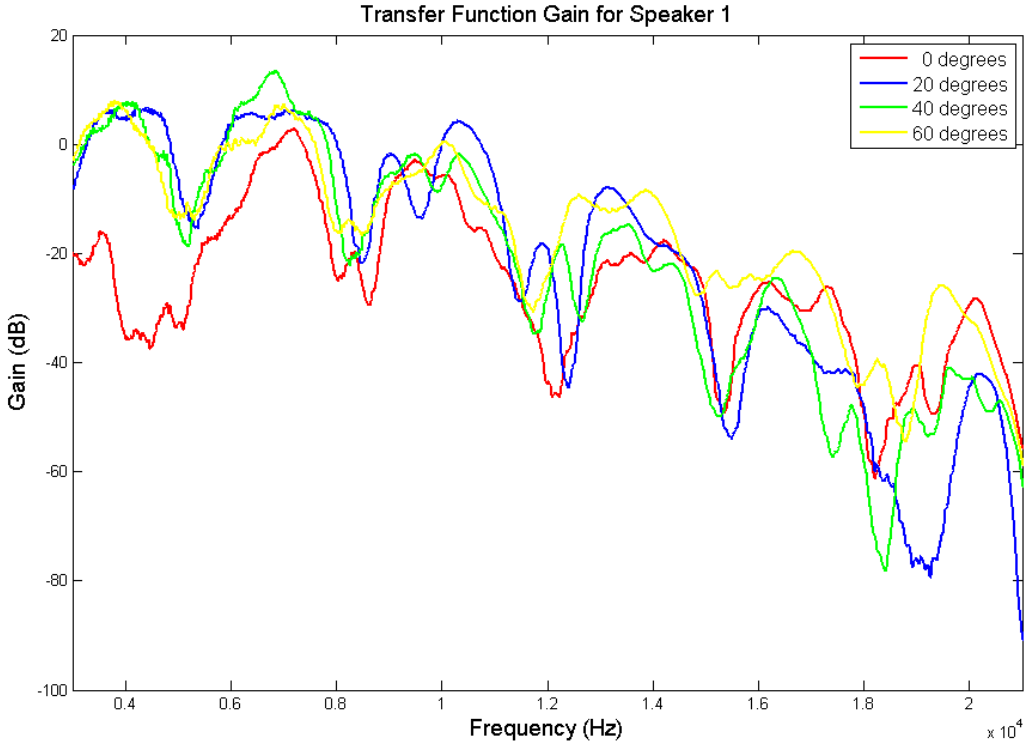


Figure 5.2. Transfer function gain for speaker 1

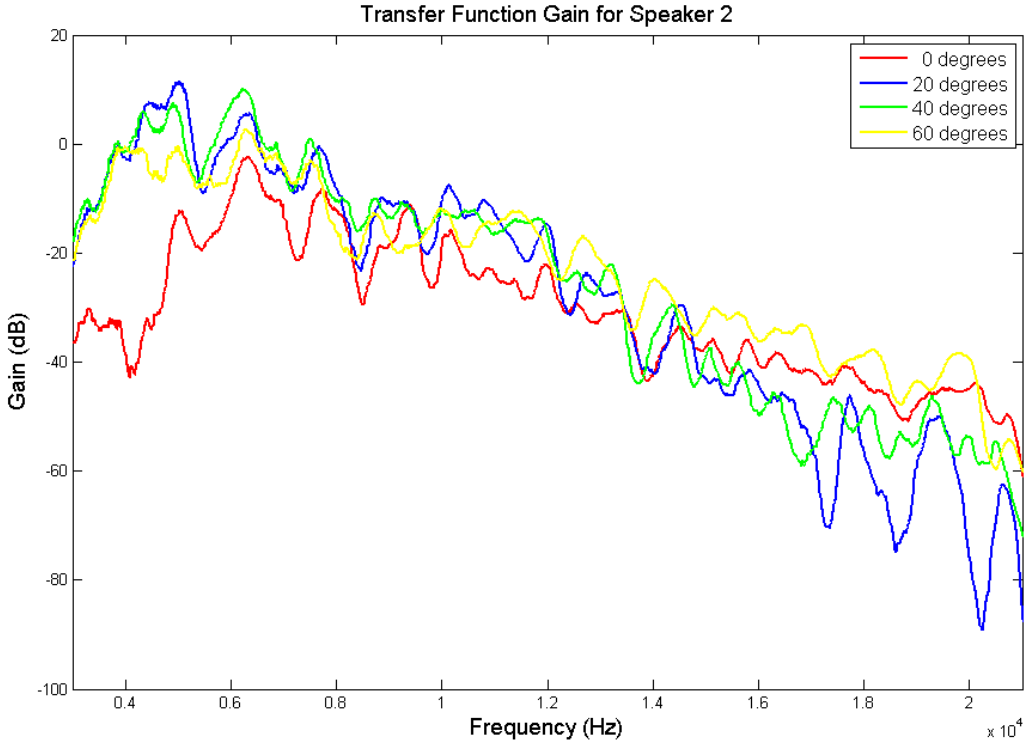


Figure 5.3. Transfer function gain for speaker 2

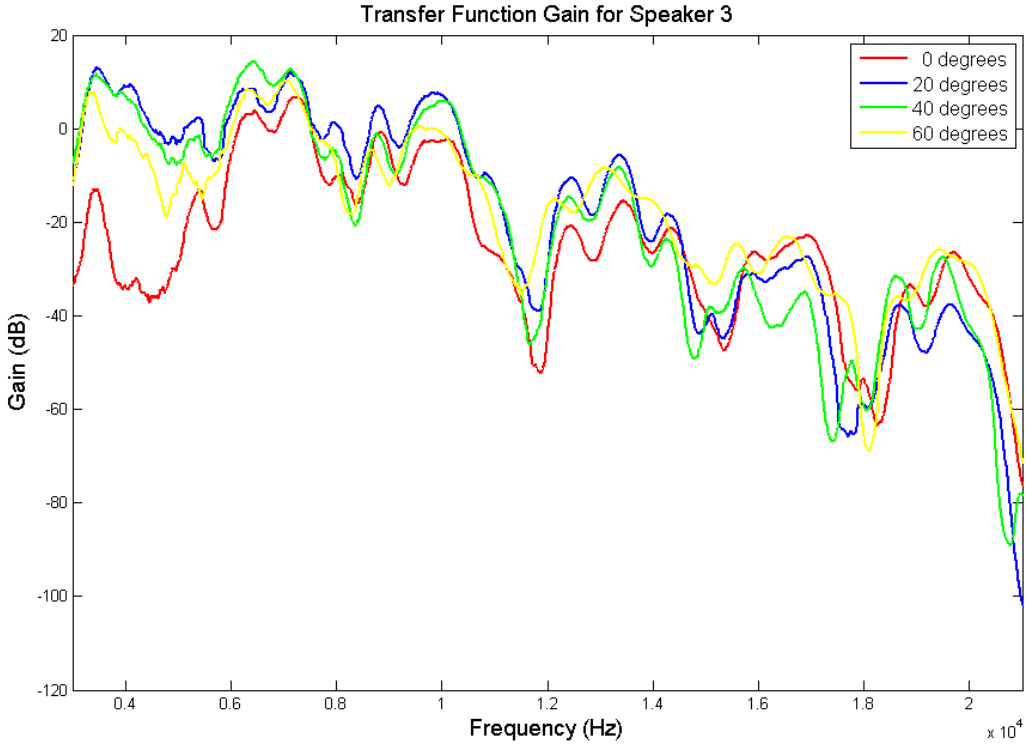


Figure 5.4. Transfer function gain for speaker 3

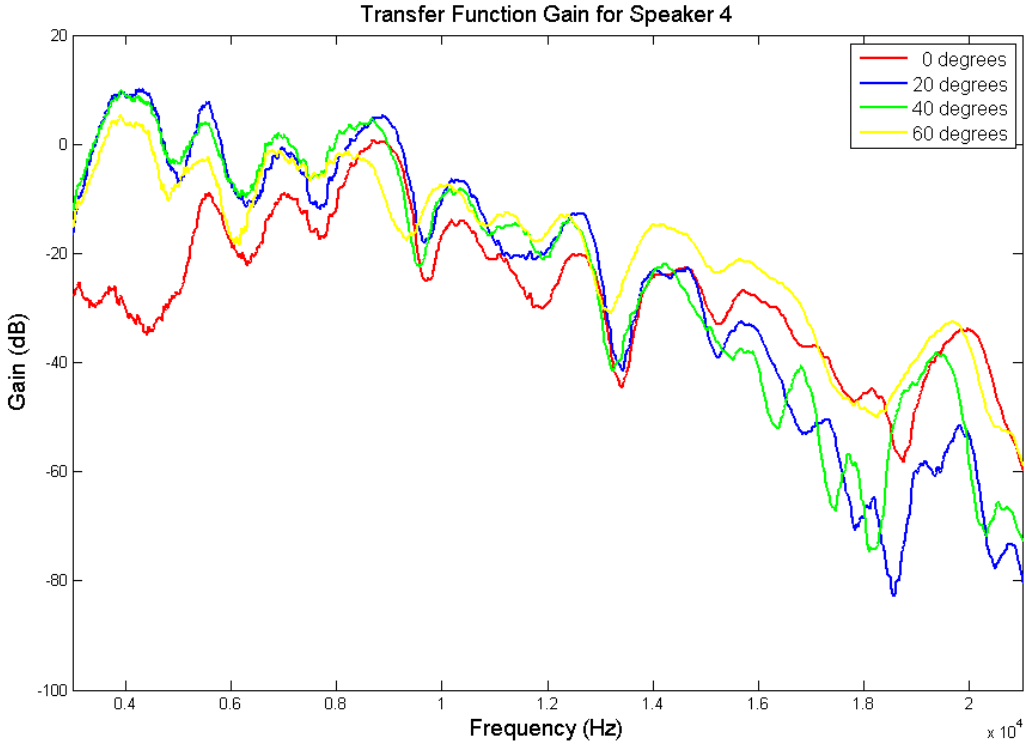


Figure 5.5. Transfer function gain for speaker 4

As it is seen from the figures, the transfer function gains show variations at different inclines. Furthermore, they do not show smooth characteristic through the frequency spectrum as it is expected. Since the transfer function gains are not only the frequency responses of speakers. They are the combination of frequency responses of the speakers, microphones and the channels.

After obtaining the transfer function gain of the system, the optimum values for the length of Gold code sequence, sampling frequency, ratio of carrier frequency to chip frequency and frequency parameters were obtained. Percentages of realizations for different parameters within different position error tolerances were observed. In order to do that a microphone was placed to a predefined location and its location was estimated for 250 times. The estimates were not separated as valid or non valid as in (Prieto, et al. 2009). In that paper, the estimates that have more than 5 cm position errors are considered as non valid readings. Therefore they were rejected by the system and not considered in the error distribution. Despite that in location system that we have proposed, all estimates were considered in order to see the performance of the system.

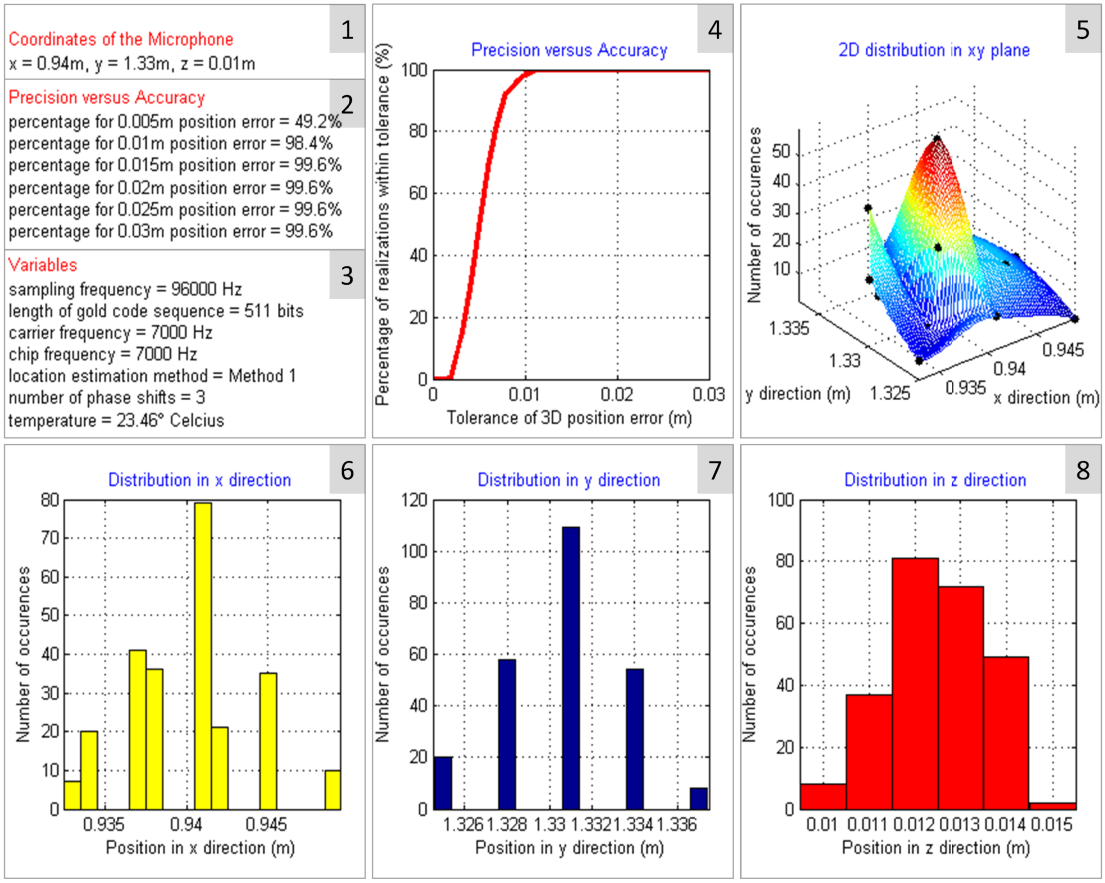


Figure 5.6. Sample localization performance screen for a sample position

For easy and intelligible display, localization performance screens are constituted for each value of each variable and attached to the appendices. For instance, Figure 5.6 illustrates a sample screen. Each screen is constituted of eight partitions. Three partitions illustrate data and the rest illustrate graphs. The partitions can be listed as;

1. Coordinates of the microphone data partition

   This partition gives information about location of the microphone in x, y and z coordinates.
2. Precision versus accuracy data partition

   This partition gives data obtained from precision versus accuracy graph. It gives the percentage of realizations within tolerance of 3D position error that starts from 0.5 cm to 3 cm by increasing 0.5 cm each.
3. Variables data partition

   This partition gives information about variables that are used in that test. Amplitudes of data signals are not given, since they are taken as one for all tests. Instead, the temperature of the environment is given.
4. Precision versus accuracy graph

   In forth partition of the screen, precision versus accuracy graph is illustrated. The graph shows percentage of realizations within tolerance for a given maximum allowed 3D position error.
5. 2D distribution in xy-plane graph

   In the fifth partition of the screen, 2D distribution in xy-plane graph is illustrated. Number of occurrences for different x and y pairs are computed and plotted.
6. Distribution in x-direction graph

   Distribution in x-direction graph is placed into the sixth partition. It shows the distribution of 3D position error in the x-direction within 3 cm tolerance.
7. Distribution in y-direction graph

   Distribution in y-direction graph is placed into the seventh partition. It shows the distribution of 3D position error in the y-direction within 3 cm tolerance.
8. Distribution in z-direction graph

   Distribution in z-direction graph is placed into the eighth partition. It shows the distribution of 3D position error in the z-direction within 3 cm tolerance.

First, the performance of the system corresponding to the change in length of Gold code sequence was evaluated. The length was increased from 31 bits to 2047 bits while the other variables were fixed. Sampling frequency was taken 96000 Hz. Carrier and chip frequencies were taken 15000 Hz. Original data signal and two shifted versions were used in correlation and Method II was applied for estimating the location. Figure 5.7 depicts the performance of the system with respect to the chance in length of the Gold code sequence.

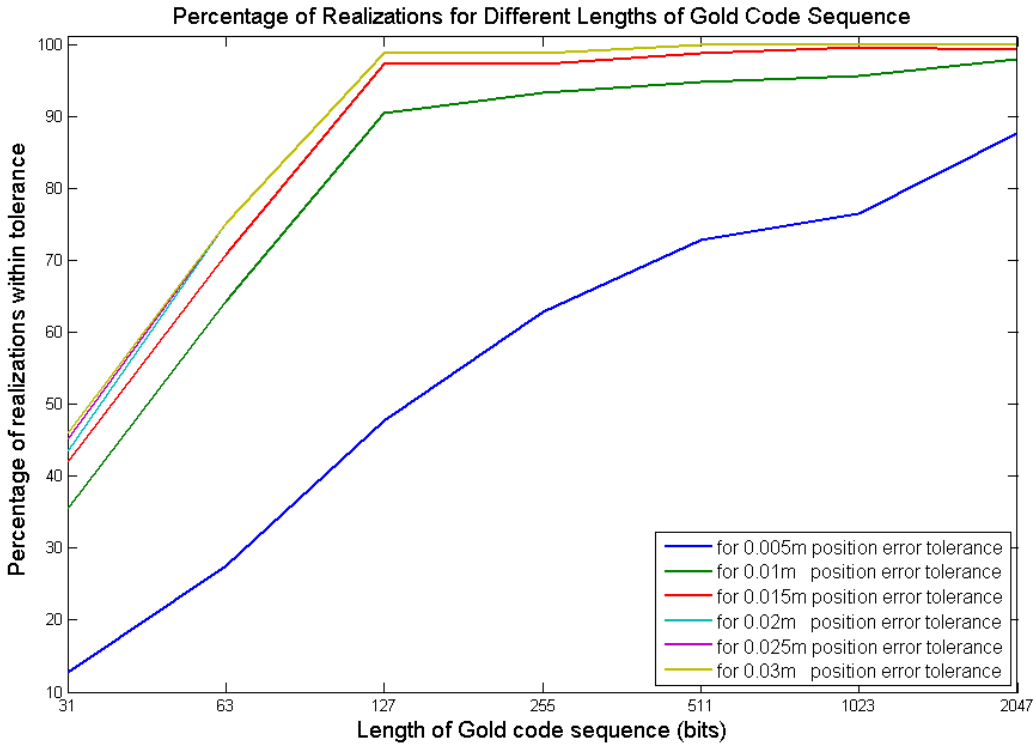


Figure 5.7. Performance of the system against the length of Gold code sequence

If the graph is examined, it is seen that 127 bits and 256 bits Gold codes exhibit substantially close results among them. Besides that, there is no significant change after 511 bits. So 511 bits is sufficient to have accurate results. In addition to that 127 bits may be chosen in order to reduce computational time. Because of these reasons, 127 bits and 511 bits Gold codes were selected. The localization performance screens related to this graph were attached to Appendix A.

Second, the performance of the system corresponding to change in sampling frequency was evaluated. The sampling frequency was taken 44100 Hz, 48000 Hz and 96000 Hz, respectively. Length of Gold code sequence was selected as 127 bits. Carrier frequency, chip frequency and number of phase shifts were taken the same with the first case. Method I was applied for estimating the location. Figure 5.8 depicts the performance of the system with respect to the chance in sampling frequency.

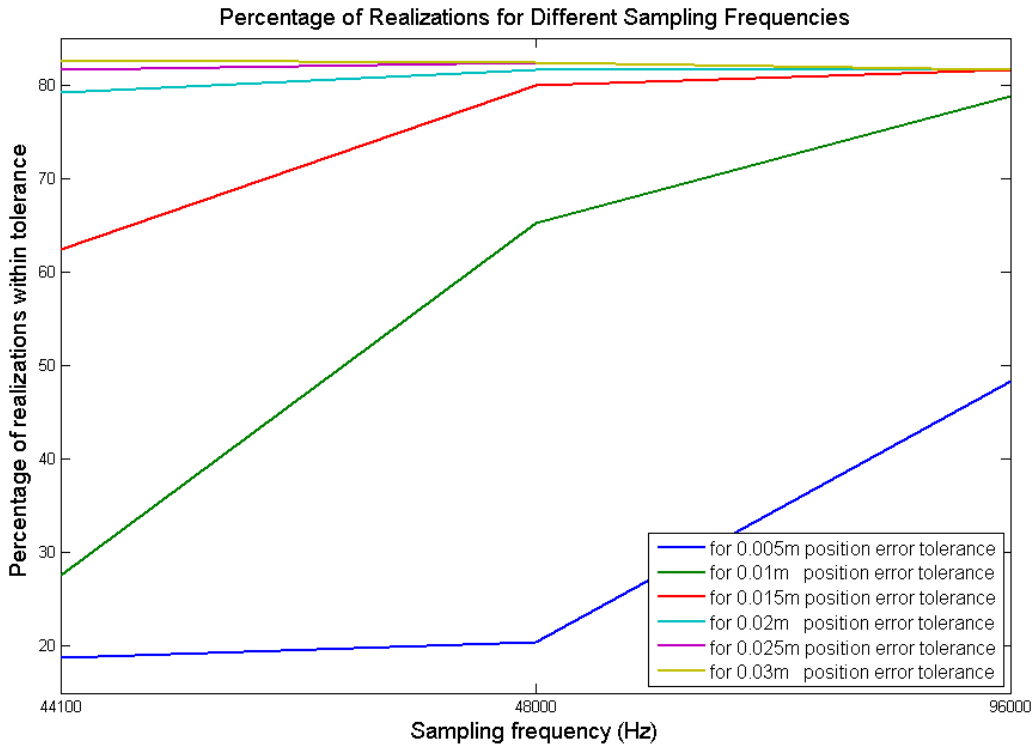


Figure 5.8. Performance of the system against to sampling frequency

Three sampling frequencies showed approximately the same performance for 3D position error tolerances of higher than 1.5 cm, but for lower tolerances 96000 Hz sampling frequency showed a better performance as it can be seen from the graph. The reason is that a distance can be measured with finer resolution by selecting a higher sampling frequency compared to lower ones. In addition to that, the correlation gives better results with higher sampling frequencies. Therefore 96000 Hz was selected as sampling frequency. The localization performance screens related to sampling frequency are attached to Appendix B.

Third, the performance as a function of the ratio of carrier frequency to chip frequency was evaluated. Carrier frequency was selected as 15000 Hz and chip frequency got values corresponding to the ratio. The other variables were selected as in the previous one. Figure 5.9 depicts the performance of the system with respect to the chance in ratio between carrier frequency and chip frequency.

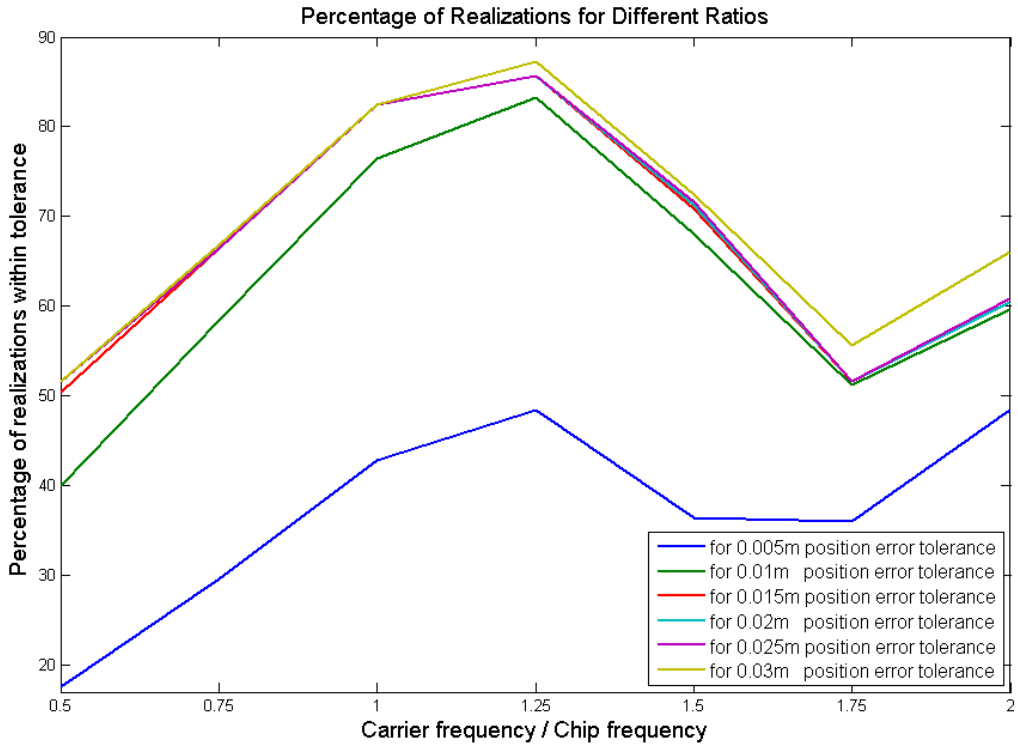


Figure 5.9. Performance of the system against the ratio of carrier frequency to chip frequency

It is obvious that ratio 1 and ratio 1.25 gave better results compared to others. For computational convenience ratio 1, which means carrier frequency and chip frequency take the same value, was selected. Related localization performance screens are attached to Appendix C.

Forth, the performance of system was evaluated against the frequency. Carrier and chip frequencies took the same values from 5 kHz to 22 kHz. All the other variables were taken the same as in the previous case. Figure 5.10 depicts the performance of the system with respect to the chance in frequency.

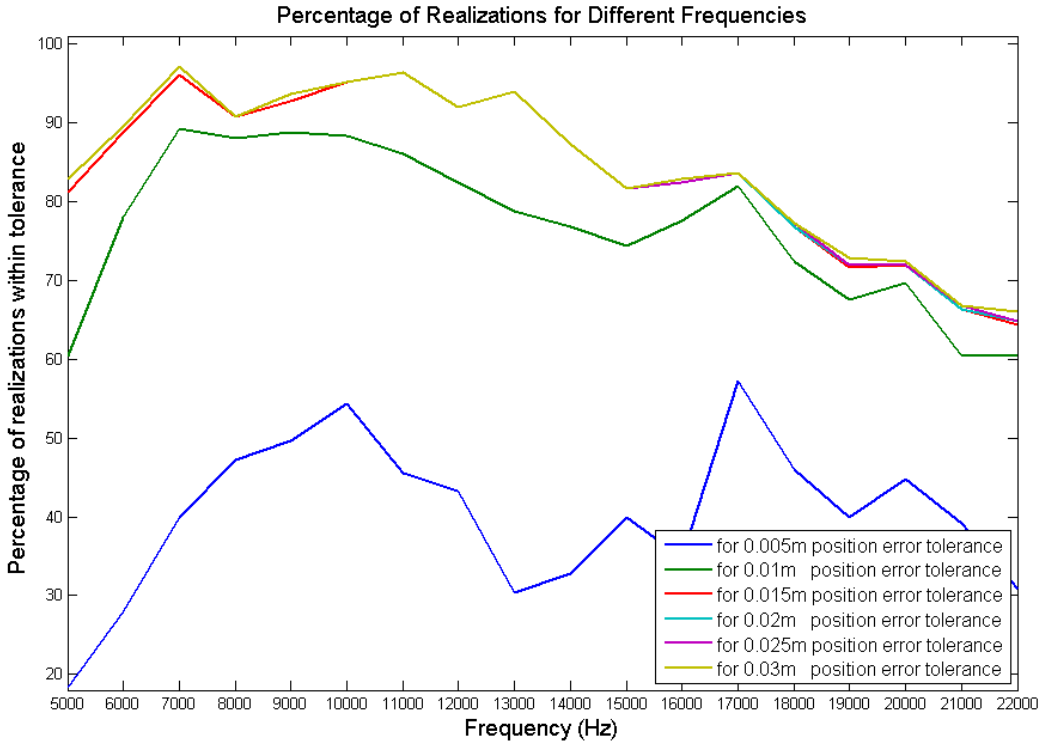


Figure 5.10. Performance of the system against the frequency

Remarkable results were obtained at frequencies 7 kHz and 17 kHz. The system exhibited the most precise result at 7 kHz; on the other hand, 17 kHz can also be chosen because of ease in computation and requirement of less computation time. Related localization performance screens are attached to Appendix D.

Methods for location estimation and number of phase shifts were also examined. Method I gives good results when length of Gold code sequence is long, and Method II gives good results when length of Gold code sequence is shorter. In the case that the length of Gold code sequence is long, the correlations show better properties. So, the four distances can be measured and the four locations can be estimated accurately. Applying Method I that takes the average of the four location estimates gives better results than applying Method II. On the other hand, in the case that the length of Gold code sequence is short, the correlations do not show properties as good as in the previous case. So, one of the distances, usually the longest one, can not be measured

accurately enough. Therefore applying Method II instead of Method I robustifies the location estimate.

The number of phase shifts is also effective on the performance of the system. When the number of phase shifts is increased, the performance of the system is increasing because; the number of phase shifts improves the correlation property. However, it is not much effective in the case that the correlation property is already good. Hence the number of phase shifts can be taken small in the case that Gold code sequence is long. This recommendation is essential in order to decrease the required computation and elapsed time.

After these evaluations, two sets of variables were selected. The first set of variables are chosen in order to investigate the system's accuracy with reasonable computation time and update rate whereas the second set of variables are aimed to investigate the system's fastness without sacrificing the accuracy .

In the first set, the variables were selected as;

- 96000 Hz for sampling frequency,
- 511 bits for length of Gold code sequence,
- 7000 Hz for carrier and chip frequencies,
- Method I for location estimation method,
- 3 for number of phase shifts.

In the second the set, the variables were selected as;

- 96000 Hz for sampling frequency,
- 127 bits for length of Gold code sequence,
- 17000 Hz for carrier and chip frequencies,
- Method II for location estimation method,
- 1 for number of phase shifts.

After selecting the sets of variables, the test points were defined. To minimize the number of the test points, the work area was divided into four rectangular regions as shown in Figure 5.11.

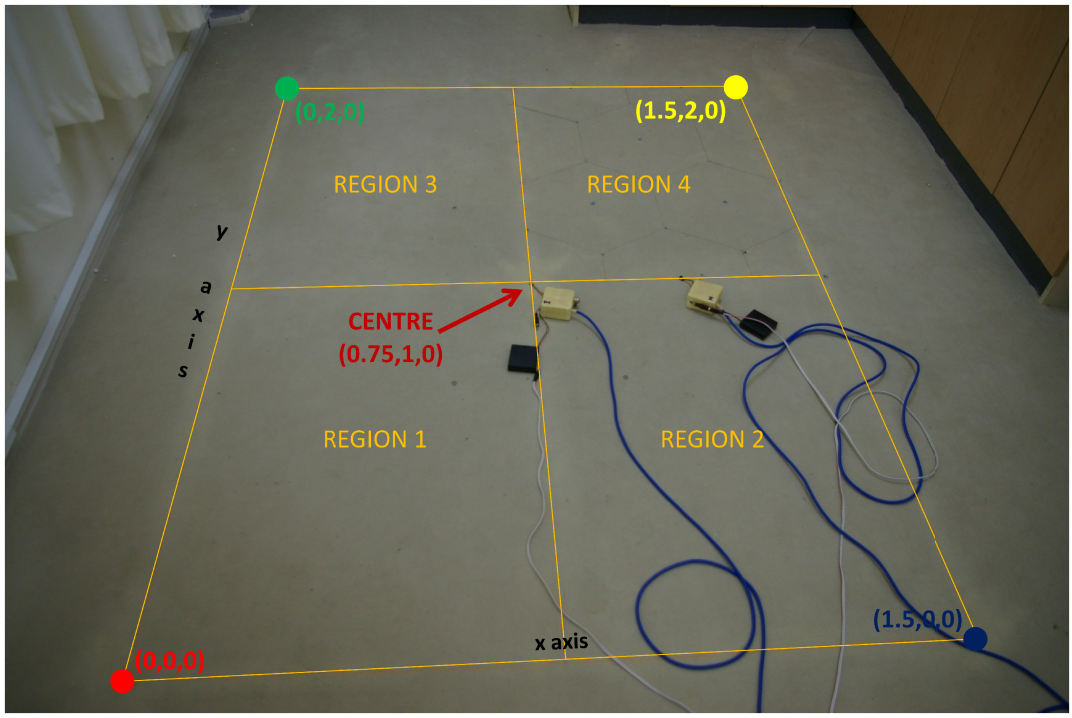


Figure 5.11. The regions of the work area

In order to validate that the defined regions are equivalent regarding the performance of the proposed location system, four points were selected from different regions. The selected points are illustrated in Figure 5.12.

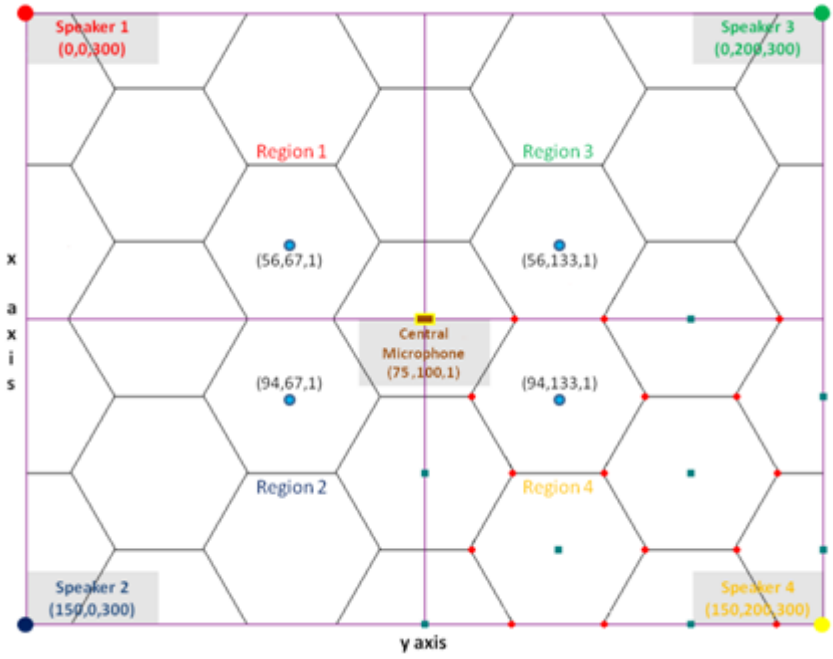


Figure 5.12. The points taken from each region

Precision versus accuracy graphs of the four points were plotted over and over as one graph. Graphs for the first and second sets of variables are illustrated in Figure 5.13 and Figure 5.14, respectively. Related localization performance screens are attached to the Appendix E and F.

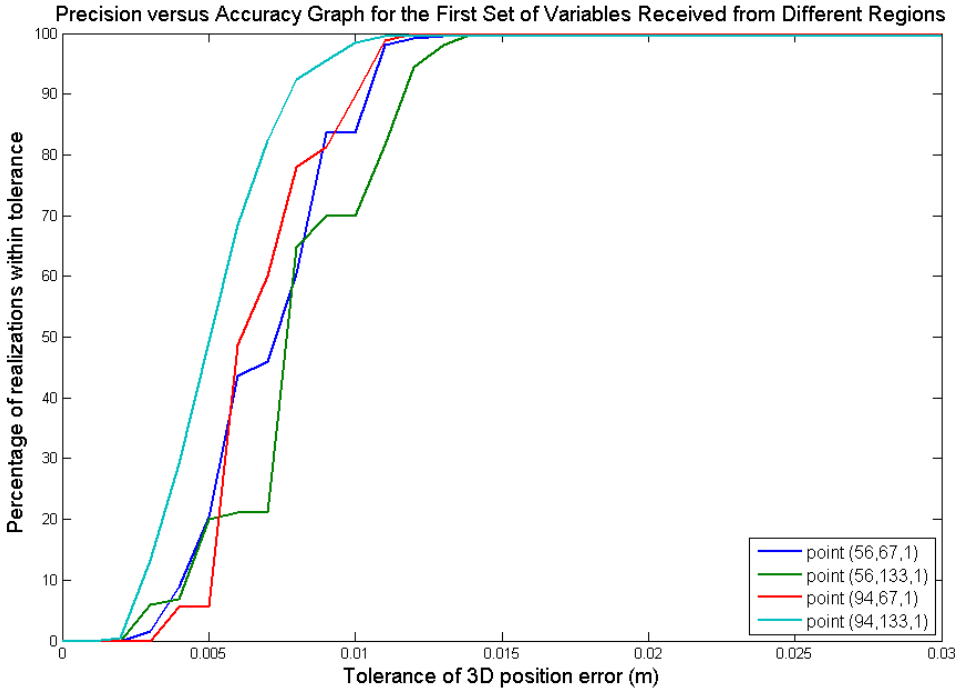


Figure 5.13. Precision versus accuracy of the four points for the first set of variables

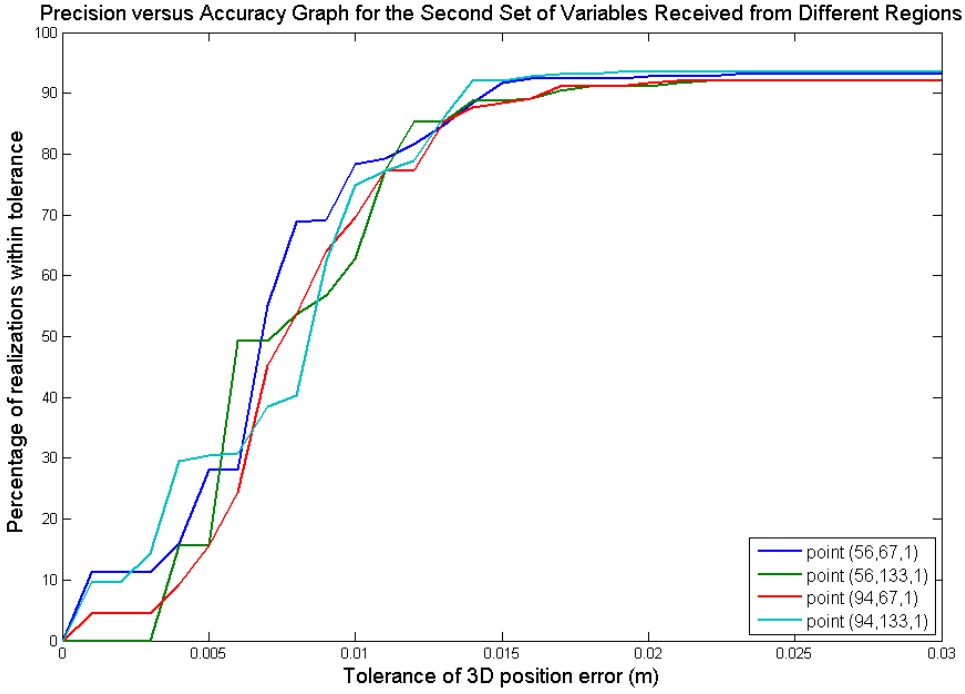


Figure 5.14. Precision versus accuracy of the four points for the second set of variables

Comparing Figures 5.13 and 5.14 it is observed that there is somewhat less variation in the performance curve for the second set of variables which means that the degree of equivalence of the four regions is higher with the second set of parameters. Nevertheless, the performance curves with the first set of parameters also do not show significant variation.

Regarding the considerably close results obtained for the points in both cases, it was deduced that the regions can be assumed as equivalent. So, it is decided to use test points only in Region 4. A group of test points were selected at the ground level that is 3 meters below the speakers and another group of test points were selected at a level which is 1 meter above the ground level. Figure 5.15 illustrates the ground level test points. The ground level test points were taken as the centers of hexagons as it is seen in figure.

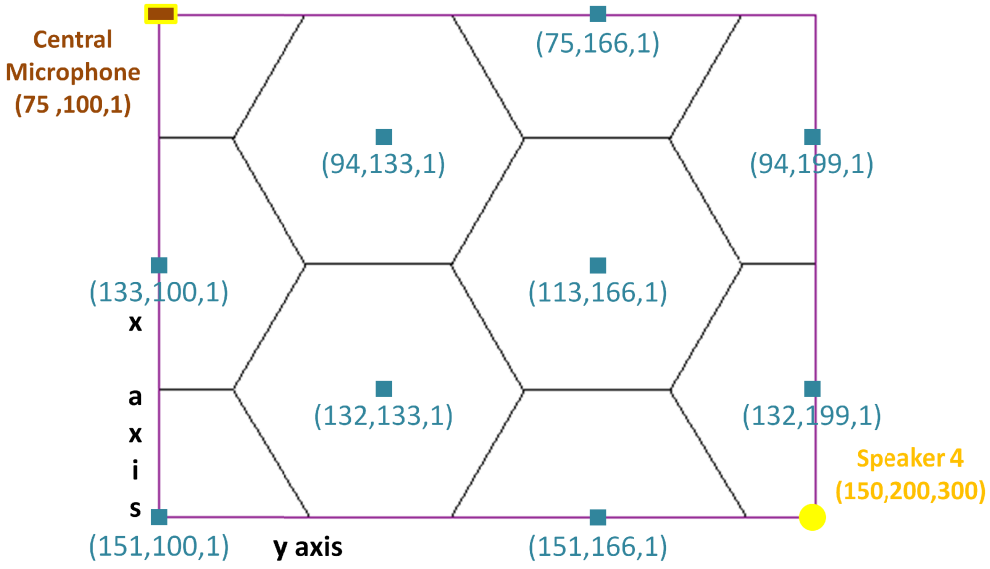


Figure 5.15. Ground level test points

The precision results corresponding to several accuracy levels obtained from ground level test points were collected in Table 5.1. They were sorted into two groups: precision results for the first set of variables and precision results for the second set of variables. Related localization performance screens of the first set and the second set of variables are attached to Appendix G and Appendix H, respectively.

Table 5.1. Precisions at the ground level

| Points | First set of variables | | | | | | Second set of variables | | | | | |
|---|---|---|---|---|---|---|---|---|---|---|---|---|
| | 0.05m | 0.01m | 0.015m | 0.02m | 0.025m | 0.03m | 0.05m | 0.01m | 0.015m | 0.02m | 0.025m | 0.03m |
| 113,100,1 | 37.6% | 97.6% | 99.6% | 99.6% | 99.6% | 99.6% | 9.6% | 77.6% | 95.2% | 97.2% | 97.6% | 97.6% |
| 151,100,1 | 17.2% | 91.2% | 100% | 100% | 100% | 100% | 22% | 65.2% | 90.4% | 92.8% | 93.2% | 93.2% |
| 94,133,1 | 49.2% | 98.4% | 99.6% | 99.6% | 99.6% | 99.6% | 30.4% | 74.8% | 92% | 93.6% | 93.6% | 93.6% |
| 132,133,1 | 51.2% | 99.2% | 100% | 100% | 100% | 100% | 46% | 69.2% | 83.6% | 87.2% | 87.6% | 87.6% |
| 75,166,1 | 16% | 92.4% | 99.6% | 99.6% | 99.6% | 99.6% | 12.8% | 60.8% | 77.2% | 77.6% | 77.6% | 77.6% |
| 113,166,1 | 13.6% | 80% | 98.8% | 98.8% | 98.8% | 98.8% | 8% | 54% | 72.4% | 86.3% | 86.8% | 86.8% |
| 151,166,1 | 0% | 64.8% | 99.2% | 99.2% | 99.2% | 99.2% | 6% | 19.2% | 84.4% | 89.2% | 90.8% | 90.8% |
| 94,199,1 | 0% | 20.4% | 79.6% | 98.8% | 99.6% | 99.6% | 0% | 42% | 73.6% | 79.2% | 80% | 80% |
| 132,199,1 | 0% | 47.2% | 93.2% | 100% | 100% | 100% | 1.2% | 30.8% | 68.8% | 82% | 83.2% | 83.2% |

The precision results of the first set of variables are plotted for the accuracies 0.02 m and 0.03 m in order to illustrate the precision distributions in Figure 5.16 and Figure 5.17, respectively. These precision distributions are such close that the difference can not be observed from the graphs. The precision results vary from 98.8% to 100% which means that the system is very precise for the accuracies of 0.02m and higher at the ground level.

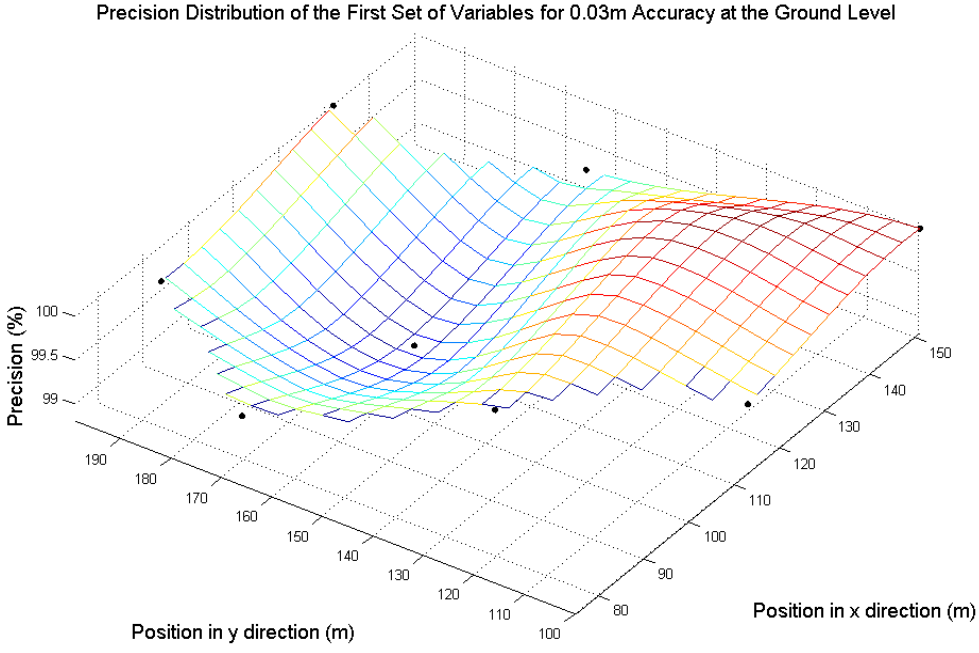


Figure 5.16. Precision distribution of the first set of variables for 0.03 m accuracy at the ground level

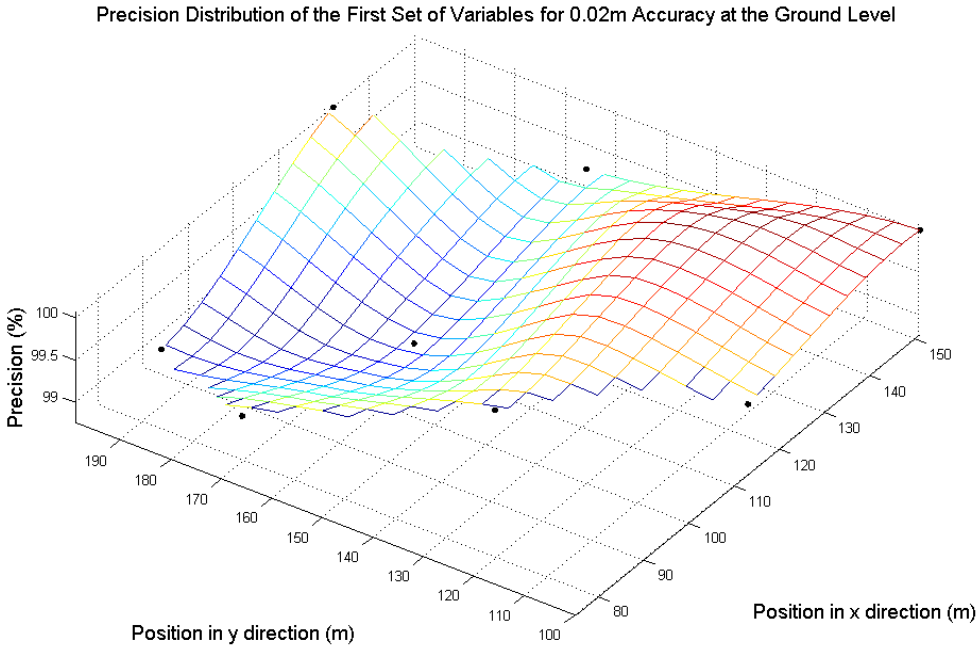


Figure 5.17. Precision distribution of the first set of variables for 0.02 m accuracy at the ground level

The precision results of second set of variables are also plotted for the accuracies of 0.02 m and 0.03 m in Figures 5.18 and 5.19, respectively. The precision distributions are very close again. The precision results vary from 77.6% to 97.6%.

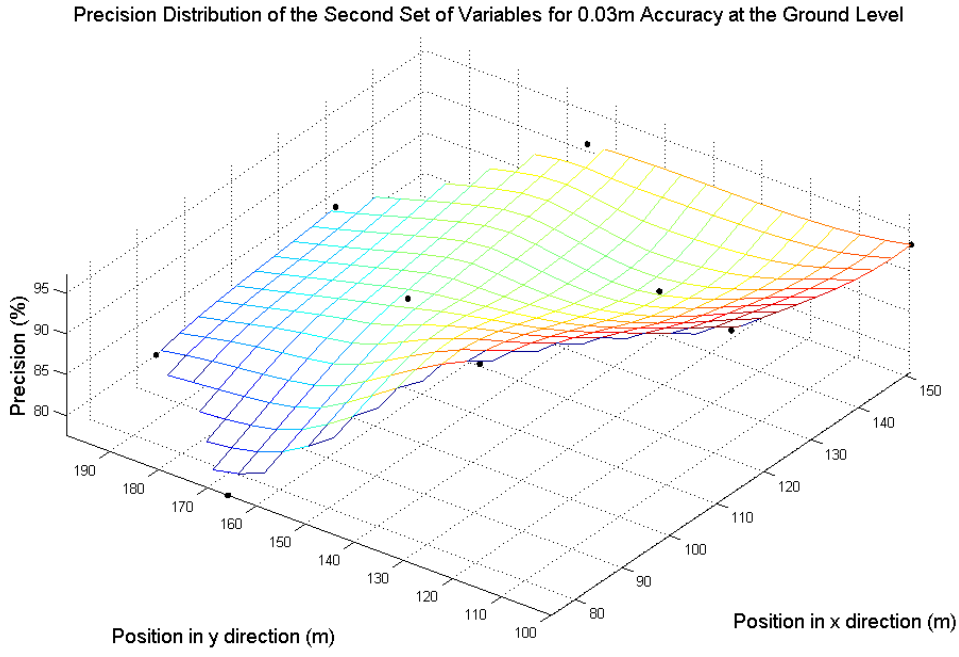


Figure 5.18. Precision distribution of the second set of variables for 0.03 m accuracy at the ground level

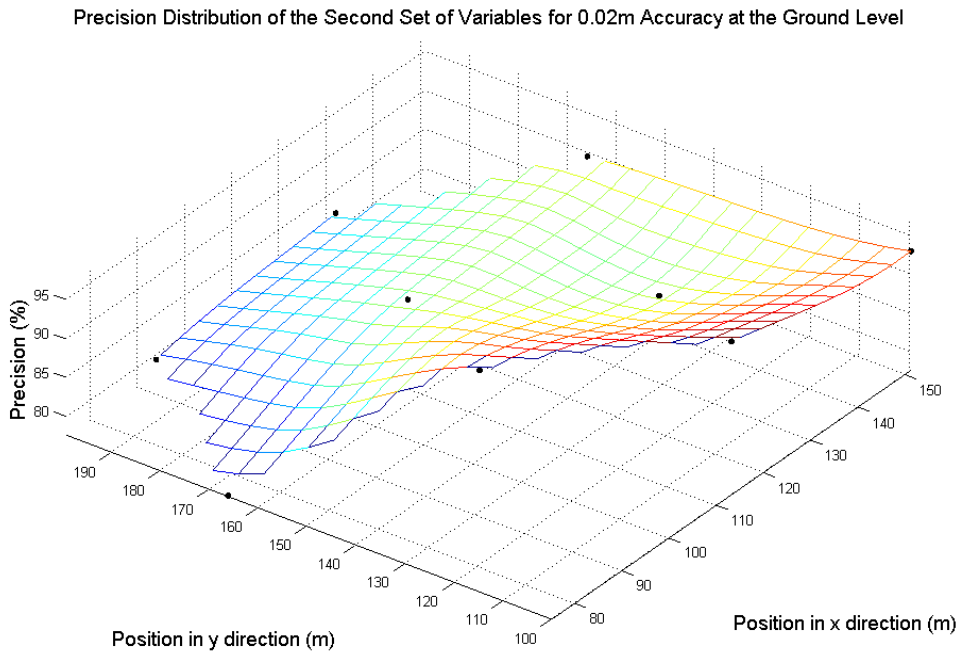


Figure 5.19. Precision distribution of the second set of variables for 0.02 m accuracy at the ground level

The upper level test points were taken as the corners of hexagons as it is seen in Figure 5.20.

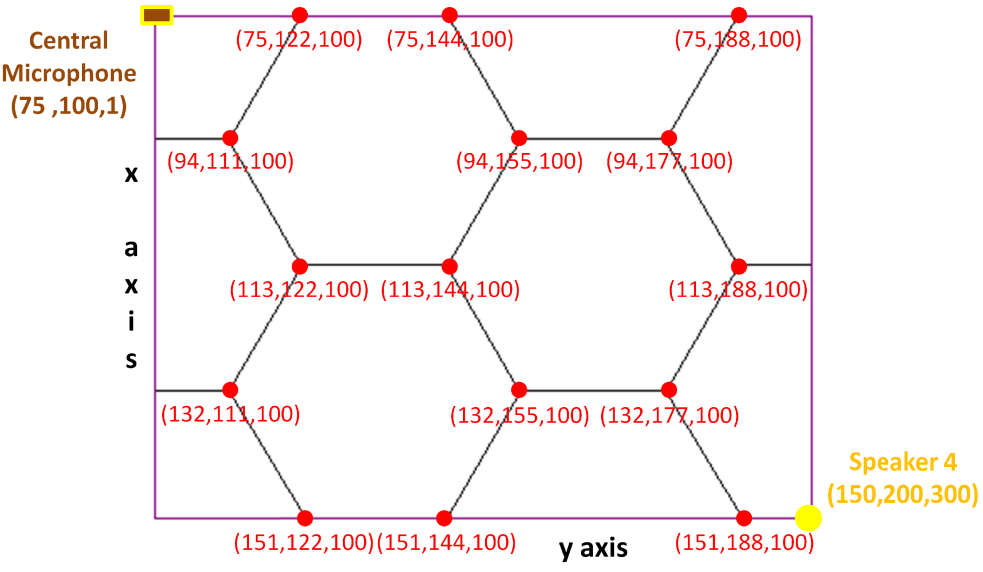


Figure 5.20. Upper level test points

The precision results obtained from upper level test points are illustrated in Table 5.2 which is constructed in a similar way as Table 5.1. Related localization performance screens of the first set and the second set of variables are attached to Appendix I and J, respectively.

Table 5.2. Precisions at the upper level

| Points | First Set of Variables | | | | | | Second Set of Variables | | | | | |
|---|---|---|---|---|---|---|---|---|---|---|---|---|
| | 0.05m | 0.01m | 0.015m | 0.02m | 0.025m | 0.03m | 0.05m | 0.01m | 0.015m | 0.02m | 0.025m | 0.03m |
| 94,111,100 | 0% | 14.8% | 100% | 100% | 100% | 100% | 0% | 9.2% | 76.8% | 86% | 86.8% | 86.8% |
| 132,111,100 | 31.2% | 98.8% | 99.6% | 99.6% | 99.6% | 99.6% | 0.8% | 48.4% | 79.2% | 83.6% | 84% | 84% |
| 75,122,100 | 0.4% | 75.2% | 100% | 100% | 100% | 100% | 0.4% | 27.2% | 82.8% | 87.6% | 87.6% | 88% |
| 113,122,100 | 6.4% | 99.2% | 100% | 100% | 100% | 100% | 12.8% | 82.8% | 88% | 88% | 88% | 88% |
| 151,122,100 | 36.8% | 99.2% | 100% | 100% | 100% | 100% | 12% | 56% | 79.2% | 80% | 80.8% | 81.2% |
| 75,144,100 | 0% | 5.6% | 58.8% | 99.2% | 100% | 100% | 0% | 1.2% | 30.4% | 69.6% | 75.6% | 76% |
| 113,144,100 | 0.8% | 79.2% | 99.2% | 99.2% | 99.2% | 99.2% | 0% | 58% | 80.4% | 82% | 82.4% | 82.4% |
| 151,144,100 | 16% | 84% | 99.6% | 99.6% | 99.6% | 99.6% | 6% | 51.2% | 68.4% | 72.8% | 72.8% | 73.2% |
| 94,155,100 | 2% | 70.4% | 99.2% | 99.2% | 99.2% | 99.2% | 13,6% | 50.8% | 63.2% | 65.2% | 66% | 66.4% |
| 132,155,100 | 0% | 6.8% | 53.2% | 96% | 100% | 100% | 0.4% | 11.6% | 43.6% | 68% | 76% | 76% |
| 94,177,100 | 0% | 0.4% | 47.2% | 96.8% | 100% | 100% | 5.6% | 26.8% | 60% | 75.2% | 76% | 76.4% |
| 132,177,100 | 0% | 0.4% | 62.8% | 94.4% | 99.2% | 99.2% | 1.6% | 16% | 48.8% | 55.2% | 57.6% | 58.8% |
| 75,188,100 | 0% | 2.4% | 49.6% | 98.4% | 99.6% | 99.6% | 1.6% | 35.2% | 55.6% | 58.4% | 58.8% | 58.8% |
| 113,188,100 | 0% | 53.2% | 96.4% | 99.2% | 99.6% | 99.6% | 8% | 37.6% | 48.8% | 50.8% | 50.8% | 50.8% |
| 151,188,100 | 0% | 0.8% | 64.4% | 95.6% | 98.8% | 98.8% | 4.4% | 29.6% | 47.6% | 52% | 53.6% | 54.8% |

The precision results of first set of variables are plotted for the accuracies 0.02 m and 0.03 m in Figure 5.21 and Figure 5.22, respectively. The precision results vary from 95.6% to 100%. Although, precision reduces a bit at the upper level test points compared to ground level test points, it is again sufficiently good.

The precision results of second set of variables are also plotted for the accuracies 0.02 m and 0.03 m in Figure 5.23 and Figure 5.24, respectively. Precision distributions for accuracies 0.03 m and 0.02 m are very close as well. The precision results vary from 50.8% to 88%.

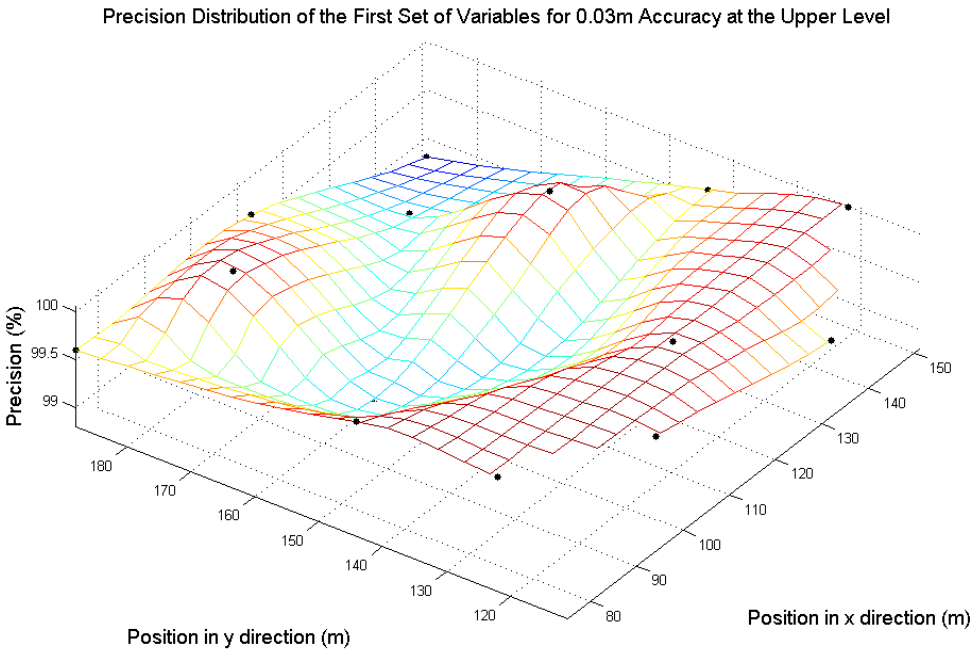


Figure 5.21. Precision distribution of the first set of variables for 0.03 m accuracy at the upper level

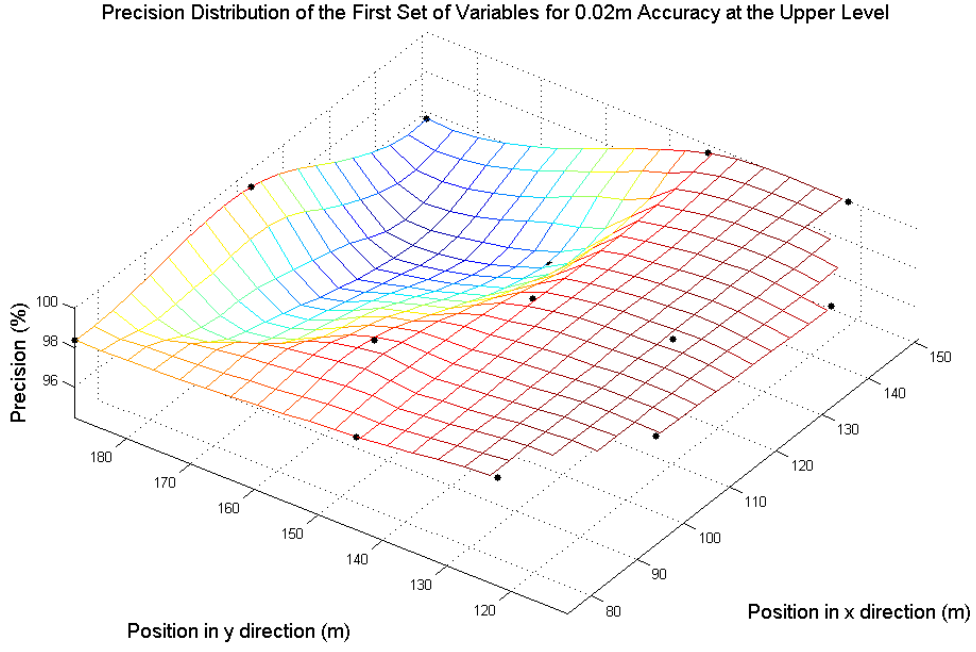


Figure 5.22. Precision distribution of the first set of variables for 0.02 m accuracy at the upper level

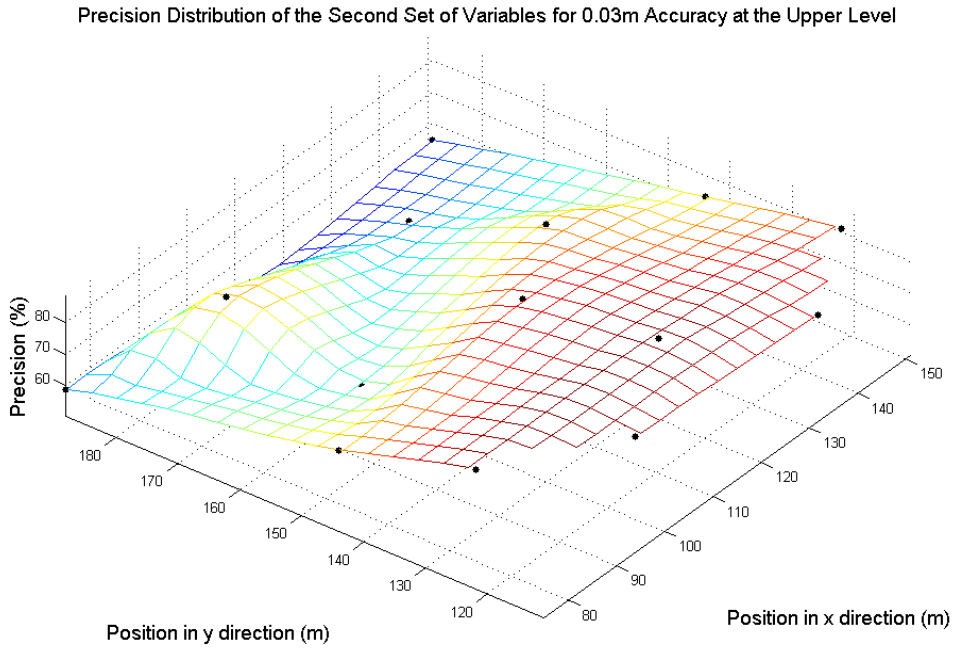


Figure 5.23. Precision distribution of the second set of variables for 0.03 m accuracy at the upper level

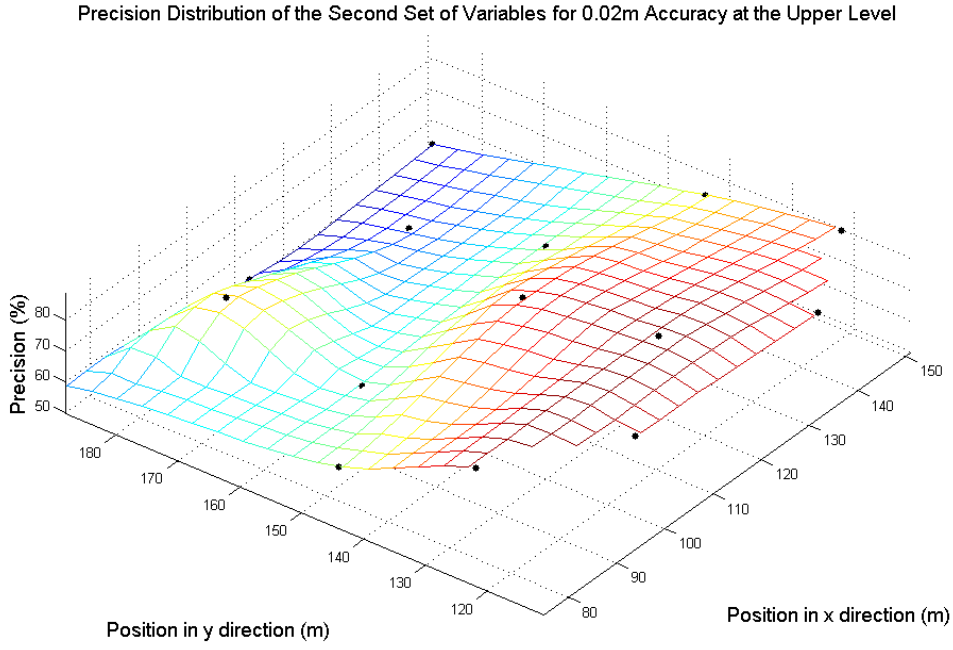


Figure 5.24. Precision distribution of the second set of variables for 0.02 m accuracy at the upper level

After these results were obtained, a conclusion can be drawn as;

1. Precision decreases when the test point is moved away from the centre,
2. Precision decreases while the test point is getting closer to speakers level in height,
3. Results of the first set of variables for all tests points show that the proposed system can be used for the applications that require approximately 2 cm accuracy with substantially precise results,
4. Result of the second set of variables, that is less time consuming and less precise set-up, for all tests points shows the precision distribution for this structure more obviously,
5. Results were examined up to 3 cm position error. Consequently, it was seen that the precision does not vary much from 2 cm accuracy to 3 cm accuracy.

After examining the precision results, the precision versus accuracy graphs were plotted in order to see the overall performance of the system. Firstly, precision versus accuracy at ground level is illustrated in Figure 5.25.

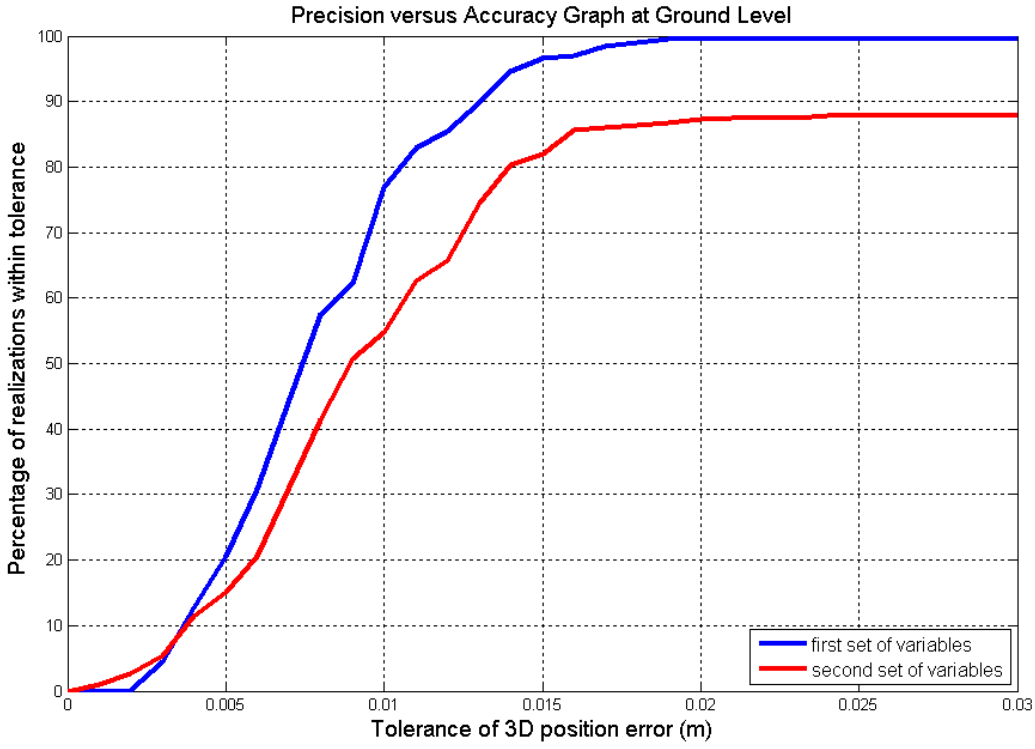


Figure 5.25. Precision versus accuracy graph at ground level for different set of variables

As it is seen, first set of variables can achieve 100% precision at 1.9 cm accuracy, while the second set of variables can reach only about 88% precision at 3 cm accuracy at the ground level.

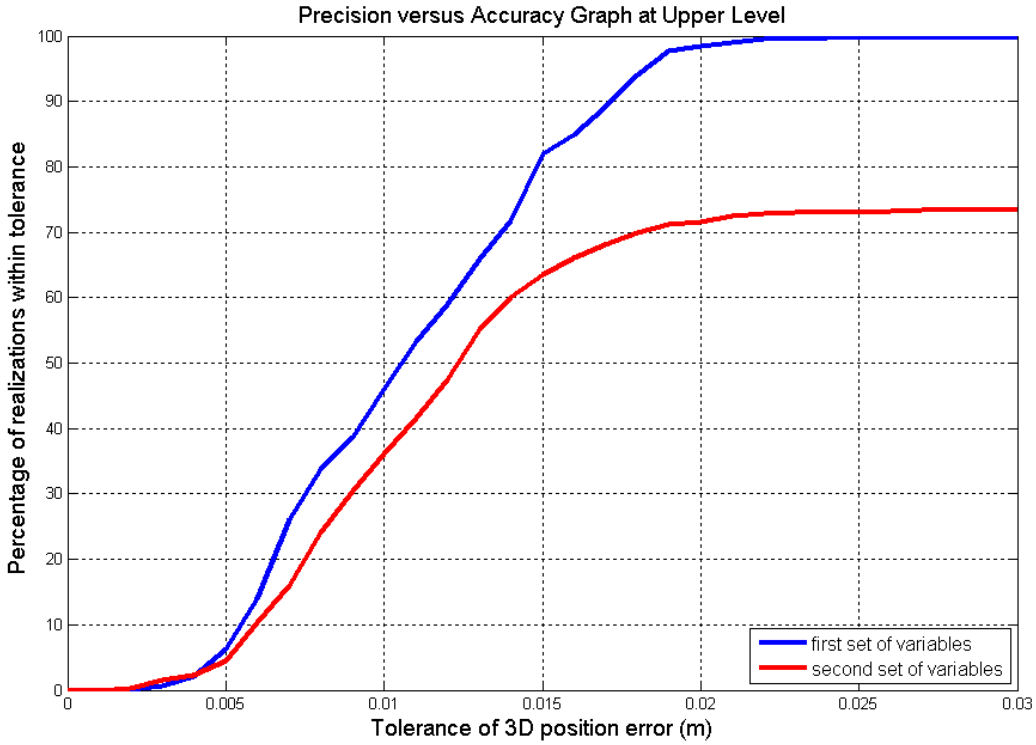


Figure 5.26. Precision versus accuracy graph at upper level for different set of variables

Similarly at the upper level, the first set of variables can achieve 100% precision at 2.2 cm accuracy, while the second set of variables can reach only about 74% precision at 3 cm accuracy as it is seen in Figure 5.26. These results also verify the second statement that has been made above.

Secondly, the precision versus accuracy graphs for the first set of variables and for the second set of variables are illustrated in Figure 5.27 and 5.28, respectively. The graphs illustrate the results for ground level, upper level and the total of them.

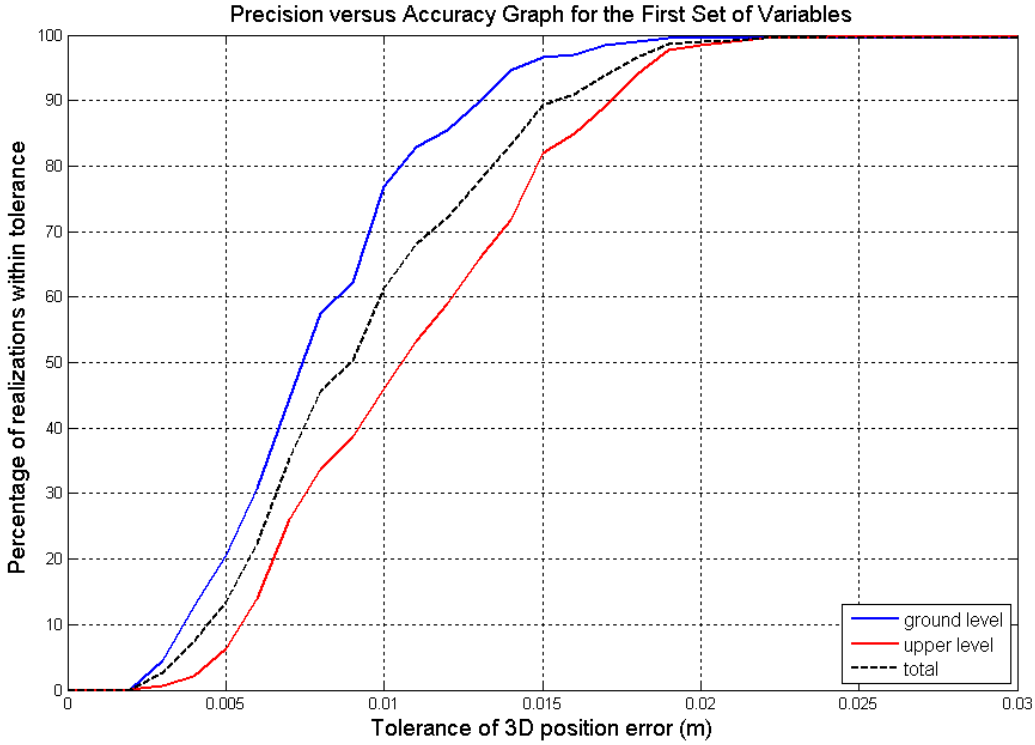


Figure 5.27. Precision versus accuracy graph for the first set of variables

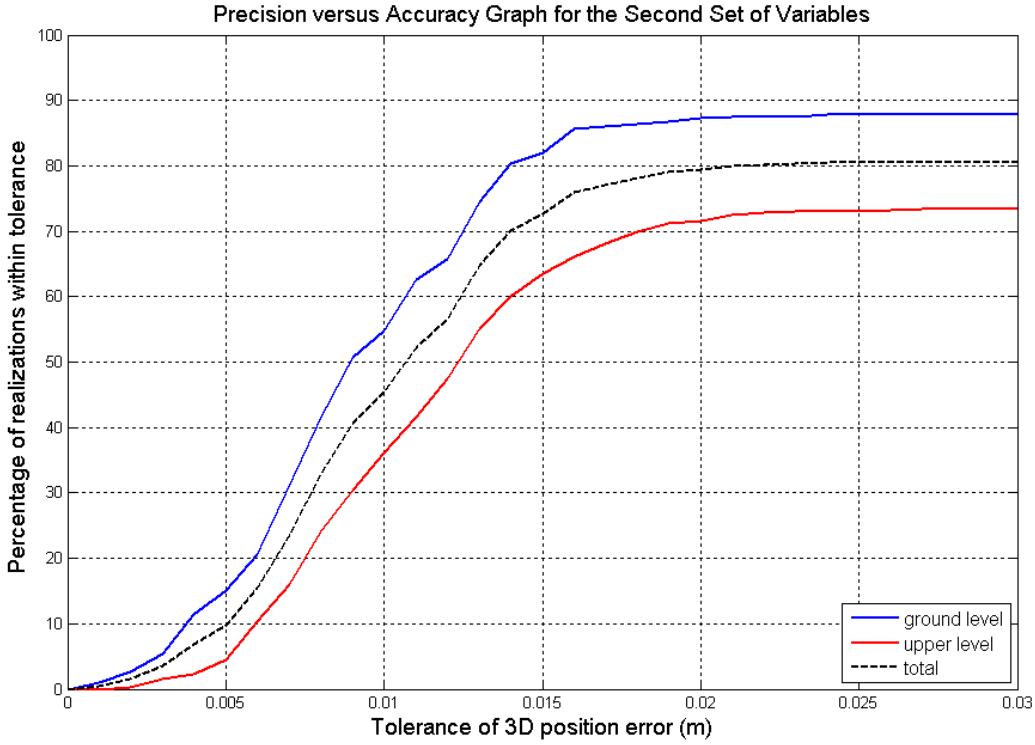


Figure 5.28. Precision versus accuracy graph for the second set of variables

Last two figures depict that ground level and upper level measurements can achieve 100% precision for the first set of variables since the first set of variables provides sufficient processing gain, while the second set of variables does not. With the second set of variables, the ground level, upper level and total measurements can attain only 88%, 74% and 81% precision at 3 cm accuracy, respectively.

Finally, the overall precision versus accuracy graph for the first and the second sets of variables incorporating all of the measurements are illustrated in Figure 5.29.

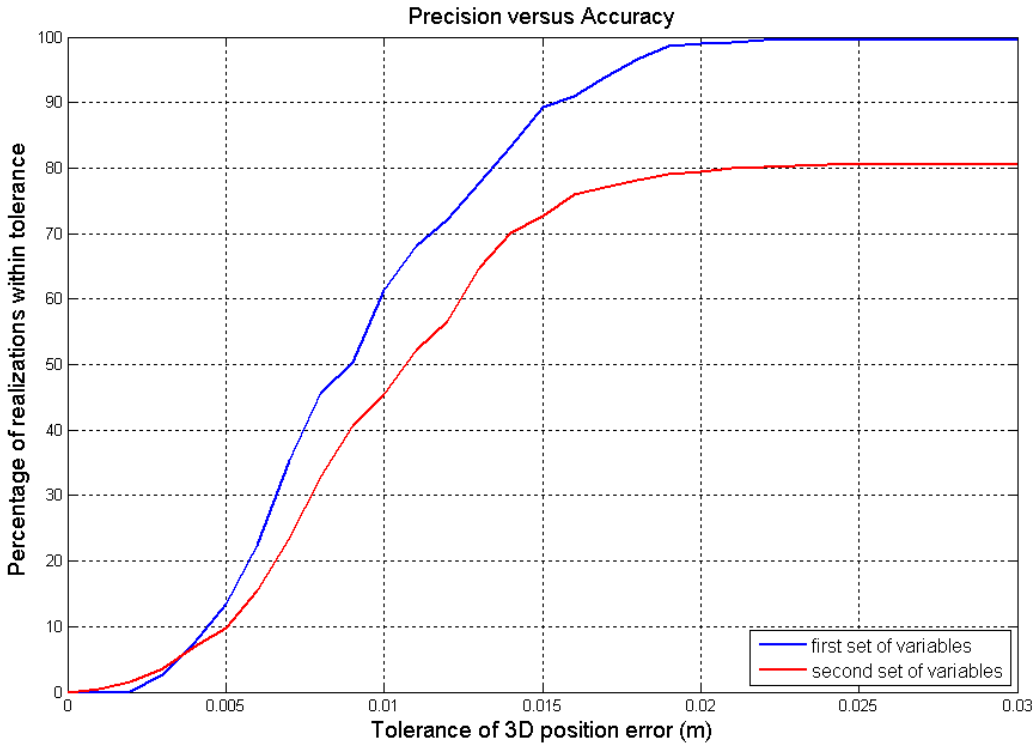


Figure 5.29. The overall precision versus accuracy graph

The first set of variables reaches 100% precision at 2.2 cm accuracy while the second set of variables reaches 81% precision at 3 cm accuracy. This overall performance evaluation demonstrates that the system that uses the first set of variables can achieve the requirement that is aimed.

The extended overall precision and accuracy graphs to 3 dm and 3 m are also illustrated in Figure 5.30 and 5.31, respectively.

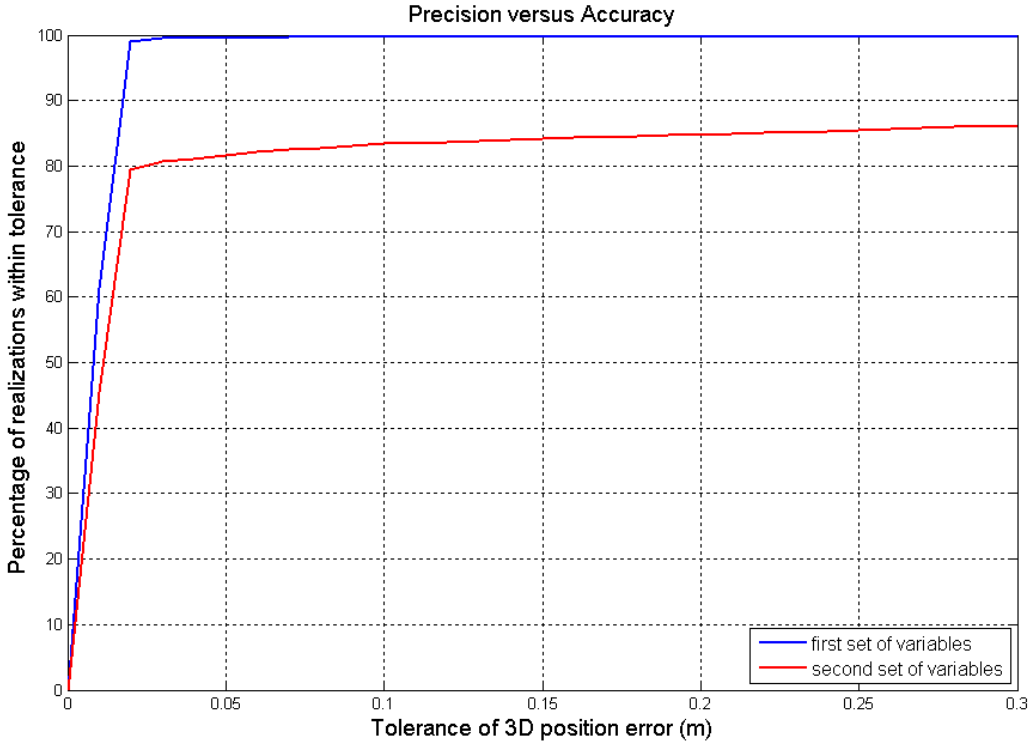


Figure 5.30. 3 dm extended overall precision versus accuracy graph

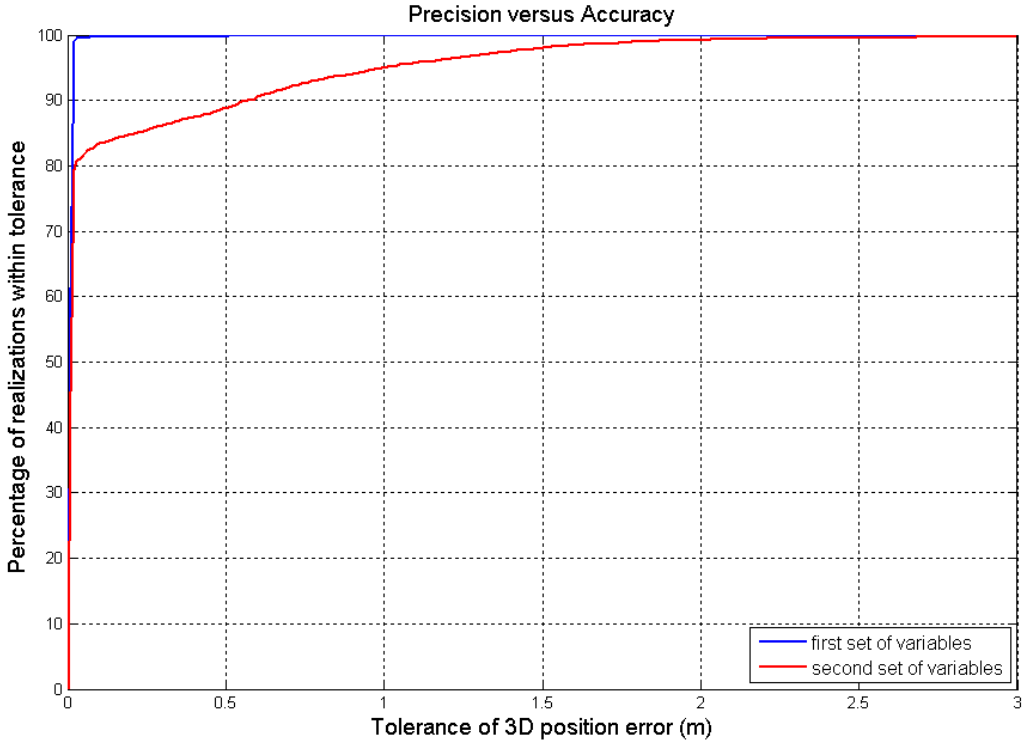


Figure 5.31. 3 m extended overall precision versus accuracy graph

Although the proposed system performs the computations in a central unit, it can be accepted as a privacy-oriented system, since the system does not emit any detectable signals and uses its transducer to receive the signals as it is mentioned in (Hazas and Hopper 2006).

If a performance comparison is made among Dolphin system, 3D-LOCUS LPS and the proposed location system, it is seen that the proposed system provides location estimation better than 2 cm accuracy within 99% precision, while Dolphin system provides accuracy about 4.9 cm within 67% returned readings in synchronous privacy-oriented mode and 3D-LOCUS system provides 13.5 mm accuracy in 95% confidence level within 94.7% valid readings in private CDMA configuration. But, the reader should not miss out that in the experiment with the proposed system the results were not separated as valid and non valid as in the other systems, so none of them was rejected in order to see the general attitude of the system. The comparison of the results shows that the proposed system provides successful results as good as the ones offered by other systems utilizing only ordinary, inexpensive equipment.

# CHAPTER 6

# CONCLUSION

In this thesis, a new indoor location system has been proposed and an implementation has been applied in order to see the overall performance of the system. The implementation has been realized using ordinary and inexpensive off-the-shelf devices. The proposed system uses acoustic signals that are phase-modulated Gold code sequences using DSSS technique. ToA is preferred for the distance measurement rather than SS because of the accuracy concern. DS-CDMA is applied to perform simultaneous distance measurements and it provides accurate results, immunity to noise and interference. There is no limitation for the number of users using the system due to the privacy oriented structure. The only limitation is the system's computational capacity.

The proposed system can be used for large area deployments like museums. In this case, the number of distinct Gold codes gains importance, since every speaker has its own unique Gold code sequence. But this challenge can be surpassed by reusing a used code where it does not affect the others as in the case of cellular communication systems.

In the proposed system, the speakers and the microphones are synchronized due to the centralized structure. However some unpredictable delays occur in the transmission of acoustic signal while creating two objects for four channels in Matlab. In order to overcome this challenge a central microphone for reference is used to find the delays.

Throughout the preparation, first, the devices that are needed for implementation were chosen and gathered together. Later, the preparation of the work area was done since the office room that is assigned was not suitable for that implementation. After these preparations, the codes were written in Matlab and a GUI was developed that allows working with different variables in an easy way.

Two methods have been proposed for location estimation. The first method uses four different position estimates obtained by trilateration technique and takes their averages to locate the microphone. In the second method, only a robust location estimate is done using three distances while the least reliable fourth distance measurement is not taken into account.

In experimental study, the transfer function gains of the system were obtained by emitting signals from each speaker. The parameter selections were done according to the obtained experimental results. As a result two set of variables were selected; one aims considerably good accuracy and the other aims fastness without sacrificing the accuracy.

Eventually, the data was collected at the defined test points. The test points were chosen from two different heights located in the fourth region defined in Figures 5.11 and 5.12. The area was divided into hexagonal sub areas. The test points in the ground level were taken as the centre of the hexagons and the test points in the upper level were taken as the corners of the hexagons. The precision tables were presented for these points. In addition, precision distribution and precision versus accuracy graphs were illustrated. The related localization performance screens illustrating the data for each test point are given in the appendices section.

The main contributions of this thesis study and differences from related work can be listed as follows:

- An accuracy of 2 cm with 99% precision was attained in the proposed system using ordinary, inexpensive off-the-shelf devices.
- A microphone was first used to find the delays of the system.
- Two methods have been proposed for location estimation.
- The real performances of the parameters were evaluated by the experimental results.
- Precision distributions of work area at two height levels were analyzed that have not been done before.
- The performances of two sets of variables were compared using precision versus accuracy graphs.
- A GUI that provides convenience for working with different variables was created with practical visual form.

As a future work, different geometric configurations can be investigated and their precision distributions can be analyzed. Moreover, another method that is a combination of Method I and Method II can be implemented for location estimation. The method can automatically select Method I when four peak correlation values are approximately equal and Method II when one of the peak correlations is low with respect to the others. Furthermore, MAI can be reduced by selecting efficient codes and the update rate can be increased using the data tables formed for the data signals of these efficient codes.

# REFERENCES


Bahl, P. and V.N. Padmanabhan. 2000. RADAR: An In-Building RF-Based User Location and Tracking System. *Proc. IEEE INFOCOM* (2):775-784.

Bahl, P., V.N. Padmanabhan, and A. Balachandran. 2000. Enhancements to the RADAR user location and tracking system. *Microsoft Research Technical Report*. http://research.microsoft.com/~bahl/papers/pdf/msr-tr-2000-12.pdf (accessed April 25, 2009).

Bucur, D. 2006. Location Sensing in Ubiquitous Computing. http://www.daimi.au.dk /~doina/absg-loc/absg-loc.pdf (accessed June 11, 2009).

Cyril, B., T. Conners, G. Leon, and S. Pradhan. 2005. An autonomous, self-assembling sensor network for indoor asset and system management. *HP Laboratories Technical Report*. http://www.hpl.hp.com/techreports/2003/HPL-2003-41.pdf (accessed April 26, 2009).

Daly, P. 1993. Navstar GPS and GLONASS: global satellite navigation system. *Electronics & Communication Engineering Journal* 349-357.

Harter, A., A. Hopper, P. Steggles, A. Ward, and P. Webster. 2002. The Anatomy of a Context-Aware Application. *Wireless Networks* 8(2):187-197.

Hazas, M. and A. Hopper. 2006. Broadband Ultrasonic Location Systems for Improved Indoor Positioning. *IEEE Transactions on Mobile Computing* 5(5):536-547.

Hazas, M. and A. Ward. 2003. A High Performance Privacy-Oriented Location System. *Proceedings of the first IEEE International Conference on Pervasive Computing and Communications* 216-223.

Hightower, J. and G. Borriello. 2001. Location Systems for Ubiquitous Computing. *Computer* 34(8):57-66.

Hightower, J., G. Borriello, and R. Want. 2000. SpotON: An indoor 3D location sensing technology based on RF signal strength. *UW CSE Technical Report*. http://www.cs.washington.edu/homes/jeffro/pubs/hightower2000indoor /hightower2000indoor.pdf (accessed July 11, 2009).

Juang, P., H. Oki, Y. Wang, M. Martonosi, L.S. Peh, and D. Rubenstein. 2002. Energy-efficient computing for wildlife tracking: design tradeoffs and early experiences with ZebraNet. *ACM SIGOPS Operating Systems Review* 36(5):96-107.

Martin, J.M., A.R. Jimenez, F. Seco, L. Calderon, J.L. Pons, and R. Ceres. 2002. Estimating the 3D-position from time delay data of US-waves: experimental analysis and a new processing algorithm. *Sensors and Actuators A* 101(3):311-321.

Ni, L.M., Y. Liu, Y.C. Lau, and A.P. Patil. 2004. LANDMARC: Indoor Location Sensing Using Active RFID. *Wireless Networks* 10(6):701-710.

Pandey, S. and P. Agrawal. 2006. A survey on localization techniques for wireless networks. *Journal of the Chinese Institute of Engineers* 29(7):1125-1147.

Piontek, H., M. Seyfferm, and J. Kaiser. 2007. Improving the accuracy of ultrasound-based localisation systems. *Personal and Ubiquitous Computing* 11(6):439-449.

Prieto, J.C., A.R. Jiménez, J. Guevara, J.L. Ealo, F. Seco, J.O. Roa, and F. Ramos. 2009. Performance Evaluation of 3D-LOCUS Advanced Acoustic LPS. *IEEE Transactions on Instrumental and Measurement* 58(8):2385-2395.

Prieto, J.C., A.R. Jiménez, J. I. Guevara, J.L. Ealo, F. A. Seco, J.O. Roa, and J.X. Ramos. 2007. Subcentimeter-accuracy localization through broadband acoustic transducers. *Proc. IEEE International Symposium on Intelligent Signal Processing* 1–6.

Priyantha, N.B. 2005. The Cricket Indoor Location System. PhD Thesis, Massachusetts Institute of Tehnology.

Priyantha, N.B., A. Chakraborty, and H. Balakrishnan. 2000. The Cricket location-support system. *Proceedings of the 6th Annual international Conference on Mobile Computing and Networking* 32-43.

Priyantha, N.B., A.K. Miu, H. Balakrishnan, and S. Teller. 2001. The cricket compass for context-aware mobile applications. *Proceedings of the 7th Annual International Conference on Mobile Computing and Networking* 1-14.

Proakis, John G. 2001. *Digital Communications*. New York: McGraw-Hill.

Schulze, H. and C. Lüders. 2005. *Theory and Applications of OFDM and CDMA Wideband Wireless Communications*. West Sussex: Wiley.

Tilak, S., V. Kolar, N.B. Abu-Ghazaleh, and K.D. Kang. 2005. Dynamic localization control for mobile sensor networks. *Proc. IEEE International Performance Computing and Communications Conference* 587-592.

Want, R., A. Hopper, V. Falcão, and J. Gibbons. 1992. The active badge location system. *ACM Transactions on Information Systems.* 10(1):91-102.

# APPENDIX A

# LOCALIZATION PERFORMANCE SCREENS FOR DIFFERENT LENGHTS OF GOLD CODE

In this section, the localization performance screens for different lengths of Gold code, vary from 31 bits to 2047 bits, were illustrated. All tests were made with the same predefined variables for each length of Gold code value at a fix point.

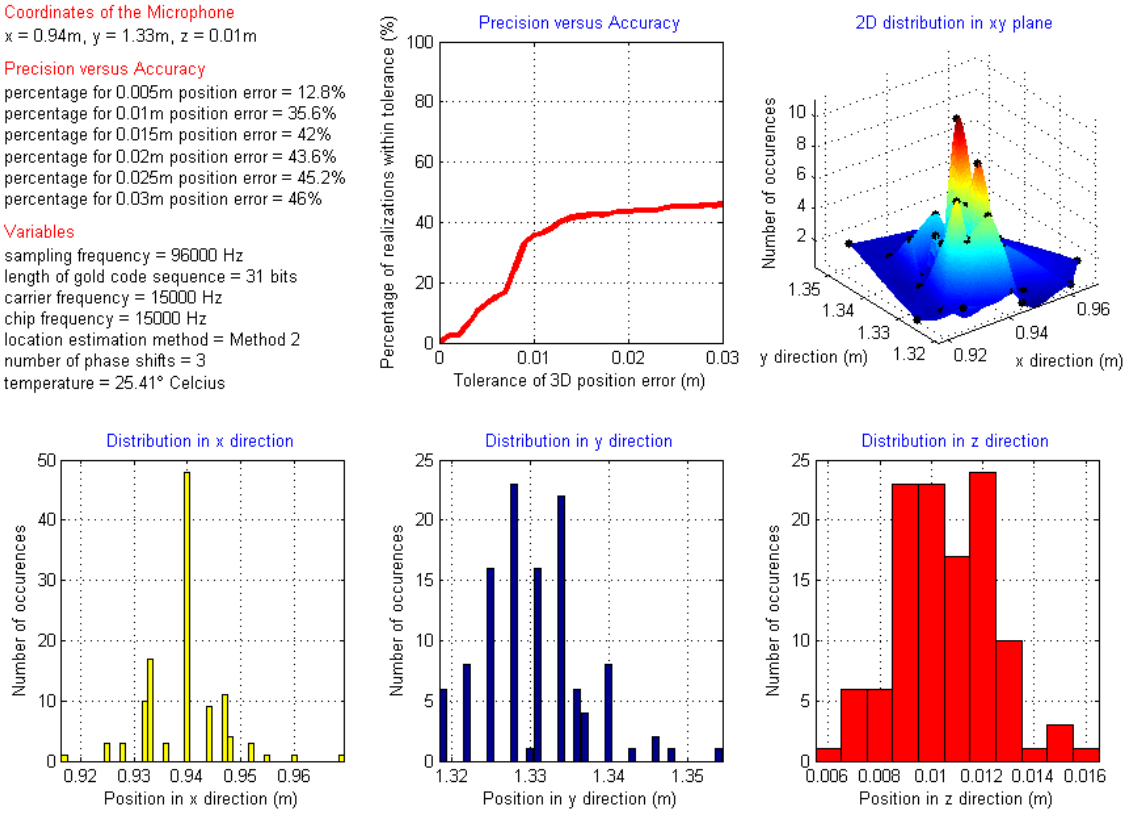


Figure A.1. 31-bit-long Gold code

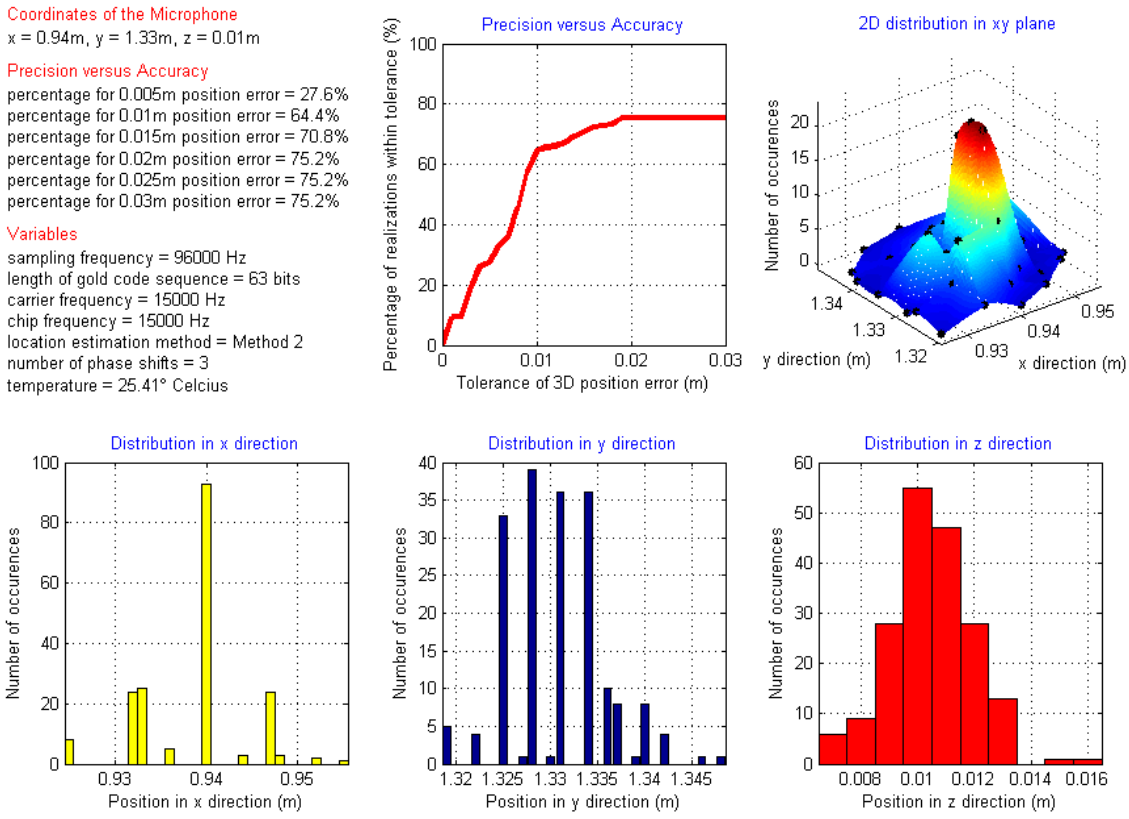


Figure A.2. 63-bit-long Gold code

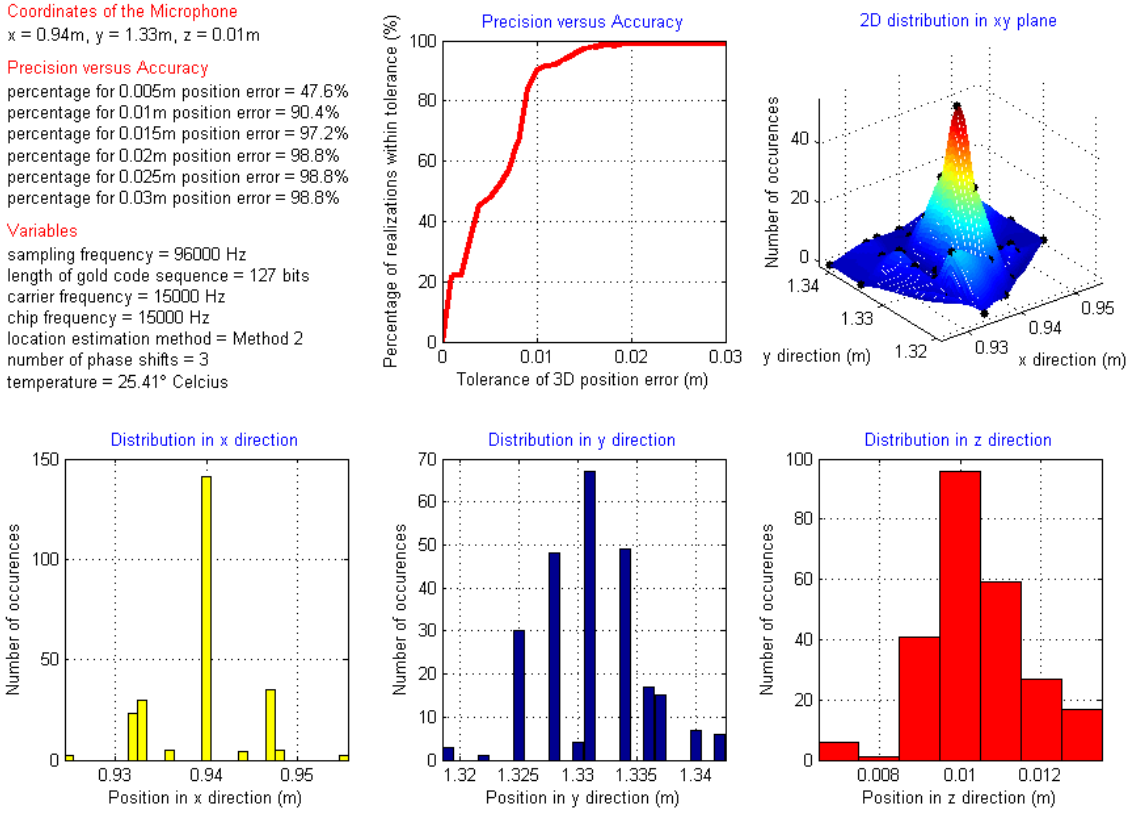


Figure A.3. 127-bit-long Gold code

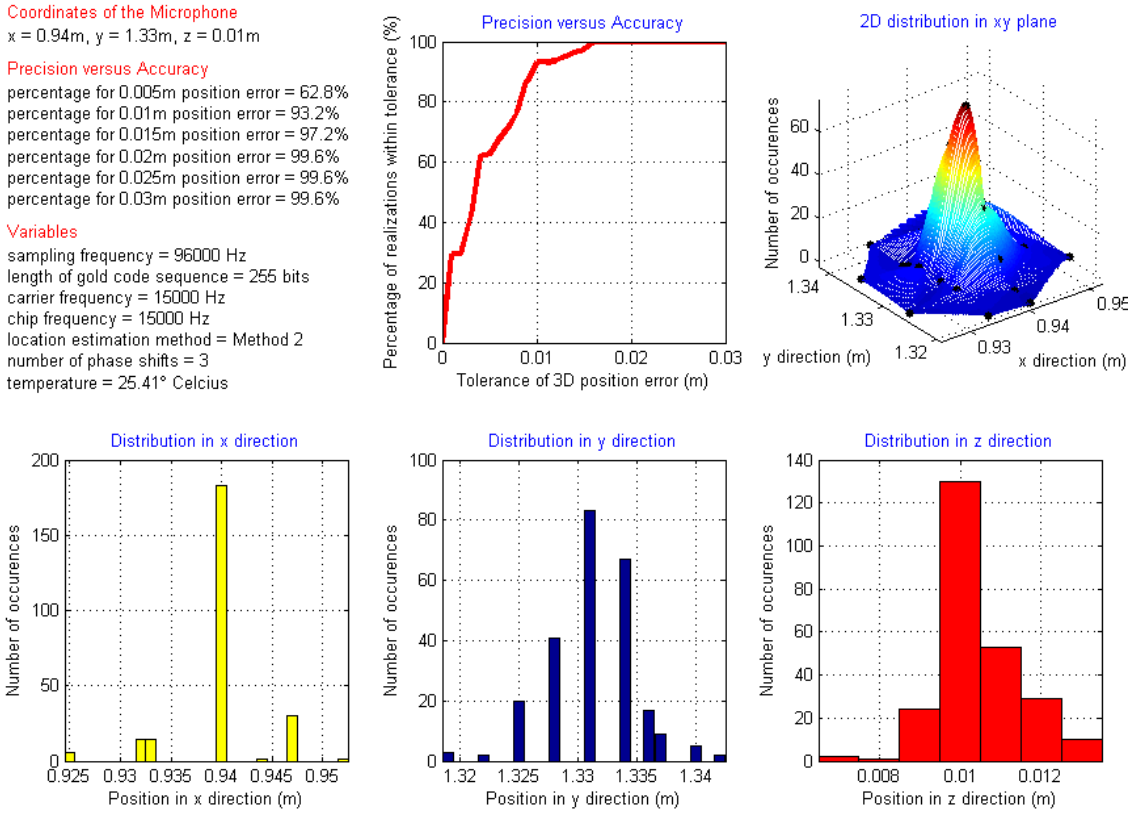


Figure A.4 255-bit-long Gold code.

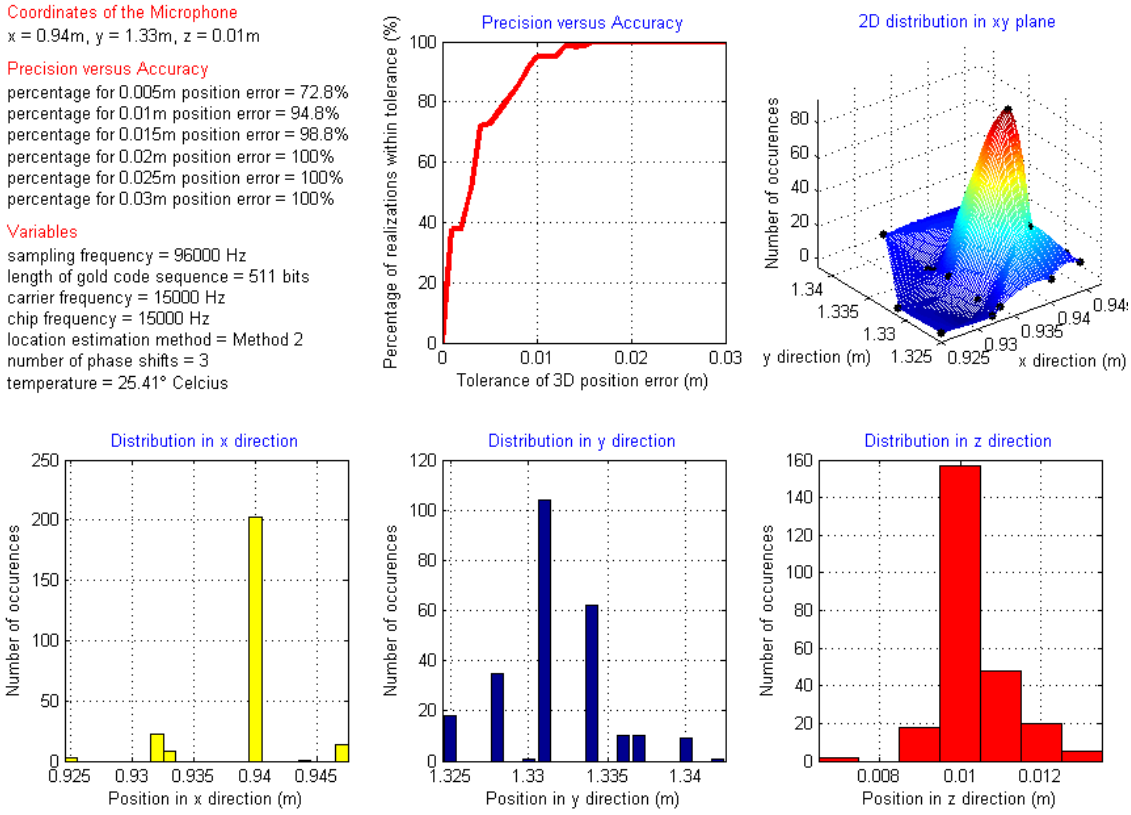


Figure A.5. 511-bit-long Gold code

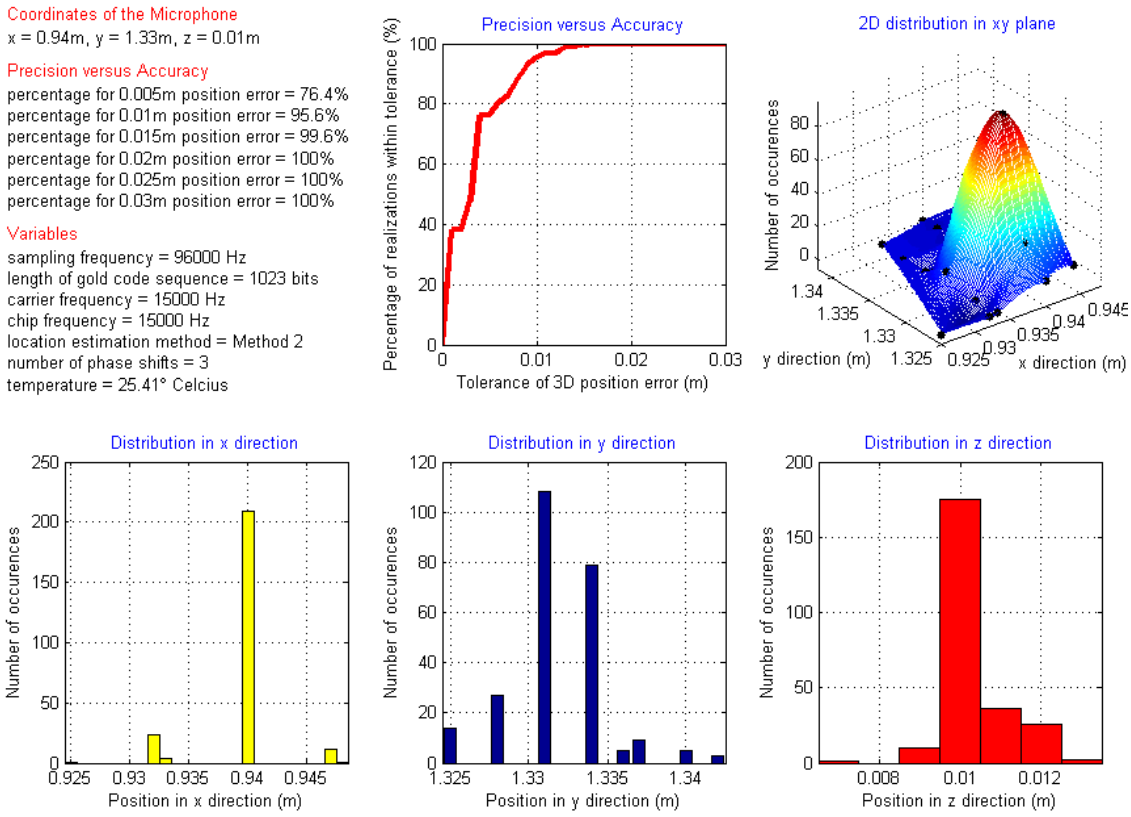


Figure A.6. 1023-bit-long Gold code

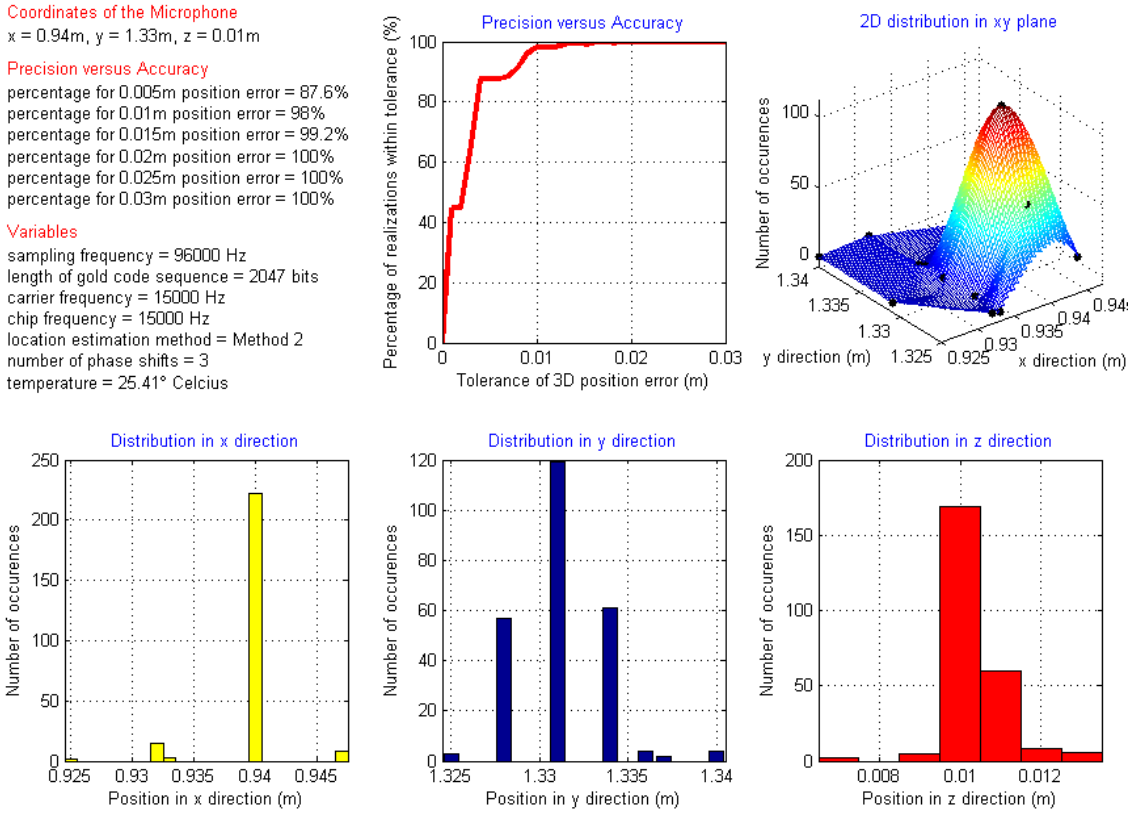


Figure A.7. 2047-bit-long Gold code

# APPENDIX B

# LOCALIZATION PERFORMANCE SCREENS FOR DIFFERENT SAMPLING FREQUENCIES

In this section, the localization performance screens for sampling frequencies: 44100 Hz, 48000 Hz and 96000 Hz were illustrated. All tests were made with the same predefined variables for each sampling frequency value at a fix point.

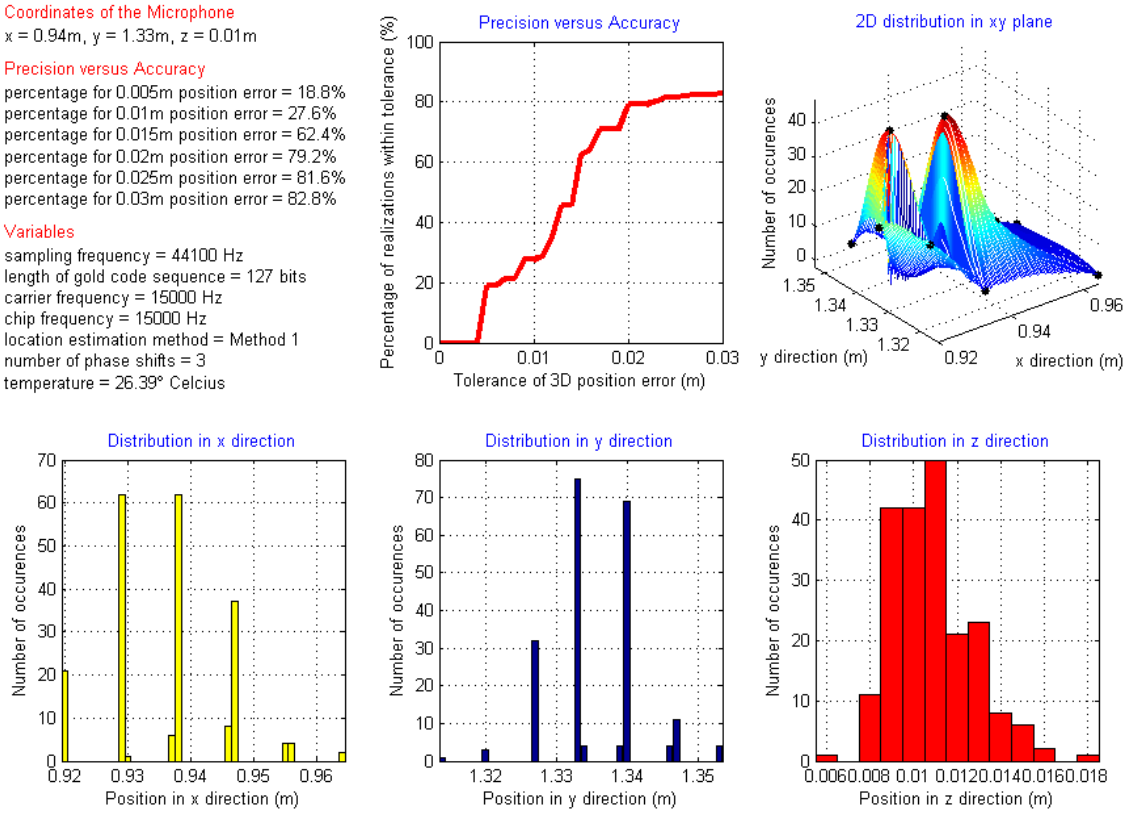


Figure B.1 44100 Hz sampling frequency

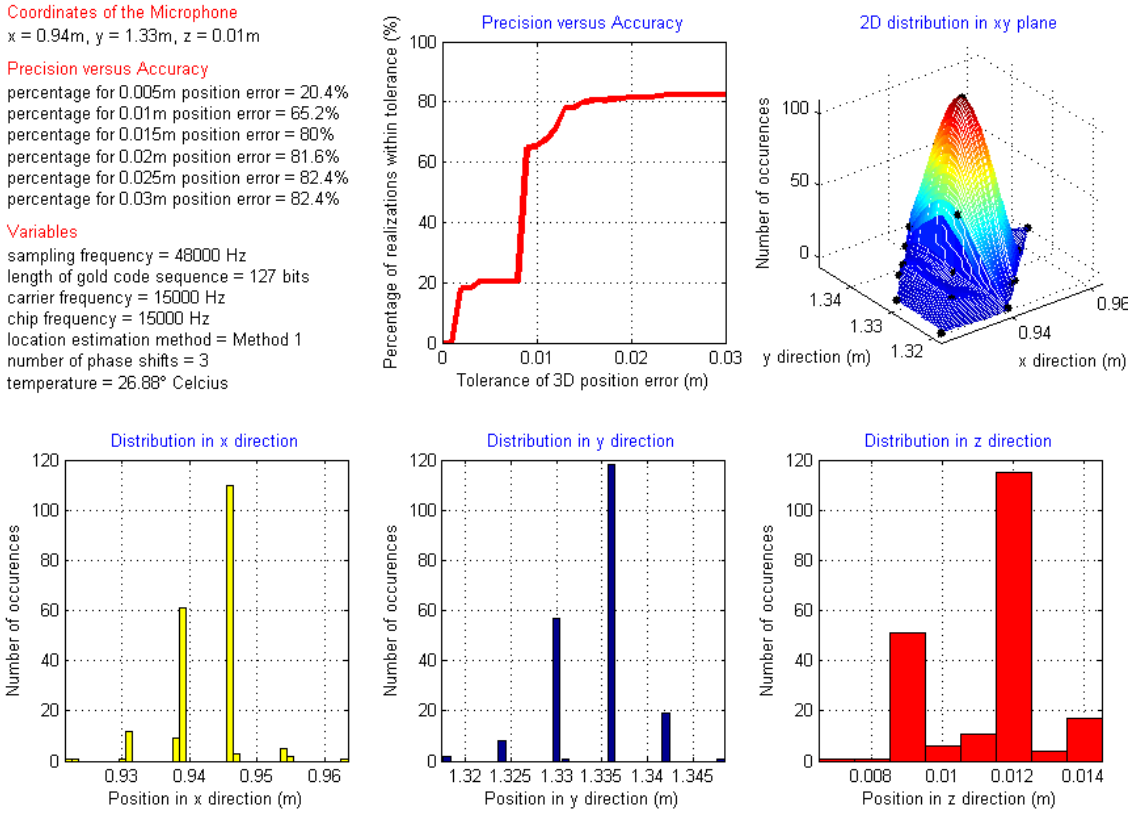


Figure B.2. 48000 Hz sampling frequency

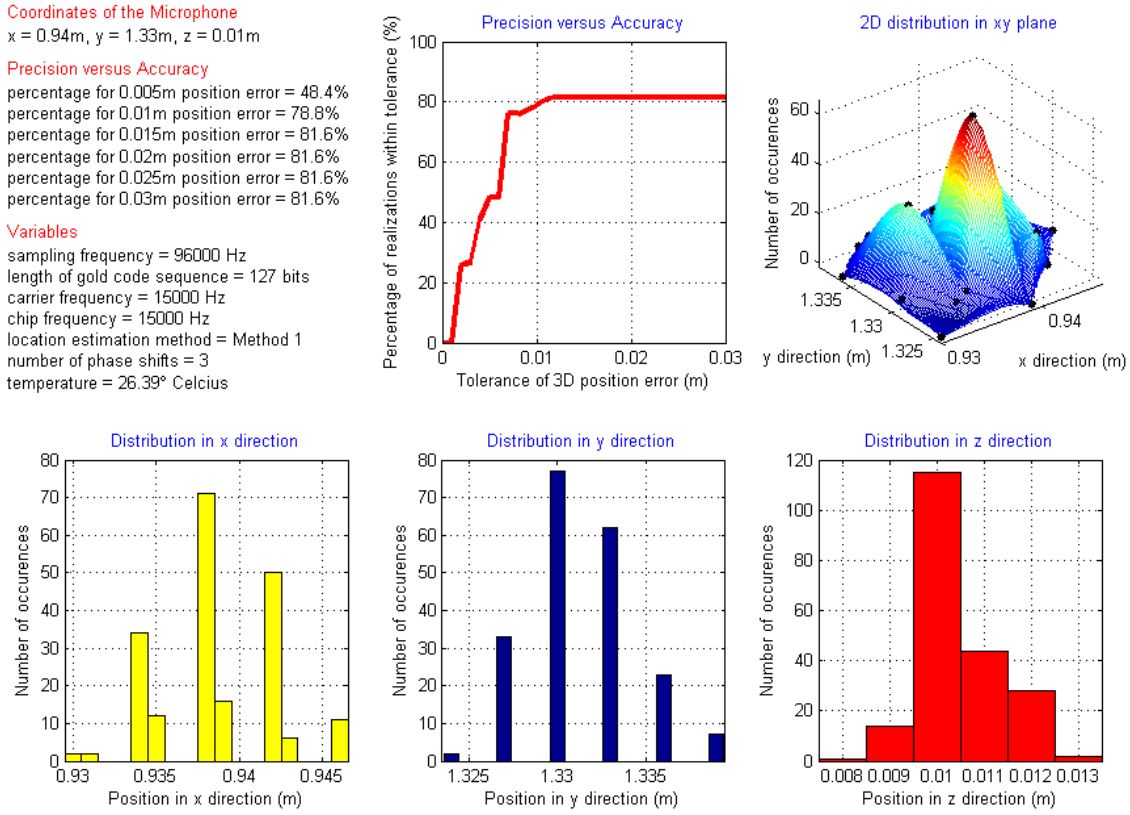


Figure B.3. 96000 Hz sampling frequency

# APPENDIX C

# LOCALIZATION PERFORMANCE SCREENS FOR DIFFERENT RATIOS

In this section, the localization performance screens for different ratios of carrier frequency to chip frequency, vary from 0.5 to 2, were illustrated. All tests were made with the same predefined variables for each ratio at a fix point.

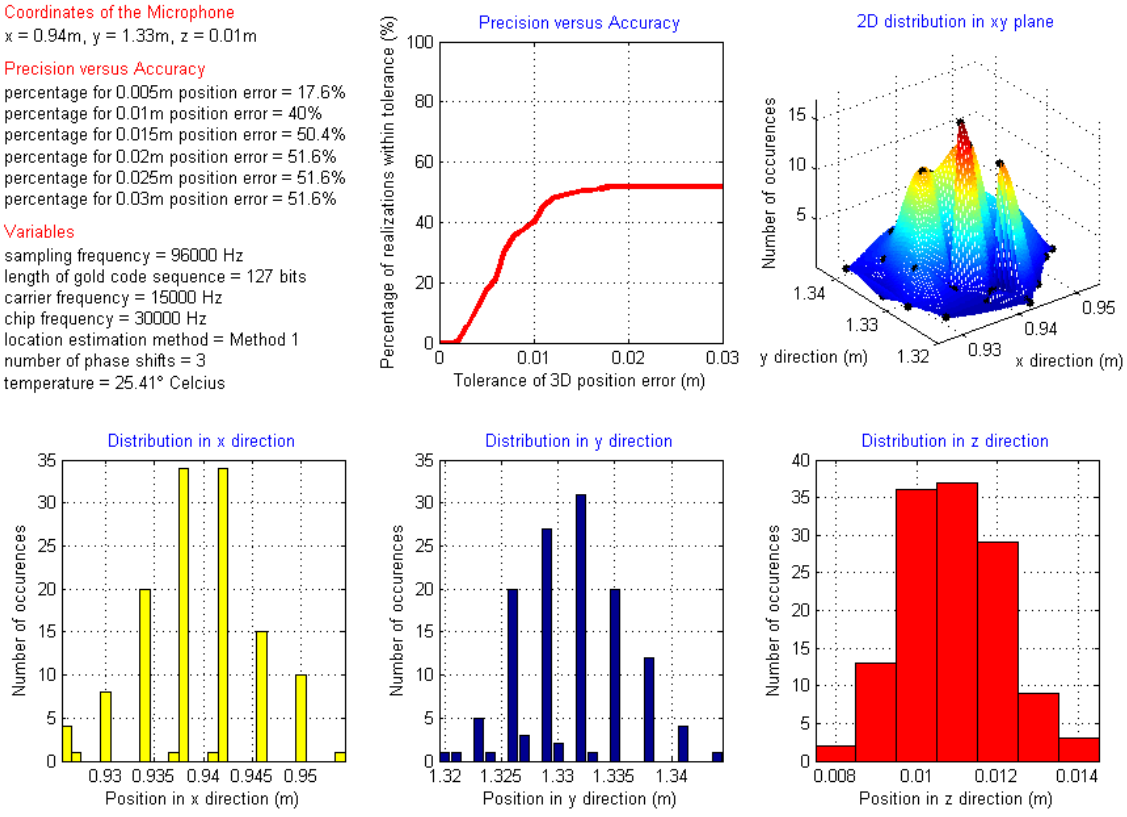


Figure C.1. Ratio of carrier frequency to chip frequency equal to 0.5

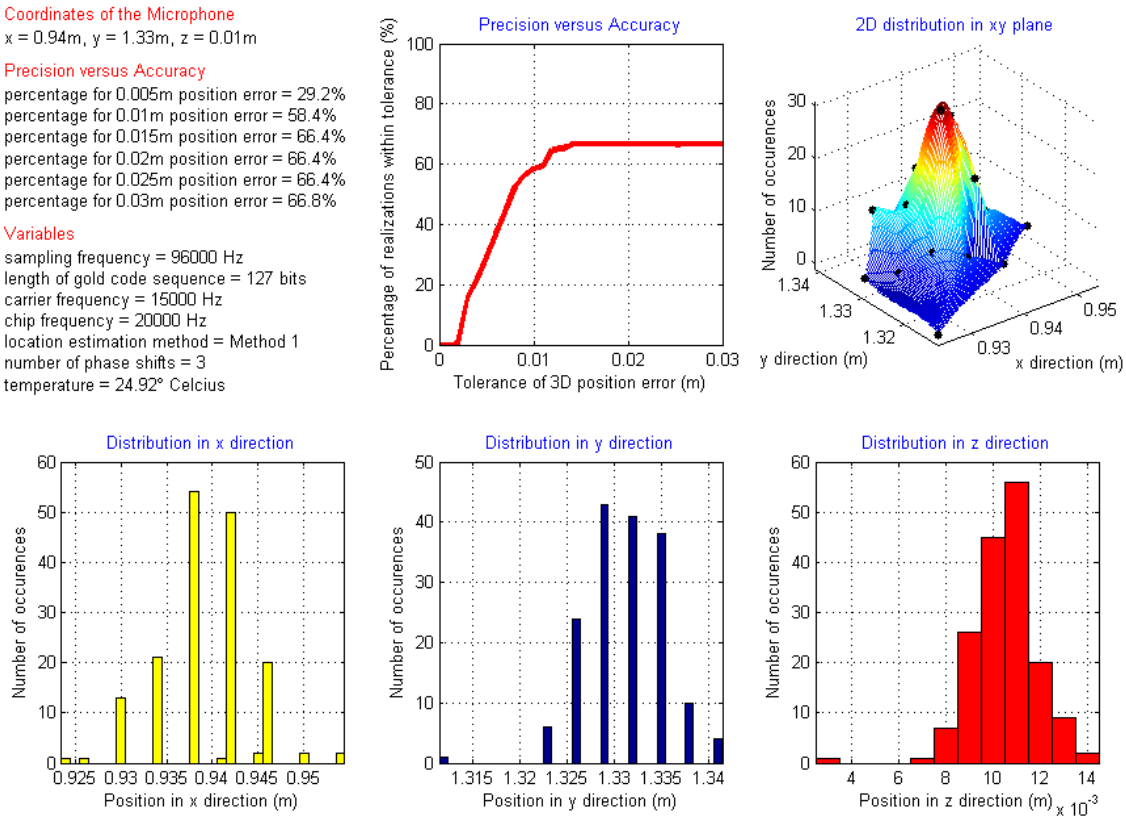


Figure C.2. Ratio of carrier frequency to chip frequency equal to 0.75

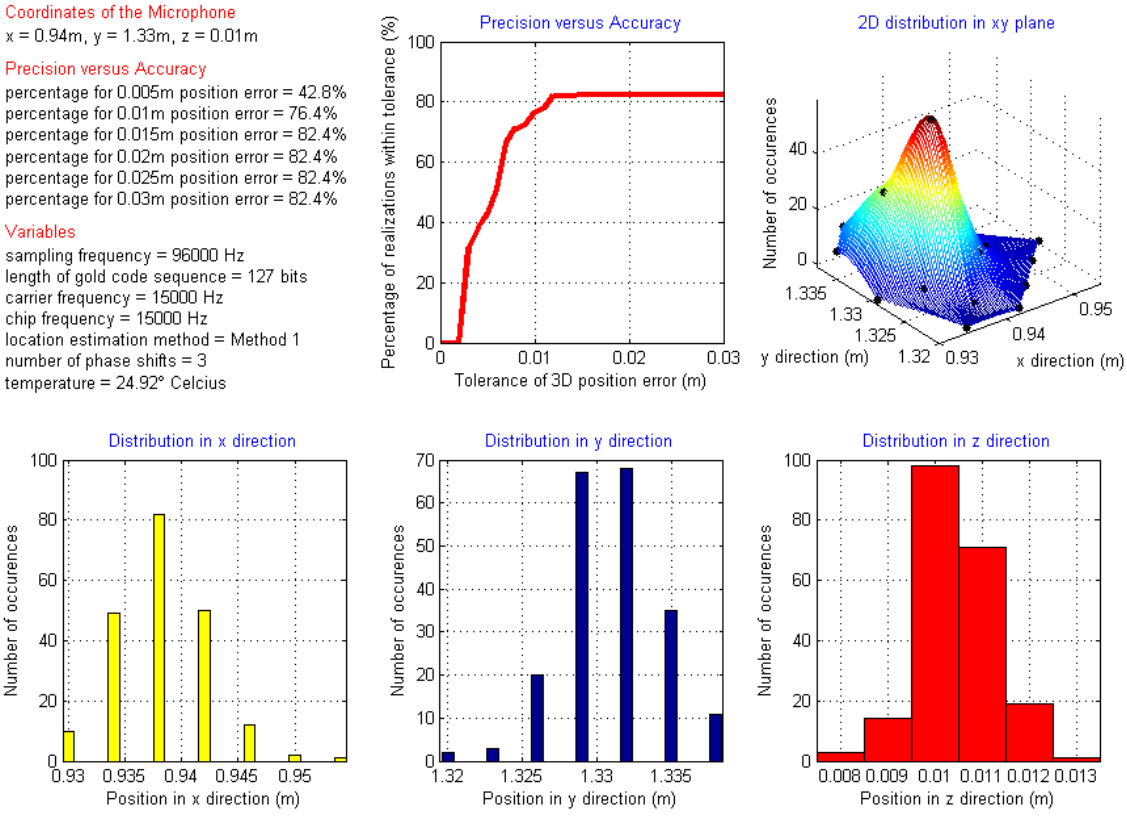


Figure C.3. Ratio of carrier frequency to chip frequency equal to 1

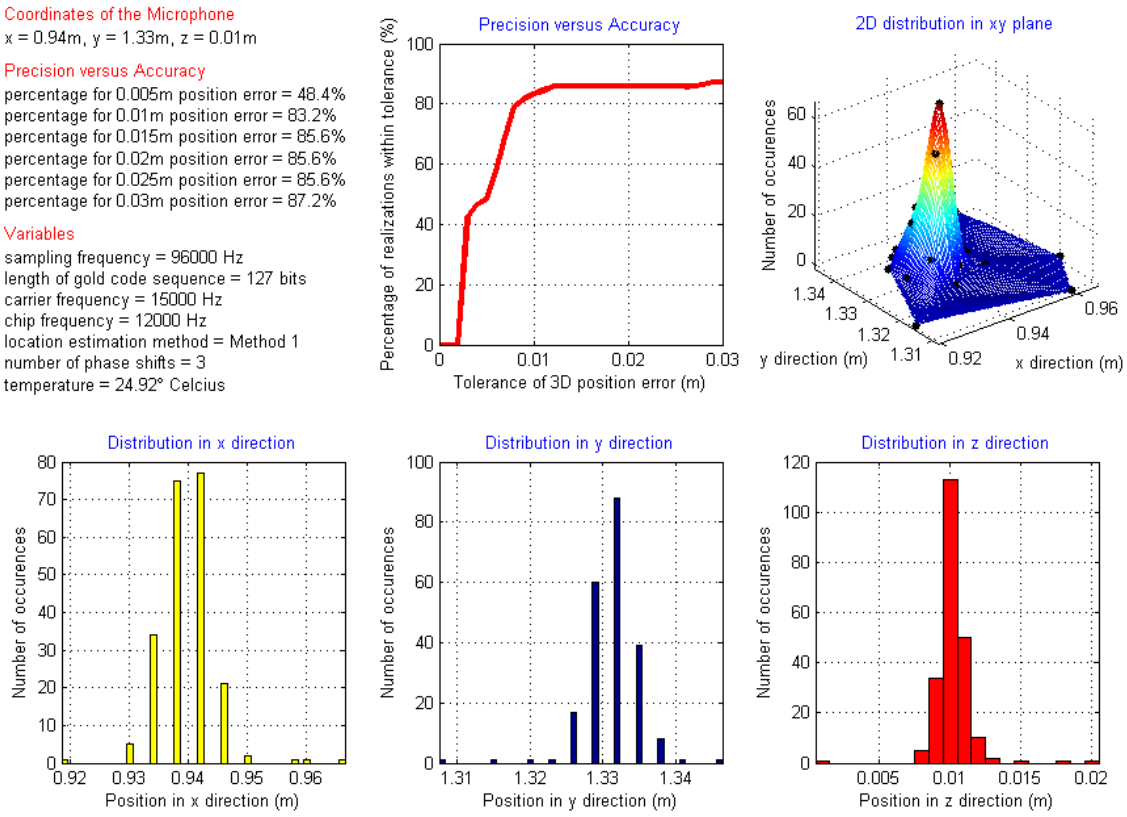


Figure C.4. Ratio of carrier frequency to chip frequency equal to 1.25

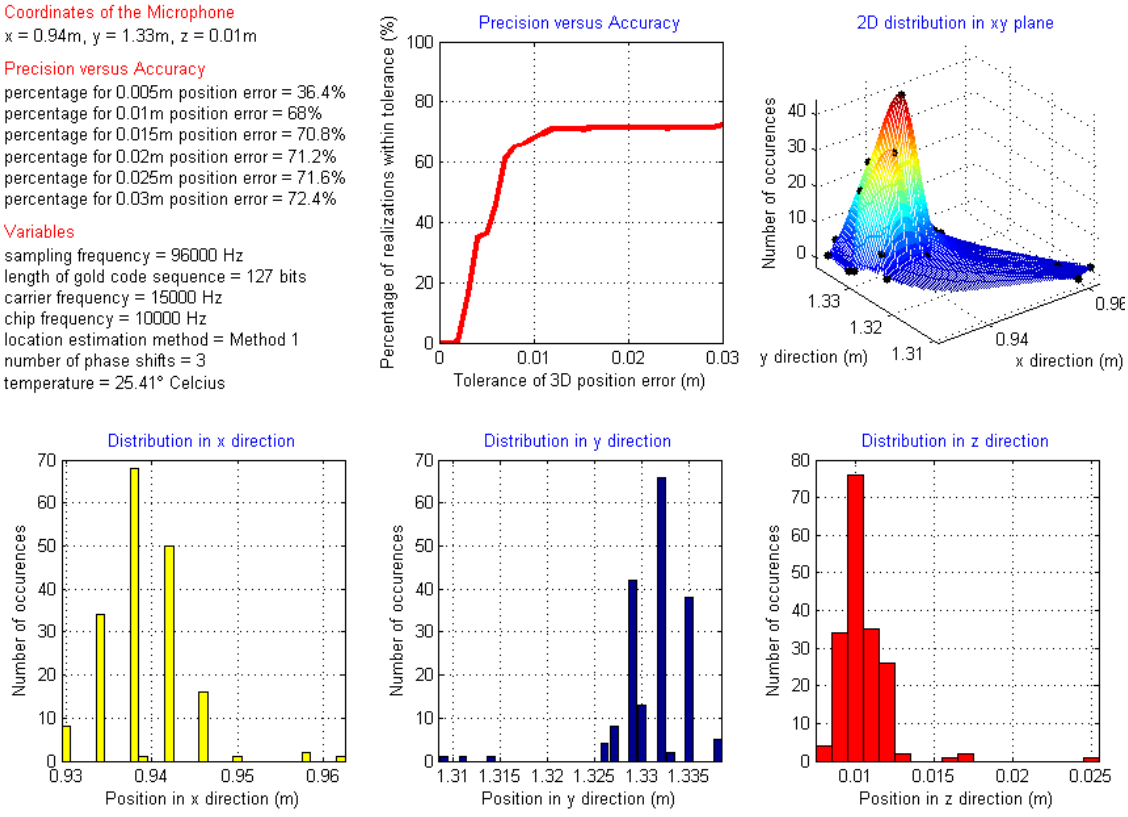


Figure C.5. Ratio of carrier frequency to chip frequency equal to 1.5

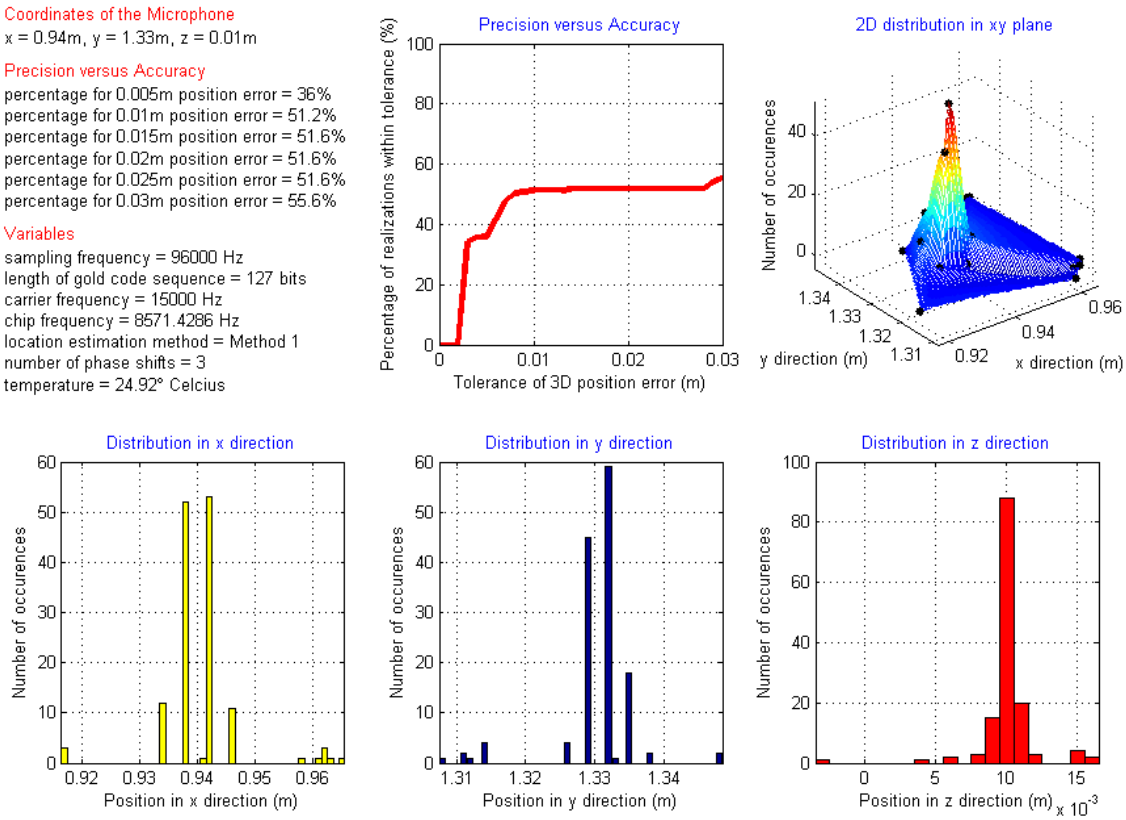


Figure C.6. Ratio of carrier frequency to chip frequency equal to 1.75

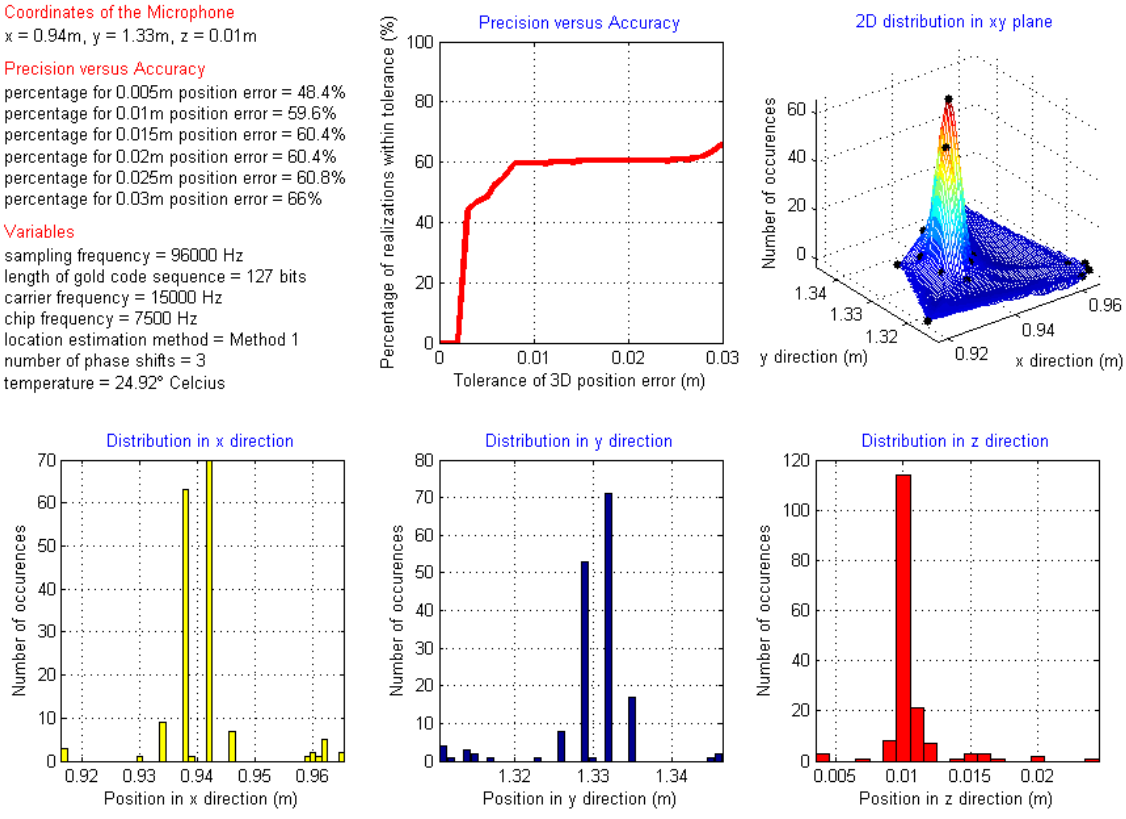


Figure C.7. Ratio of carrier frequency to chip frequency equal to 2

# APPENDIX D

# LOCALIZATION PERFORMANCE SCREENS FOR DIFFERENT FREQUENCIES

In this section, the localization performance screens for different frequencies, vary from 5000 Hz to 22000 Hz, were illustrated. Carrier and chip frequencies were taken equal for each case. All tests were made with the same predefined variables for each frequency value at a fix point.

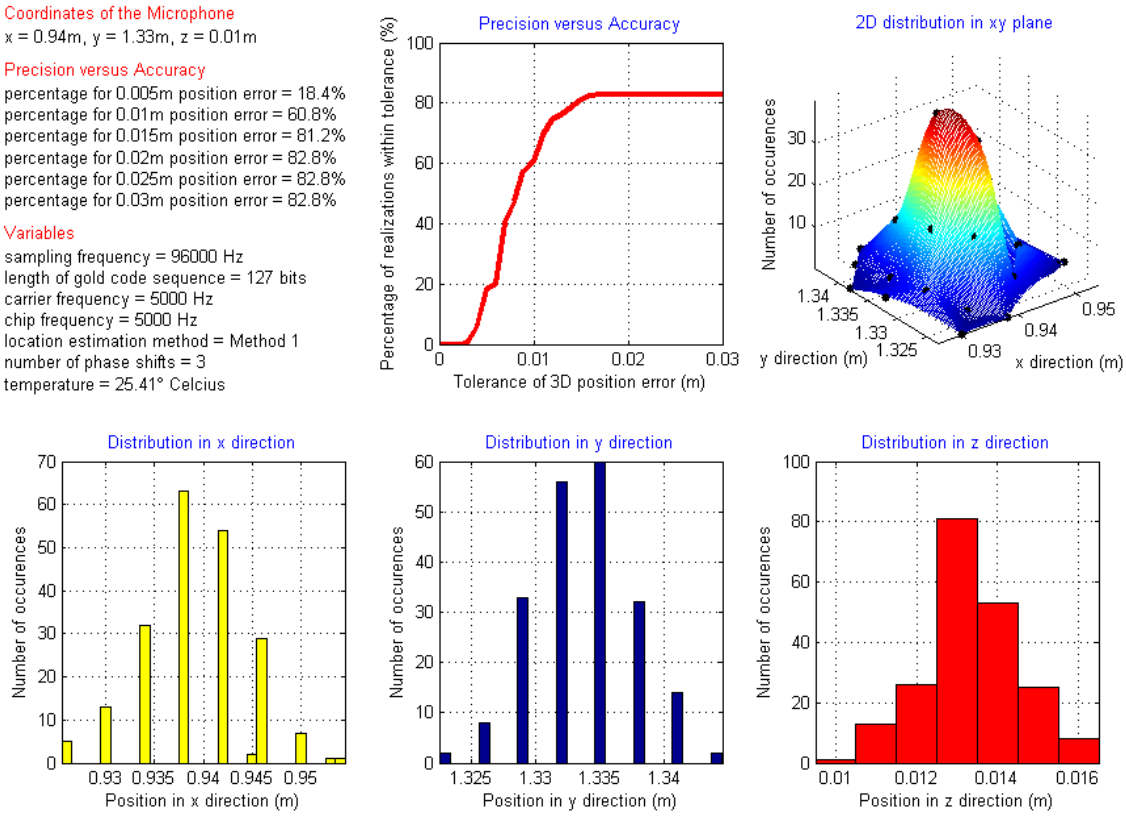


Figure D.1. 5 kHz carrier and chip frequencies

Coordinates of the Microphone
x = 0.94m, y = 1.33m, z = 0.01m

Precision versus Accuracy
percentage for 0.005m position error = 28%
percentage for 0.01m position error = 78%
percentage for 0.015m position error = 88.8%
percentage for 0.02m position error = 89.6%
percentage for 0.025m position error = 89.6%
percentage for 0.03m position error = 89.6%

Variables
sampling frequency = 96000 Hz
length of gold code sequence = 127 bits
carrier frequency = 6000 Hz
chip frequency = 6000 Hz
location estimation method = Method 1
number of phase shifts = 3
temperature = 25.41° Celcius

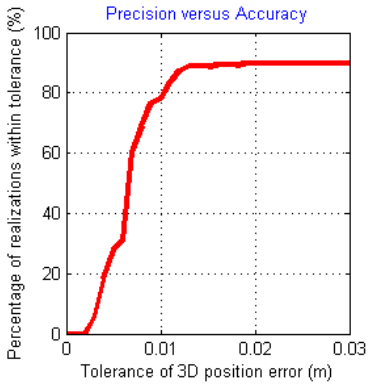


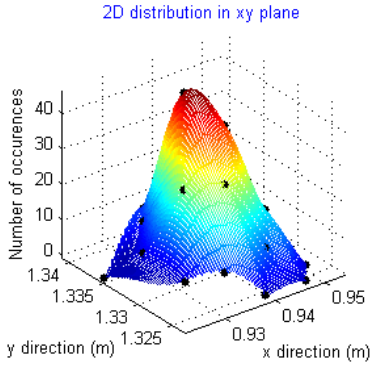


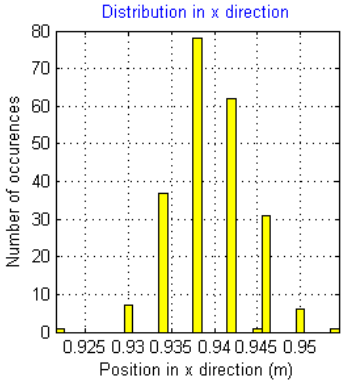


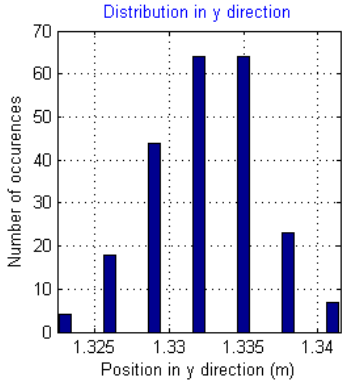


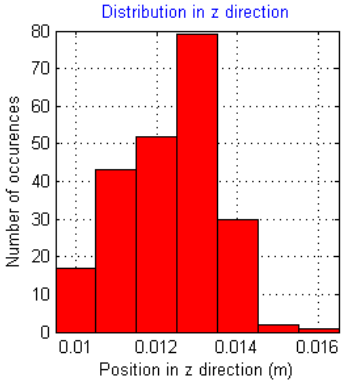


Figure D.2. 6 kHz carrier and chip frequencies

Coordinates of the Microphone
x = 0.94m, y = 1.33m, z = 0.01m

Precision versus Accuracy
percentage for 0.005m position error = 40%
percentage for 0.01m position error = 89.2%
percentage for 0.015m position error = 96%
percentage for 0.02m position error = 97.2%
percentage for 0.025m position error = 97.2%
percentage for 0.03m position error = 97.2%

Variables
sampling frequency = 96000 Hz
length of gold code sequence = 127 bits
carrier frequency = 7000 Hz
chip frequency = 7000 Hz
location estimation method = Method 1
number of phase shifts = 3
temperature = 26.39° Celcius

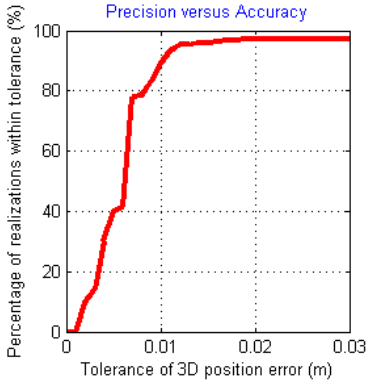


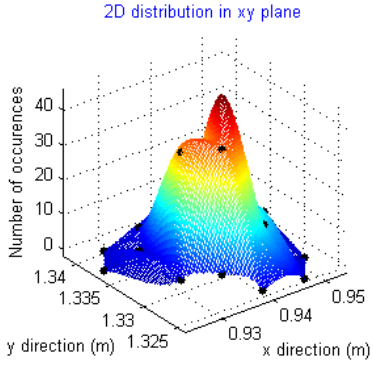


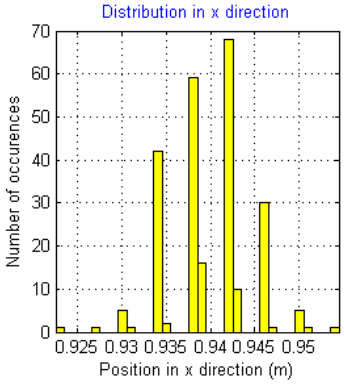


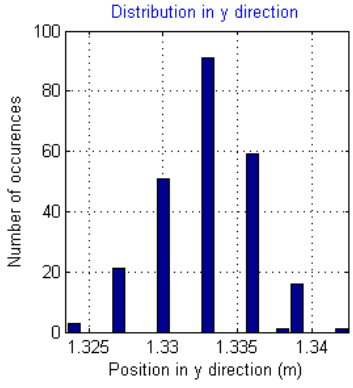


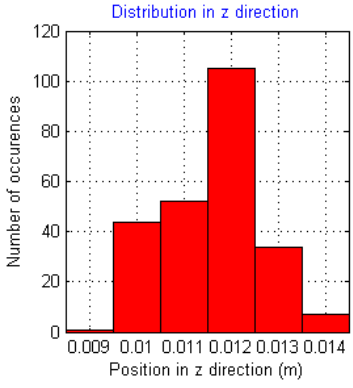


Figure D.3. 7 kHz carrier and chip frequencies

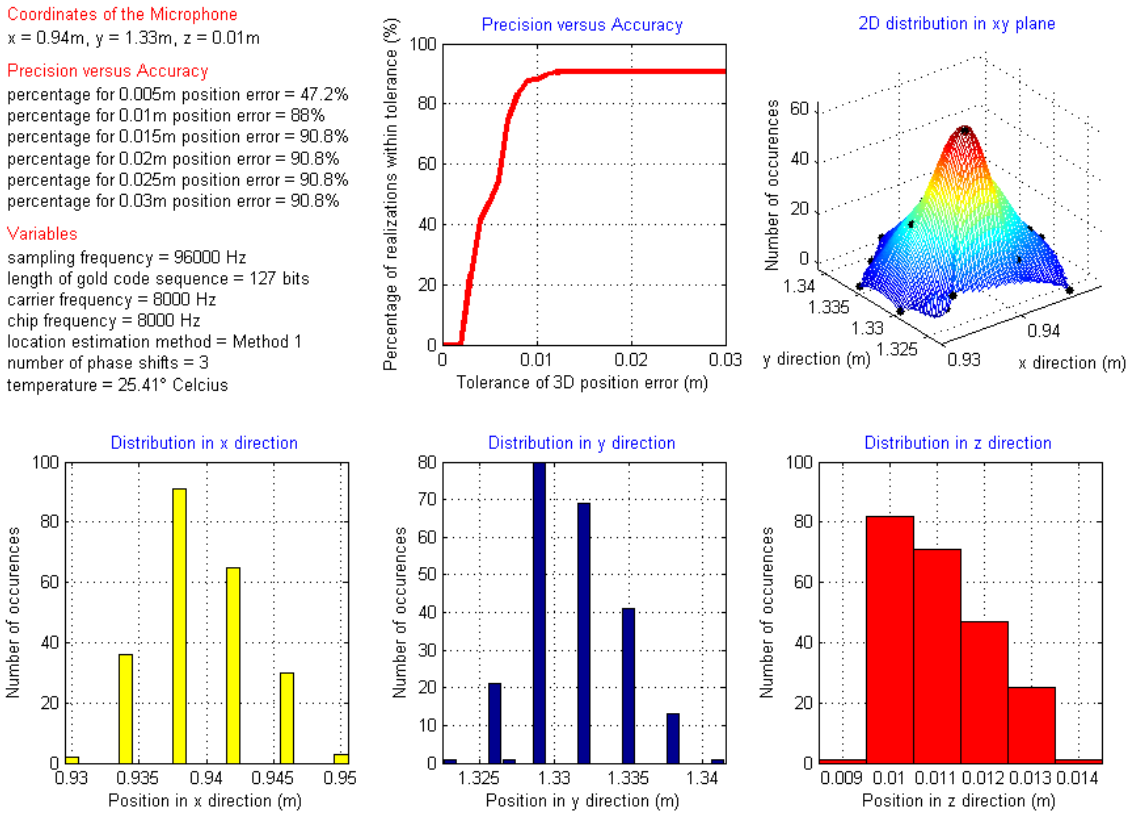


Figure D.4. 8 kHz carrier and chip frequencies

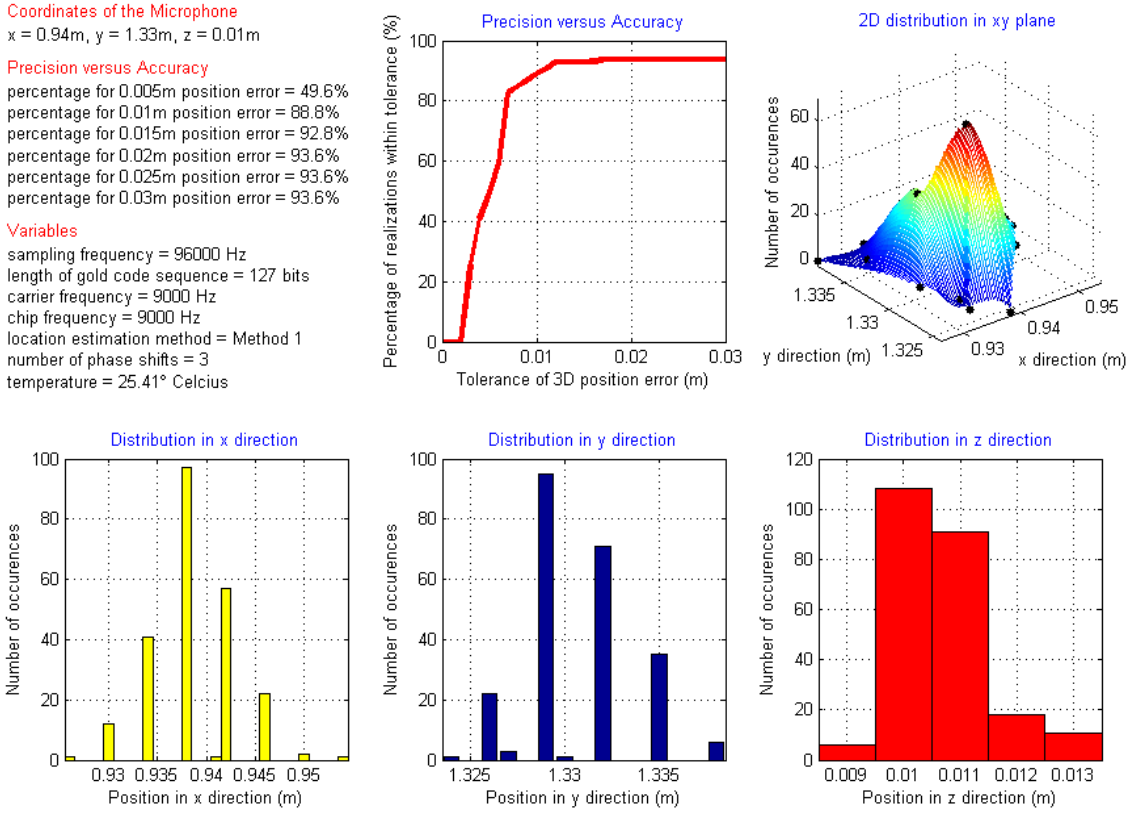


Figure D.5. 9 kHz carrier and chip frequencies

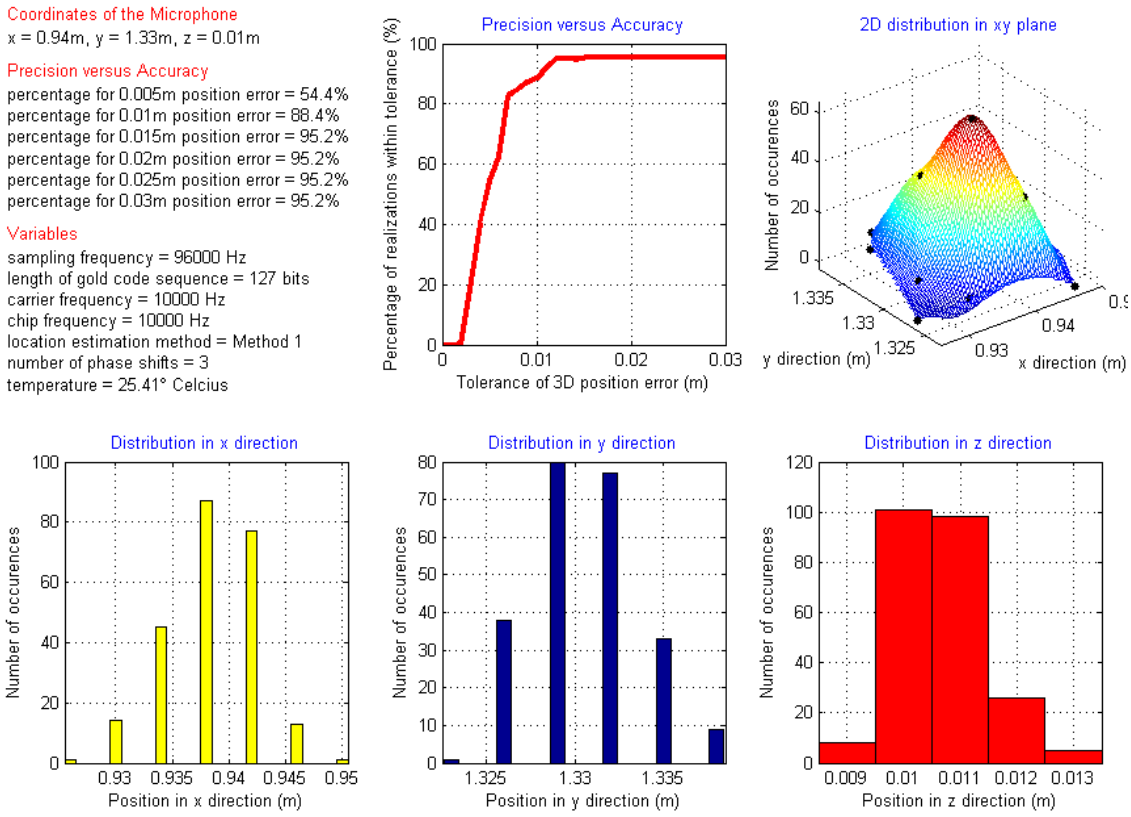


Figure D.6. 10 kHz carrier and chip frequencies

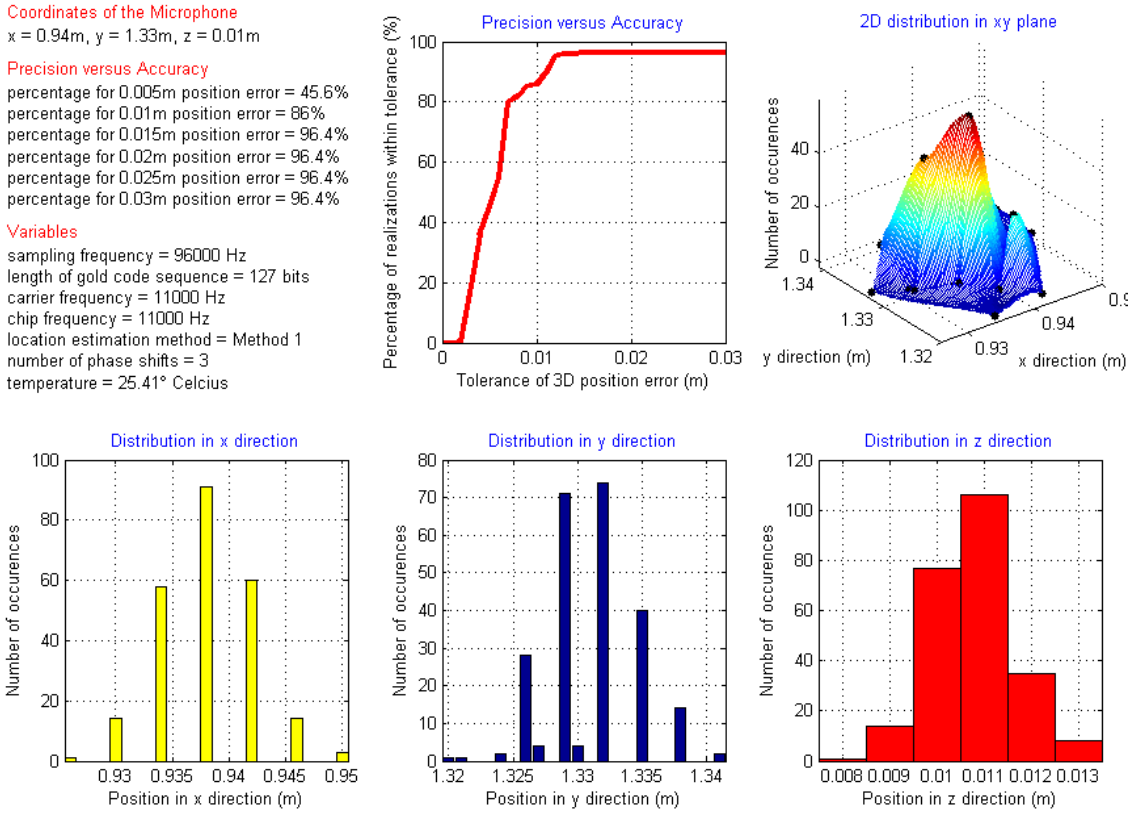


Figure D.7. 11 kHz carrier and chip frequencies

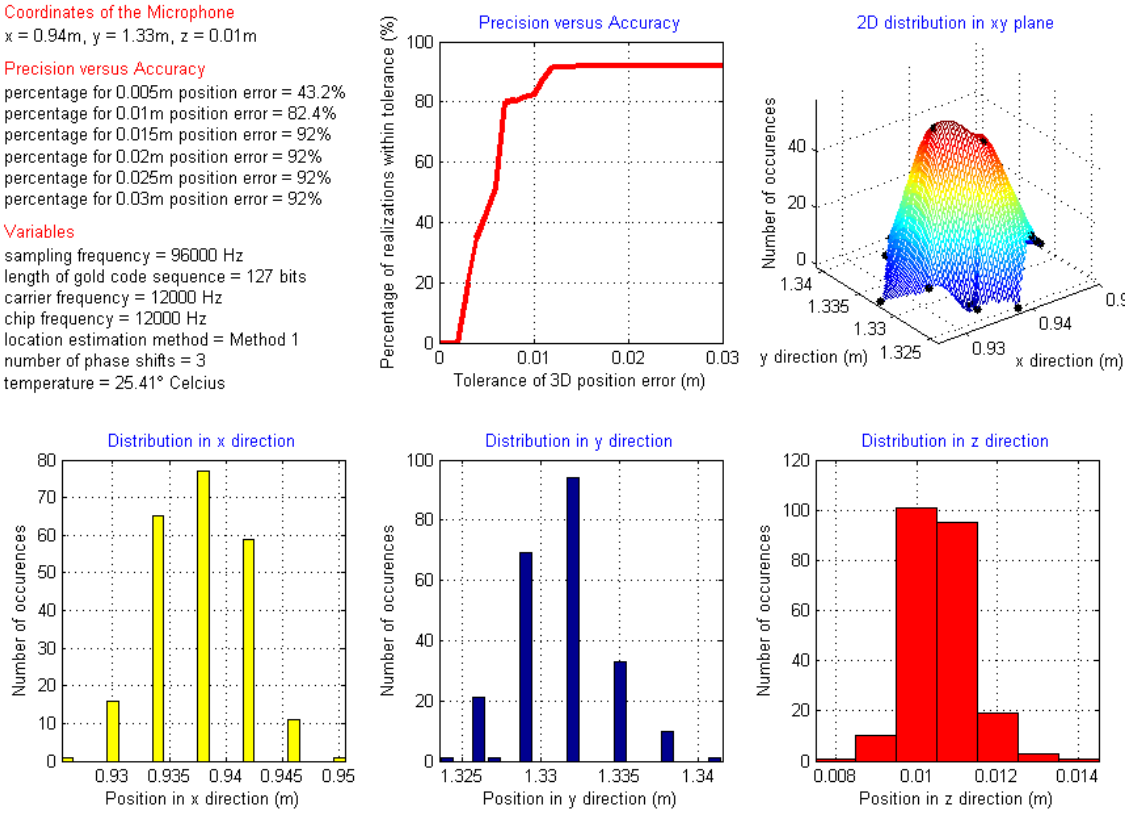


Figure D.8. 12 kHz carrier and chip frequencies

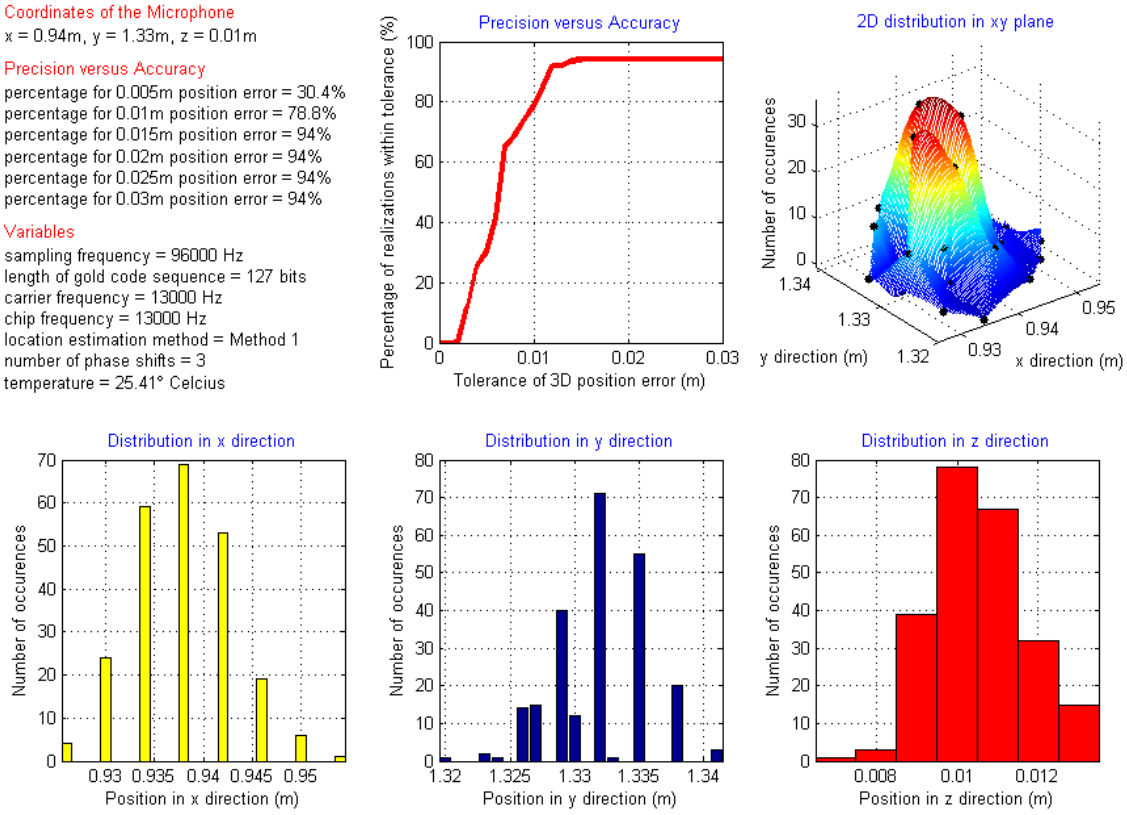


Figure D.9. 13 kHz carrier and chip frequencies

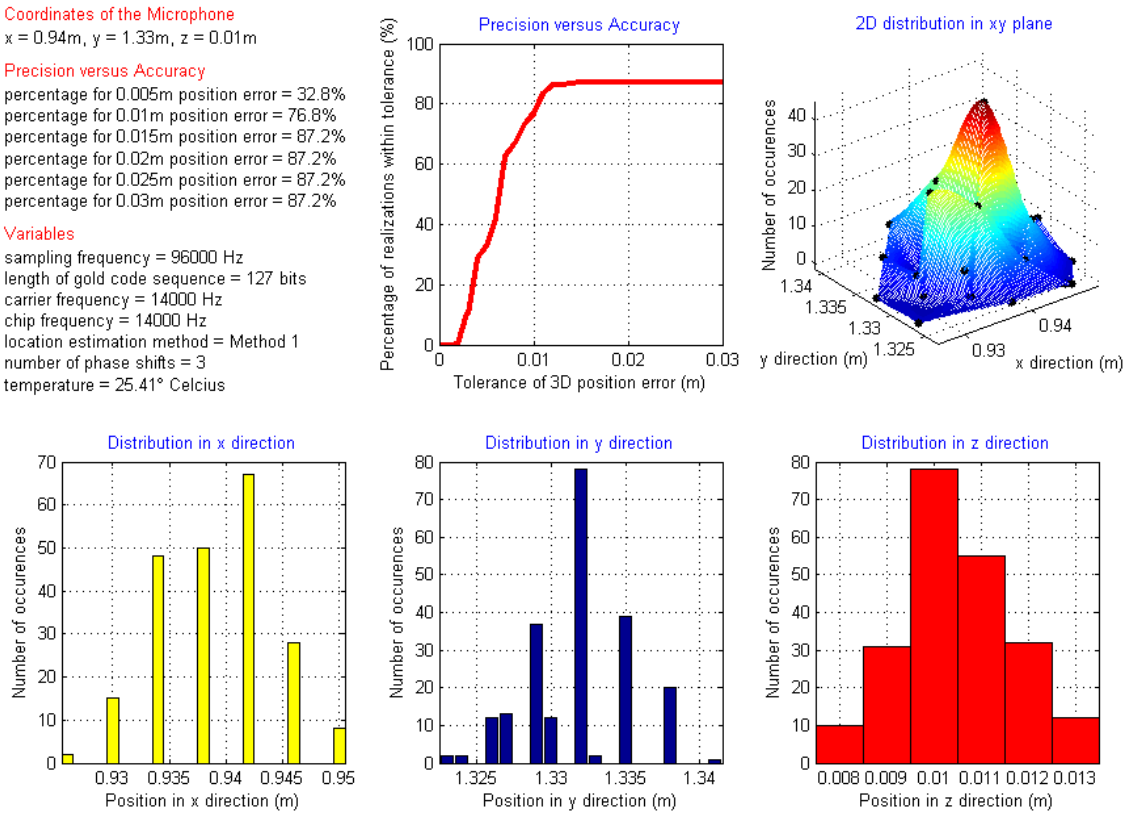


Figure D.10. 14 kHz carrier and chip frequencies

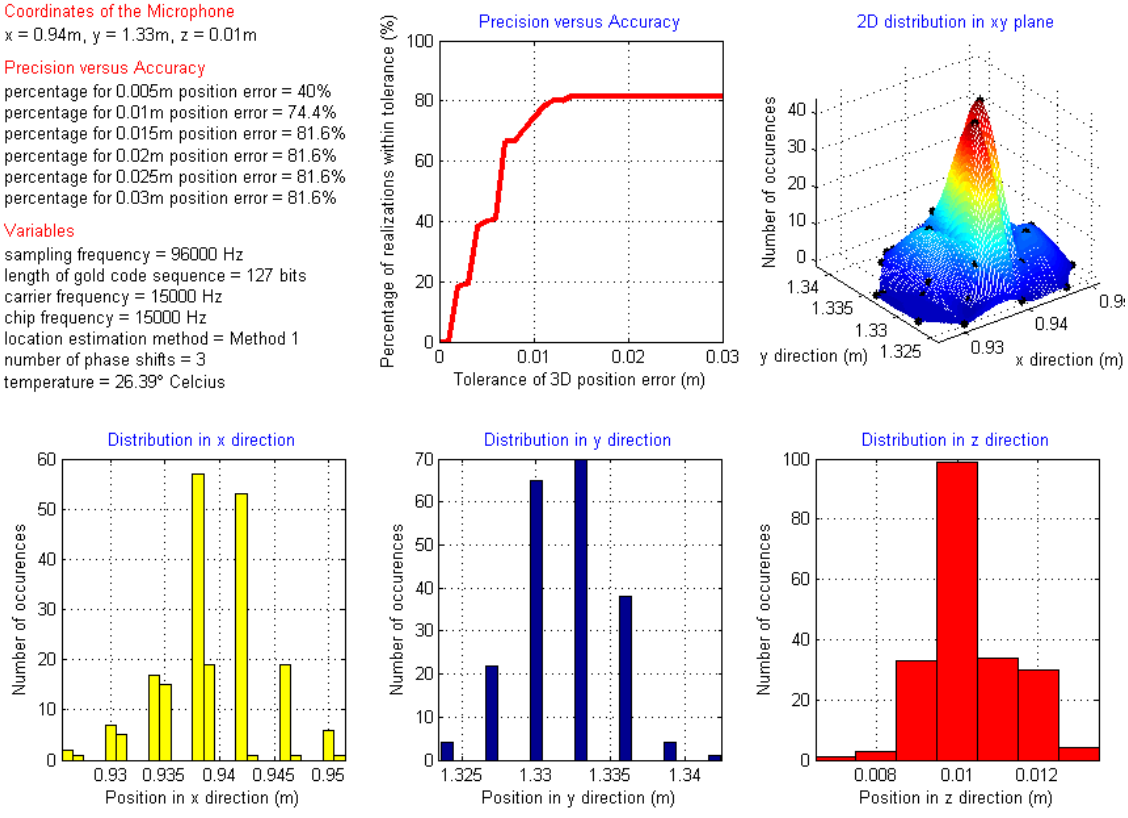


Figure D.11. 15 kHz carrier and chip frequencies

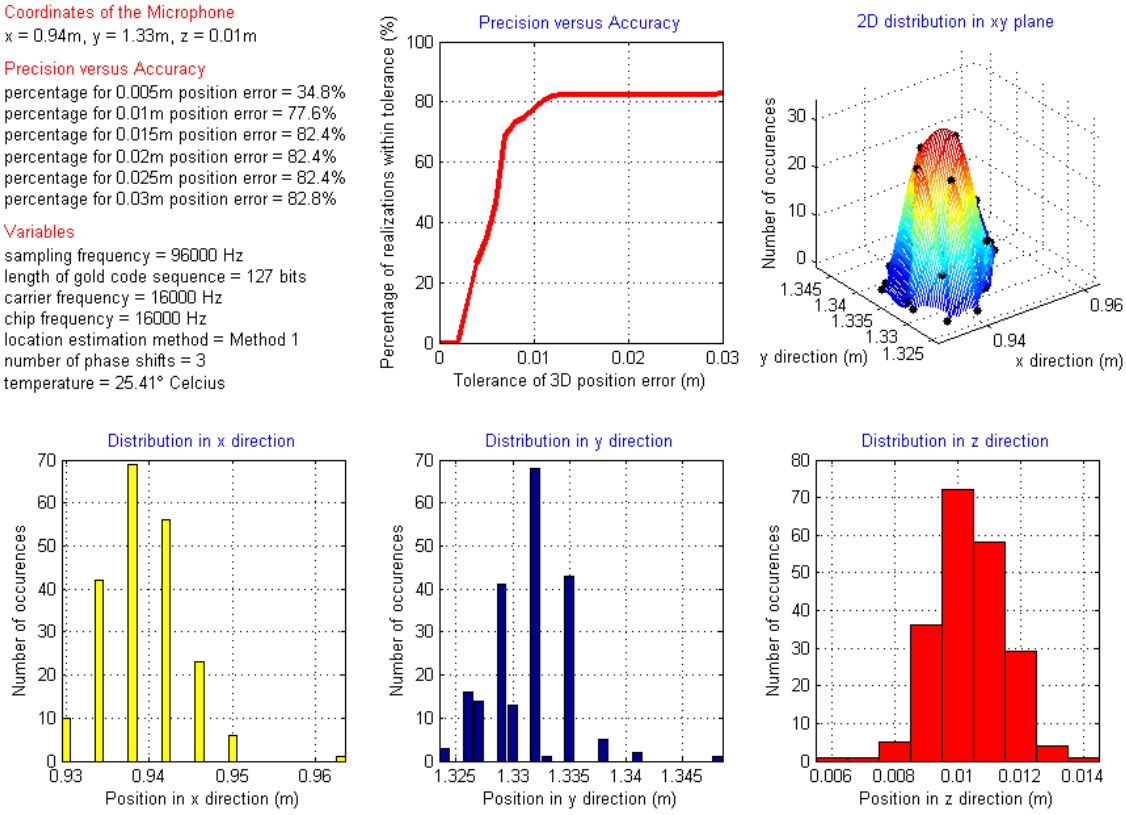


Figure D.12. 16 kHz carrier and chip frequencies

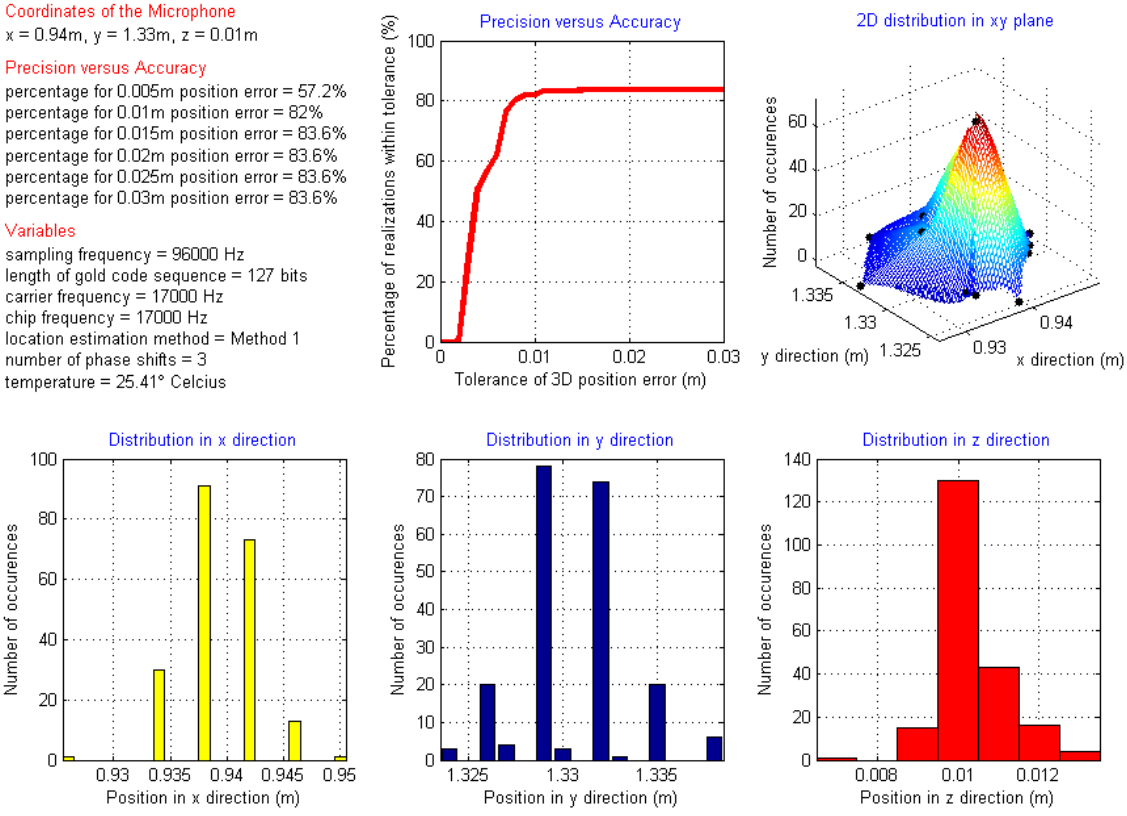


Figure D.13. 17 kHz carrier and chip frequencies

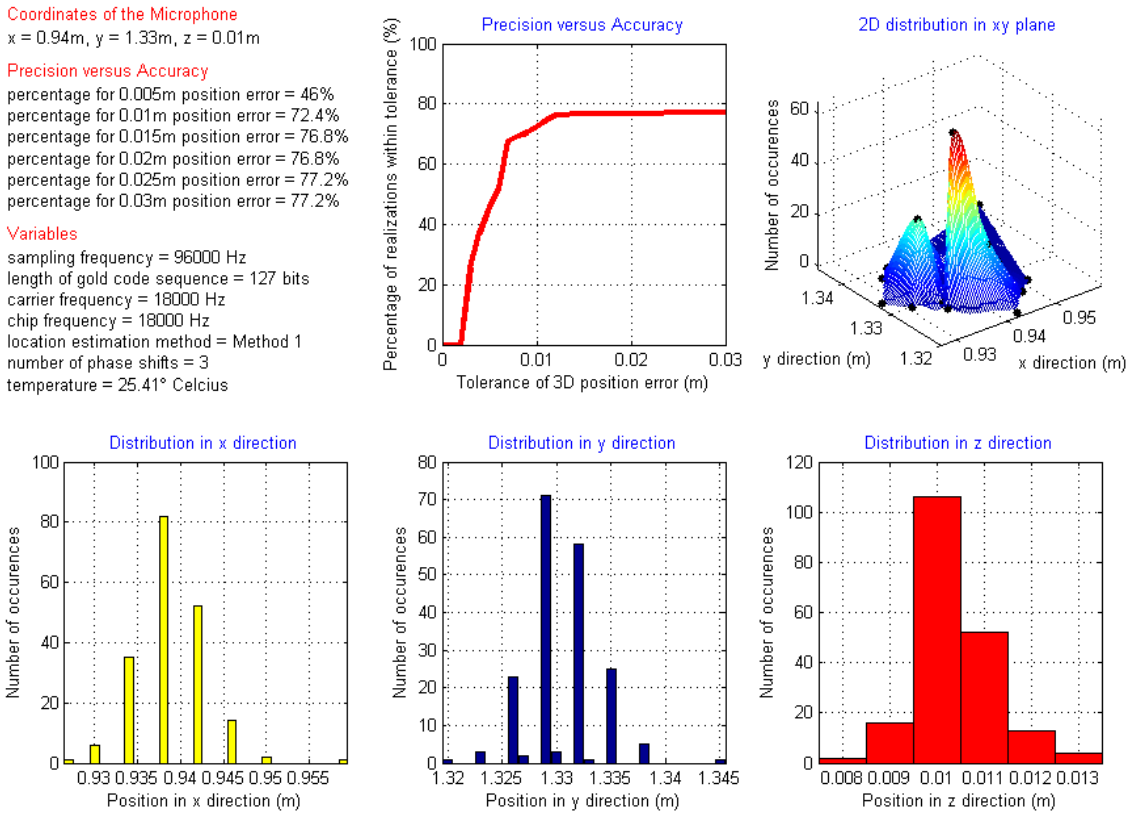


Figure D.14. 18 kHz carrier and chip frequencies

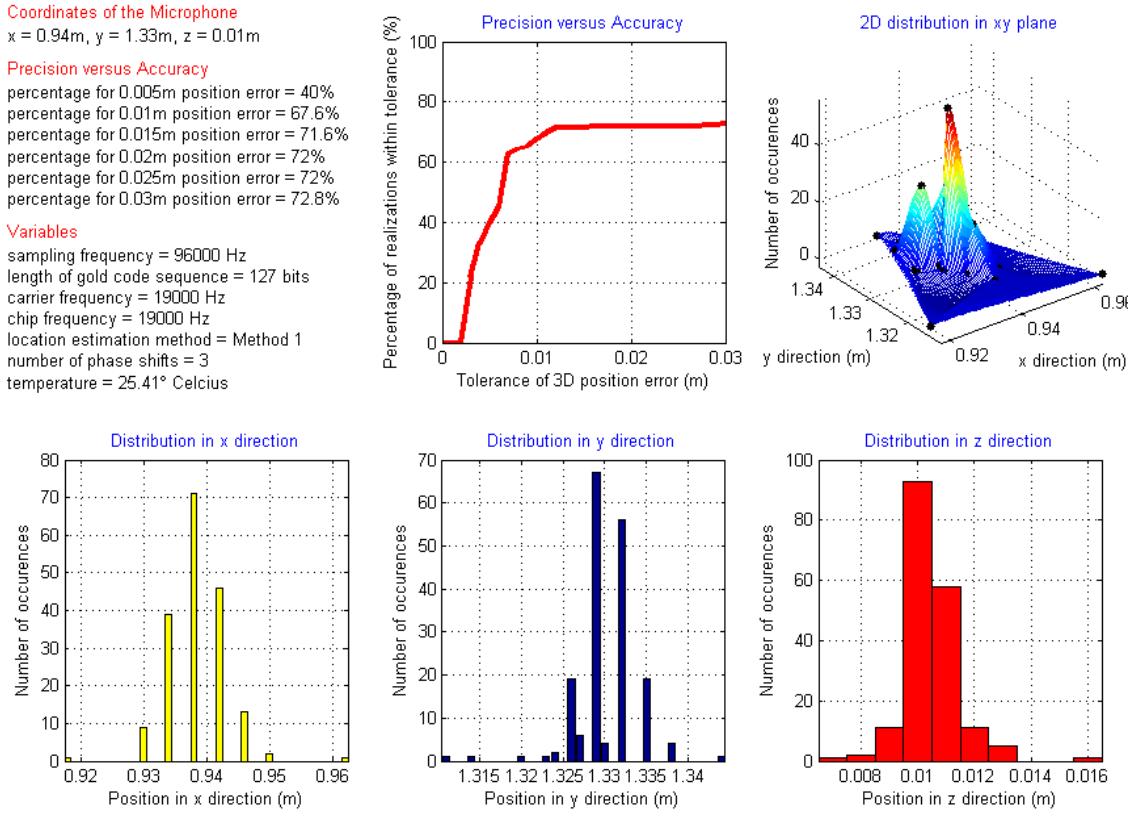


Figure D.15. 19 kHz carrier and chip frequencies

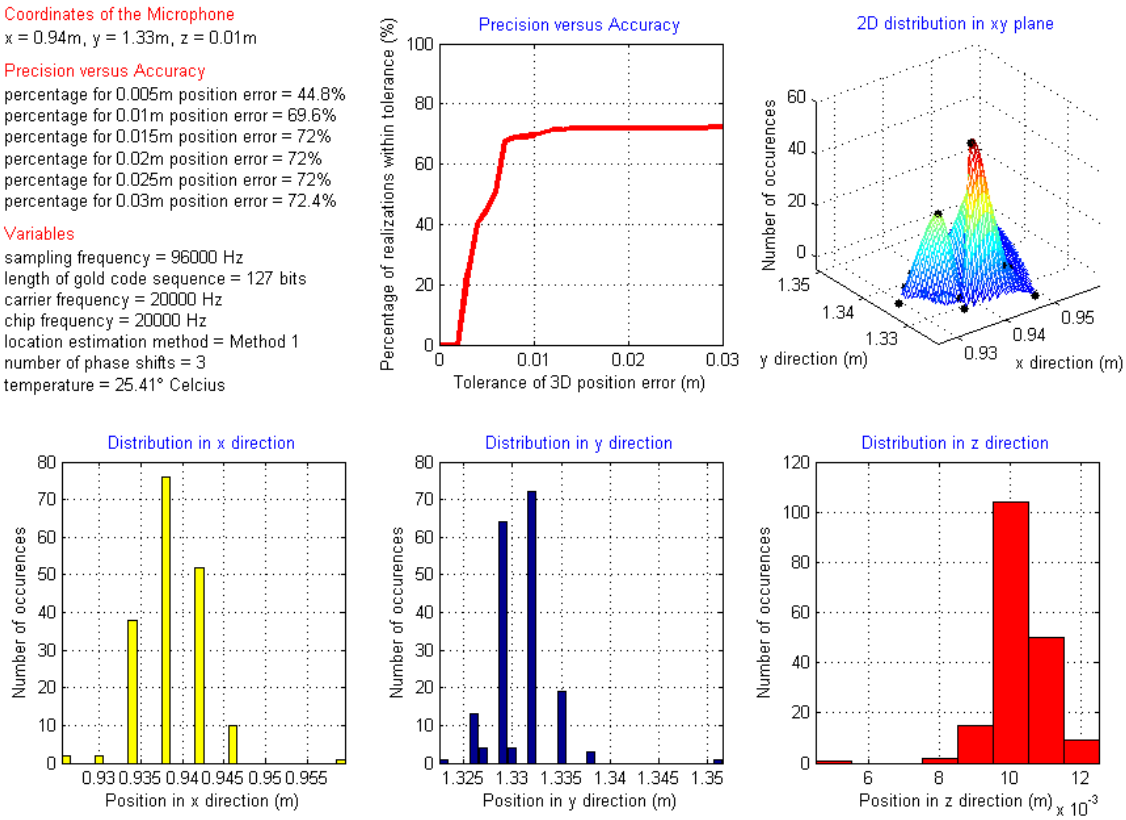


Figure D.16. 20 kHz carrier and chip frequencies

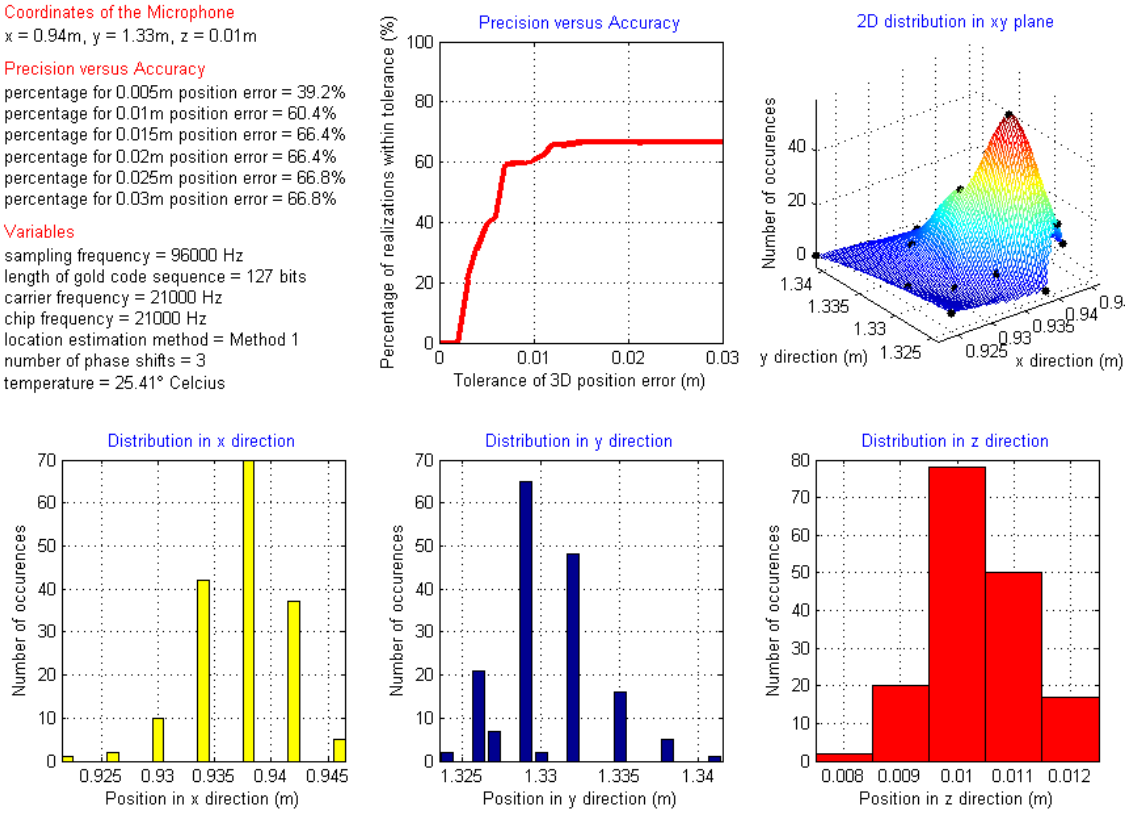


Figure D.17. 21 kHz carrier and chip frequencies

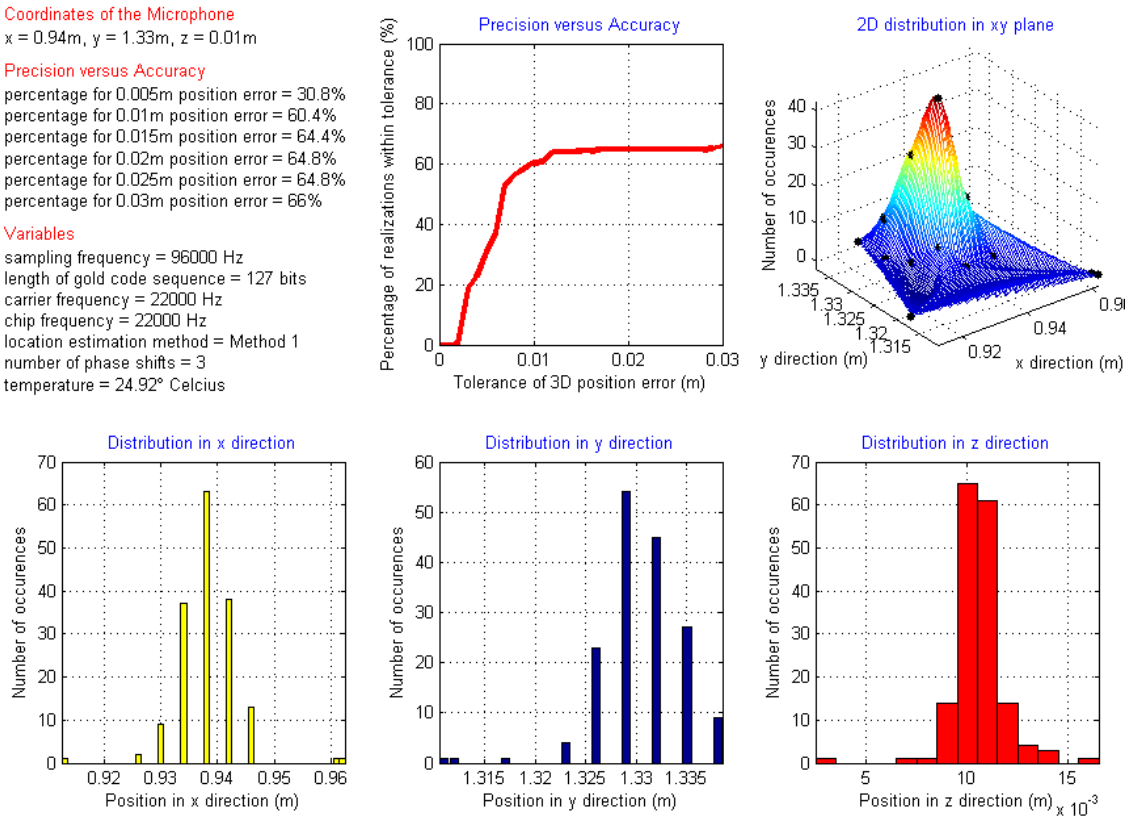


Figure D.18. 22 kHz carrier and chip frequencies

# APPENDIX E

# LOCALIZATION PERFORMANCE SCREENS FOR THE FIRST SET OF VARIABLES TAKEN FROM FOUR DIFFERENT REGIONS

In this section, the localization performance screens taken from four different regions were illustrated. The first set of variables was used for the tests.

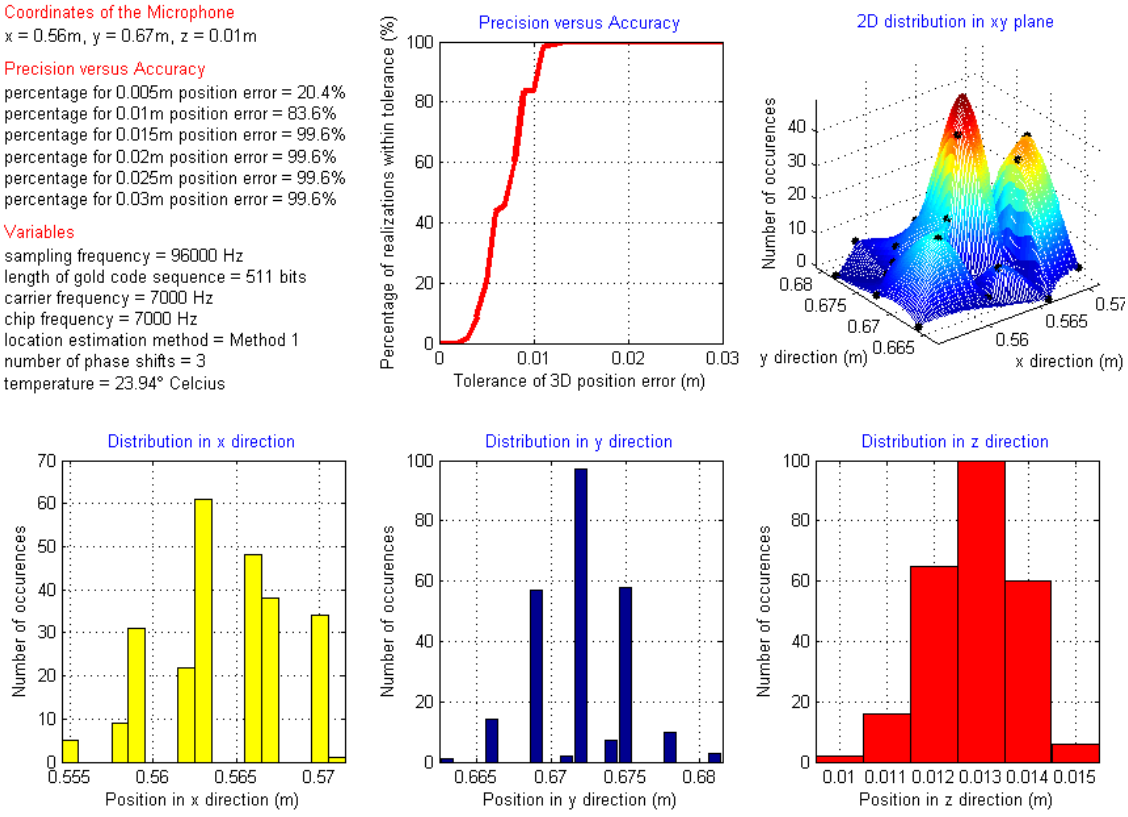


Figure E.1. x = 0.56 m, y = 0.67 m, z = 0.01 m

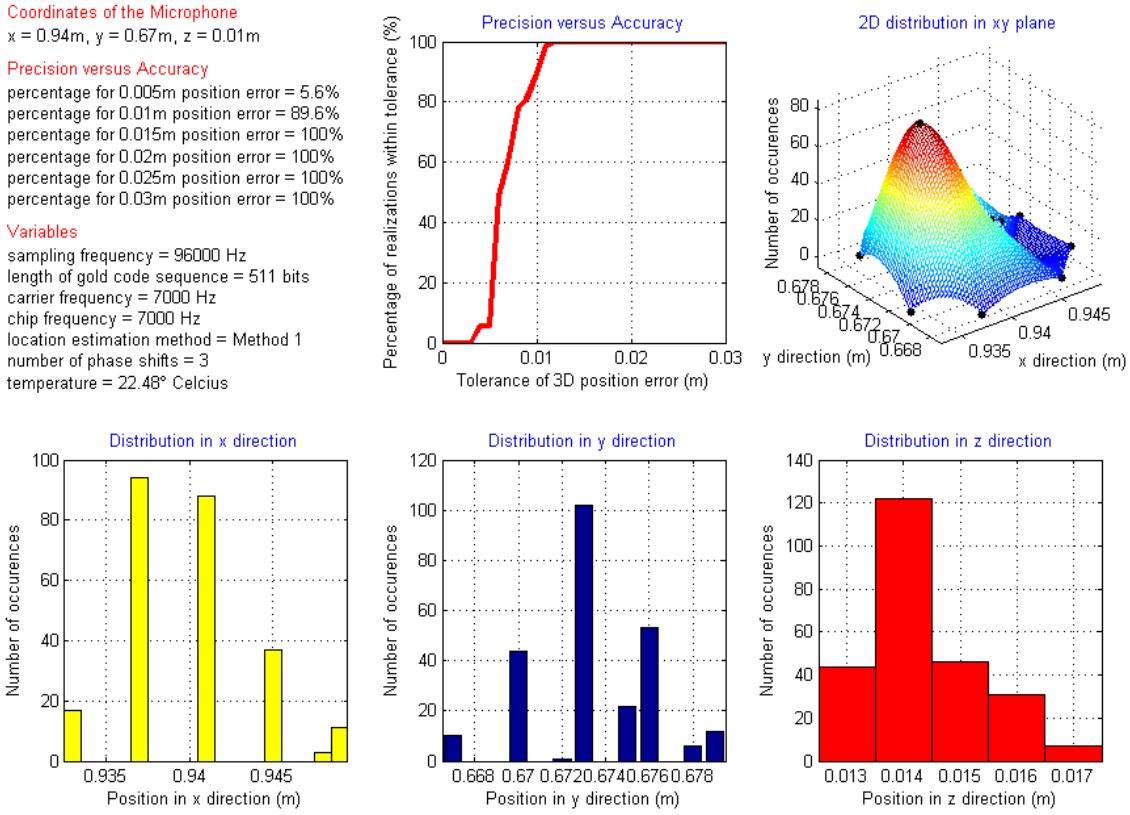


Figure E.2. x = 0.94 m, y = 0.67 m, z = 0.01 m

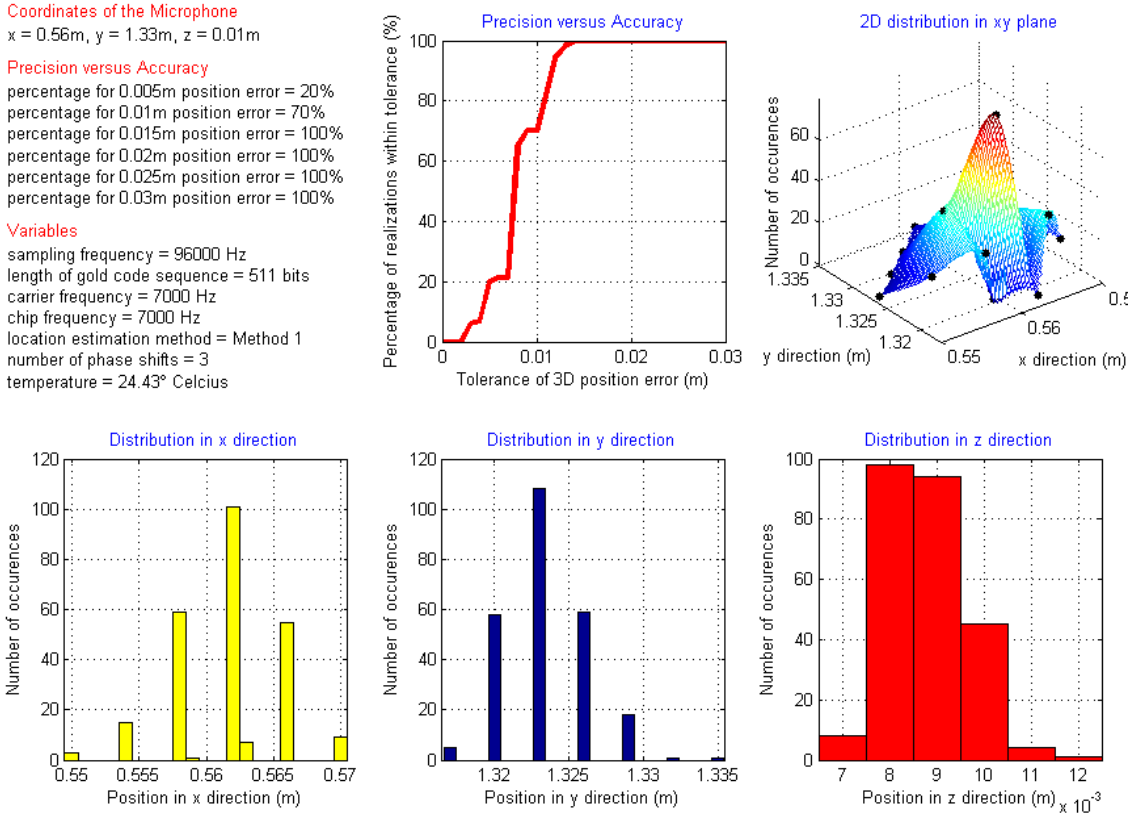


Figure E.3. x = 0.56 m, y = 1.33 m, z = 0.01 m

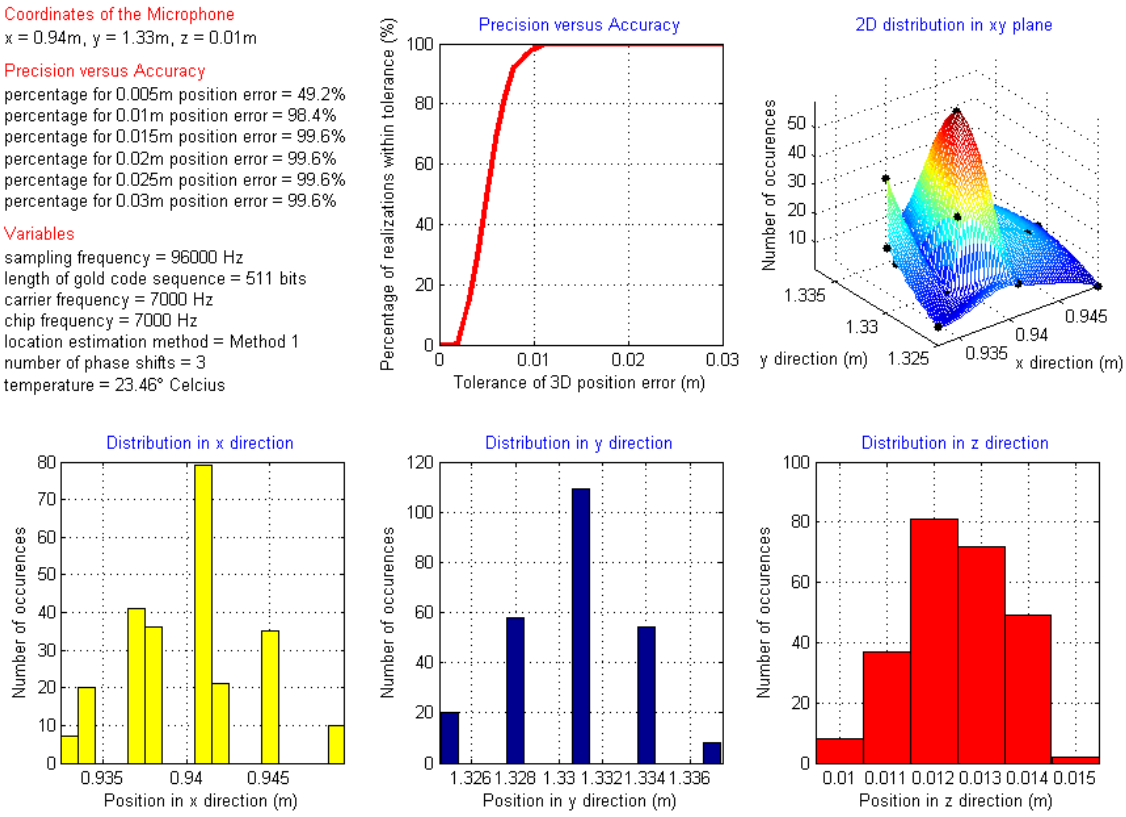


Figure E.4. x = 0.94 m, y = 1.33 m, z = 0.01 m

# APPENDIX F

# LOCALIZATION PERFORMANCE SCREENS FOR THE SECOND SET OF VARIABLES TAKEN FROM FOUR DIFFERENT REGIONS

In this section, the localization performance screens taken from four different regions were illustrated. The second set of variables was used for the tests.

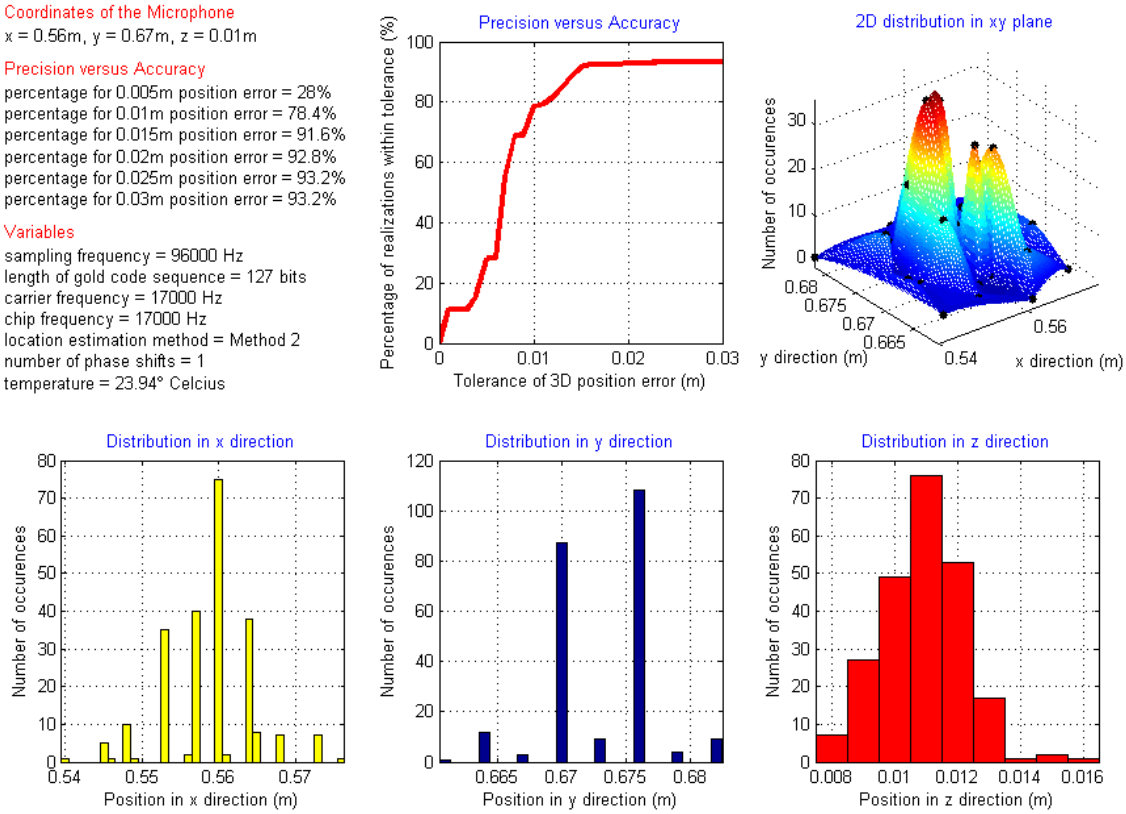


Figure F.1. x = 0.56 m, y = 0.67 m, z = 0.01 m

Coordinates of the Microphone
x = 0.94m, y = 0.67m, z = 0.01m

Precision versus Accuracy
percentage for 0.005m position error = 15.6%
percentage for 0.01m position error = 69.6%
percentage for 0.015m position error = 88.4%
percentage for 0.02m position error = 91.6%
percentage for 0.025m position error = 92%
percentage for 0.03m position error = 92%

Variables
sampling frequency = 96000 Hz
length of gold code sequence = 127 bits
carrier frequency = 17000 Hz
chip frequency = 17000 Hz
location estimation method = Method 2
number of phase shifts = 1
temperature = 23.46° Celcius

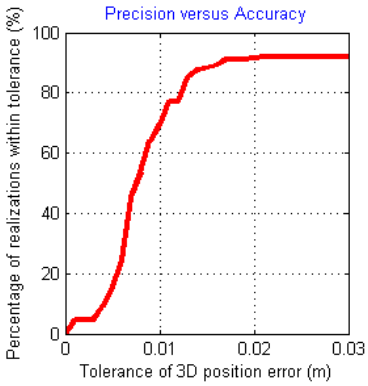


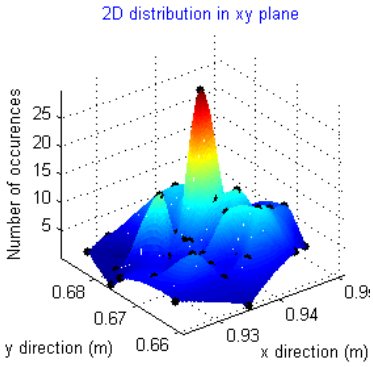


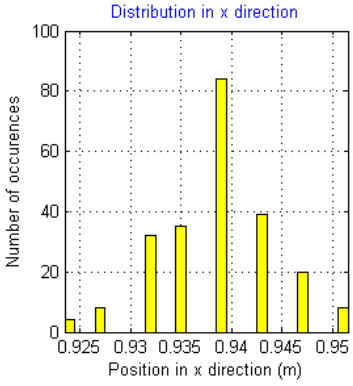


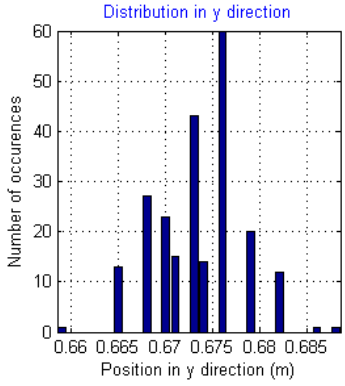


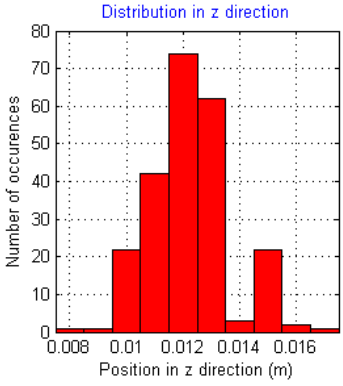


Figure F.2. x = 0.94 m, y = 0.67 m, z = 0.01 m

Coordinates of the Microphone
x = 0.56m, y = 1.33m, z = 0.01m

Precision versus Accuracy
percentage for 0.005m position error = 15.6%
percentage for 0.01m position error = 62.8%
percentage for 0.015m position error = 88.8%
percentage for 0.02m position error = 91.2%
percentage for 0.025m position error = 92%
percentage for 0.03m position error = 92%

Variables
sampling frequency = 96000 Hz
length of gold code sequence = 127 bits
carrier frequency = 17000 Hz
chip frequency = 17000 Hz
location estimation method = Method 2
number of phase shifts = 1
temperature = 24.43° Celcius

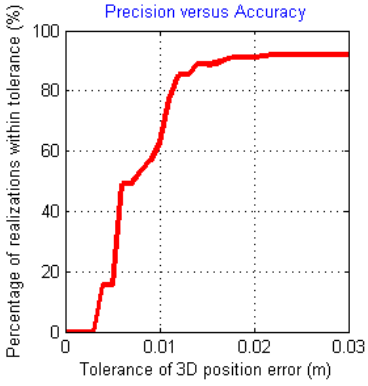


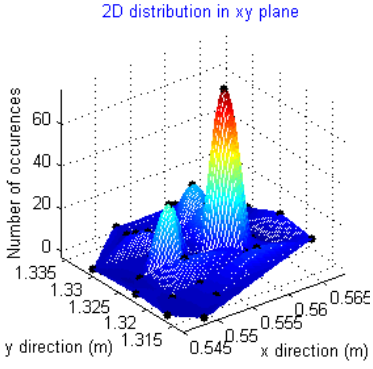


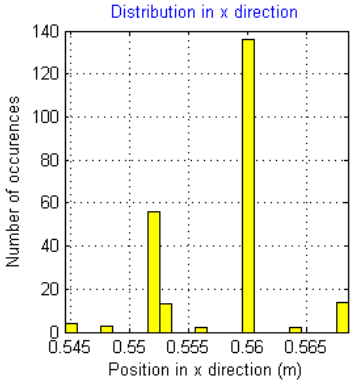


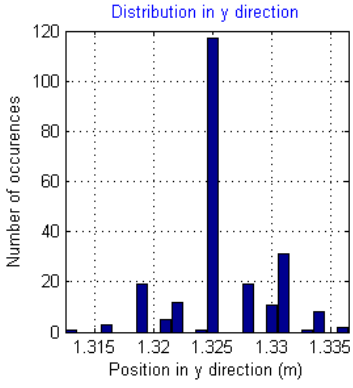


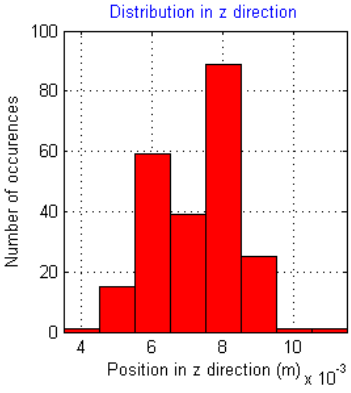


Figure F.3. x = 0.56 m, y = 1.33 m, z = 0.01 m

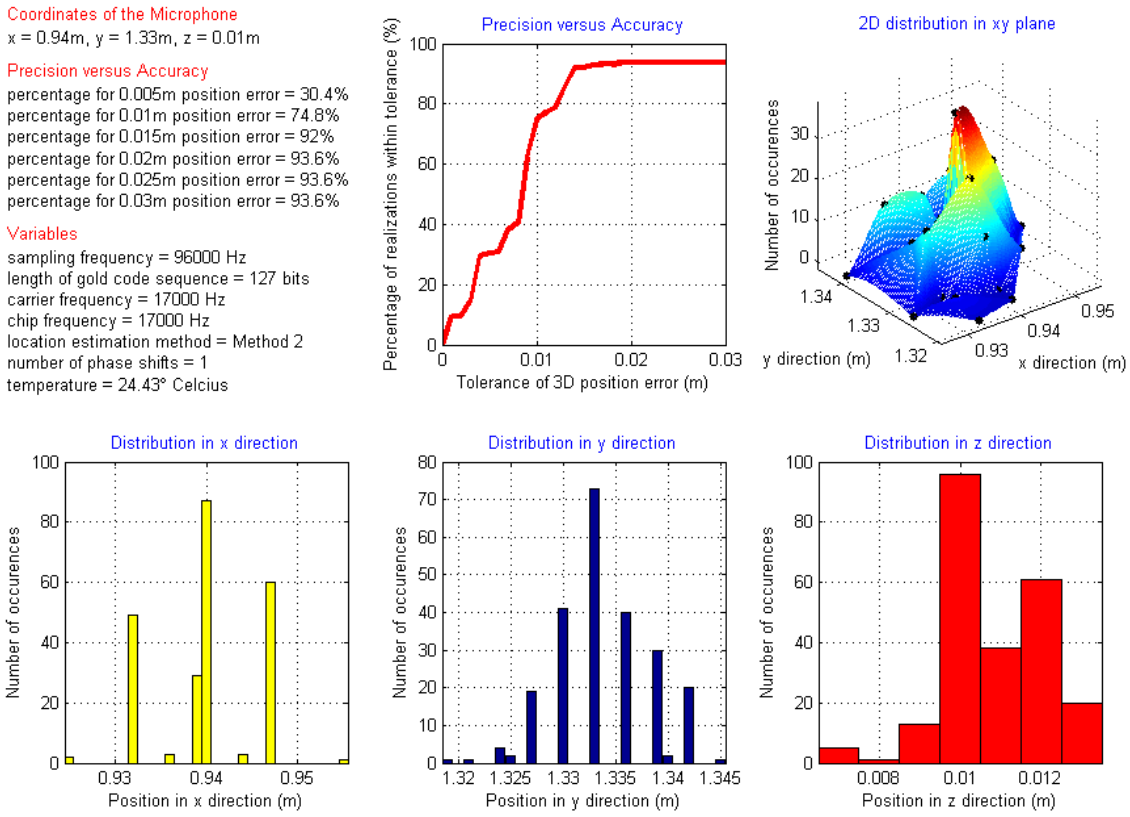


Figure F.4. x = 0.94 m, y = 1.33 m, z = 0.01 m

# APPENDIX G

# LOCALIZATION PERFORMANCE SCREENS FOR THE FIRST SET OF VARIABLES TAKEN FROM GROUND LEVEL TEST POINTS

In this section, the localization performance screens taken from ground level test points were illustrated. The first set of variables was used for the tests.

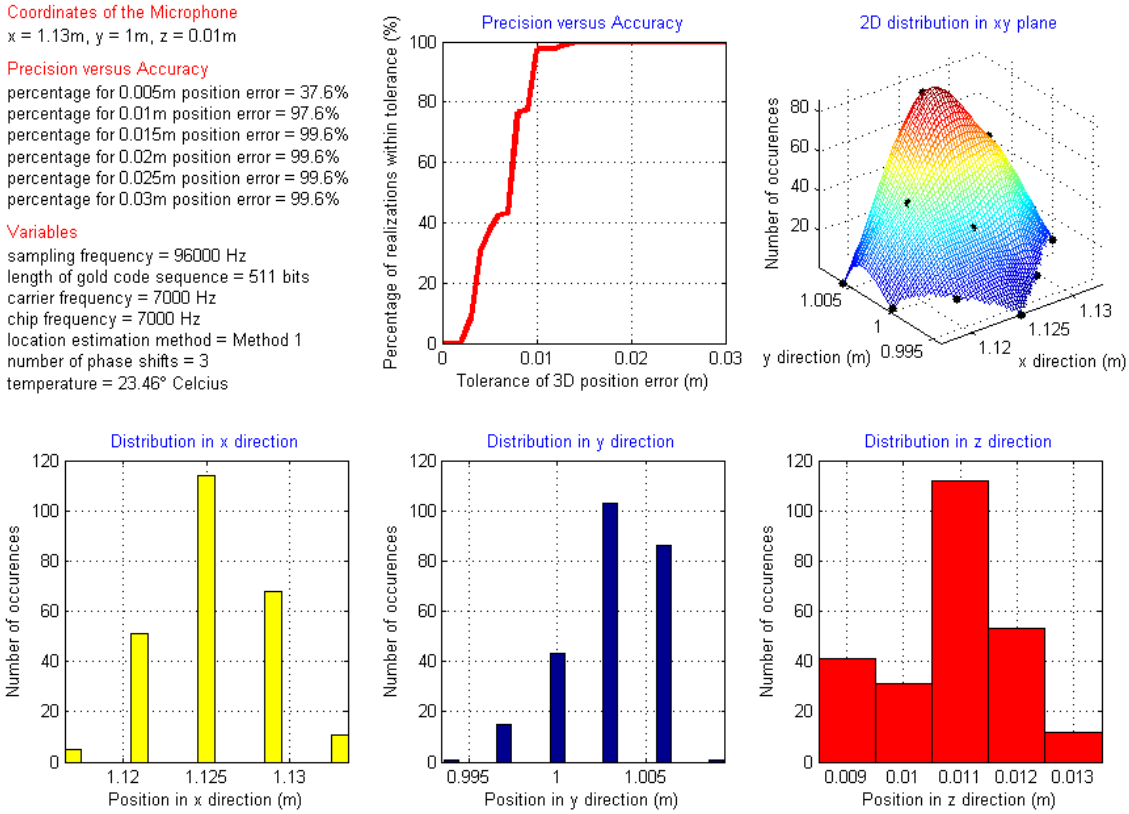


Figure G.1. x = 1.13 m, y = 1 m, z = 0.01 m

Coordinates of the Microphone
x = 1.51m, y = 1m, z = 0.01m

Precision versus Accuracy
percentage for 0.005m position error = 17.6%
percentage for 0.01m position error = 91.2%
percentage for 0.015m position error = 100%
percentage for 0.02m position error = 100%
percentage for 0.025m position error = 100%
percentage for 0.03m position error = 100%

Variables
sampling frequency = 96000 Hz
length of gold code sequence = 511 bits
carrier frequency = 7000 Hz
chip frequency = 7000 Hz
location estimation method = Method 1
number of phase shifts = 3
temperature = 23.94° Celcius

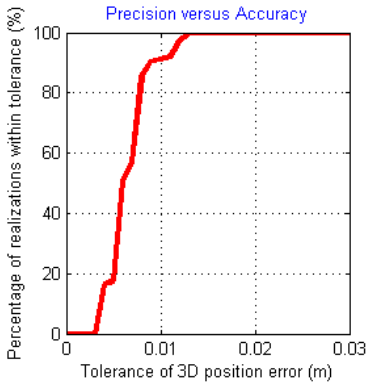


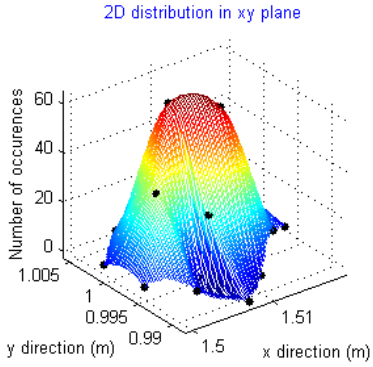


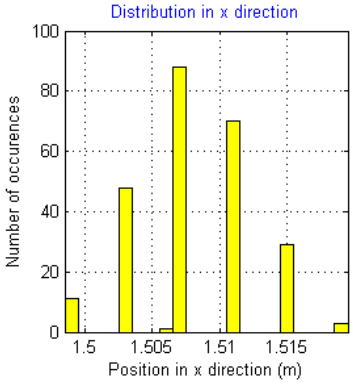


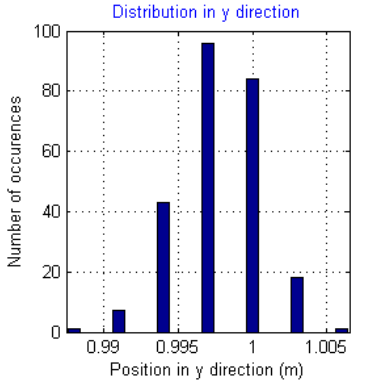


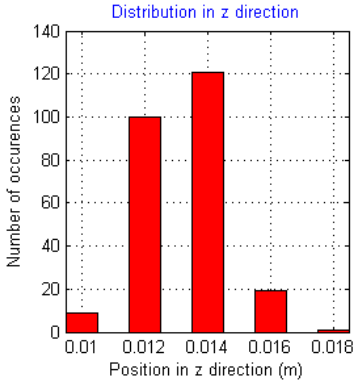


Figure G.2. x = 1.51 m, y = 1 m, z = 0.01 m

Coordinates of the Microphone
x = 0.94m, y = 1.33m, z = 0.01m

Precision versus Accuracy
percentage for 0.005m position error = 49.2%
percentage for 0.01m position error = 98.4%
percentage for 0.015m position error = 99.6%
percentage for 0.02m position error = 99.6%
percentage for 0.025m position error = 99.6%
percentage for 0.03m position error = 99.6%

Variables
sampling frequency = 96000 Hz
length of gold code sequence = 511 bits
carrier frequency = 7000 Hz
chip frequency = 7000 Hz
location estimation method = Method 1
number of phase shifts = 3
temperature = 23.46° Celcius

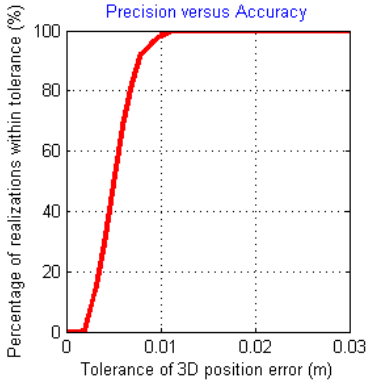


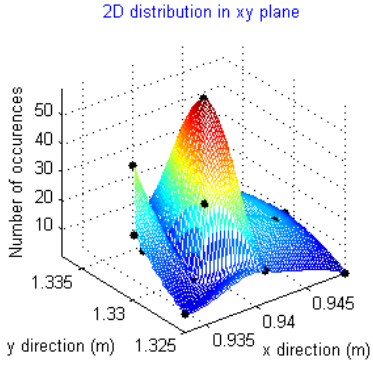


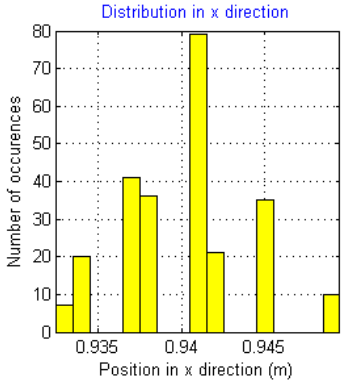


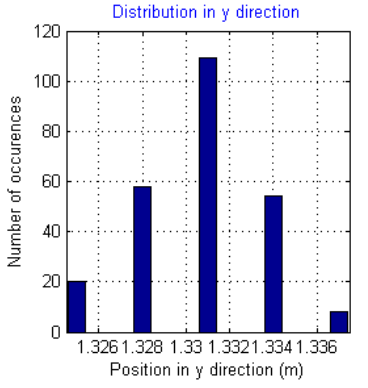


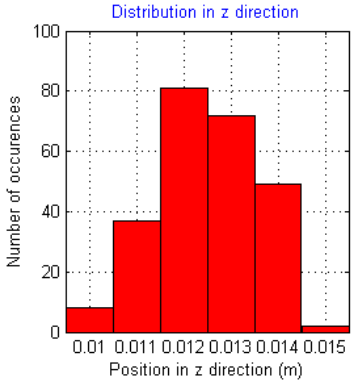


Figure G.3. x = 0.94 m, y = 1.33 m, z = 0.01 m

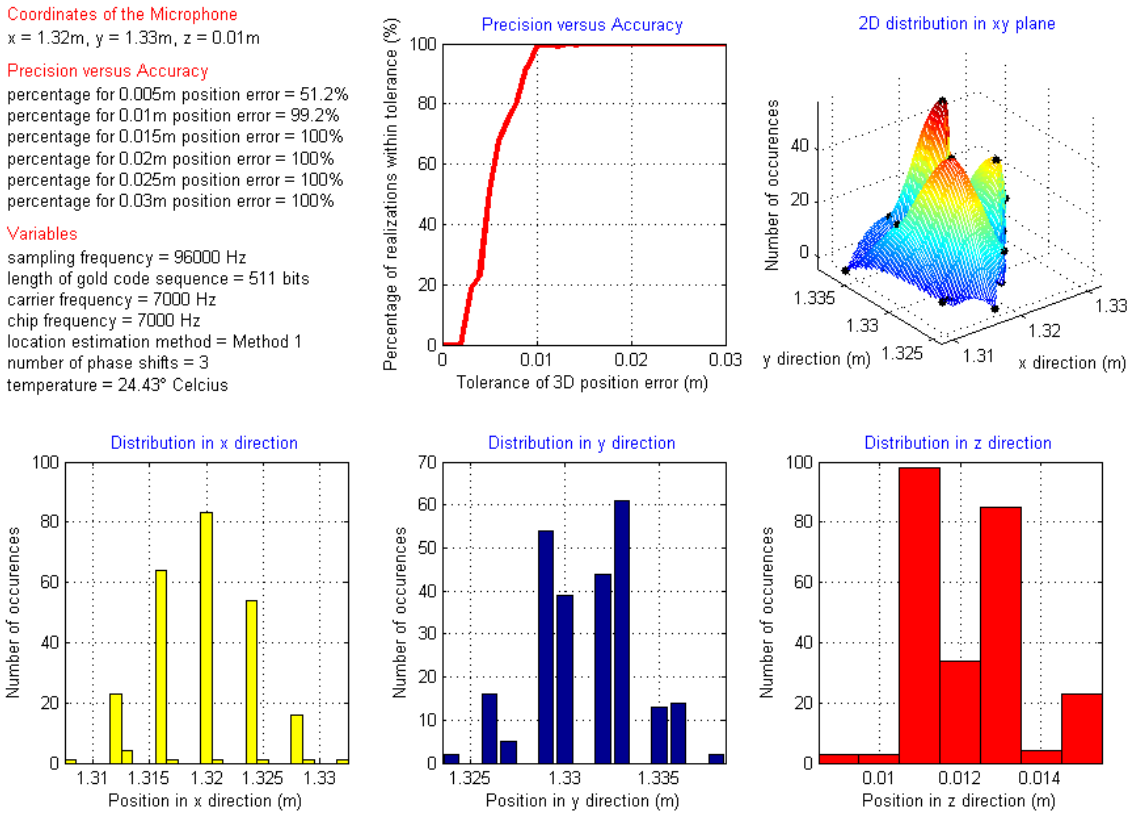


Figure G.4. x = 1.32 m, y = 1.33 m, z = 0.01 m

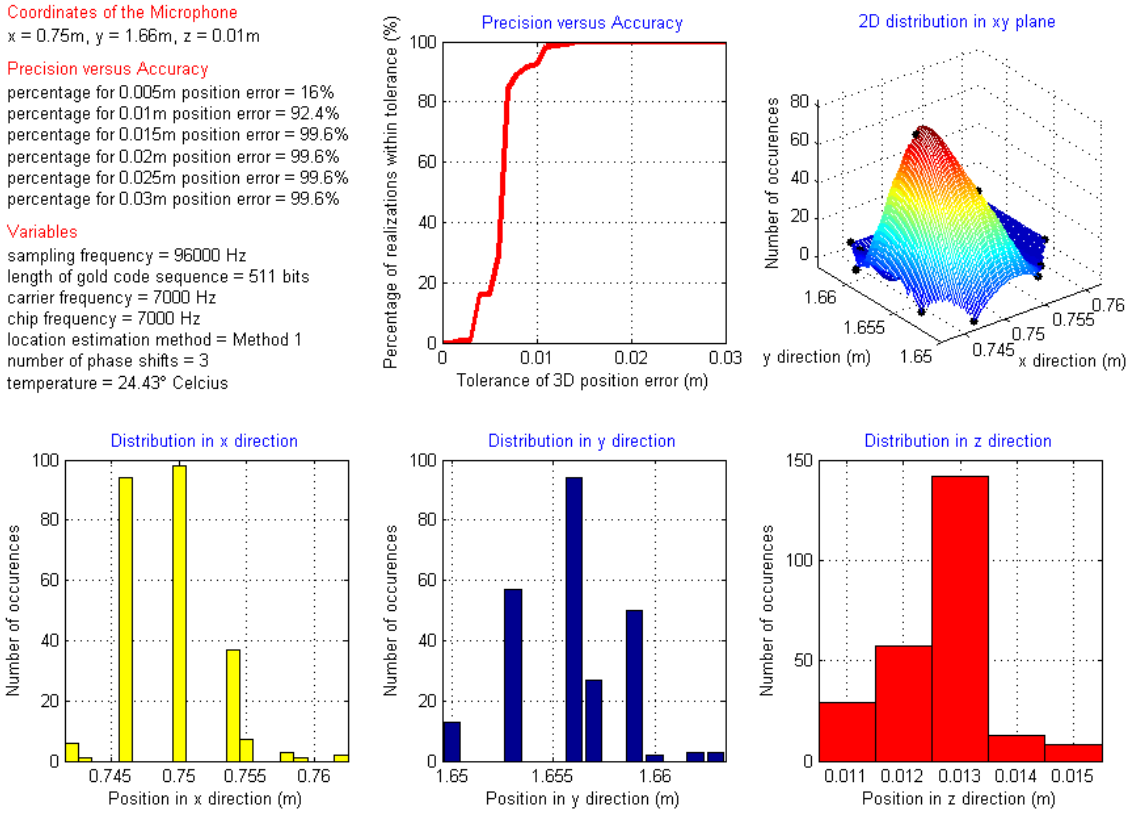


Figure G.5. x = 0.75 m, y = 1.66 m, z = 0.01 m

Coordinates of the Microphone
x = 1.13m, y = 1.66m, z = 0.01m

Precision versus Accuracy
percentage for 0.005m position error = 13.6%
percentage for 0.01m position error = 80%
percentage for 0.015m position error = 98.8%
percentage for 0.02m position error = 98.8%
percentage for 0.025m position error = 98.8%
percentage for 0.03m position error = 98.8%

Variables
sampling frequency = 96000 Hz
length of gold code sequence = 511 bits
carrier frequency = 7000 Hz
chip frequency = 7000 Hz
location estimation method = Method 1
number of phase shifts = 3
temperature = 24.43° Celcius

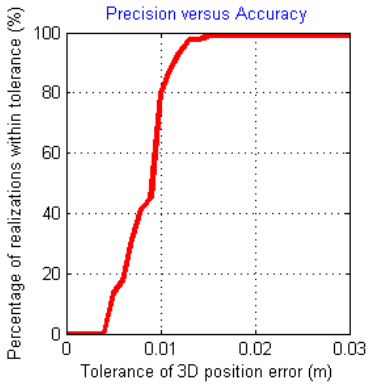


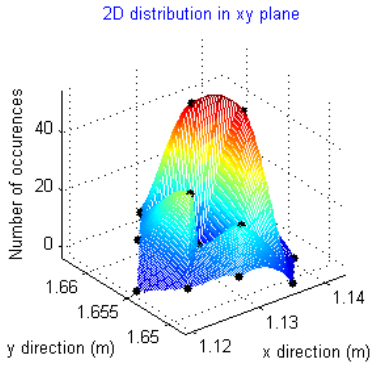


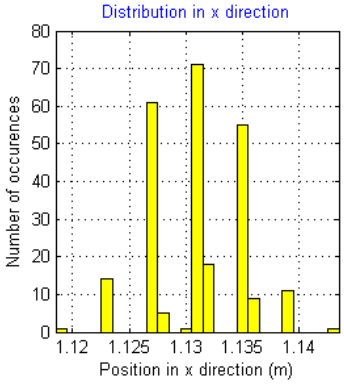


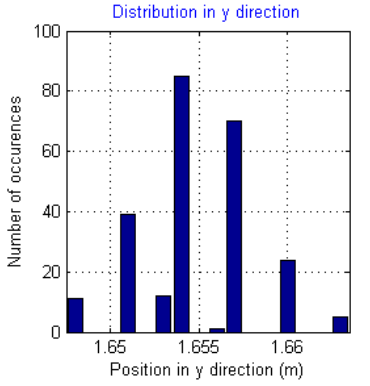


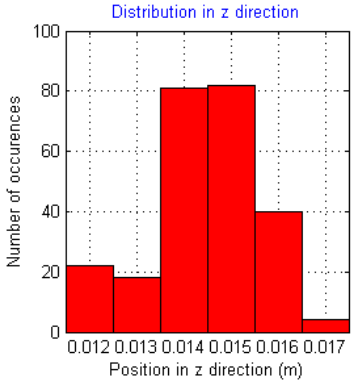


Figure G.6. x = 1.13 m, y = 1.66 m, z = 0.01 m

Coordinates of the Microphone
x = 1.51m, y = 1.66m, z = 0.01m

Precision versus Accuracy
percentage for 0.005m position error = 0%
percentage for 0.01m position error = 64.8%
percentage for 0.015m position error = 99.2%
percentage for 0.02m position error = 99.2%
percentage for 0.025m position error = 99.2%
percentage for 0.03m position error = 99.2%

Variables
sampling frequency = 96000 Hz
length of gold code sequence = 511 bits
carrier frequency = 7000 Hz
chip frequency = 7000 Hz
location estimation method = Method 1
number of phase shifts = 3
temperature = 23.94° Celcius

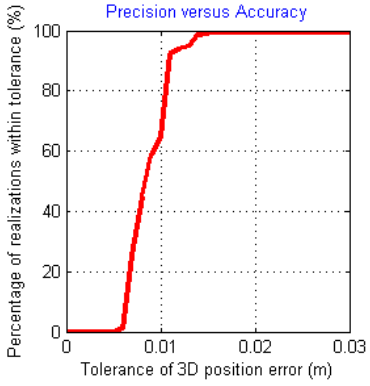


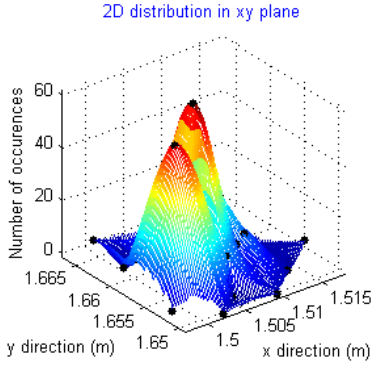


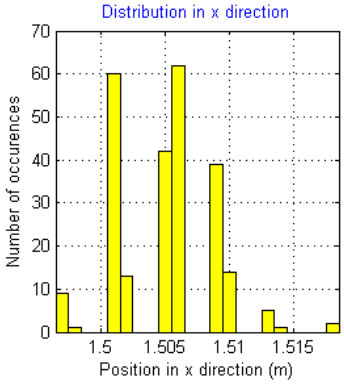


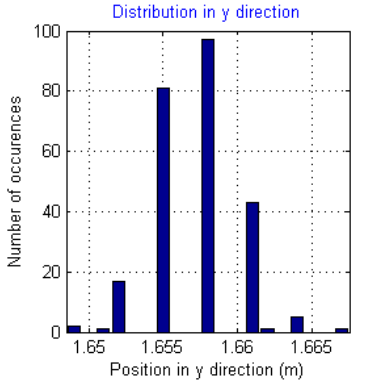


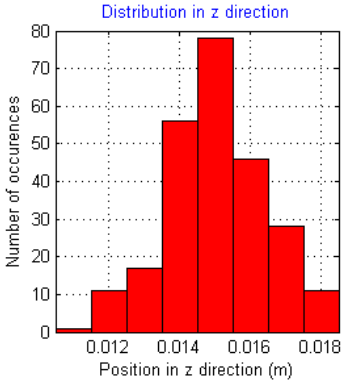


Figure G.7. x = 1.51 m, y = 1.66 m, z = 0.01 m

Coordinates of the Microphone
x = 0.94m, y = 1.99m, z = 0.01m

Precision versus Accuracy
percentage for 0.005m position error = 0%
percentage for 0.01m position error = 20.4%
percentage for 0.015m position error = 79.6%
percentage for 0.02m position error = 98.8%
percentage for 0.025m position error = 99.6%
percentage for 0.03m position error = 99.6%

Variables
sampling frequency = 96000 Hz
length of gold code sequence = 511 bits
carrier frequency = 7000 Hz
chip frequency = 7000 Hz
location estimation method = Method 1
number of phase shifts = 3
temperature = 24.43° Celcius

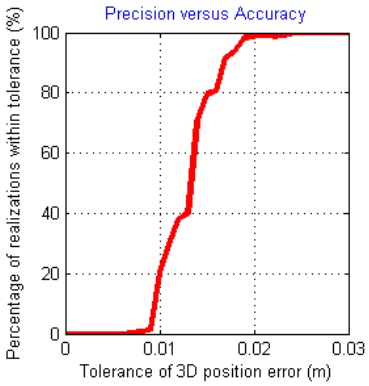


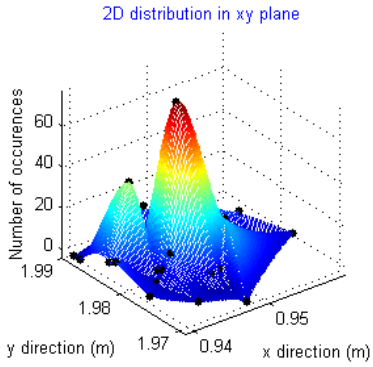


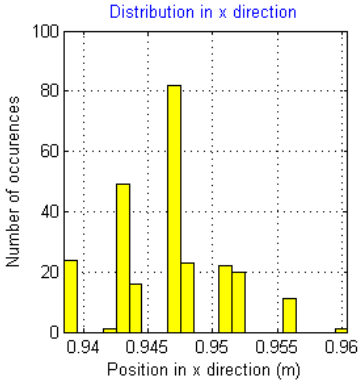


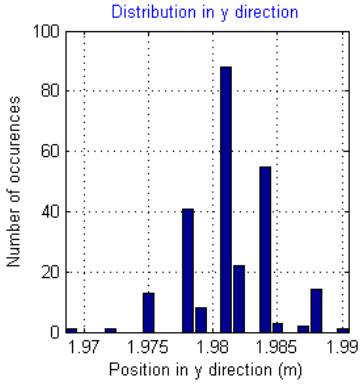


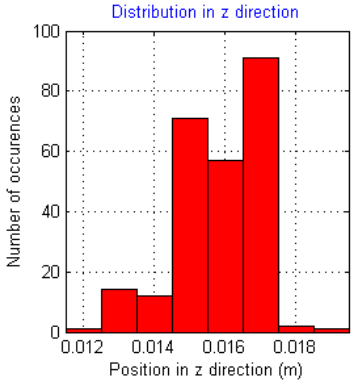


Figure G.8. x = 0.94 m, y = 1.99 m, z = 0.01 m

Coordinates of the Microphone
x = 1.32m, y = 1.99m, z = 0.01m

Precision versus Accuracy
percentage for 0.005m position error = 0%
percentage for 0.01m position error = 47.2%
percentage for 0.015m position error = 93.2%
percentage for 0.02m position error = 100%
percentage for 0.025m position error = 100%
percentage for 0.03m position error = 100%

Variables
sampling frequency = 96000 Hz
length of gold code sequence = 511 bits
carrier frequency = 7000 Hz
chip frequency = 7000 Hz
location estimation method = Method 1
number of phase shifts = 3
temperature = 23.94° Celcius

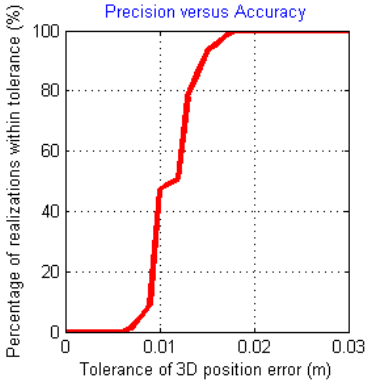


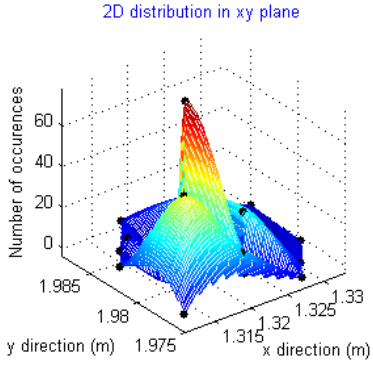


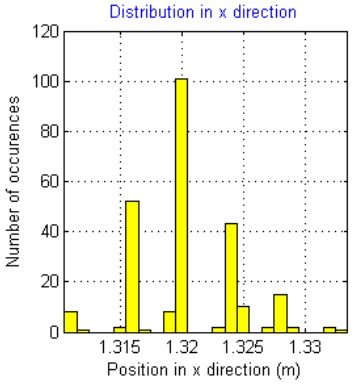


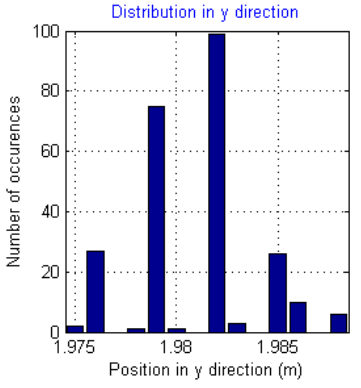


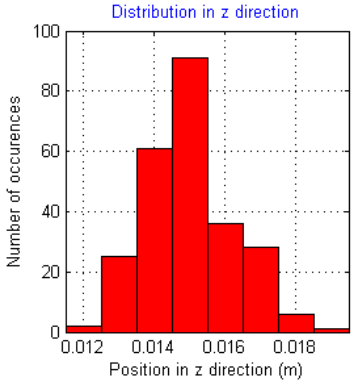


Figure G.9. x = 1.32 m, y = 1.99 m, z = 0.01 m

# APPENDIX H

# LOCALIZATION PERFORMANCE SCREENS FOR THE SECOND SET OF VARIABLES TAKEN FROM GROUND LEVEL TEST POINTS

In this section, the localization performance screens taken from ground level test points were illustrated. The second set of variables was used for the tests.

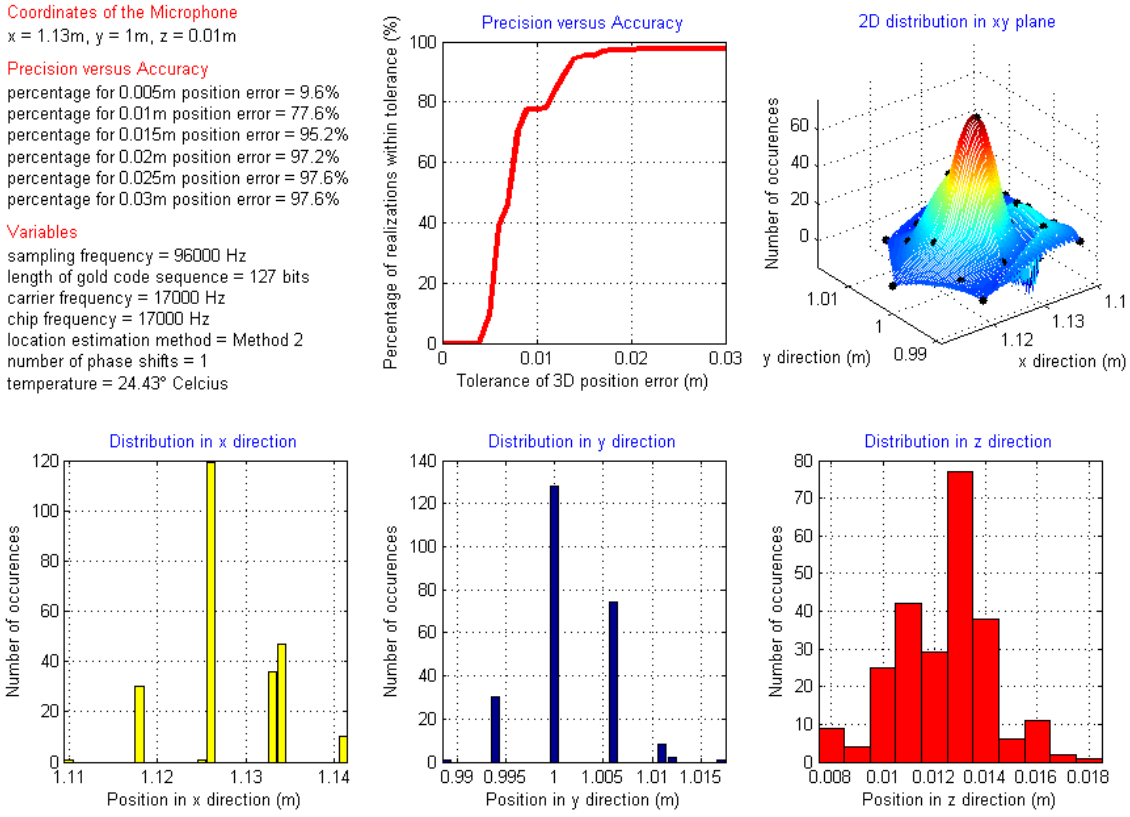


Figure H.1. x = 1.13 m, y = 1 m, z = 0.01 m

Coordinates of the Microphone
x = 1.51m, y = 1m, z = 0.01m

Precision versus Accuracy
percentage for 0.005m position error = 22%
percentage for 0.01m position error = 65.2%
percentage for 0.015m position error = 90.4%
percentage for 0.02m position error = 92.8%
percentage for 0.025m position error = 93.2%
percentage for 0.03m position error = 93.2%

Variables
sampling frequency = 96000 Hz
length of gold code sequence = 127 bits
carrier frequency = 17000 Hz
chip frequency = 17000 Hz
location estimation method = Method 2
number of phase shifts = 1
temperature = 24.43° Celcius

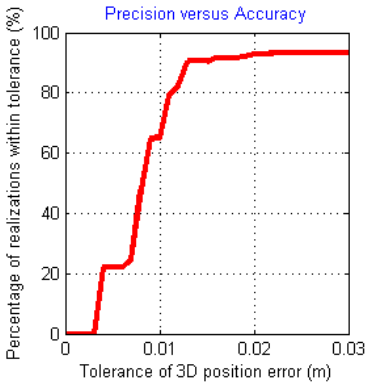


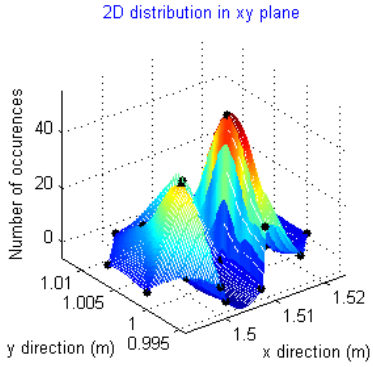


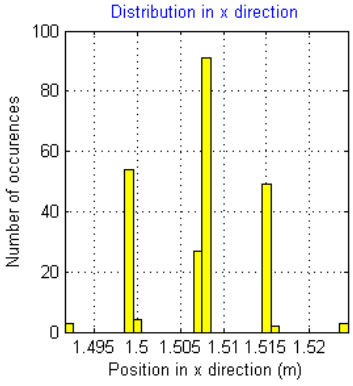


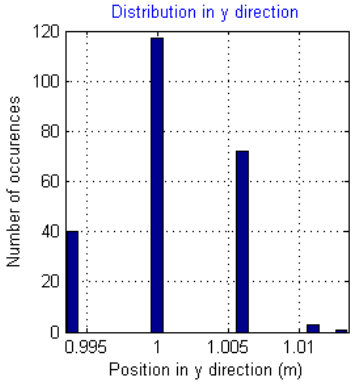


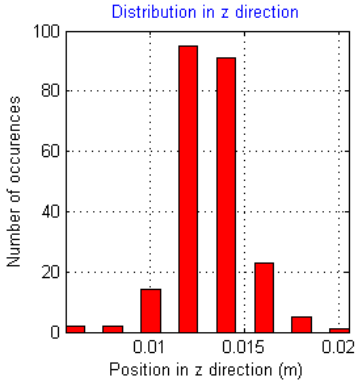


Figure H.2. x = 1.51 m, y = 1 m, z = 0.01 m

Coordinates of the Microphone
x = 0.94m, y = 1.33m, z = 0.01m

Precision versus Accuracy
percentage for 0.005m position error = 30.4%
percentage for 0.01m position error = 74.8%
percentage for 0.015m position error = 92%
percentage for 0.02m position error = 93.6%
percentage for 0.025m position error = 93.6%
percentage for 0.03m position error = 93.6%

Variables
sampling frequency = 96000 Hz
length of gold code sequence = 127 bits
carrier frequency = 17000 Hz
chip frequency = 17000 Hz
location estimation method = Method 2
number of phase shifts = 1
temperature = 24.43° Celcius

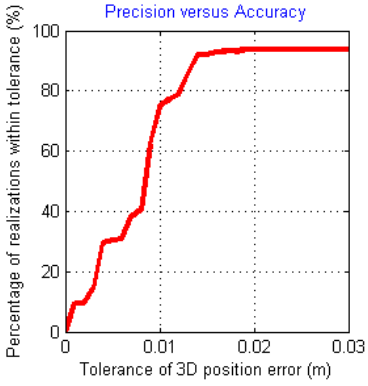


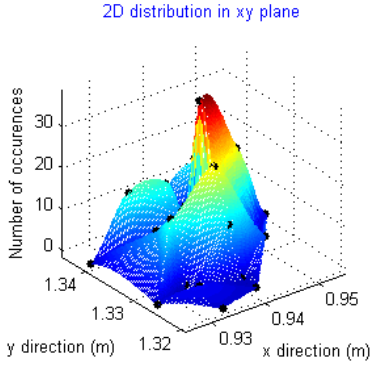


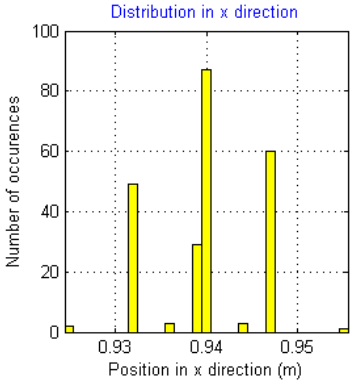


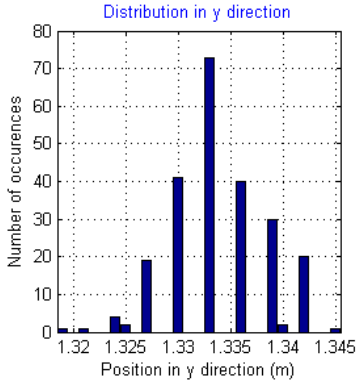


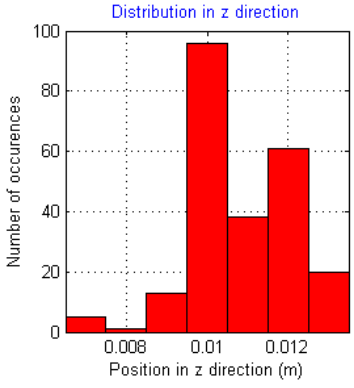


Figure H.3. x = 0.94 m, y = 1.33 m, z = 0.01 m

Coordinates of the Microphone
x = 1.32m, y = 1.33m, z = 0.01m

Precision versus Accuracy
percentage for 0.005m position error = 46%
percentage for 0.01m position error = 69.2%
percentage for 0.015m position error = 83.6%
percentage for 0.02m position error = 87.2%
percentage for 0.025m position error = 87.6%
percentage for 0.03m position error = 87.6%

Variables
sampling frequency = 96000 Hz
length of gold code sequence = 127 bits
carrier frequency = 17000 Hz
chip frequency = 17000 Hz
location estimation method = Method 2
number of phase shifts = 1
temperature = 23.46° Celcius

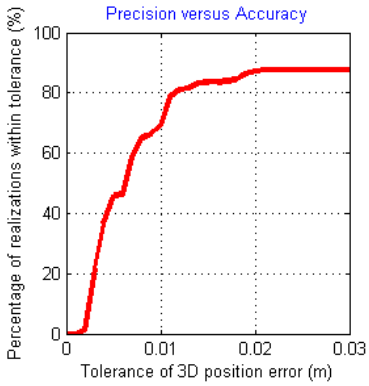


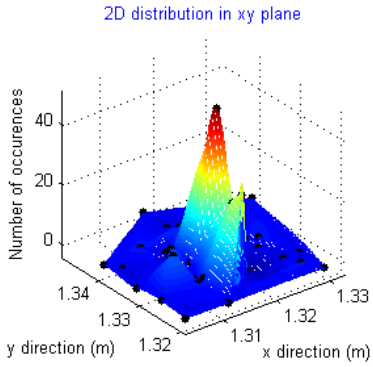


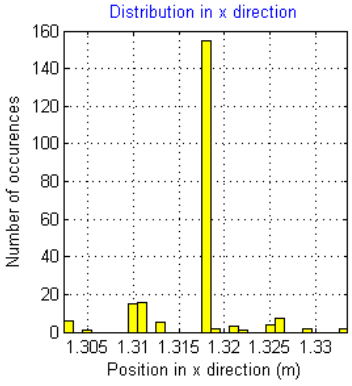


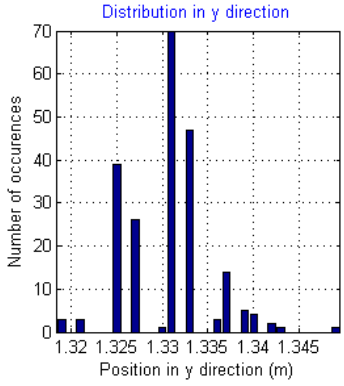


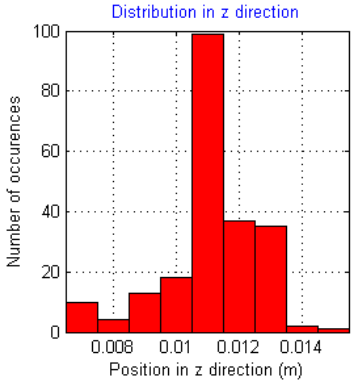


Figure H.4. x = 1.32 m, y = 1.33 m, z = 0.01 m

Coordinates of the Microphone
x = 0.75m, y = 1.66m, z = 0.01m

Precision versus Accuracy
percentage for 0.005m position error = 12.8%
percentage for 0.01m position error = 60.8%
percentage for 0.015m position error = 77.2%
percentage for 0.02m position error = 77.6%
percentage for 0.025m position error = 77.6%
percentage for 0.03m position error = 77.6%

Variables
sampling frequency = 96000 Hz
length of gold code sequence = 127 bits
carrier frequency = 17000 Hz
chip frequency = 17000 Hz
location estimation method = Method 2
number of phase shifts = 1
temperature = 24.43° Celcius

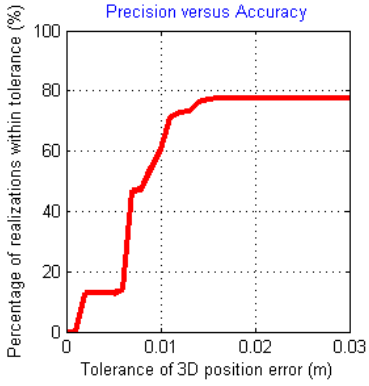


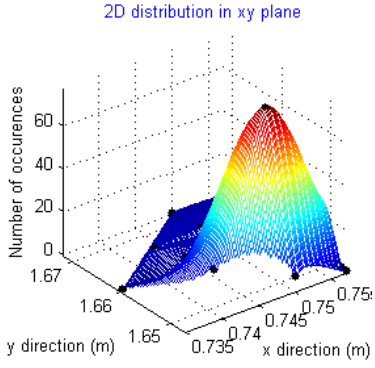


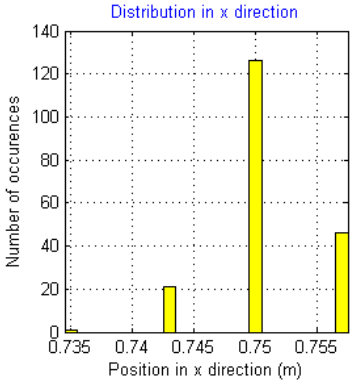


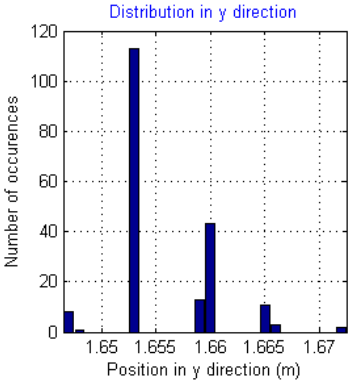


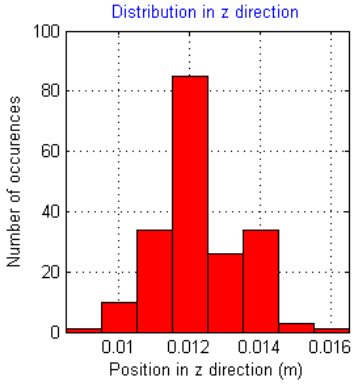


Figure H.5. x = 0.75 m, y = 1.66 m, z = 0.01 m

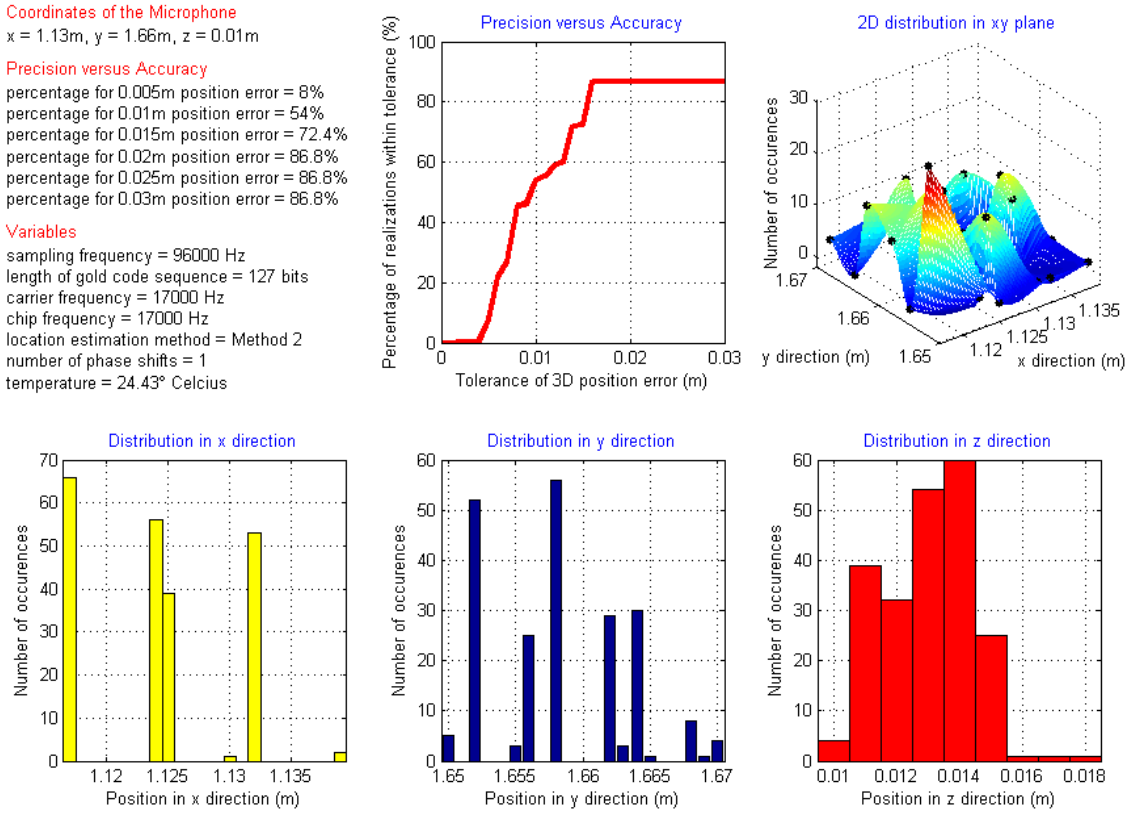


Figure H.6. x = 1.13 m, y = 1.66 m, z = 0.01 m

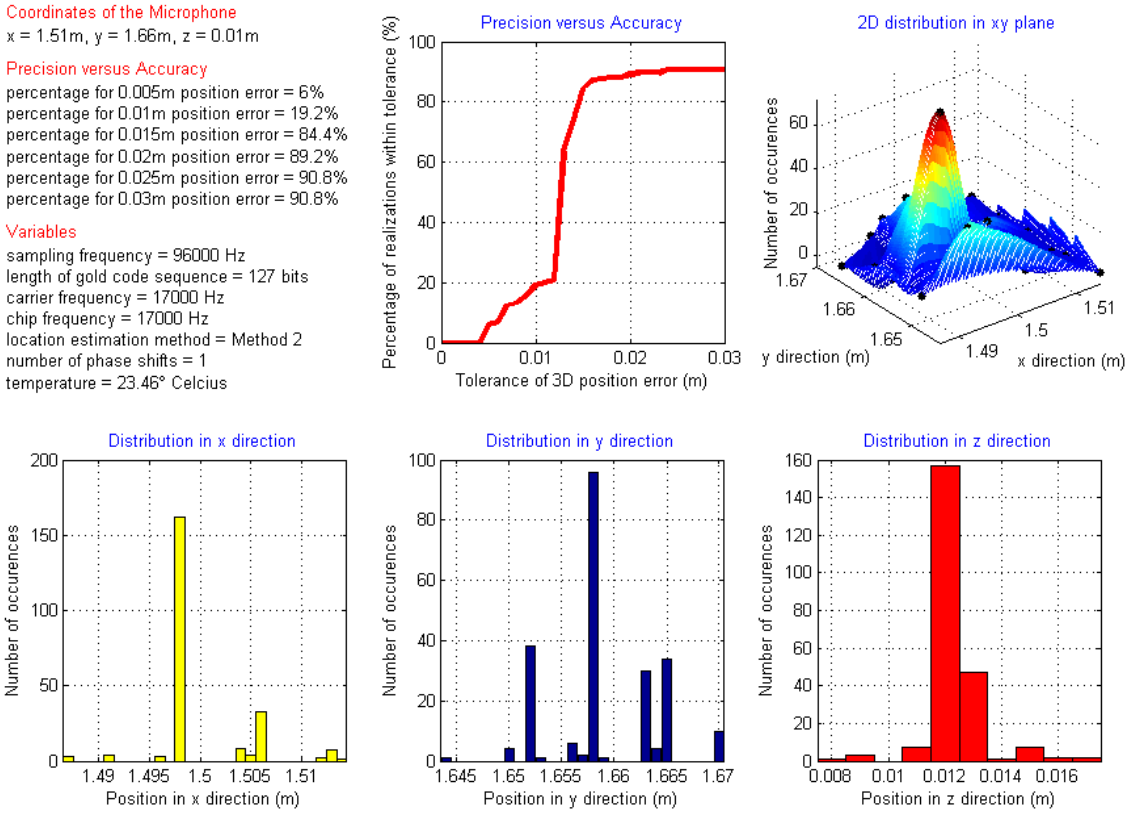


Figure H.7. x = 1.51 m, y = 1.66 m, z = 0.01 m

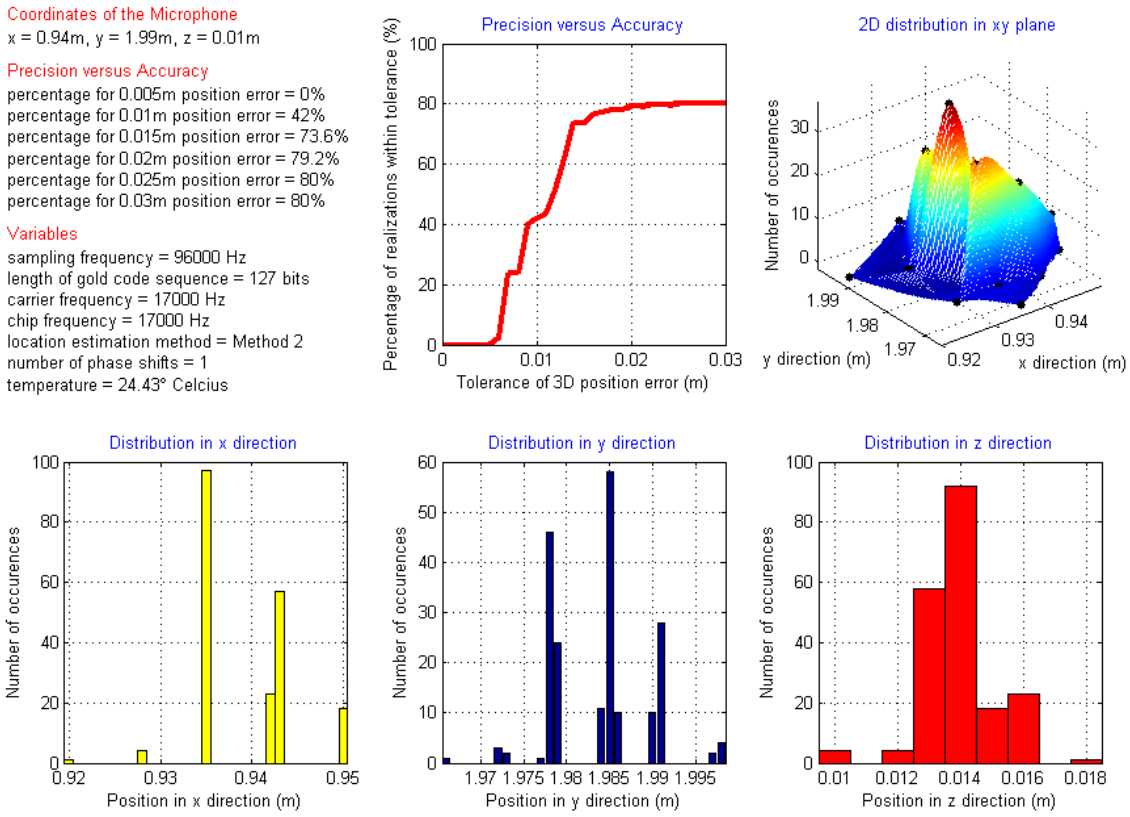


Figure H.8. x = 0.94 m, y = 1.99 m, z = 0.01 m

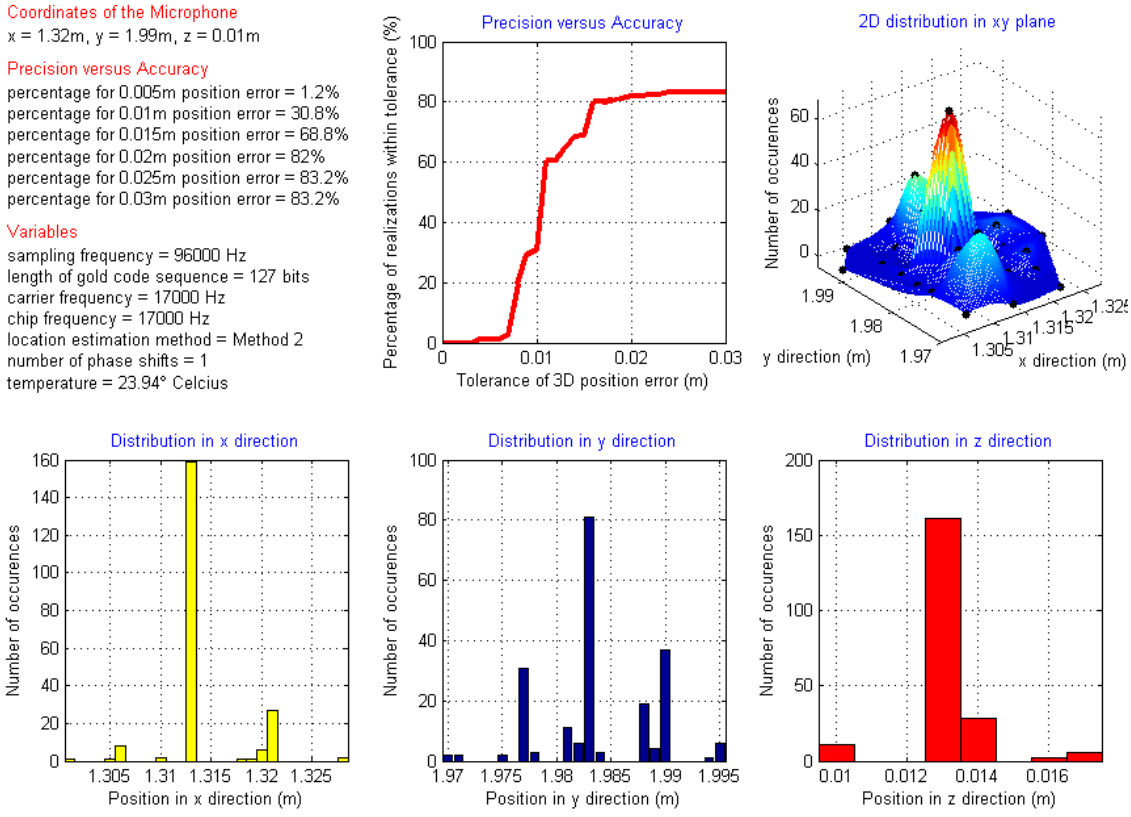


Figure H.9. x = 1.32 m, y = 1.99 m, z = 0.01 m

# APPENDIX I

# LOCALIZATION PERFORMANCE SCREENS FOR THE FIRST SET OF VARIABLES TAKEN FROM UPPER LEVEL TEST POINTS

In this section, the localization performance screens taken from upper level test points were illustrated. The first set of variables was used for the tests.

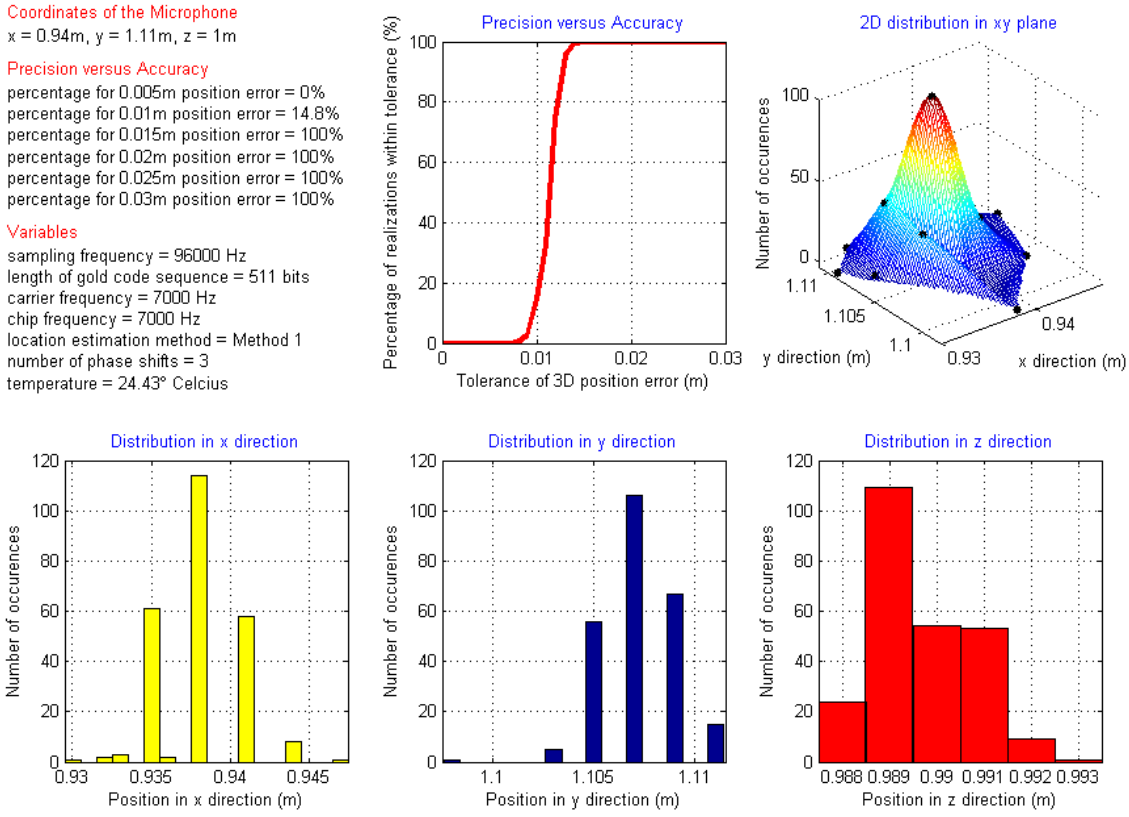


Figure I.1. x = 0.94 m, y = 1.11 m, z = 1 m

Coordinates of the Microphone
x = 1.32m, y = 1.11m, z = 1m

Precision versus Accuracy
percentage for 0.005m position error = 31.2%
percentage for 0.01m position error = 98.8%
percentage for 0.015m position error = 99.6%
percentage for 0.02m position error = 99.6%
percentage for 0.025m position error = 99.6%
percentage for 0.03m position error = 99.6%

Variables
sampling frequency = 96000 Hz
length of gold code sequence = 511 bits
carrier frequency = 7000 Hz
chip frequency = 7000 Hz
location estimation method = Method 1
number of phase shifts = 3
temperature = 24.43° Celcius

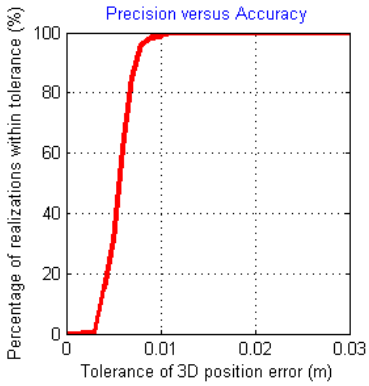


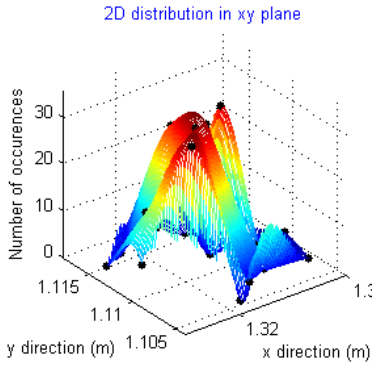


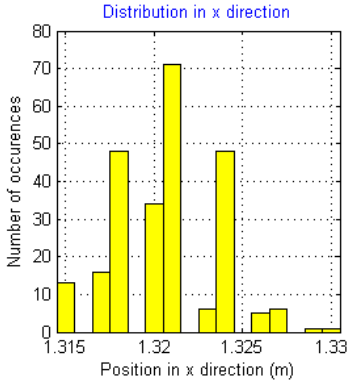


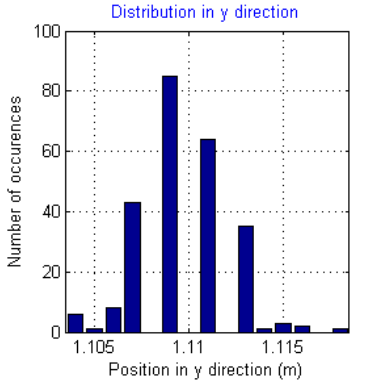


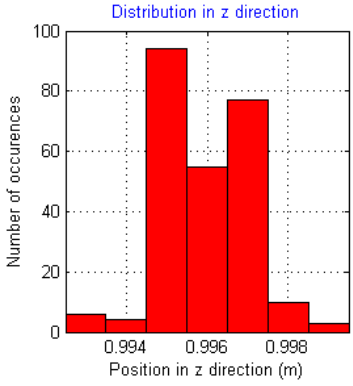


Figure I.2. x = 1.32 m, y = 1.11 m, z = 1 m

Coordinates of the Microphone
x = 0.75m, y = 1.22m, z = 1m

Precision versus Accuracy
percentage for 0.005m position error = 0.4%
percentage for 0.01m position error = 75.2%
percentage for 0.015m position error = 100%
percentage for 0.02m position error = 100%
percentage for 0.025m position error = 100%
percentage for 0.03m position error = 100%

Variables
sampling frequency = 96000 Hz
length of gold code sequence = 511 bits
carrier frequency = 7000 Hz
chip frequency = 7000 Hz
location estimation method = Method 1
number of phase shifts = 3
temperature = 24.43° Celcius

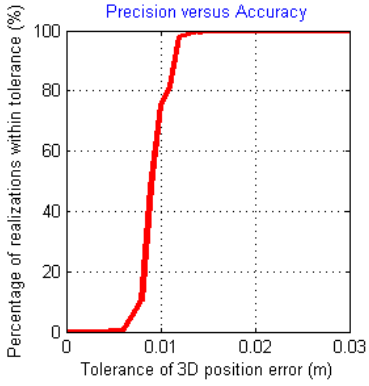


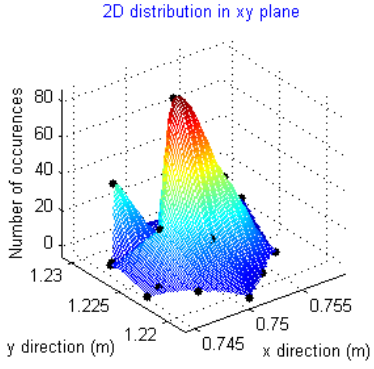


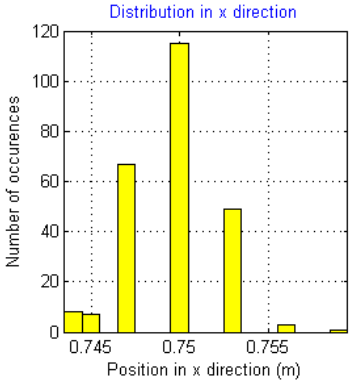


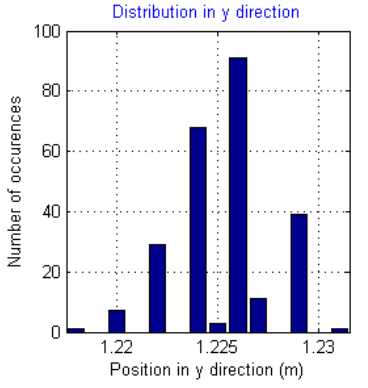


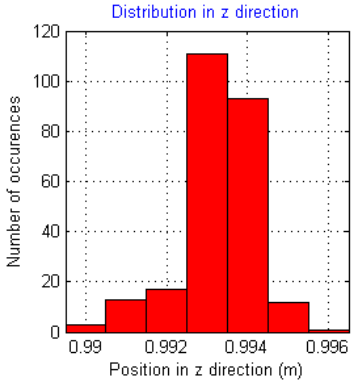


Figure I.3. x = 0.75 m, y = 1.22 m, z = 1 m

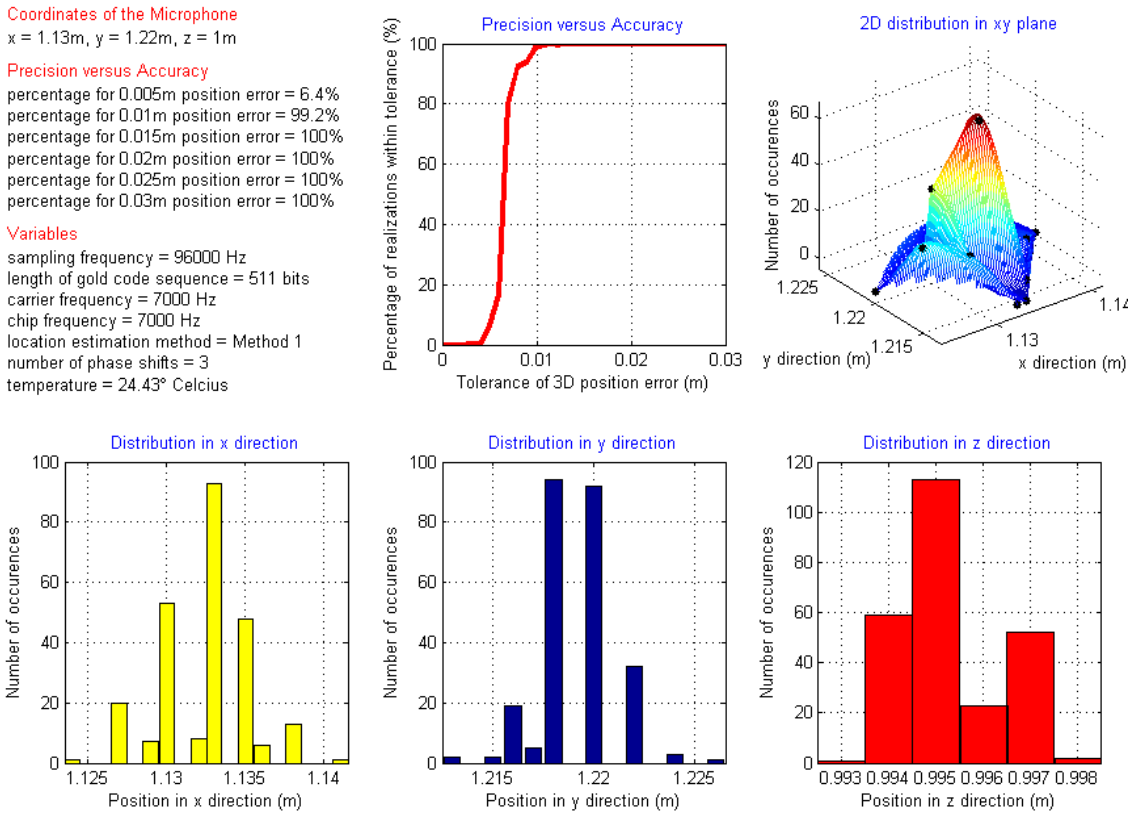


Figure I.4. x = 1.13 m, y = 1.22 m, z = 1 m

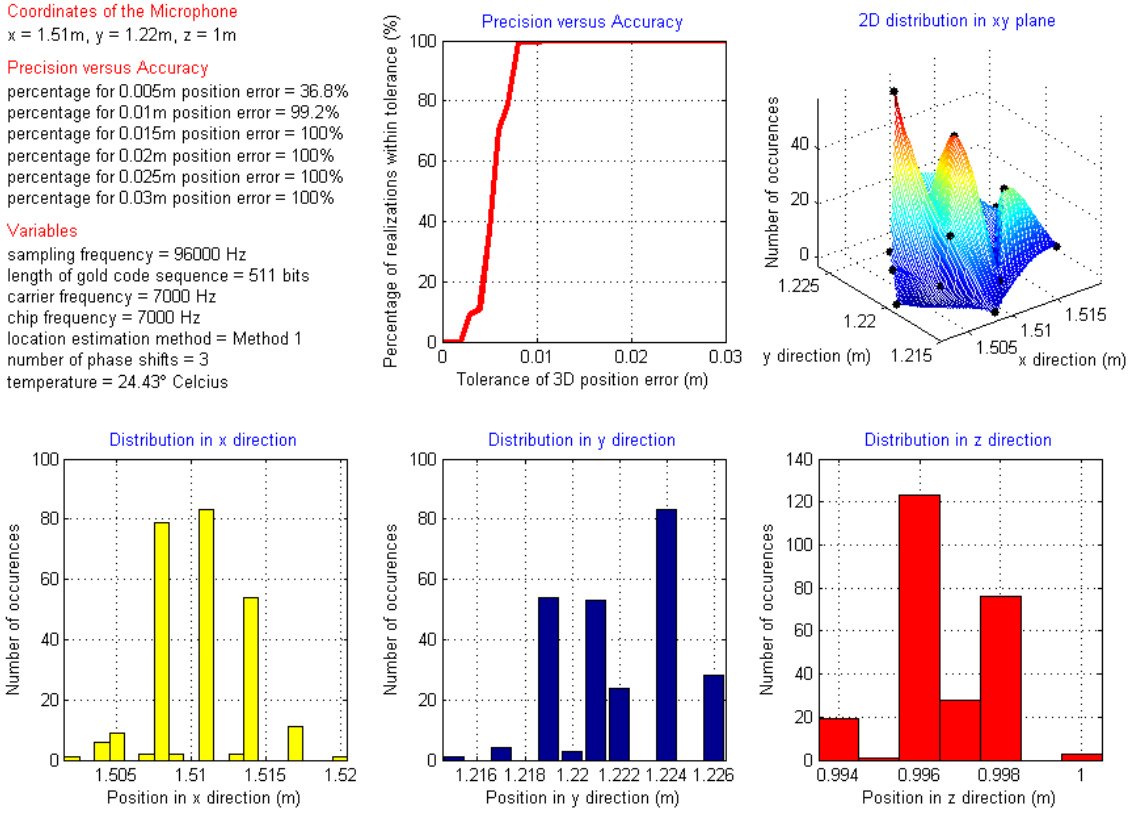


Figure I.5. x = 1.51 m, y = 1.22 m, z = 1 m

Coordinates of the Microphone
x = 0.75m, y = 1.44m, z = 1m

Precision versus Accuracy
percentage for 0.005m position error = 0%
percentage for 0.01m position error = 5.6%
percentage for 0.015m position error = 58.8%
percentage for 0.02m position error = 99.2%
percentage for 0.025m position error = 100%
percentage for 0.03m position error = 100%

Variables
sampling frequency = 96000 Hz
length of gold code sequence = 511 bits
carrier frequency = 7000 Hz
chip frequency = 7000 Hz
location estimation method = Method 1
number of phase shifts = 3
temperature = 24.43° Celcius

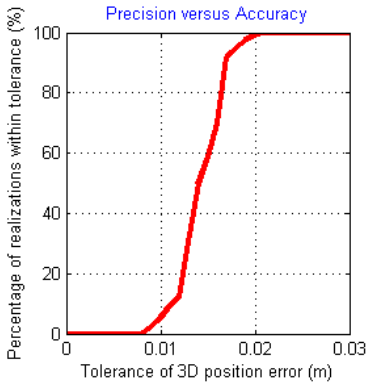


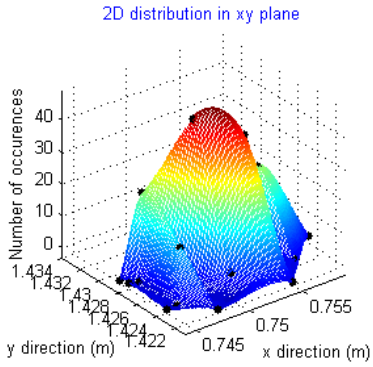


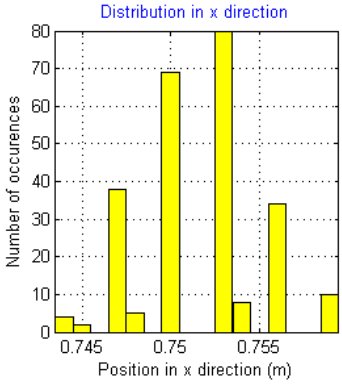


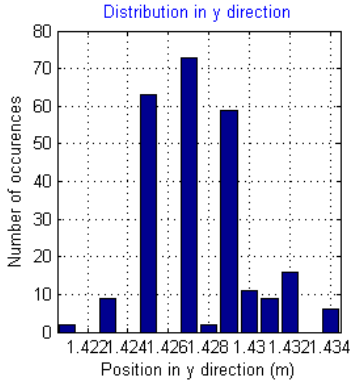


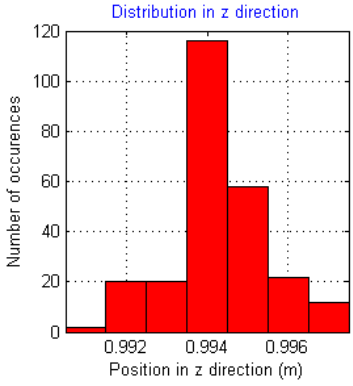


Figure I.6. x = 0.75 m, y = 1.44 m, z = 1 m

Coordinates of the Microphone
x = 1.13m, y = 1.44m, z = 1m

Precision versus Accuracy
percentage for 0.005m position error = 0.8%
percentage for 0.01m position error = 79.2%
percentage for 0.015m position error = 99.2%
percentage for 0.02m position error = 99.2%
percentage for 0.025m position error = 99.2%
percentage for 0.03m position error = 99.2%

Variables
sampling frequency = 96000 Hz
length of gold code sequence = 511 bits
carrier frequency = 7000 Hz
chip frequency = 7000 Hz
location estimation method = Method 1
number of phase shifts = 3
temperature = 24.92° Celcius

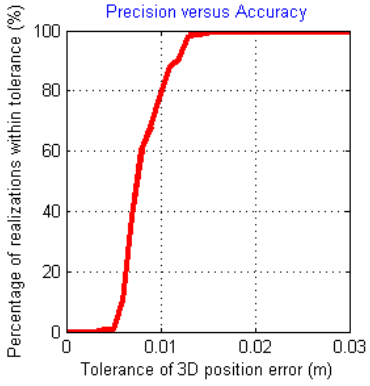


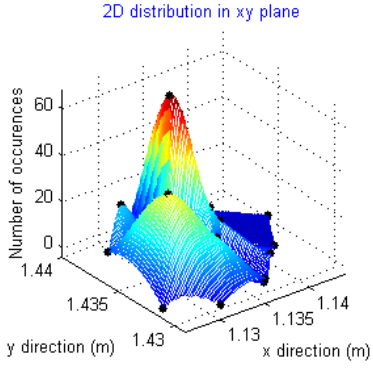


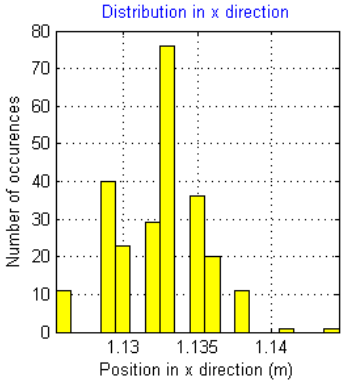


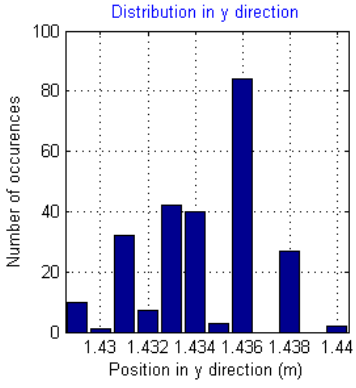


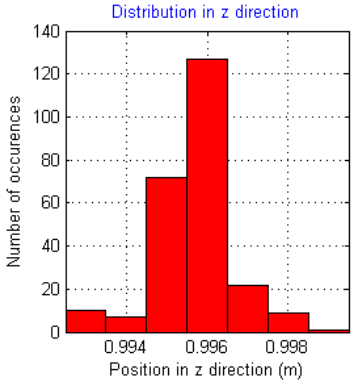


Figure I.7. x = 1.13 m, y = 1.44 m, z = 1 m

Coordinates of the Microphone
x = 1.51m, y = 1.44m, z = 1m

Precision versus Accuracy
percentage for 0.005m position error = 16%
percentage for 0.01m position error = 84%
percentage for 0.015m position error = 99.6%
percentage for 0.02m position error = 99.6%
percentage for 0.025m position error = 99.6%
percentage for 0.03m position error = 99.6%

Variables
sampling frequency = 96000 Hz
length of gold code sequence = 511 bits
carrier frequency = 7000 Hz
chip frequency = 7000 Hz
location estimation method = Method 1
number of phase shifts = 3
temperature = 23.46° Celcius

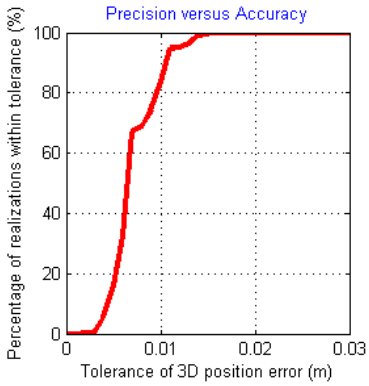


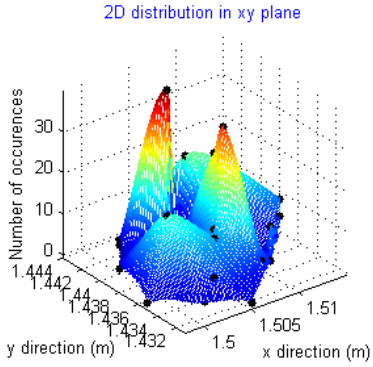


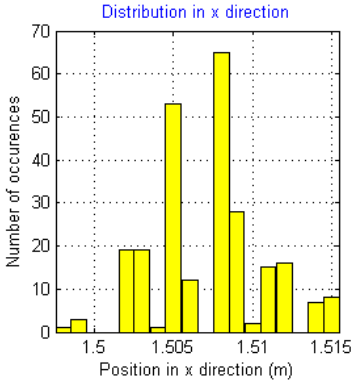


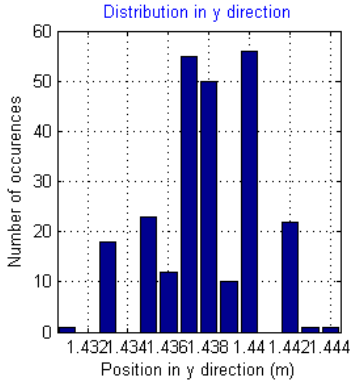


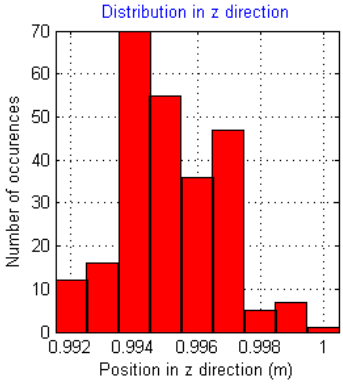


Figure I.8. x = 1.51 m, y = 1.44 m, z = 1 m

Coordinates of the Microphone
x = 0.94m, y = 1.55m, z = 1m

Precision versus Accuracy
percentage for 0.005m position error = 2%
percentage for 0.01m position error = 70.4%
percentage for 0.015m position error = 99.2%
percentage for 0.02m position error = 99.2%
percentage for 0.025m position error = 99.2%
percentage for 0.03m position error = 99.2%

Variables
sampling frequency = 96000 Hz
length of gold code sequence = 511 bits
carrier frequency = 7000 Hz
chip frequency = 7000 Hz
location estimation method = Method 1
number of phase shifts = 3
temperature = 23.46° Celcius

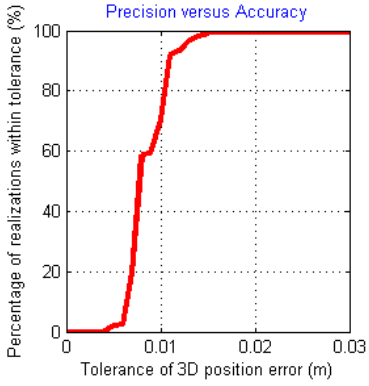


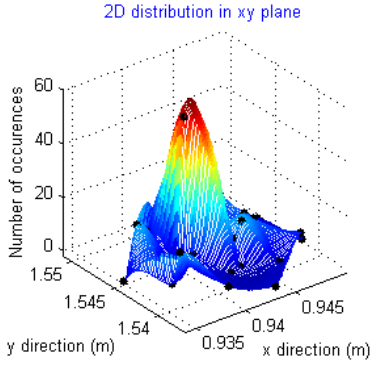


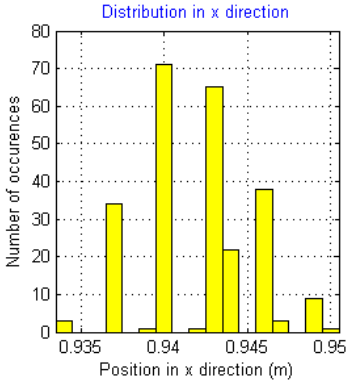


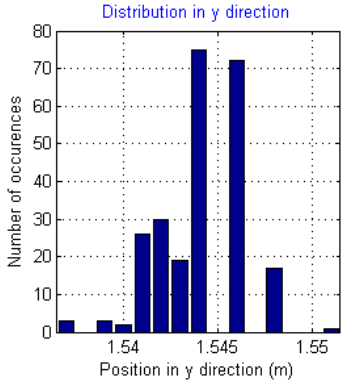


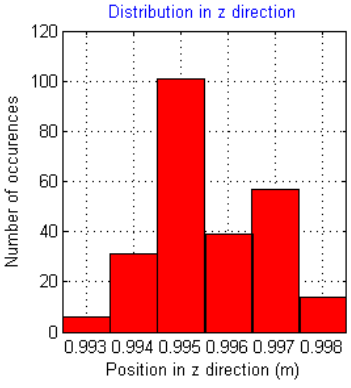


Figure I.9. x = 0.94 m, y = 1.55 m, z = 1 m

Coordinates of the Microphone
x = 1.32m, y = 1.55m, z = 1m

Precision versus Accuracy
percentage for 0.005m position error = 0%
percentage for 0.01m position error = 6.8%
percentage for 0.015m position error = 53.2%
percentage for 0.02m position error = 96%
percentage for 0.025m position error = 100%
percentage for 0.03m position error = 100%

Variables
sampling frequency = 96000 Hz
length of gold code sequence = 511 bits
carrier frequency = 7000 Hz
chip frequency = 7000 Hz
location estimation method = Method 1
number of phase shifts = 3
temperature = 24.43° Celcius

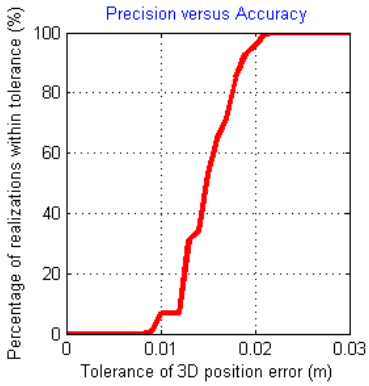


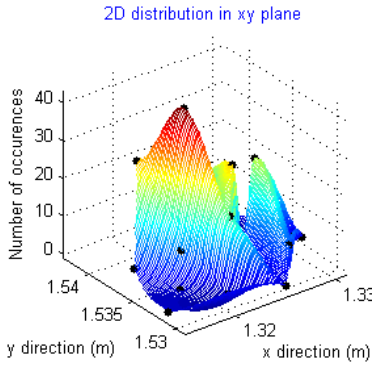


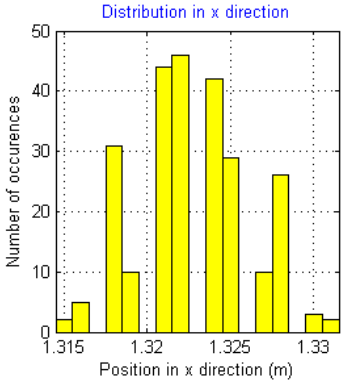


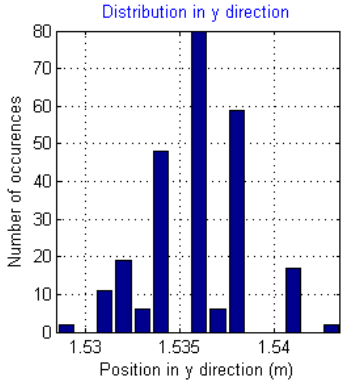


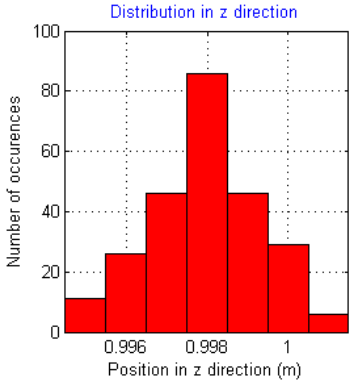


Figure I.10. x = 1.32 m, y = 1.55 m, z = 1 m

Coordinates of the Microphone
x = 0.94m, y = 1.77m, z = 1m

Precision versus Accuracy
percentage for 0.005m position error = 0%
percentage for 0.01m position error = 0.4%
percentage for 0.015m position error = 47.2%
percentage for 0.02m position error = 96.8%
percentage for 0.025m position error = 100%
percentage for 0.03m position error = 100%

Variables
sampling frequency = 96000 Hz
length of gold code sequence = 511 bits
carrier frequency = 7000 Hz
chip frequency = 7000 Hz
location estimation method = Method 1
number of phase shifts = 3
temperature = 24.43° Celcius

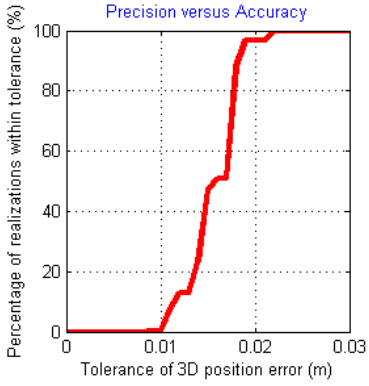


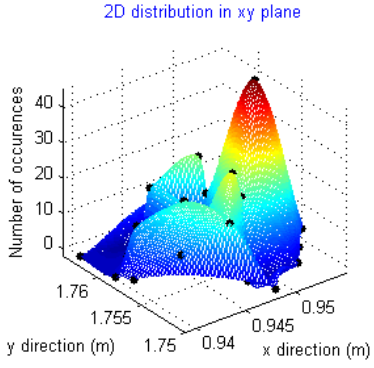


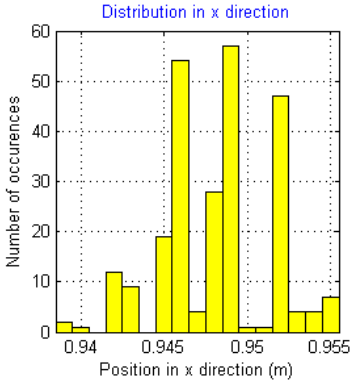


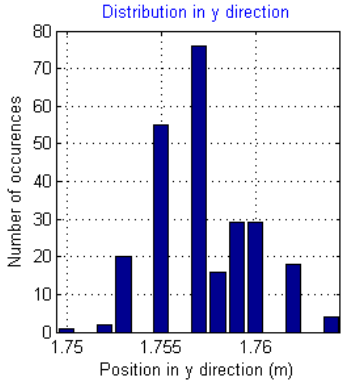


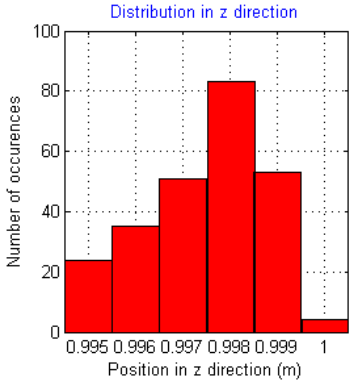


Figure I.11. x = 0.94 m, y = 1.77 m, z = 1 m

Coordinates of the Microphone
x = 1.32m, y = 1.77m, z = 1m

Precision versus Accuracy
percentage for 0.005m position error = 0%
percentage for 0.01m position error = 0.4%
percentage for 0.015m position error = 62.8%
percentage for 0.02m position error = 94.4%
percentage for 0.025m position error = 99.2%
percentage for 0.03m position error = 99.2%

Variables
sampling frequency = 96000 Hz
length of gold code sequence = 511 bits
carrier frequency = 7000 Hz
chip frequency = 7000 Hz
location estimation method = Method 1
number of phase shifts = 3
temperature = 24.43° Celcius

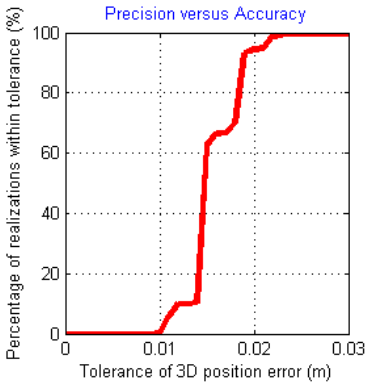


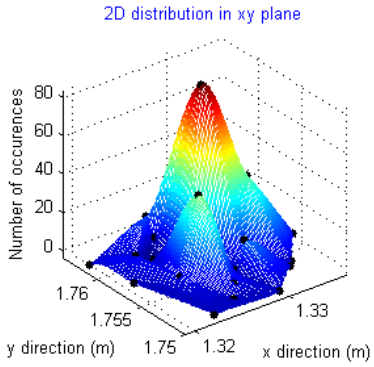


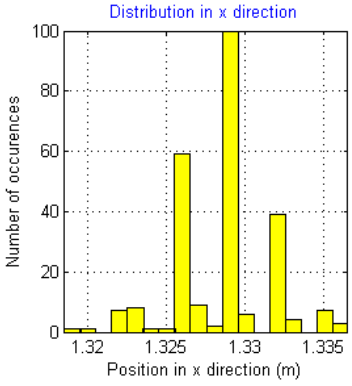


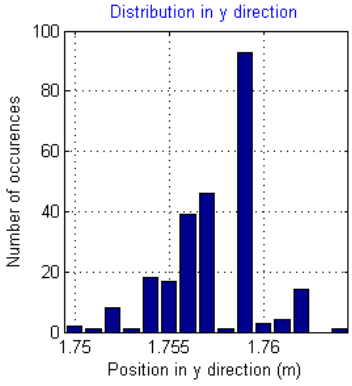


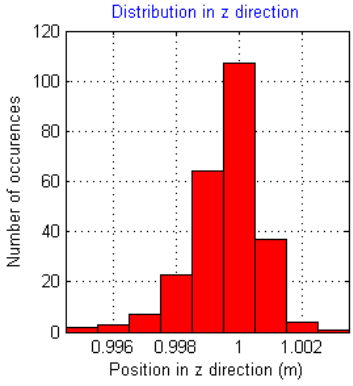


Figure I.12. x = 1.32 m, y = 1.77 m, z = 1 m

Coordinates of the Microphone
x = 0.75m, y = 1.88m, z = 1m

Precision versus Accuracy
percentage for 0.005m position error = 0%
percentage for 0.01m position error = 2.4%
percentage for 0.015m position error = 49.6%
percentage for 0.02m position error = 98.4%
percentage for 0.025m position error = 99.6%
percentage for 0.03m position error = 99.6%

Variables
sampling frequency = 96000 Hz
length of gold code sequence = 511 bits
carrier frequency = 7000 Hz
chip frequency = 7000 Hz
location estimation method = Method 1
number of phase shifts = 3
temperature = 25.41° Celcius

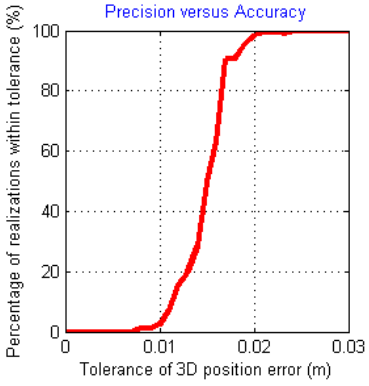


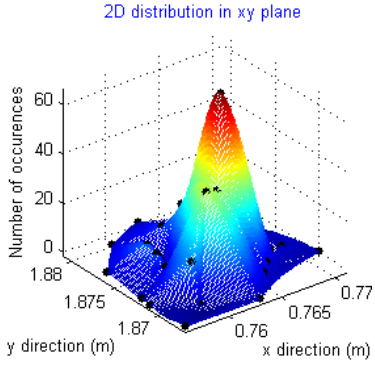


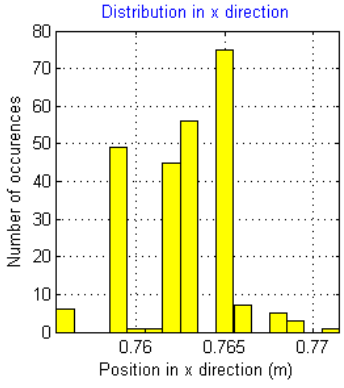


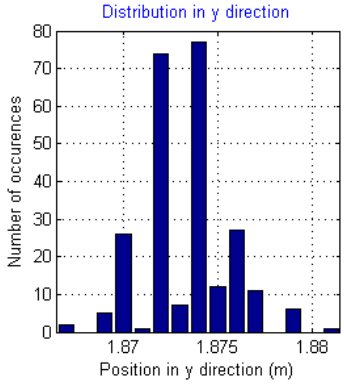


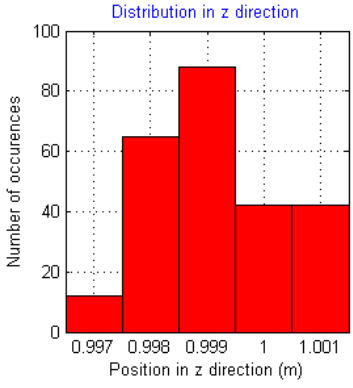


Figure I.13. x = 0.75 m, y = 1.88 m, z = 1 m

Coordinates of the Microphone
x = 1.13m, y = 1.88m, z = 1m

Precision versus Accuracy
percentage for 0.005m position error = 0%
percentage for 0.01m position error = 53.2%
percentage for 0.015m position error = 96.4%
percentage for 0.02m position error = 99.2%
percentage for 0.025m position error = 99.6%
percentage for 0.03m position error = 99.6%

Variables
sampling frequency = 96000 Hz
length of gold code sequence = 511 bits
carrier frequency = 7000 Hz
chip frequency = 7000 Hz
location estimation method = Method 1
number of phase shifts = 3
temperature = 23.94° Celcius

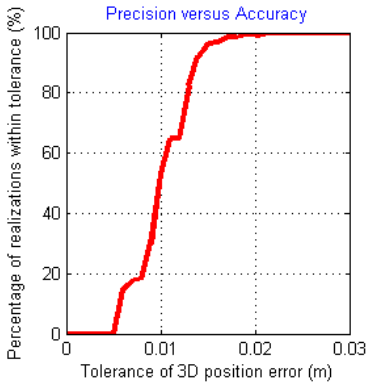


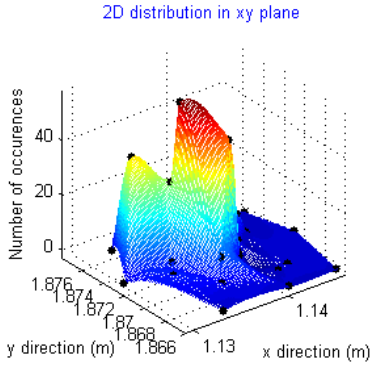


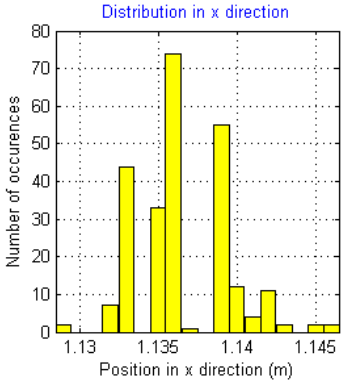


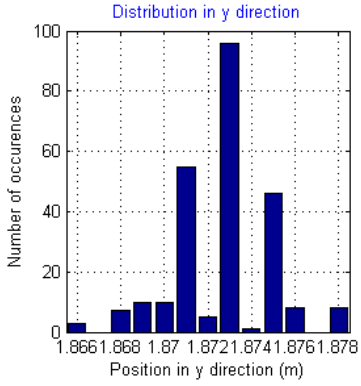


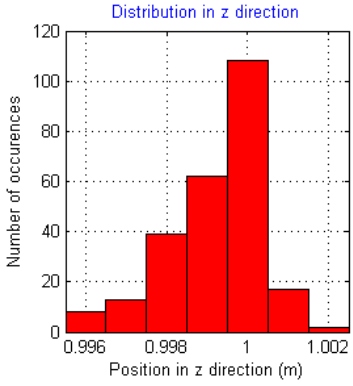


Figure I.14. x = 1.13 m, y = 1.88 m, z = 1 m

Coordinates of the Microphone
x = 1.51m, y = 1.88m, z = 1m

Precision versus Accuracy
percentage for 0.005m position error = 0%
percentage for 0.01m position error = 0.8%
percentage for 0.015m position error = 64.4%
percentage for 0.02m position error = 95.6%
percentage for 0.025m position error = 98.8%
percentage for 0.03m position error = 98.8%

Variables
sampling frequency = 96000 Hz
length of gold code sequence = 511 bits
carrier frequency = 7000 Hz
chip frequency = 7000 Hz
location estimation method = Method 1
number of phase shifts = 3
temperature = 24.92° Celcius

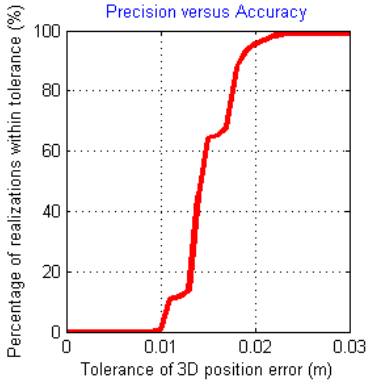


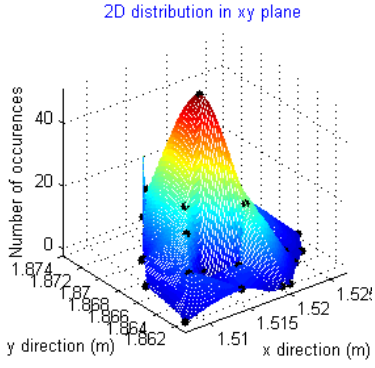


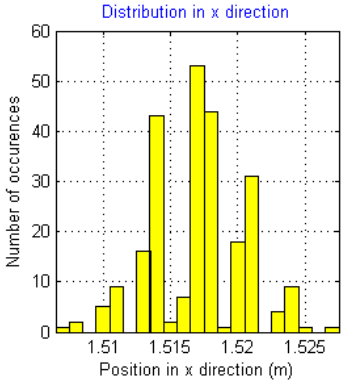


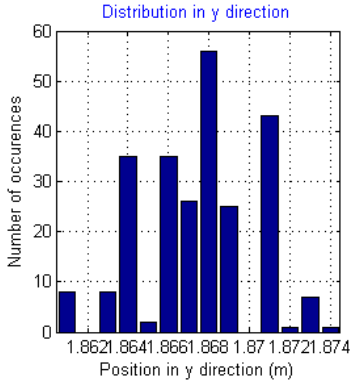


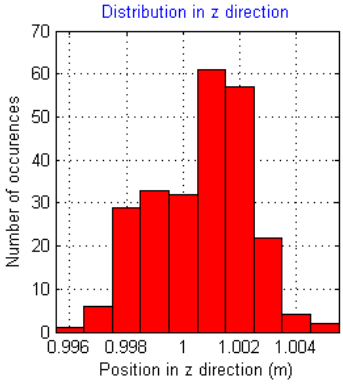


Figure I.15. x = 1.51 m, y = 1.88 m, z = 1 m

# APPENDIX J

# LOCALIZATION PERFORMANCE SCREENS FOR THE SECOND SET OF VARIABLES TAKEN FROM UPPER LEVEL TEST POINTS

In this section, the localization performance screens taken from ground level test points were illustrated. The second set of variables was used for the tests.

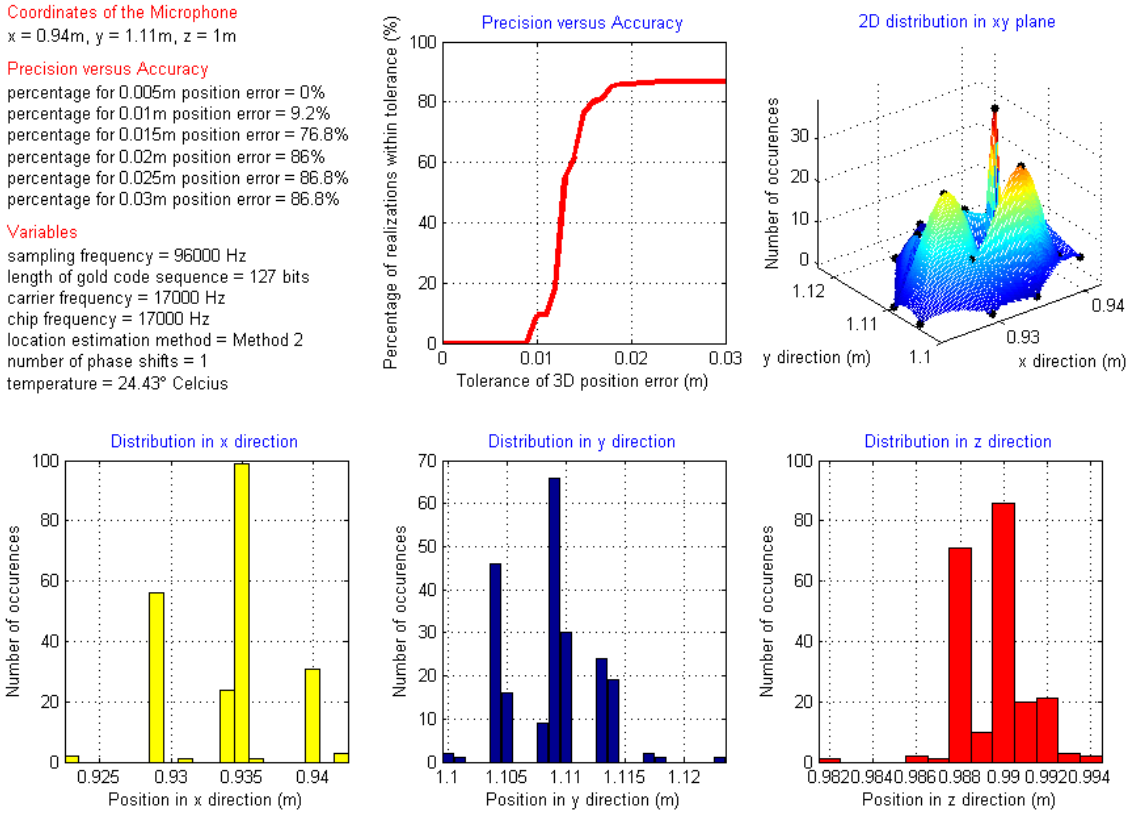


Figure J.1. x = 0.94 m, y = 1.11 m, z = 1 m

Coordinates of the Microphone
x = 1.32m, y = 1.11m, z = 1m

Precision versus Accuracy
percentage for 0.005m position error = 0.8%
percentage for 0.01m position error = 48.4%
percentage for 0.015m position error = 79.2%
percentage for 0.02m position error = 83.6%
percentage for 0.025m position error = 84%
percentage for 0.03m position error = 84%

Variables
sampling frequency = 96000 Hz
length of gold code sequence = 127 bits
carrier frequency = 17000 Hz
chip frequency = 17000 Hz
location estimation method = Method 2
number of phase shifts = 1
temperature = 23.46° Celcius

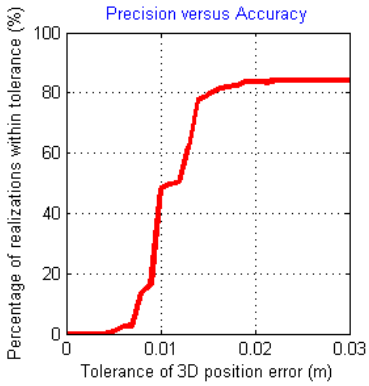


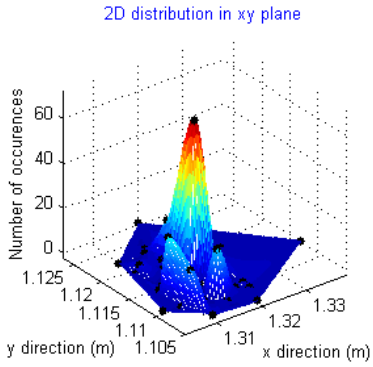


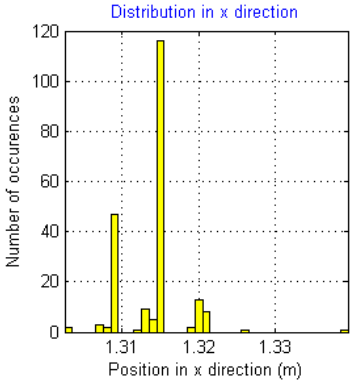


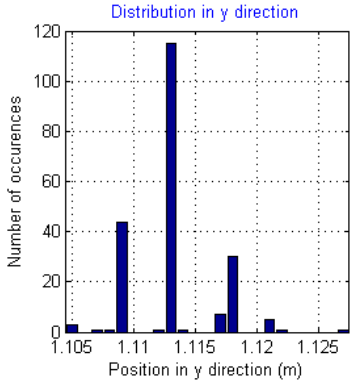


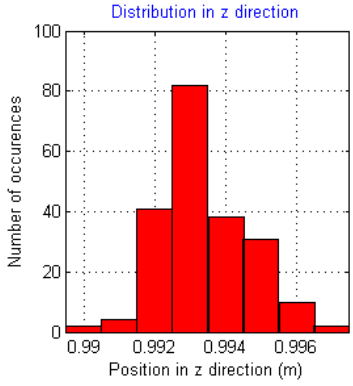


Figure J.2. x = 1.32 m, y = 1.11 m, z = 1 m

Coordinates of the Microphone
x = 0.75m, y = 1.22m, z = 1m

Precision versus Accuracy
percentage for 0.005m position error = 0.4%
percentage for 0.01m position error = 27.2%
percentage for 0.015m position error = 82.8%
percentage for 0.02m position error = 87.6%
percentage for 0.025m position error = 87.6%
percentage for 0.03m position error = 88%

Variables
sampling frequency = 96000 Hz
length of gold code sequence = 127 bits
carrier frequency = 17000 Hz
chip frequency = 17000 Hz
location estimation method = Method 2
number of phase shifts = 1
temperature = 24.43° Celcius

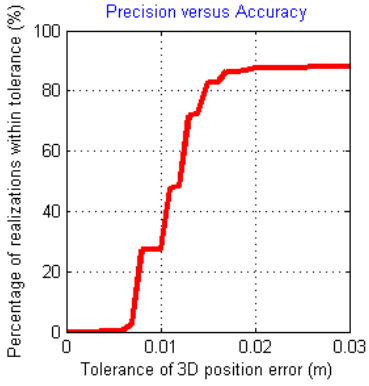


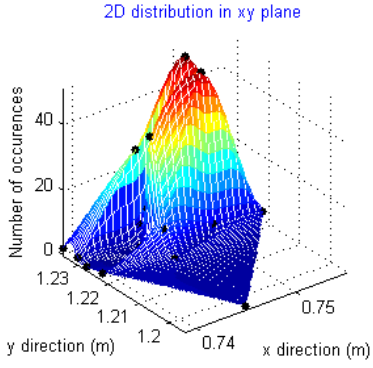


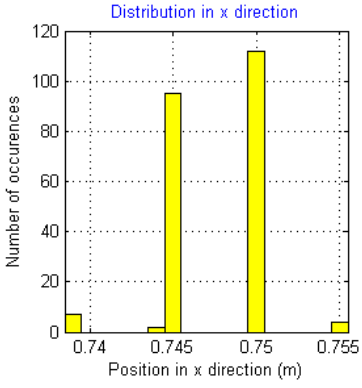


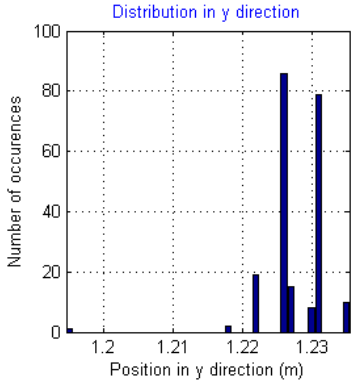


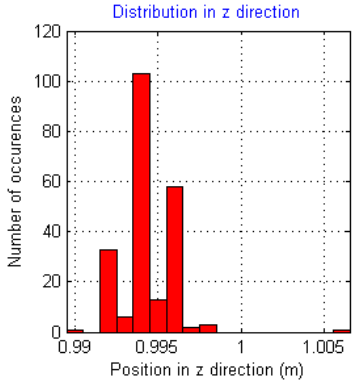


Figure J.3. x = 0.75 m, y = 1.22 m, z = 1 m

Coordinates of the Microphone
x = 1.13m, y = 1.22m, z = 1m

Precision versus Accuracy
percentage for 0.005m position error = 12.8%
percentage for 0.01m position error = 82.8%
percentage for 0.015m position error = 88%
percentage for 0.02m position error = 88%
percentage for 0.025m position error = 88%
percentage for 0.03m position error = 88%

Variables
sampling frequency = 96000 Hz
length of gold code sequence = 127 bits
carrier frequency = 17000 Hz
chip frequency = 17000 Hz
location estimation method = Method 2
number of phase shifts = 1
temperature = 24.43° Celcius

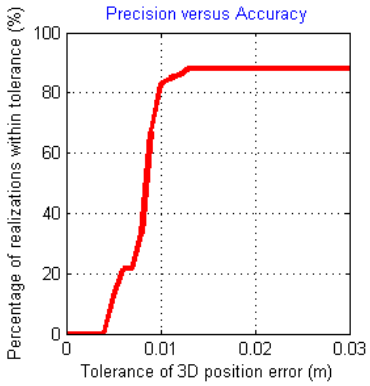


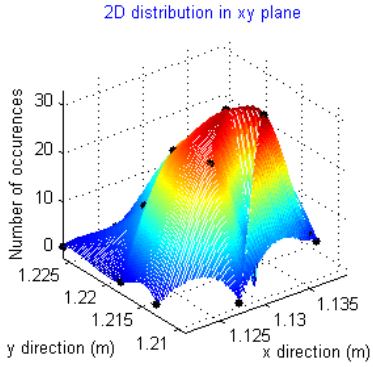


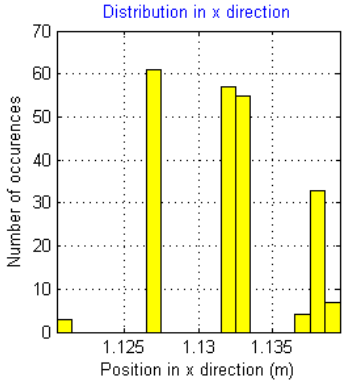


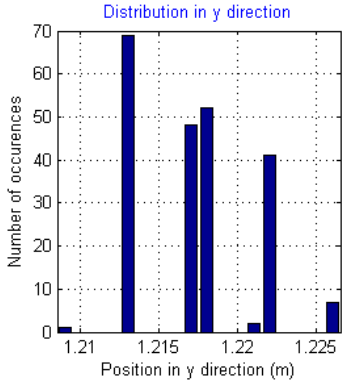


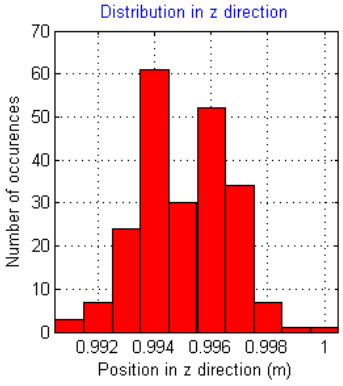


Figure J.4. x = 1.13 m, y = 1.22 m, z = 1 m

Coordinates of the Microphone
x = 1.51m, y = 1.22m, z = 1m

Precision versus Accuracy
percentage for 0.005m position error = 12%
percentage for 0.01m position error = 56%
percentage for 0.015m position error = 79.2%
percentage for 0.02m position error = 80%
percentage for 0.025m position error = 80.8%
percentage for 0.03m position error = 81.2%

Variables
sampling frequency = 96000 Hz
length of gold code sequence = 127 bits
carrier frequency = 17000 Hz
chip frequency = 17000 Hz
location estimation method = Method 2
number of phase shifts = 1
temperature = 24.43° Celcius

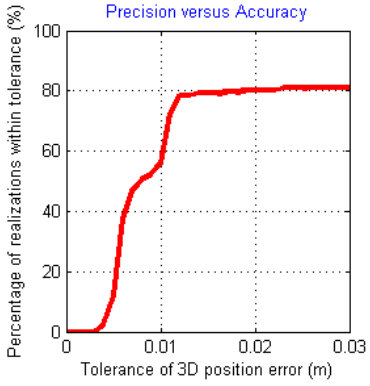


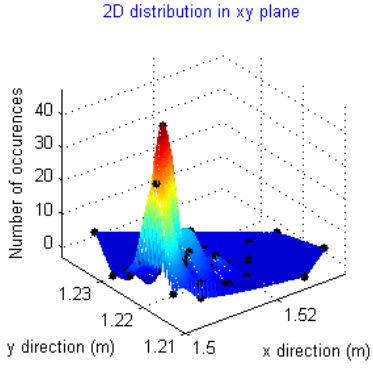


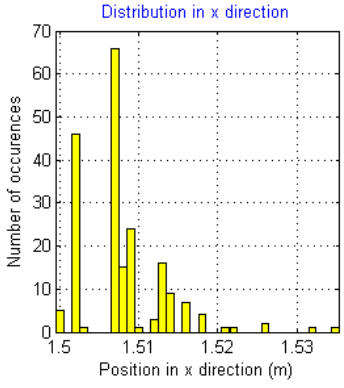


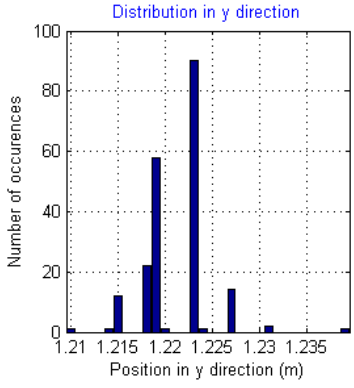


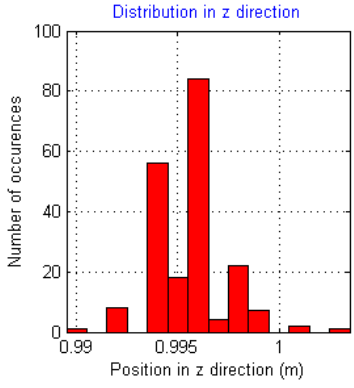


Figure J.5. x = 1.51 m, y = 1.22 m, z = 1 m

Coordinates of the Microphone
x = 0.75m, y = 1.44m, z = 1m

Precision versus Accuracy
percentage for 0.005m position error = 0%
percentage for 0.01m position error = 1.2%
percentage for 0.015m position error = 30.4%
percentage for 0.02m position error = 69.6%
percentage for 0.025m position error = 75.6%
percentage for 0.03m position error = 76%

Variables
sampling frequency = 96000 Hz
length of gold code sequence = 127 bits
carrier frequency = 17000 Hz
chip frequency = 17000 Hz
location estimation method = Method 2
number of phase shifts = 1
temperature = 24.43° Celcius

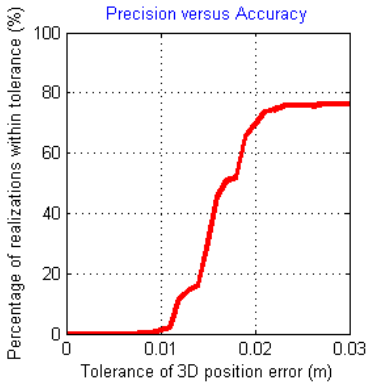


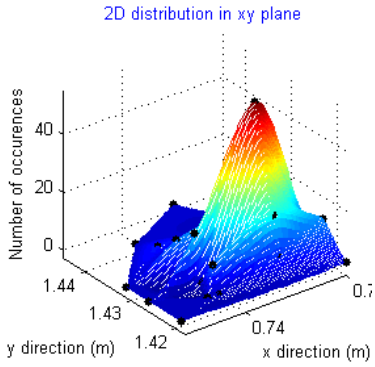


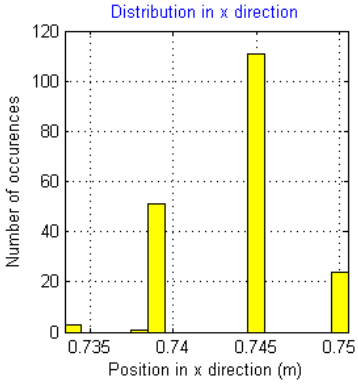


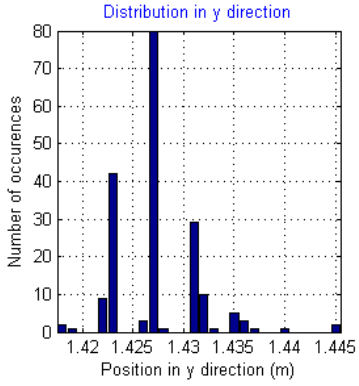


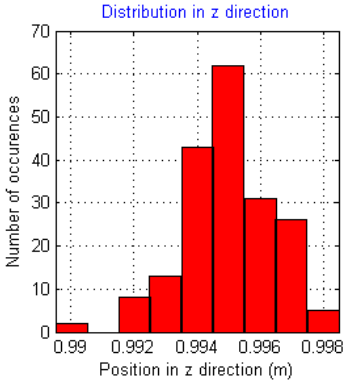


Figure J.6. x = 0.75 m, y = 1.44 m, z = 1 m

Coordinates of the Microphone
x = 1.13m, y = 1.44m, z = 1m

Precision versus Accuracy
percentage for 0.005m position error = 0%
percentage for 0.01m position error = 58%
percentage for 0.015m position error = 80.4%
percentage for 0.02m position error = 82%
percentage for 0.025m position error = 82.4%
percentage for 0.03m position error = 82.4%

Variables
sampling frequency = 96000 Hz
length of gold code sequence = 127 bits
carrier frequency = 17000 Hz
chip frequency = 17000 Hz
location estimation method = Method 2
number of phase shifts = 1
temperature = 23.94° Celcius

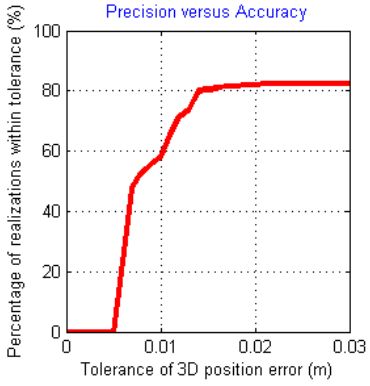


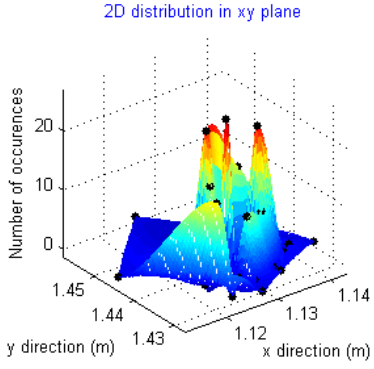


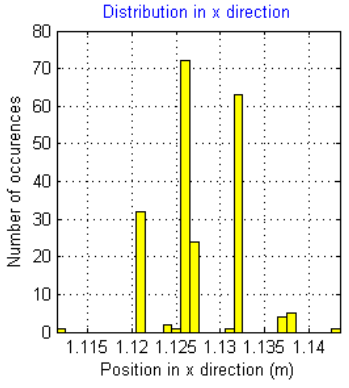


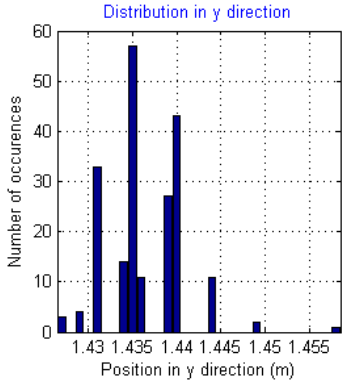


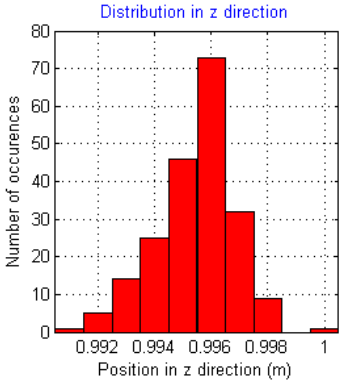


Figure J.7. x = 1.13 m, y = 1.44 m, z = 1 m

Coordinates of the Microphone
x = 1.51m, y = 1.44m, z = 1m

Precision versus Accuracy
percentage for 0.005m position error = 6%
percentage for 0.01m position error = 51.2%
percentage for 0.015m position error = 68.4%
percentage for 0.02m position error = 72.8%
percentage for 0.025m position error = 72.8%
percentage for 0.03m position error = 73.2%

Variables
sampling frequency = 96000 Hz
length of gold code sequence = 127 bits
carrier frequency = 17000 Hz
chip frequency = 17000 Hz
location estimation method = Method 2
number of phase shifts = 1
temperature = 24.43° Celcius

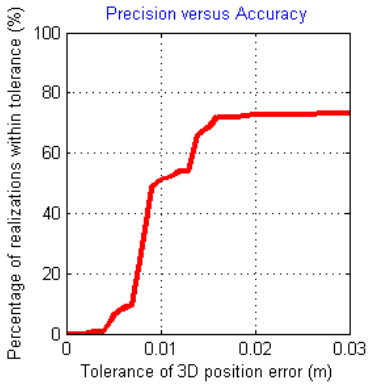


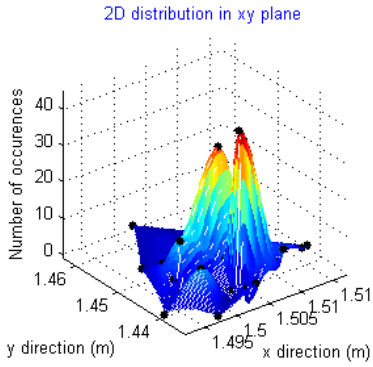


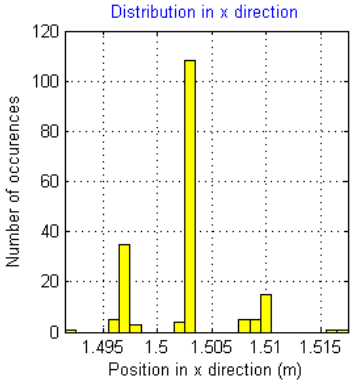


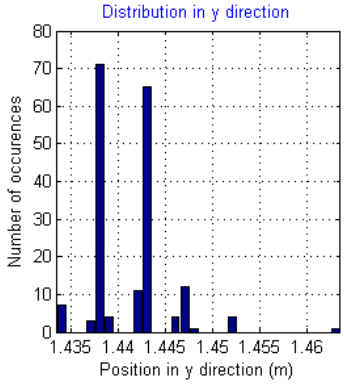


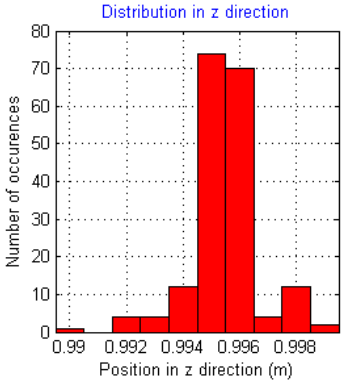


Figure J.8. x = 1.51 m, y = 1.44 m, z = 1 m

Coordinates of the Microphone
x = 0.94m, y = 1.55m, z = 1m

Precision versus Accuracy
percentage for 0.005m position error = 13.6%
percentage for 0.01m position error = 50.8%
percentage for 0.015m position error = 63.2%
percentage for 0.02m position error = 65.2%
percentage for 0.025m position error = 66%
percentage for 0.03m position error = 66.4%

Variables
sampling frequency = 96000 Hz
length of gold code sequence = 127 bits
carrier frequency = 17000 Hz
chip frequency = 17000 Hz
location estimation method = Method 2
number of phase shifts = 1
temperature = 24.43° Celcius

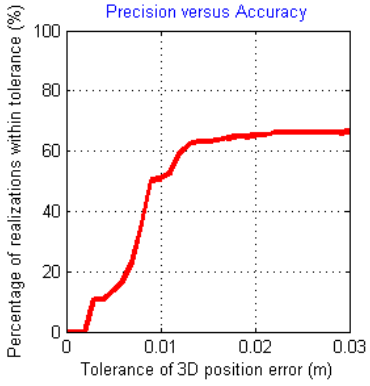


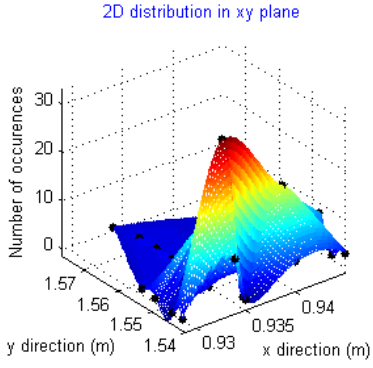


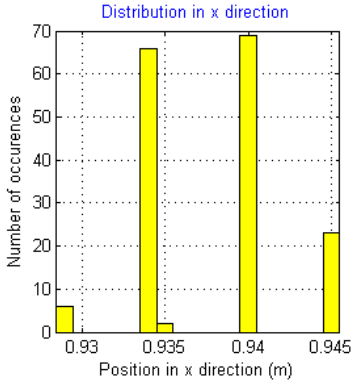


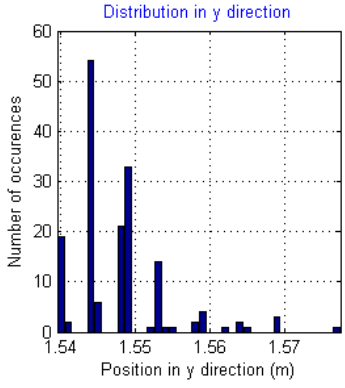


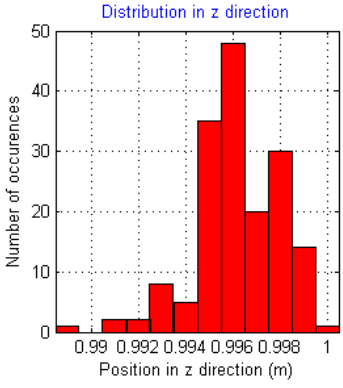


Figure J.9. x = 0.94 m, y = 1.55 m, z = 1 m

Coordinates of the Microphone
x = 1.32m, y = 1.55m, z = 1m

Precision versus Accuracy
percentage for 0.005m position error = 0.4%
percentage for 0.01m position error = 11.6%
percentage for 0.015m position error = 43.6%
percentage for 0.02m position error = 68%
percentage for 0.025m position error = 76%
percentage for 0.03m position error = 76%

Variables
sampling frequency = 96000 Hz
length of gold code sequence = 127 bits
carrier frequency = 17000 Hz
chip frequency = 17000 Hz
location estimation method = Method 2
number of phase shifts = 1
temperature = 24.92° Celcius

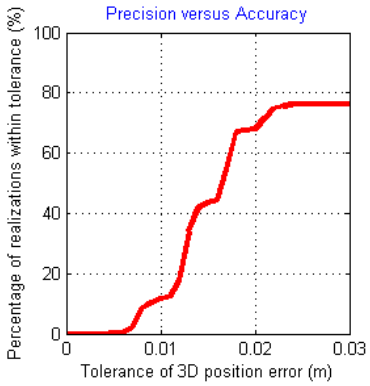


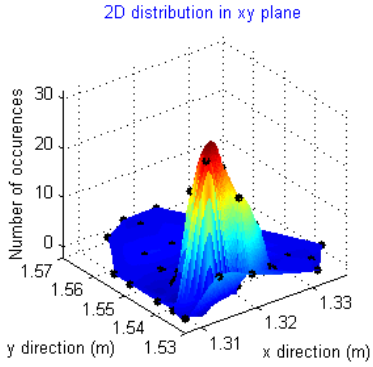


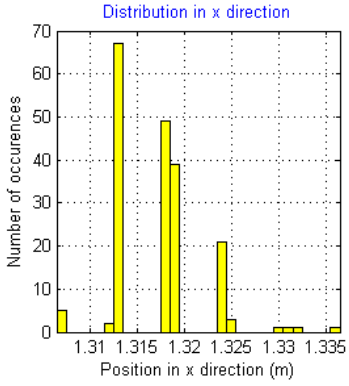


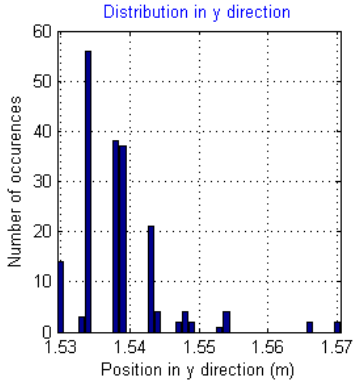


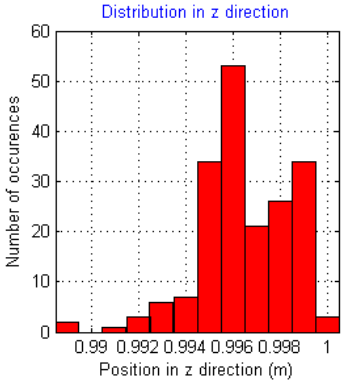


Figure J.10. x = 1.32 m, y = 1.55 m, z = 1 m

Coordinates of the Microphone
x = 0.94m, y = 1.77m, z = 1m

Precision versus Accuracy
percentage for 0.005m position error = 5.6%
percentage for 0.01m position error = 26.8%
percentage for 0.015m position error = 60%
percentage for 0.02m position error = 75.2%
percentage for 0.025m position error = 76%
percentage for 0.03m position error = 76.4%

Variables
sampling frequency = 96000 Hz
length of gold code sequence = 127 bits
carrier frequency = 17000 Hz
chip frequency = 17000 Hz
location estimation method = Method 2
number of phase shifts = 1
temperature = 24.43° Celcius

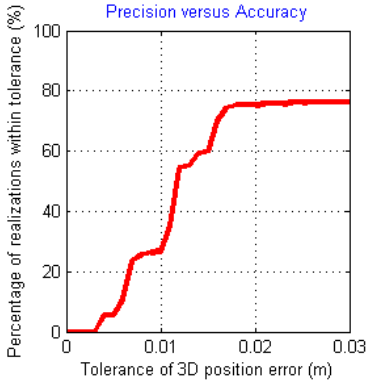


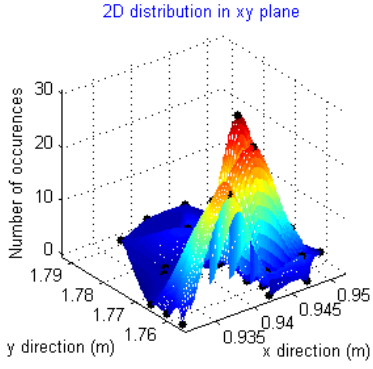


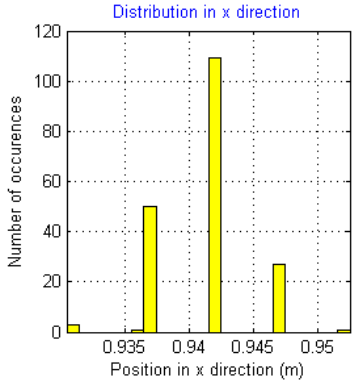


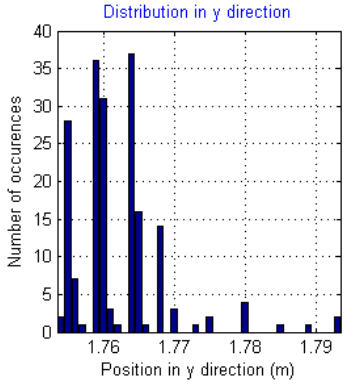


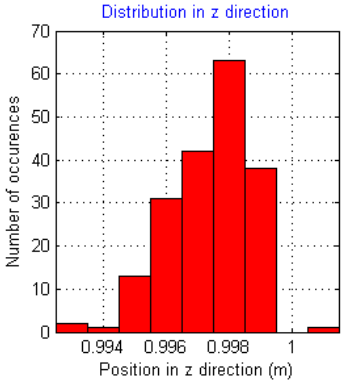


Figure J.11. x = 0.94 m, y = 1.77 m, z = 1 m

Coordinates of the Microphone
x = 1.32m, y = 1.77m, z = 1m

Precision versus Accuracy
percentage for 0.005m position error = 1.6%
percentage for 0.01m position error = 16%
percentage for 0.015m position error = 48.8%
percentage for 0.02m position error = 55.2%
percentage for 0.025m position error = 57.6%
percentage for 0.03m position error = 58.8%

Variables
sampling frequency = 96000 Hz
length of gold code sequence = 127 bits
carrier frequency = 17000 Hz
chip frequency = 17000 Hz
location estimation method = Method 2
number of phase shifts = 1
temperature = 24.92° Celcius

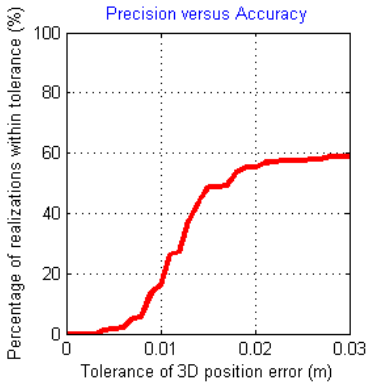


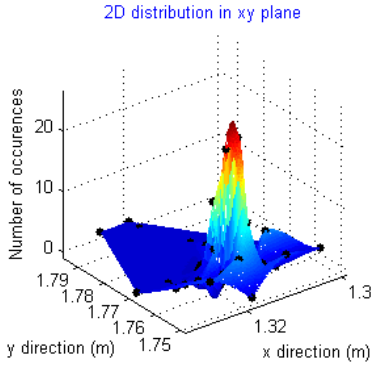


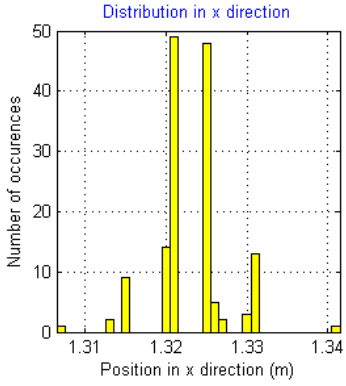


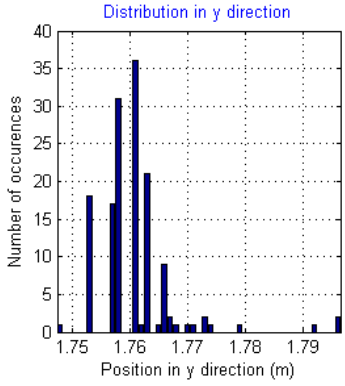


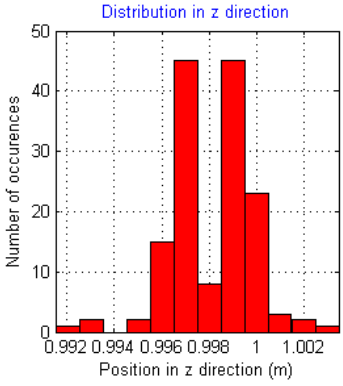


Figure J.12. x = 1.32 m, y = 1.77 m, z = 1 m

Coordinates of the Microphone
x = 0.75m, y = 1.88m, z = 1m

Precision versus Accuracy
percentage for 0.005m position error = 1.6%
percentage for 0.01m position error = 35.2%
percentage for 0.015m position error = 55.6%
percentage for 0.02m position error = 58.4%
percentage for 0.025m position error = 58.8%
percentage for 0.03m position error = 58.8%

Variables
sampling frequency = 96000 Hz
length of gold code sequence = 127 bits
carrier frequency = 17000 Hz
chip frequency = 17000 Hz
location estimation method = Method 2
number of phase shifts = 1
temperature = 24.43° Celcius

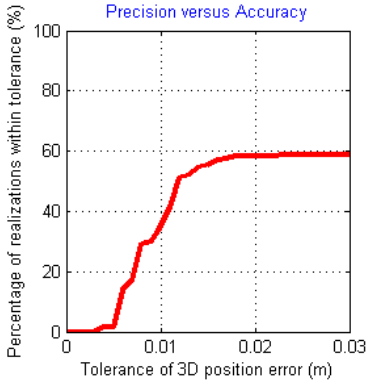


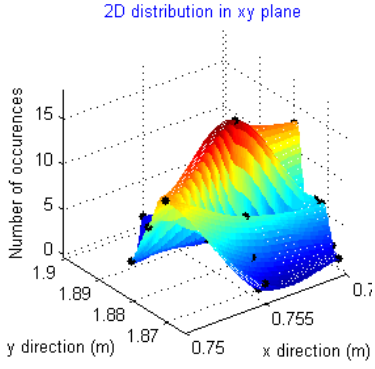


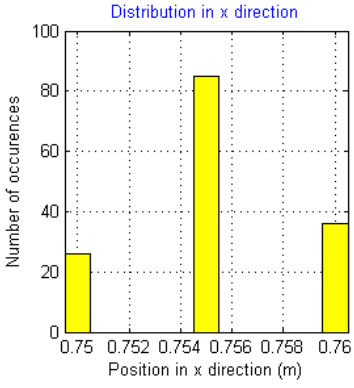


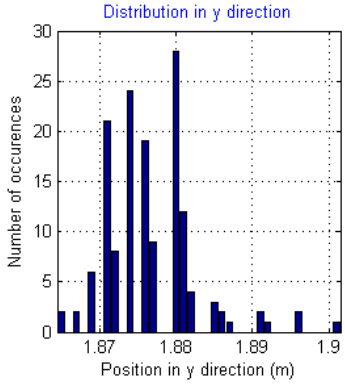


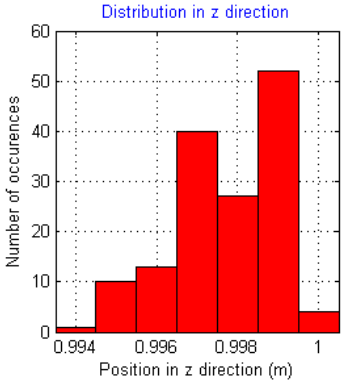


Figure J.13. x = 0.75 m, y = 1.88 m, z = 1 m

Coordinates of the Microphone
x = 1.13m, y = 1.88m, z = 1m

Precision versus Accuracy
percentage for 0.005m position error = 8%
percentage for 0.01m position error = 37.6%
percentage for 0.015m position error = 48.8%
percentage for 0.02m position error = 50.8%
percentage for 0.025m position error = 50.8%
percentage for 0.03m position error = 50.8%

Variables
sampling frequency = 96000 Hz
length of gold code sequence = 127 bits
carrier frequency = 17000 Hz
chip frequency = 17000 Hz
location estimation method = Method 2
number of phase shifts = 1
temperature = 24.43° Celcius

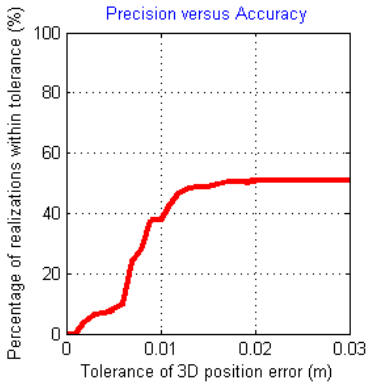


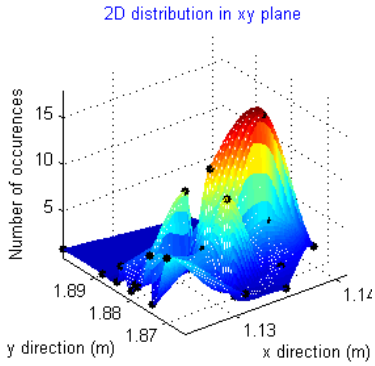


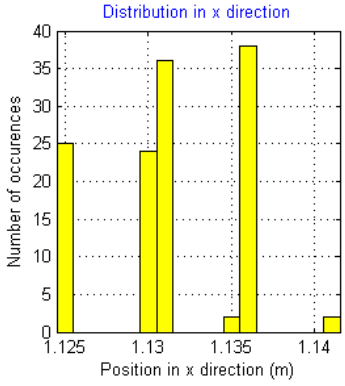


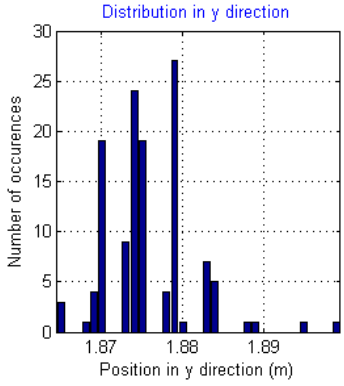


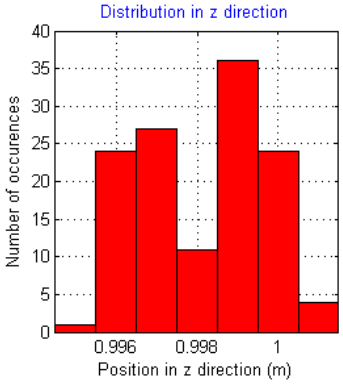


Figure J.14. x = 1.13 m, y = 1.88 m, z = 1 m

Coordinates of the Microphone
x = 1.51m, y = 1.88m, z = 1m

Precision versus Accuracy
percentage for 0.005m position error = 4.4%
percentage for 0.01m position error = 29.6%
percentage for 0.015m position error = 47.6%
percentage for 0.02m position error = 52%
percentage for 0.025m position error = 53.6%
percentage for 0.03m position error = 54.8%

Variables
sampling frequency = 96000 Hz
length of gold code sequence = 127 bits
carrier frequency = 17000 Hz
chip frequency = 17000 Hz
location estimation method = Method 2
number of phase shifts = 1
temperature = 24.92° Celcius

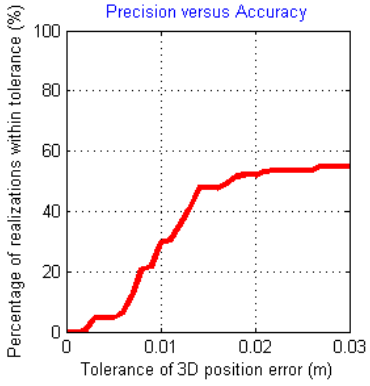


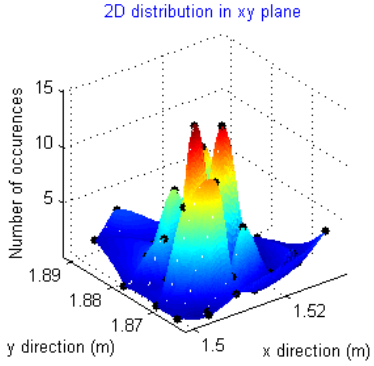


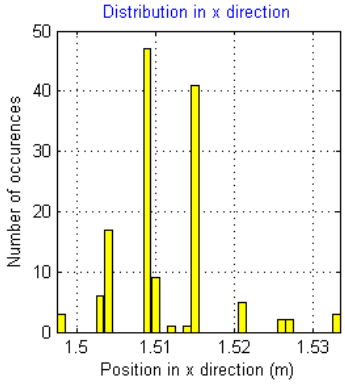


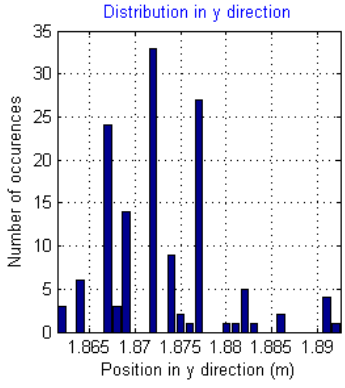


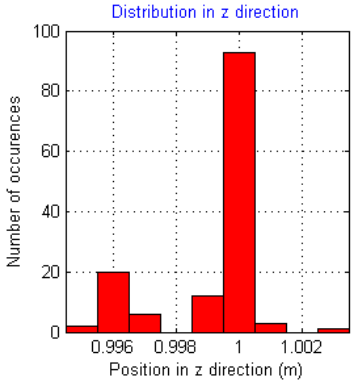


Figure J.15. x = 1.51 m, y = 1.88 m, z = 1 m